

UNCLASSIFIED

AD NUMBER

AD909656

LIMITATION CHANGES

TO:

Approved for public release; distribution is unlimited.

FROM:

Distribution authorized to U.S. Gov't. agencies only; Test and Evaluation; 21 DEC 1972. Other requests shall be referred to Aeronautical Systems Div., Wright-Patterson AFB, OH 45433.

AUTHORITY

ASD ltr 21 May 1974

THIS PAGE IS UNCLASSIFIED

L

ASD-TR-73-2

AD 909656

**ADVANCED CONCEPT EJECTION SEAT (ACES)
DEVELOPMENT AND QUALIFICATION**

HAMMOND R. MOY
DOUGLAS AIRCRAFT COMPANY
McDONNELL DOUGLAS CORPORATION

TECHNICAL REPORT ASD-TR-73-2

JANUARY 1973



Distribution limited to U.S. Government agencies only; Test and Evaluation; 21 December 1972. Other requests for this document must be referred to ASD/SML, Wright-Patterson Air Force Base, Ohio 45433.

**LIFE SUPPORT SYSTEM PROGRAM OFFICE
AERONAUTICAL SYSTEMS DIVISION
WRIGHT-PATTERSON AIR FORCE BASE, OHIO**

**Best
Available
Copy**

NOTICE

When Government drawings, specifications, or other data are used for any purpose other than in connection with a definitely related Government procurement operation, the United States Government thereby incurs no responsibility nor any obligation whatsoever; and the fact that the Government may have formulated, furnished, or in any way supplied the said drawings, specifications, or other data, is not to be regarded by implication or otherwise as in any manner licensing the holder or any other person or corporation, or conveying any rights or permission to manufacture, use, or sell any patented invention that may in any way be related thereto.

Copies of this report should not be returned unless return is required by security considerations, contractual obligations, or notice on a specific document.

ADVANCED CONCEPT EJECTION SEAT (ACES) DEVELOPMENT AND QUALIFICATION

HAMMOND R. MOY

**Distribution limited to U.S. Government agencies only; Test and Evaluation; 21
December 1972. Other requests for this document must be referred to ASD/SML,
Wright-Patterson Air Force Base, Ohio 45433.**

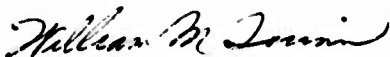
FOREWORD

This report was prepared by the Douglas Aircraft Company, McDonnell Douglas Corporation, 3855 Lakewood Blvd., Long Beach, California, 90846. This document covers the design, development, and qualification of the Advanced Concept Ejection Seat (ACES), which was accomplished under U. S. Air Force Contract F33657-69-C-0223 during the period from September 1968 through April 1972. The program was administered for the Air Force by the Life Support System Program Office, Aeronautical Systems Division (AFSC), with Mr. A. S. Mastriana (ASD/SML) acting as program manager. Technical coordination was provided by Captain E. M. Chase (ASD/SML), during the early phases of the program and, subsequently, by Mr. G. G. Dickson (ASD/SML).

The Douglas Principal Investigator was Mr. Hammond R. Moy of the Interior Design Section, Engineering and Product Development Department. Significant technical contributions were made by Messrs. R. G. McIntyre, B. Nichols, Jr., M. E. Wilfert, H. W. Jones, et al. of the Interior Design Section. Testing was carried out at Long Beach, California; Holloman Air Force Base, New Mexico; and at the Department of Defense Joint Parachute Test Facility, El Centro, California. Mr. A. R. Barker of the Interior Design Section coordinated the testing activity. The overall Douglas program effort was under the administrative direction of Mr. J. M. Palmer, Jr., Director for Research and Development.

This report was submitted by the author in April 1972.

This report has been reviewed and approved.



WILLIAM M. QUINN, Colonel, USAF
System Program Director
Life Support System Program Office
Deputy for Subsystems

ABSTRACT

The development of the Advanced Concept Ejection Seat (ACES) was proposed by the Douglas Aircraft Company of the McDonnell Douglas Corporation as a solution to critical operational problems experienced with current U. S. Air Force escape systems and to provide a major improvement in escape capability, especially under low-level, adverse attitude situations where relatively high crew fatality rates have been encountered. A program encompassing design, as well as development and qualification testing, resulted in the successful demonstration of the ACES system at speeds up to 590 KEAS and at altitudes up to 41,000 feet (MSL). The major performance improvement was achieved by incorporation of a multi-mode recovery sequencing system, mortar-deployed recovery subsystem with variable effective reefing, and a gyro-controlled vernier rocket to pitch-stabilize the seat during the initial part of its trajectory. Onboard speed/altitude sensors and an automatic programmer, containing logic and electronic time delays, were used to establish the seat environment, select the recovery mode, and initiate ejection and recovery events. Performance requirements of MIL-S-9479A were satisfied, with the exception that accelerations (spinal axis), in some instances, exceeded specified limits. An improvement in ACES escape capability can be effected by releasing the seat from the crewman earlier, just as the recovery parachute initially inflates.

TABLE OF CONTENTS

SECTION		PAGE
I	INTRODUCTION	1
II	SEAT SYSTEM	3
	System Design Concepts	3
	System Operation	9
	Manual Backups	13
III	SEAT ASSEMBLY	17
	Structure	17
	Loads	17
	Controls	23
	Seat-Mounted Mechanism	23
IV	INITIATION SUBSYSTEM	27
V	PROPULSION SUBSYSTEM	31
VI	ENVIRONMENTAL SENSOR SUBSYSTEM	35
VII	AUTOMATIC PROGRAMMER SUBSYSTEM	39
	Initiation Sequencer	41
	Recovery Sequencer	44
	Initiation Control Unit	50
	Development Problems	50
	Squib Isolation	53
VIII	ELECTROEXPLOSIVE DEVICES	55
	Firing Characteristics	55
	External Electromagnetic Fields	58
	Static Electricity	58
IX	STABILIZATION SUBSYSTEM	61
	STAPAC	61
	STAPAC Operation	64
	STAPAC Performance	64
	Development Problems	68
	Drogue System	70
	Drogue Operation and Performance	77

PRECEDING PAGE BLANK-NOT FILMED.

TABLE OF CONTENTS (Continued)

SECTION		PAGE
X	RECOVERY SUBSYSTEM	83
	Installation and Operation	88
XI	CREW SUPPORT AND RESTRAINT SUBSYSTEM	97
	Backrest	97
	Restraint Harness	99
XII	SURVIVAL AND PERSONAL EQUIPMENT	105
	Survival Kit	105
	Outer Container	106
	HARK	108
	Locator Beacon	111
XIII	WEIGHT SUMMARY	117
XIV	TEST PROGRAM	119
	Component Development Tests	119
	Subsystem Development Tests	121
	System Development Tests	130
	Component Qualification Tests	145
	Subsystem Qualification Tests	147
	System Qualification Tests	149
	Discussion of Acceleration Data	175
	Event Timing	179
	System Improvements	180
XV	SYSTEM PERFORMANCE	181
XVI	RELIABILITY AND MAINTAINABILITY	189
	Reliability	189
	Maintainability	189
XVII	CONCLUSIONS	193

LIST OF ILLUSTRATIONS

FIGURE		PAGE
1	Advanced Concept Ejection Seat, Three-Quarter View . . .	4
2	Advanced Concept Ejection Seat, Right Side	5
3	Advanced Concept Ejection Seat, Left Side	6
4	ACES Subsystems	7
5	ACES System Schematic	10
6	Mode Envelopes	11
7	Mode 1 Operation	12
8	Mode 2 Operation	14
9	Mode 3 Operation	15
10	Parachute Manual Backup Sequence	16
11	Advanced Concept Ejection Seat Major Assemblies	18
12	ACES Seat Structure	19
13	Seat Load Data	20
14	Crash and Aerodynamic Seat Loads	21
15	Crash and Parachute Loads	22
16	Seat-Mounted Controls	24
17	Man/Seat Release System	25
18	Armrest/Restraint System	26
19	Initiation Subsystem	27
20	Initiation Sequencer	28
21	Initiation Subsystem Schematic	29
22	XM-39 Rocket Catapult Assembly	31
23	XM-39 Rocket Catapult Performance	32
24	ACES Catapult Separation Velocity Performance for Static Ejections	32

LIST OF ILLUSTRATIONS (Continued)

FIGURE		PAGE
25	Environmental Sensors	35
26	Environmental Sensor Installation	36
27	Environmental Sensor Schematic	37
28	Velocity Switch Operational Limits	38
29	Environmental Sensor Switching Matrix	38
30	Recovery Sequencer	40
31	Automatic Programmer Subsystem	41
32	Initiation Sequencer Functional Block Diagram	42
33	Programmer-Initiated Pre-Ejection Functions	43
34	Recovery Sequencer Initiation	44
35	Programmer-Initiated Recovery Functions	45
36	Recovery Sequencer Major Sections	46
37	Recovery Sequencer Operation	46
38	Typical $R_1 C_1$ Timing and Firing Circuit with Characteristic Operating Curve	47
39	Recovery Sequencer Functional Diagram	49
40	Recovery Sequencer Firing System Revision	52
41	Recovery Sequencer Logic Revision	53
42	Electrical Initiator Bridgewire Configurations	55
43	Static Electricity Discharge Protection	59
44	Gyro-Controlled Vernier Rocket (STAPAC)	61
45	Vernier Rocket Motor	62
46	Vernier Rocket Performance	63
47	STAPAC Operation	65
48	STAPAC Operation During Test	66

LIST OF ILLUSTRATIONS (Continued)

FIGURE		PAGE
49	Rocket Motor Pitching Moments	66
50	Pitch Angle vs Time (with Biasing Spring)	67
51	Computed Pitch Stabilization Performance	67
52	Pitch Stabilization for Mode 1 Ejections	68
53	STAPAC Firing Mechanism Revisions (Alternate)	69
54	Drogue Parachute System	71
55	Drogue Installation	72
56	Restrictor Band Installation	73
57	Extraction Chute Assembly	74
58	Drogue Gun	76
59	Drogue Bridle Cutters	76
60	Drogue System Operation	78
61	Drogue Operational Times	79
62	Pitch Stabilization for Mode 2 Ejections	79
63	Drogue Performance	81
64	ACES Recovery Subsystem	84
65	Deployment Bag	85
66	Pilot Chute and Pouch	86
67	Mortar Assembly	87
68	Reefing Line Cutter	87
69	Parachute Assembly	89
70	Parachute Installation	90
71	Recovery Sequence (Automatic Mode)	91
72	Parachute Operation Over the Ejection Velocity Range . . .	93

LIST OF ILLUSTRATIONS (Continued)

FIGURE		PAGE
73	Distance Traveled at Various Ejection Velocities	94
74	Maximum Reefed and Full Inflation Forces	95
75	Crew Support and Restraint Subsystem	97
76	Backrest Assembly - Forward Side	98
77	Backrest Assembly - Aft Side	100
78	Backrest Release System	101
79	Single-Point Release Harness	102
80	Crewman Wearing Harness	103
81	Oxygen Hose Disconnect	104
82	Survival Kit Assembly	105
83	Dropline Attached to Rucksack and Case	106
84	Raft Stowed in Case with Dropline	107
85	Ripcord Pins Through Ring Assembly and Cord Loops . .	107
86	Automatic Ripcord Stowed	108
87	Rucksack	109
88	Hit-and-Run Kit	109
89	Hit-and-Run Kit Contents	110
90	HARK Pins Safety Tied	110
91	Survival Kit Installation	111
92	Survival Kit Operation	114
93	AN/URT-33 Radio Beacon Installation	115
94	ACES Center of Gravity Locations	117
95	Drogue Performance (Tomahawk Test No. 4)	126
96	Base Pressure Coefficient vs Dynamic Pressure	127
97	Trajectory and Event Data for ACES Development Test No. 1	132

LIST OF ILLUSTRATIONS (Continued)

FIGURE		PAGE
98	Trajectory and Event Data for ACES Development Test No. 2	134
99	Trajectory and Event Data for ACES Development Test No. 3	135
100	Trajectory and Event Data for ACES Development Test No. 4	136
101	Trajectory and Event Data for ACES Development Test No. 5	137
102	Trajectory and Event Data for ACES Development Test No. 6	138
103	Trajectory and Event Data for ACES Development Test No. 7	140
104	Trajectory and Event Data for ACES Development Test No. 8	141
105	Trajectory and Event Data for ACES Development Test No. 9	141
106	Trajectory and Event Data for ACES Development Test No. 10	142
107	Trajectory and Event Data for ACES Development Test No. 11	143
108	Trajectory and Event Data for ACES Development Test No. 12	144
109	Trajectory Curve, ACES Qualification Sled Test No. 1 - 212 KEAS	159
110	Trajectory Curve, ACES Qualification Sled Test No. 2 - 0 KEAS	160
111	Trajectory Curve, ACES Qualification Sled Test No. 3 - 0 KEAS	161
112	Trajectory Curve, ACES Qualification Sled Test No. 4 - 151 KEAS - Aft Seat	161
113	Trajectory Curve, ACES Qualification Sled Test No. 4 - 149 KEAS - Forward Seat	162

LIST OF ILLUSTRATIONS (Concluded)

FIGURE		PAGE
114	Trajectory Curve, ACES Qualification Sled Test No. 5 - 227 KEAS	164
115	Trajectory Curve, ACES Qualification Sled Test No. 6 - 577 KEAS	165
116	Trajectory Curve, ACES Qualification Sled Test No. 7 - 578 KEAS	166
117	Trajectory Curve, ACES Qualification Sled Test No. 8 - 438 KEAS - Aft Seat	167
118	Trajectory Curve, ACES Qualification Sled Test No. 8 - 437 KEAS - Forward Seat	168
119	Trajectory, ACES Inflight Ejection Test No. 1 (155 KEAS, 5219 Ft MSL)	171
120	Trajectory, ACES Inflight Ejection Test No. 2 (281 KEAS, 16,090 Ft MSL)	172
121	Trajectory, ACES Inflight Ejection Test No. 3 (276 KEAS, 15,898 Ft MSL)	173
122	Trajectory, ACES Inflight Ejection Test No. 4 (244 KEAS, 41,759 Ft MSL)	174
123	Trajectory, ACES Inflight Ejection Test No. 5 (248 KEAS, 41,800 Ft MSL)	175
124	Trajectory, ACES Inflight Ejection Test No. 6 (173 KEAS, 5713 Ft MSL, Aircraft Rate of Descent 10,896 Ft/Min)	176
125	ACES Zero/Zero Performance	183
126	ACES Performance for Upright and Inverted Flight	184
127	ACES Sink Rate Performance	185
128	ACES Performance for Aircraft Dive Conditions	186
129	ACES Performance for Aircraft Roll Conditions	187
130	Velocity History for an ACES 600-KEAS Ejection	188

LIST OF TABLES

TABLE		PAGE
I	ACES Cartridges and Cartridge Activated Devices	8
II	Recovery Sequencer Parts Summary	54
III	Seat System Electroexplosive Devices	56
IV	Initiator Characteristics	57
V	S01-10217-21 Initiator Function Times	59
VI	Drogue System Physical Data	75
VII	ACES Survival Equipment	112
VIII	ACES Weight Summary	118
IX	Gyro Spin-Up Actuator Development Tests	120
X	Restraint Harness Drop Tower Tests	122
XI	Restraint Harness Airdrop Tests	123
XII	ACES Drogue System Test Results (Tomahawk)	125
XIII	ACES Recovery Subsystem Development Tests - 10 Percent Reefing	128
XIV	Summary of Event Times for ACES Development Ejection Tests	133
XV	Parachute Mortar and Gyro Spin-Up Actuator Qualification Tests	146
XVI	Subcontractor - Qualified Components	148
XVII	Summary of ACES Recovery Subsystem Qualification Tests	150
XVIII	Summary of ACES System Gravity-Launch Tests	151
XIX	ACES Static Structural Test Conditions	153
XX	Seat System Functional and Environmental Test Summary	154
XXI	Summary of Trajectory/Event Time Data for ACES Qualification Ejection Tests	157

LIST OF TABLES (Concluded)

TABLE		PAGE
XXII	Summary of ACES Inflight Ejection Test Event Data	169
XXIII	Drogue and Recovery Parachute Acceleration Data for Track Ejection Qualification Tests	178
XXIV	ACES System Performance	182
XXV	ACES Reliability Assessment	190

ABBREVIATIONS AND TERMS

<u>Abreviation or Term</u>	<u>Definition</u>
ABS	Acrylonitrile - Butadiene - Styrene
ACES	Advanced Concept Ejection Seat
AFB	Air Force Base
AFSC	Air Force Systems Command
C_d	Drag Coefficient
C_dS	Drag Area
C_f	Friction Coefficient
cg	Center of Gravity
DAC	Douglas Aircraft Company
Deg	Degree
DOD JPTF	Department of Defense Joint Parachute Test Facility
DRI	Dynamic Response Index
EED	Electroexplosive Device
ENSOLITE	Synthetic Closed-Cell Sponge
F	Fahrenheit
ft/sec	Feet per Second
g	Acceleration
G_x	Longitudinal Acceleration
G_y	Lateral Acceleration
G_z	Vertical Acceleration
G_t	Total Acceleration
HARK	Hit-and-Run Kit
KEAS	Knots Equivalent Airspeed
KIAS	Knots Indicated Airspeed

ABBREVIATIONS AND TERMS
(Continued)

<u>Abbreviation or Term</u>	<u>Definition</u>
lb	Pound
MDC	McDonnell Douglas Corporation
msec	Millisecond
MSL	Mean Sea Level
PSI	Pounds per Square Inch
RC	Resistor Capacitor
RF	Radio Frequency
RFI	Radio Frequency Interference
rpm	Revolutions per Minute
SCD	Specification Control Drawing
SCR	Silicon Controlled Rectifier
SMDC	Shielded Mild Detonating Cord
SPO	System Program Office
STAPAC	Gyro-Controlled Pitch Stabilization System
$\frac{(C_D^S)_R}{(C_D^S)_O}$	Parachute Reefing Ratio

SECTION I

INTRODUCTION

Studies of USAF ejections have shown that the majority of crew fatalities occur because of the deficient low-altitude, adverse-attitude, and high-sink rate performance of current aircrew escape systems. In addition, many injuries, in some cases fatal, result from collisions of the crewman and his seat during the recovery phase of the ejection.

Recognizing the deficiencies of current aircrew escape systems, the Air Force Specification for Ejection Seats, MIL-S-9479, was revised in June 1967 to establish requirements for a new, advanced-performance ejection seat. The intent of the new criteria was to provide a baseline for the development of an aircrew escape system that would provide the required operational capability, system standardization, improved reliability, and simplified maintenance.

In March 1968 a proposal for the development and qualification of an advanced-performance escape system, meeting the requirements of MIL-S-9479A, was submitted by the Douglas Aircraft Company to the Life Support System Program Office. The proposal was submitted in response to Aeronautical System Division (AFSC) RFQ No. F33657-68-Q-0700. The proposed escape system was known as the Advanced Concept Ejection Seat (ACES), Reference 1.

To achieve the required performance, reliability, and maintainability goals, the proposed ACES incorporated the following design features:

1. Redundant ejection controls and rocket catapult initiation system for high reliability.
2. Multi-mode recovery sequencing to optimize performance over the total envelope of escape conditions.
3. Seat-mounted speed/altitude sensors for a mode-select system independent of any aircraft subsystems.
4. Electroexplosive sequencing and electronic timing for close-tolerance control of system time delays and recovery functions.
5. Seat stabilization during rocket burn by a gyro-controlled vernier rocket (STAPAC) for rotation and trajectory control.
6. Seat stabilization during free-flight by a drogue parachute for attitude control as well as deceleration.
7. Forced, line-first deployment of the recovery parachute to minimize variations in deployment times.
8. Variable effective reefing of the recovery parachute to permit early deployment in high-speed ejections, without compromising performance at low speed.
9. Recovery of the crewman in the seat, with release of the seat following parachute inflation, to prevent man/seat collisions.

10. A separable backrest incorporating highly contoured, padded surfaces for maximum comfort.
11. A single-point release parachute/restraint harness, with negative g strap and integral automatic oxygen hose (mask) disconnect, for rapid ground egress.
12. A "soft" survival kit, with automatic-manual deployment selector, to minimize weight and complexity.

The design, development, and qualification of the ACES was authorized in September 1968, Reference 2. At the outset, a detailed design study was initiated to substantiate the technical approach and to optimize, where possible, the function, performance, and reliability of the various subsystems and components, Reference 3. Upon completion of the study, in which a firm escape system configuration was defined, the detailed design was implemented.

Near the completion of the design phase, a major modification was made to the upper portion of the seat structure. This modification was based on a requirement for improved rearward visibility in the F-15 aircraft, Reference 4. Revisions also were required to the recovery parachute and the guide rail assembly to achieve the desired result.

On the basis of a study conducted on the high-speed performance of the originally proposed drogue system, a recommendation was made to change from a 3-foot Ribless Guide Surface to a 5.8-foot-diameter Hemisflo drogue parachute, Reference 5. This modification, authorized by Reference 6, also included a change in the drogue gun to provide a heavier slug with a higher muzzle velocity.

This report describes the ACES system as developed and qualified under the Reference 2 contract. In addition to the presentation of data related to the design, operation, and performance of the system, results of the test program are summarized.

SECTION II
SEAT SYSTEM

SYSTEM DESIGN CONCEPTS

The design and performance criteria, specified by MIL-S-9479A, were primary considerations in the selection of the various design concepts incorporated in the Advanced Concept Ejection Seat (ACES). To satisfy these criteria in the most effective manner, the following features were integrated into the design of the ACES system:

1. A seat structure assembly conforming to the required MIL-S-9479A dimensional geometry with integral, dual-ejection firing controls, man/seat release mechanism, and armrest/restraints. The recovery sequencer and environmental sensors also are installed on the seat structure assembly.
2. Minimum time-delay from ejection initiation to parachute deployment by use of a multimode timing system. Mode selection is provided by seat-mounted speed/altitude sensors with all recovery functions controlled by close-tolerance electronic time delays and electroexplosive sequencing.
3. Pitch stability during rocket burn by a gyro-controlled vernier rocket motor (STAPAC) capable of compensating for a 4-inch system cg excursion.
4. Pitch and yaw stability and aerodynamic deceleration for high-speed ejections by a 5.8-foot Hemisflo drogue parachute. The drogue is attached to the seat structure by a 4-point bridle designed to maintain the occupied seat in the attitude required for optimum application of deceleration forces and for recovery parachute deployment.
5. Forced deployment of the recovery parachute by a mortar that projects the parachute into the airstream from the occupied, stabilized seat. The parachute is reefed to permit its deployment at relatively high speeds.
6. Man/seat separation by recovery of the crewman in the seat and subsequently releasing the seat. Man/seat collision is prevented because the seat accelerates away from the crewman. The parachute riser loads are transmitted initially to the seat structure and, when the seat is released, the residual riser loads are transferred to the crewman.
7. Seat ejection by a rocket catapult providing an impulse optimized for balanced escape system performance.
8. Crew restraint and comfort by a single-point release harness and a highly contoured and padded seat pan and backrest assembly. The restraint harness allows rapid egress from the cockpit in ground emergency by actuation of the single-point release buckle.

The ACES system is shown in Figures 1, 2, and 3. Major subsystems are illustrated in Figure 4, and a list of the ACES cartridges and cartridge-actuated devices is given in Table I.

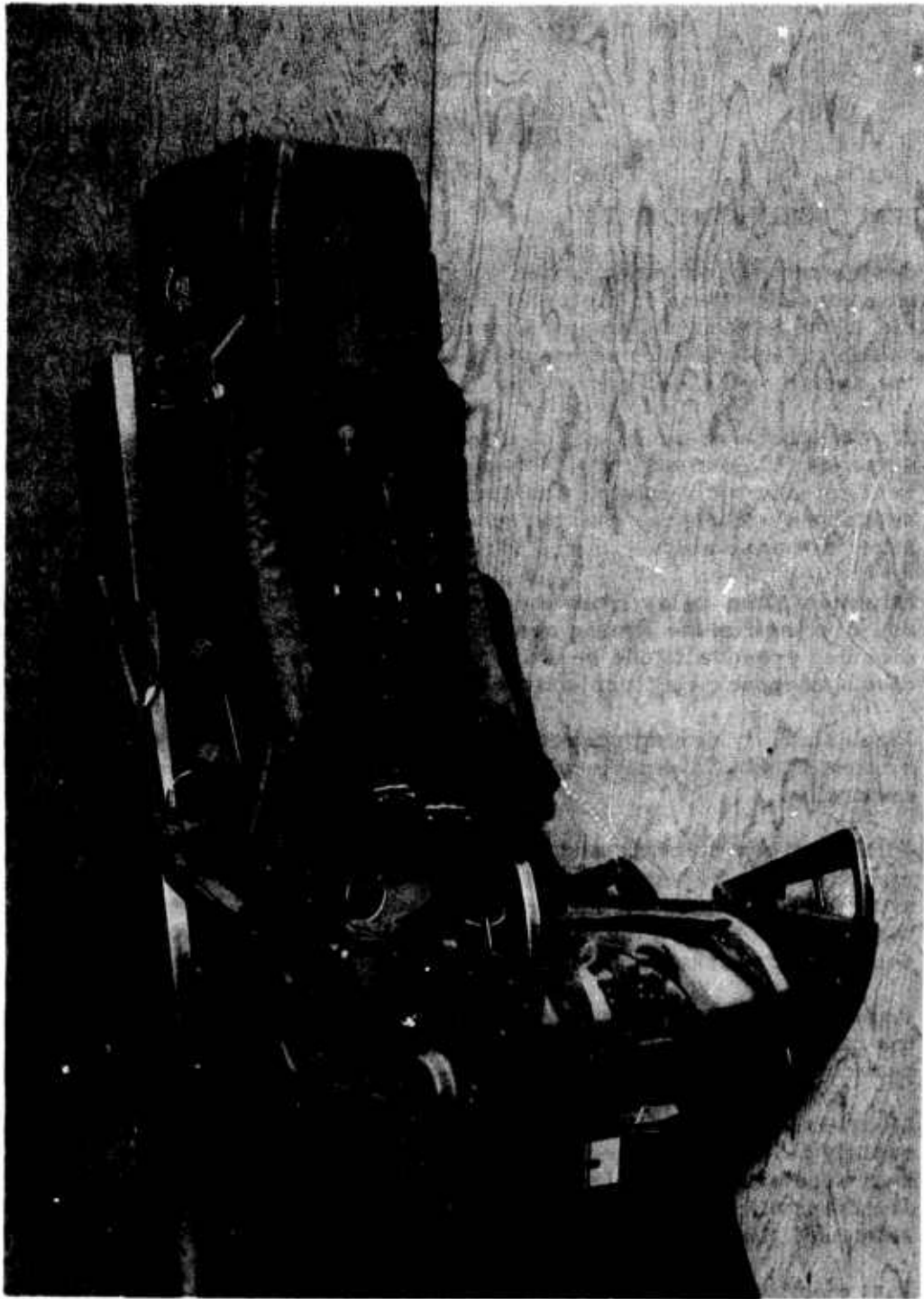


FIGURE 1. ADVANCED CONCEPT EJECTION SEAT, THREE-QUARTER VIEW

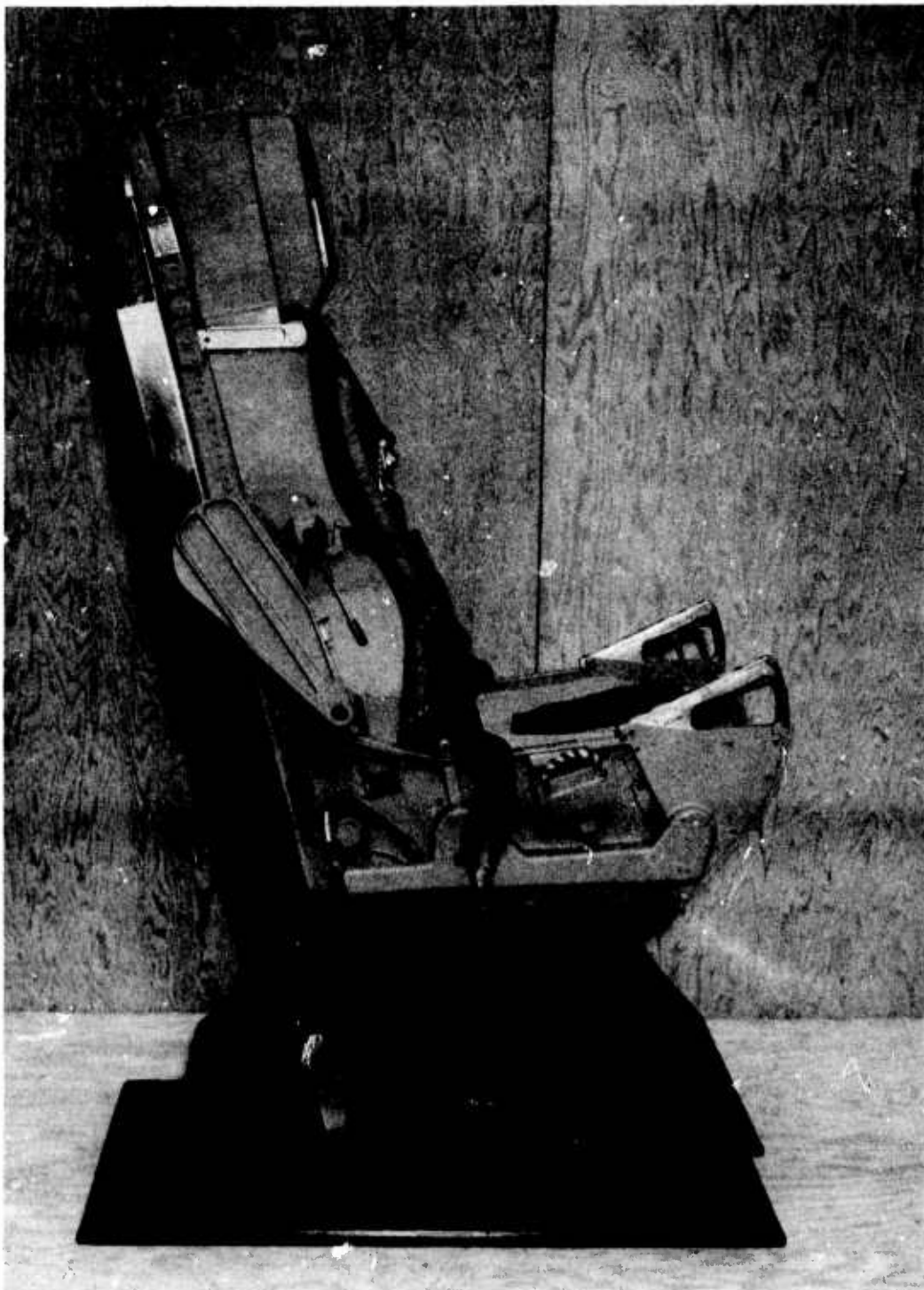


FIGURE 2. ADVANCED CONCEPT EJECTION SEAT, RIGHT SIDE

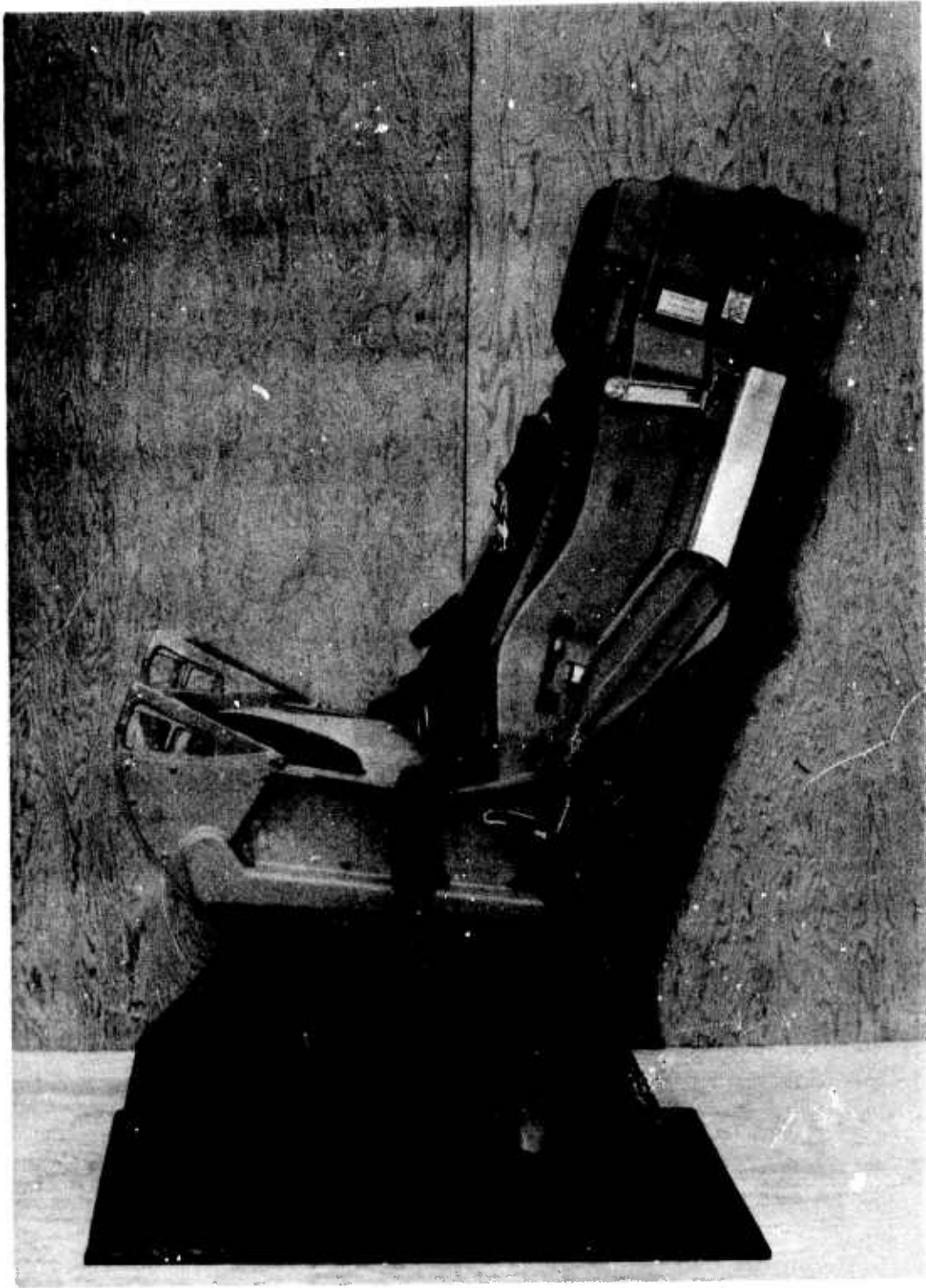


FIGURE 3. ADVANCED CONCEPT EJECTION SEAT, LEFT SIDE

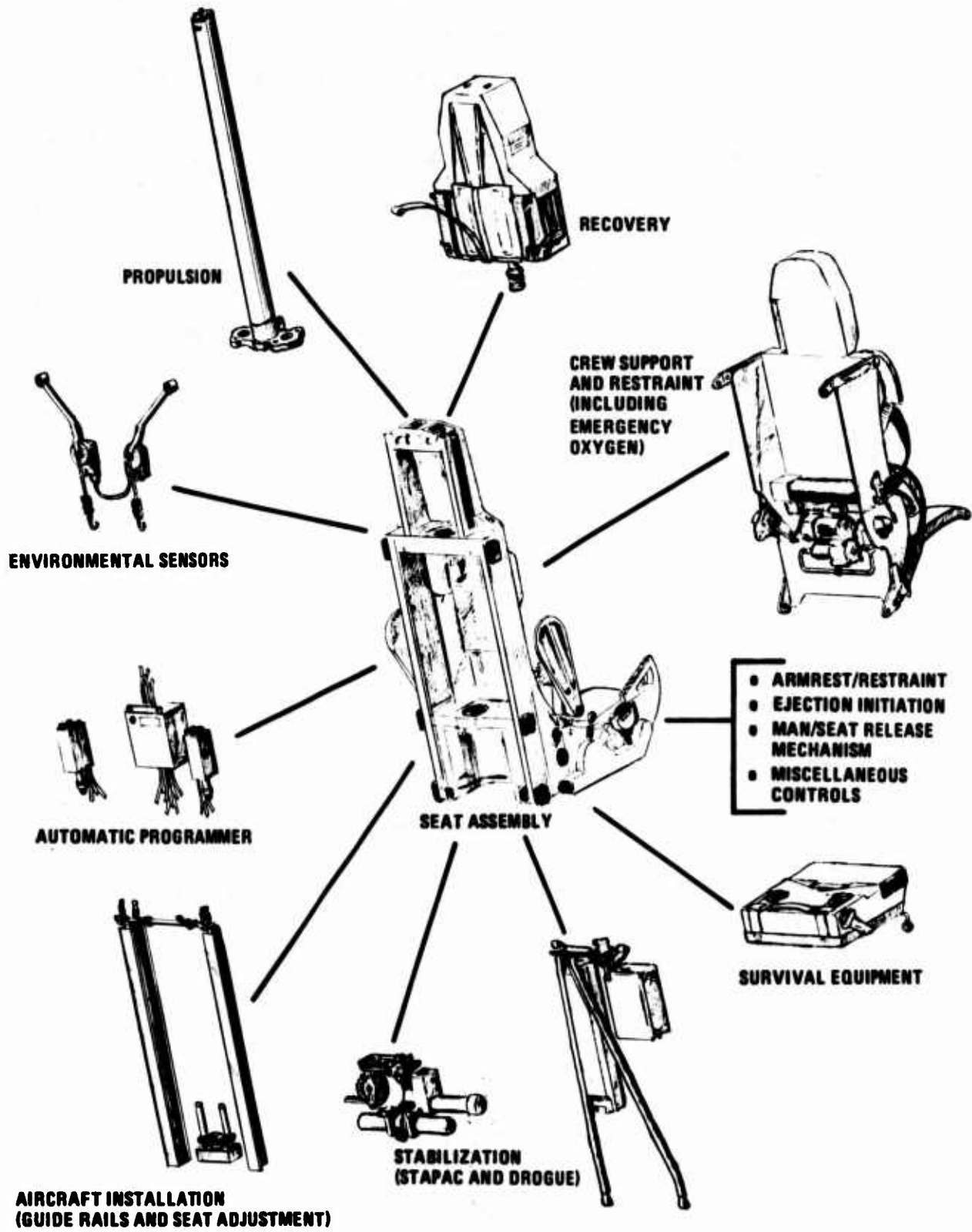


FIGURE 4. ACES SUBSYSTEMS

TABLE I
ACES CARTRIDGES AND CARTRIDGE ACTIVATED DEVICES

Component	Manufacturer	Manufacturer's Part Number
Actuator, Gyro Spin-Up	Douglas Aircraft Co.	J114099-1
Gas Generator, Gyro Spin-Up	Universal Propulsion	1004-3
Mortar, Parachute	Douglas Aircraft Co.	D114066-501
Cartridge, Mortar	Universal Propulsion	1005-2
Rocket Catapult	Frankford Arsenal	XM-39
Rocket Motor, Vernier	Talley Industries	50436-1
Severance System, Drogue	McCormick-Selph	{811363-1 & -2 811318-1
Inertia Reel, Power Haulback	Pacific Scientific	0103178-17
Gas Generator, Inertia Reel	Pacific Scientific	0113250-1
Thruster, Harness Release	Universal Propulsion	1002-1
Drogue Gun	Universal Propulsion	1003-2
Programmer, Automatic	Dorsett Electronics	93A559-2 93A479-3 & -4
Cutter, Reefing Line	Atlas Chemical	1SE172-1.3
Thruster, Arm Restraint	Universal Propulsion	1006-2

SYSTEM OPERATION

The ACES provides a completely automatic ejection sequence that is initiated when the crewman pulls either or both of the firing control handles located on the seat bucket sides. Backup systems are incorporated to allow manual actuation of the man/seat release mechanism and to permit deployment of the recovery parachute in the event of a mortar failure. The system schematic, Figure 5, illustrates the functional relationship of the ACES subsystems and components.

Ejection Automatic Sequence

The automatic ejection sequence is initiated by actuating either or both of the firing controls. This transmits motion to two pressure plates located on the guide rails which, in turn, mechanically activate an alternator contained in each of two Initiation Sequencer units, also mounted on the guide rails. Within 12 milliseconds (msec) each alternator generates sufficient electrical energy to initiate and/or power the following items:

1. 0.3-second electronic delay elements (one in each Initiation Sequencer unit).
2. Aircraft canopy remover.
3. Arm restraint thruster.
4. Power haul-back inertia reel.
5. Recovery sequencer power supply.
6. An additional Initiation Sequencer Unit containing 0.6-second electronic delay elements in a tandem ejection seat installation.

After the 0.3-second delay, the rocket catapult is fired and redundant 160-msec electronic delays are activated in the recovery sequencer. As the catapult propels the seat up the guide rails, the environmental sensor pitots are erected and the recovery sequencer interrogates the sensor transducers to establish the recovery mode. Selection of the recovery mode is dependent on the velocity and ambient pressure environment at the time the occupied seat emerges from the aircraft and penetrates the relative air. Three recovery modes are provided as follows:

Mode 1	Below 275 ± 25 KEAS at sea level
Mode 2	Above 275 ± 25 KEAS at sea level
Mode 3	Above $15,000 \pm 1000$ feet, or when an equivalent static pressure exists behind the seat

The Mode 1 - Mode 2 crossover velocity is mechanically compensated for altitude to assure that the recovery parachute is always in a safe operating regime. Because of base pressure effect, the static pressure behind the seat (at relatively high velocities) can decrease to a pressure equivalent to or less than that at 15,000 feet, even though the ambient altitude is below

15,000 feet. When this occurs, the seat, in effect, enters the Mode 3 region, which temporarily blocks initiation of the recovery parachute time delay. As the base pressure coefficient is essentially constant with altitude, the cross-over between Modes 2 and 3 is biased by both the speed and altitude. The mode envelopes are defined in Figure 6.

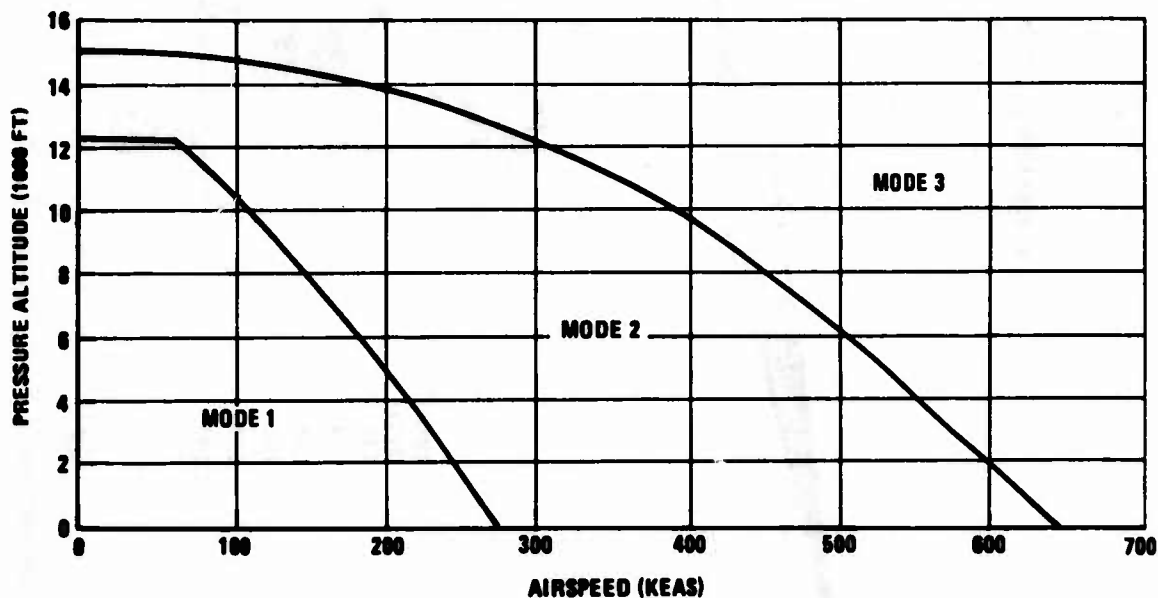
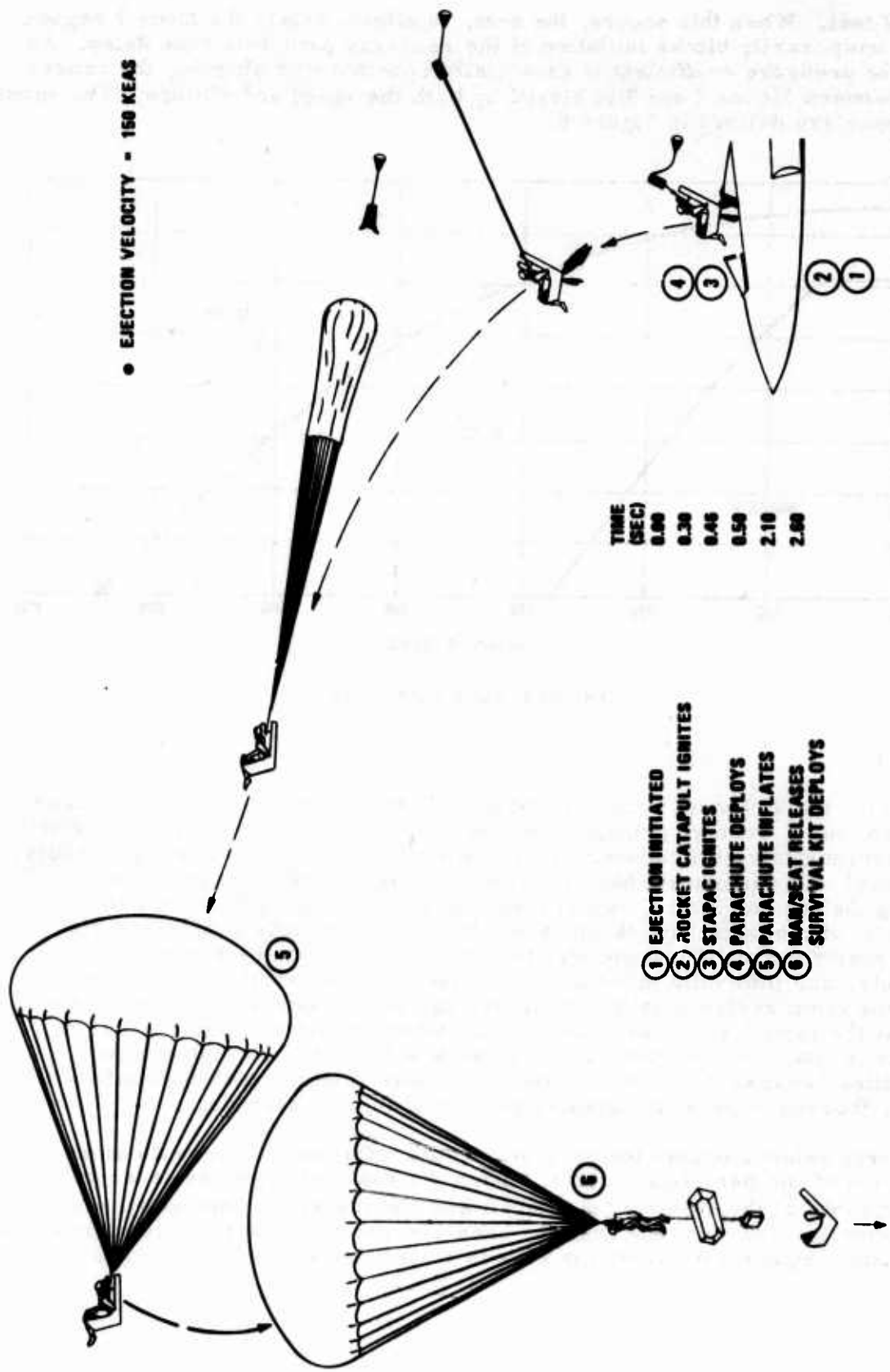


FIGURE 6. MODE ENVELOPES

Mode 1

Following the 160-msec delay, the STAPAC unit is activated, the gyro rotor spun up, the gyroscope uncaged, and the vernier rocket motor ignited. Forty milliseconds later the recovery subsystem mortar is fired and the parachute, contained in a deployment bag, is projected upward and away from the seat. During the mortar stroke, two 1.3-second reefing line cutters installed on the skirt of the parachute canopy are initiated by lanyards attached to the inner mortar tube. Subsequently, the parachute fills to the reefed condition, disreefs, and then fully inflates. The length of effective reefing time, i. e., the time from reefed inflation to disreefing, varies with the velocity of the seat at the time the mortar fires. Thus, when the aircraft velocity during escape is low, the effective reefing time is shorter than at high escape velocities because the parachute requires more time to reach the reefed-fill stage, thereby expending a greater portion of the 1.3 seconds.

Man/seat release occurs following parachute inflation, 2.1 seconds after initiation of the parachute mortar. When the seat and crewman separate, the contents of the survival kit (liferaft and rucksack) are deployed if the deployment selector on the seat has been pre-positioned to the automatic mode. The time-sequence of events for a Mode 1 ejection is illustrated in Figure 7.



TIME (SEC)
0.00
0.30
0.46
0.50
2.10
2.00

- ① EJECTION INITIATED
- ② ROCKET CATAPULT IGNITES
- ③ STAPAC IGNITES
- ④ PARACHUTE DEPLOYS
- ⑤ PARACHUTE INFLATES
- ⑥ MAIN/SEAT RELEASES SURVIVAL KIT DEPLOYS

FIGURE 7. MODE 1 OPERATION

Mode 2

Following the 160-msec delay, the STAPAC unit and drogue gun are initiated. The drogue extraction parachute, projected downstream by the drogue gun slug, inflates and strips off the main drogue sleeve, allowing the drogue to inflate, stabilize, and decelerate the occupied seat. After an 850-msec delay, the parachute mortar fires and the lower and upper drogue bridles are severed sequentially at 120 and 150 msec following parachute mortar initiation. The remainder of the recovery sequence is identical to Mode 1. The time sequence of events for a Mode 2 ejection is shown in Figure 8.

Mode 3

Following the 160 msec delay, the STAPAC and drogue parachute subsystems are activated, as in Mode 2. The remaining recovery events are interrupted until the occupied seat decelerates and/or descends to the Mode 2 - Mode 3 boundary, at which time the recovery sequencer restarts the recovery sequence. Figure 9 shows the time sequence of events for a Mode 3 ejection.

To illustrate base pressure effect, Figure 9, a simulated 600-KEAS ejection is superimposed on the mode envelope plot. In this example, the ejection occurs at 10,000-foot pressure altitude, well inside the Mode 3 region. The drogue-stabilized seat decelerates to the Mode 2 - Mode 3 cross-over point in 350-msec (from ejection initiation), at which time the recovery parachute 850-msec delay is initiated. The stabilized seat continues to decelerate and, at end of the 850-msec delay, the recovery subsystem mortar fires (seat velocity = 275 KEAS). The events following mortar initiation are the same as in Mode 2.

MANUAL BACKUPS

Man/Seat Release

In the event the man/seat release mechanism is not actuated automatically (after parachute deployment and inflation) it may be operated manually. This is accomplished by pulling a ring-shaped handle located on the right-hand side of the seat bucket. As the seat drops away, the life raft and rucksack are deployed if the deployment selector has been pre-positioned to the automatic mode.

Recovery Subsystem

If a failure of the recovery parachute initiation system occurs, the parachute mortar is disconnected from the seat structure when the man/seat release mechanism operates. When physical separation of the crewman and seat occurs, the pilot chute is extracted from a pouch installed on the seat, and deploys the recovery parachute. At line stretch, the reefing line cutters are armed by lanyards attached to the canopy suspension lines. After a 1.3-second delay, the parachute disreefs and fully inflates. The backup recovery sequence is shown in Figure 10.

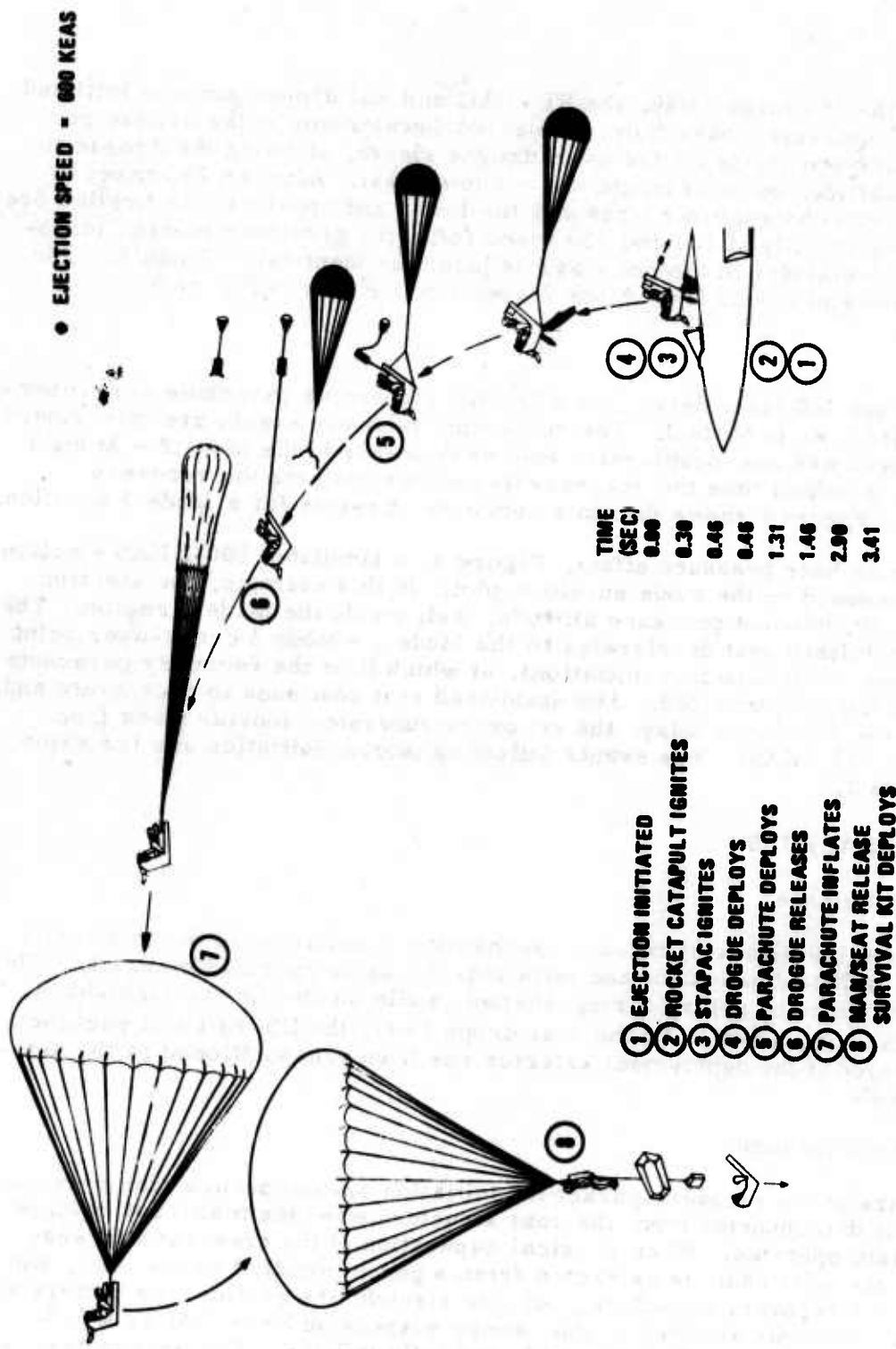


FIGURE 8. MODE 2 OPERATION

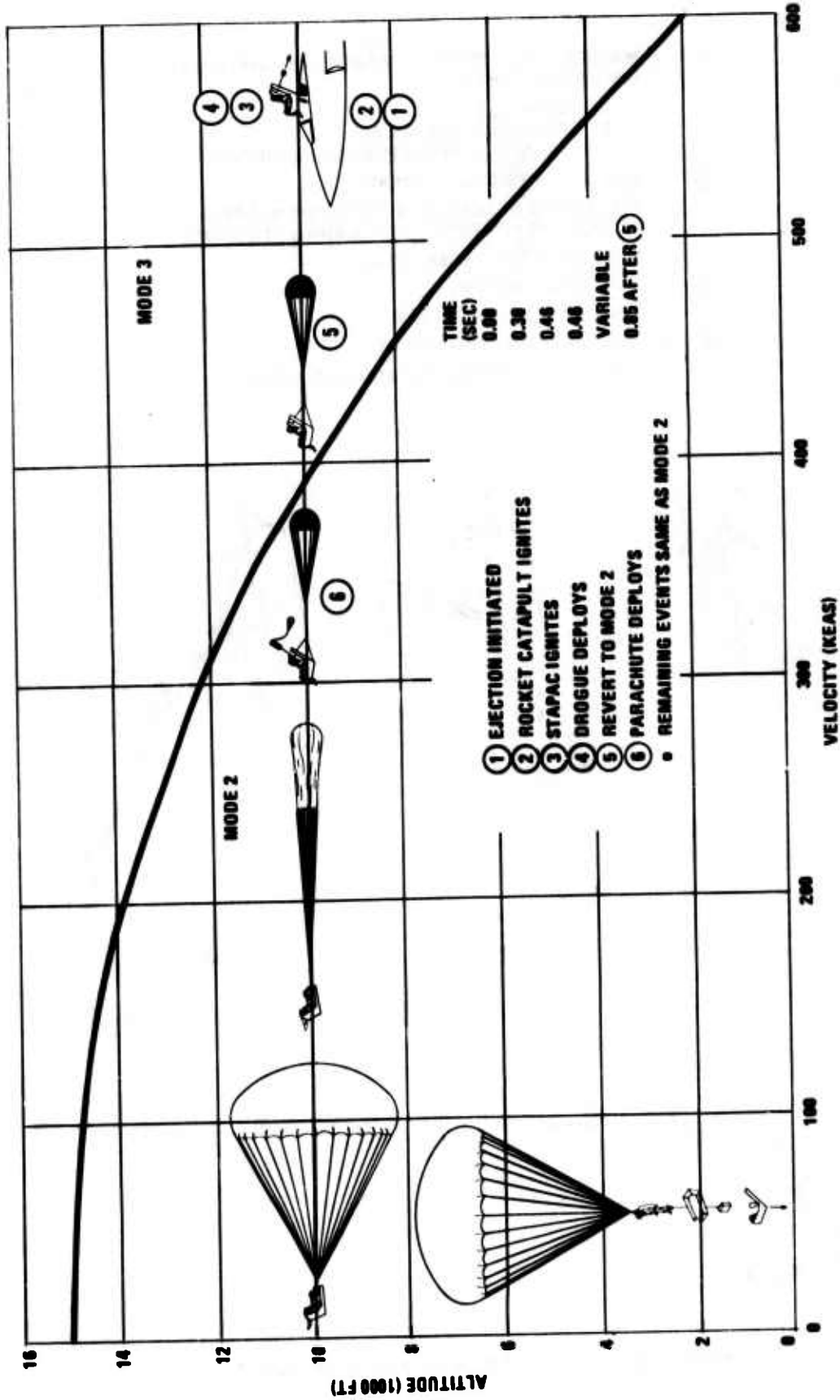


FIGURE 9. MODE 3 OPERATION

- ① ● MAN/SEAT RELEASE SYSTEM ACTUATES AUTOMATICALLY DISCONNECTING THE:
 - A. BACKREST
 - B. PARACHUTE MORTAR, AND
 - C. PARACHUTE RISERS FROM SEAT STRUCTURE
- ② ● MAN/SEAT PHYSICALLY SEPARATE
- DEPLOYMENT OF SURVIVAL KIT CONTENTS INITIATED (IF SELECTOR IS PRE-POSITIONED IN AUTOMATIC MODE)
- PILOT CHUTE DEPLOYMENT INITIATED
- ③ ● PILOT CHUTE DEPLOYS
- SURVIVAL KIT FLAPS RELEASE
- ④ ● RECOVERY PARACHUTE DEPLOYS
- REEFING LINE CUTTERS TIME DELAYS INITIATED

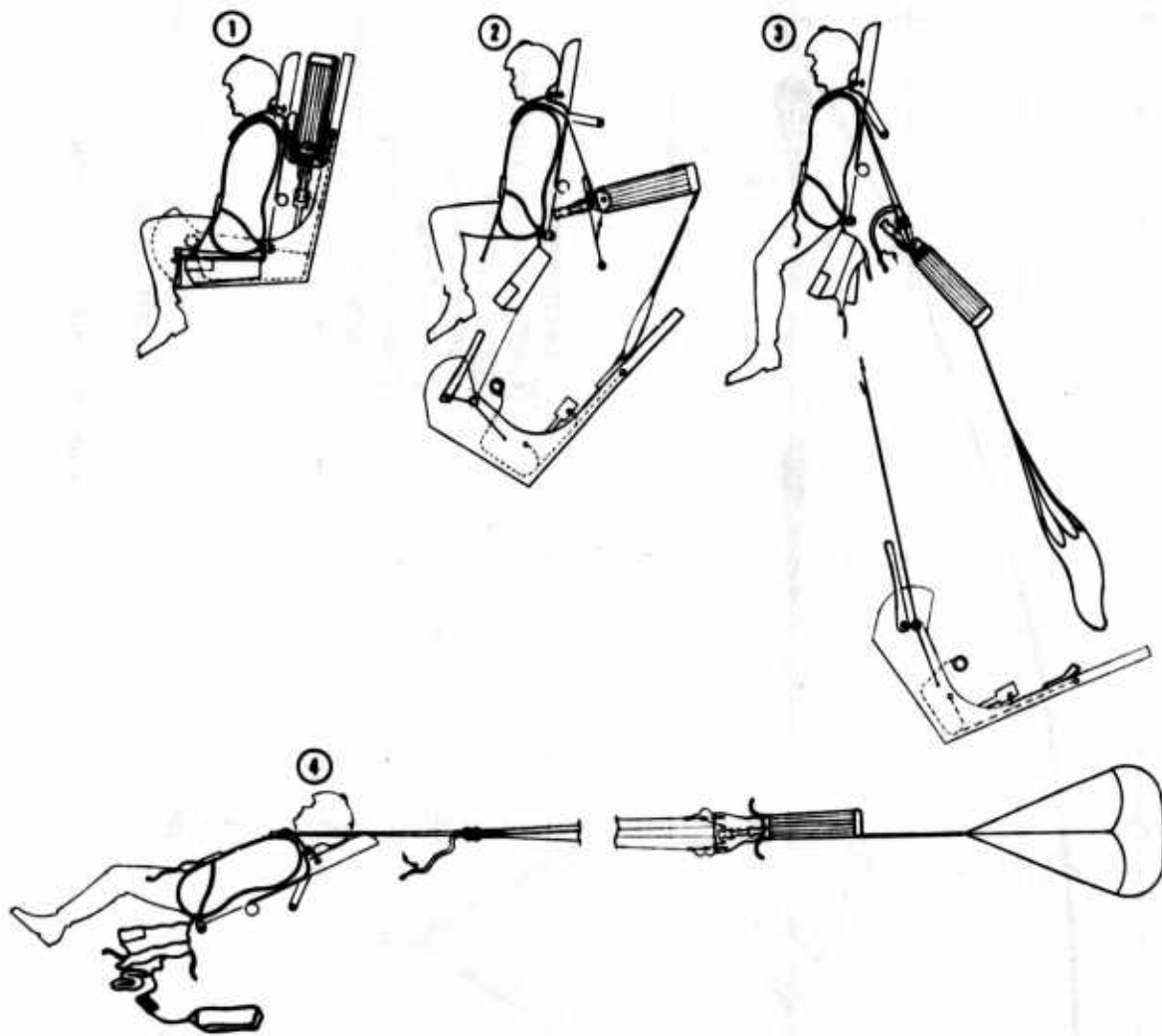


FIGURE 10. PARACHUTE MANUAL BACKUP SEQUENCE

SECTION III

SEAT ASSEMBLY

The seat assembly includes the basic seat structure and those components and subsystems that are not readily removable from the assembly. The seat assembly together with the propellant-actuated devices, recovery subsystem, drogue, backrest, restraint harness, survival kit, and guide rails, comprise the Escape System Assembly, Figure 11.

STRUCTURE

The seat structure assembly, Figure 12, consists of a back and a bucket. The back is fabricated from two aluminum channel sections spaced apart by three machined beams which are the main load-carrying members of the structure. In addition, the beams provide support for the six slide blocks. Holes are drilled through two beams to accommodate installation of the rocket catapult; attachment of the rocket catapult is accomplished through a fourth beam that ties the top of the structure together. The width of the back structure is reduced from 14.75 to 9.5 inches above the upper slide blocks to provide improved rearward vision for the crewman, Reference 4. The sides of the reduced-width portion of the back structure are slotted to allow installation and operation of the environmental sensors. The forward surface of the back structure is covered with an 0.032-inch aluminum skin.

The seat bucket comprises two chemically milled, sheet aluminum sides capped with a T-shaped extrusion. The sides are attached to the back channel sections, the sheet metal bucket bottom, and to the front beam. A rigid thermo-formable plastic fairing is installed on each seat bucket side to cover the firing control handle mechanism and linkage. The bottom of the seat bucket is a 0.040-inch aluminum panel incorporating three hat-section stiffeners.

LOADS

The seat assembly was designed to withstand the loads specified in MIL-S-9479A. In some cases the design concepts embodied in ACES dictated that certain loads be applied differently from the method specified in MIL-S-9479A. For example, this specification requires that down loads be distributed uniformly over the seat bucket bottom. In the ACES system, a rigid, removable seat pan covers the survival equipment compartment and is supported by flanges attached to the back of the bucket, each side, and to the front beam. Ejection and down crash loads are carried from the seat pan into the primary bucket structure. Therefore, the only load distributed over the seat bucket, neglecting seat pan deflection, is the weight of the survival equipment multiplied by the load factor.

Paragraph 3.6.2.5 of MIL-S-9479A requires that an ultimate load of 500 pounds be applied to the headrest on a line of action parallel to the seat bottom and evenly distributed over an area 2 inches square at the center of the headrest. The ACES headrest was designed for the 500-pound load but applied over an area equivalent to the pilot's helmeted head.

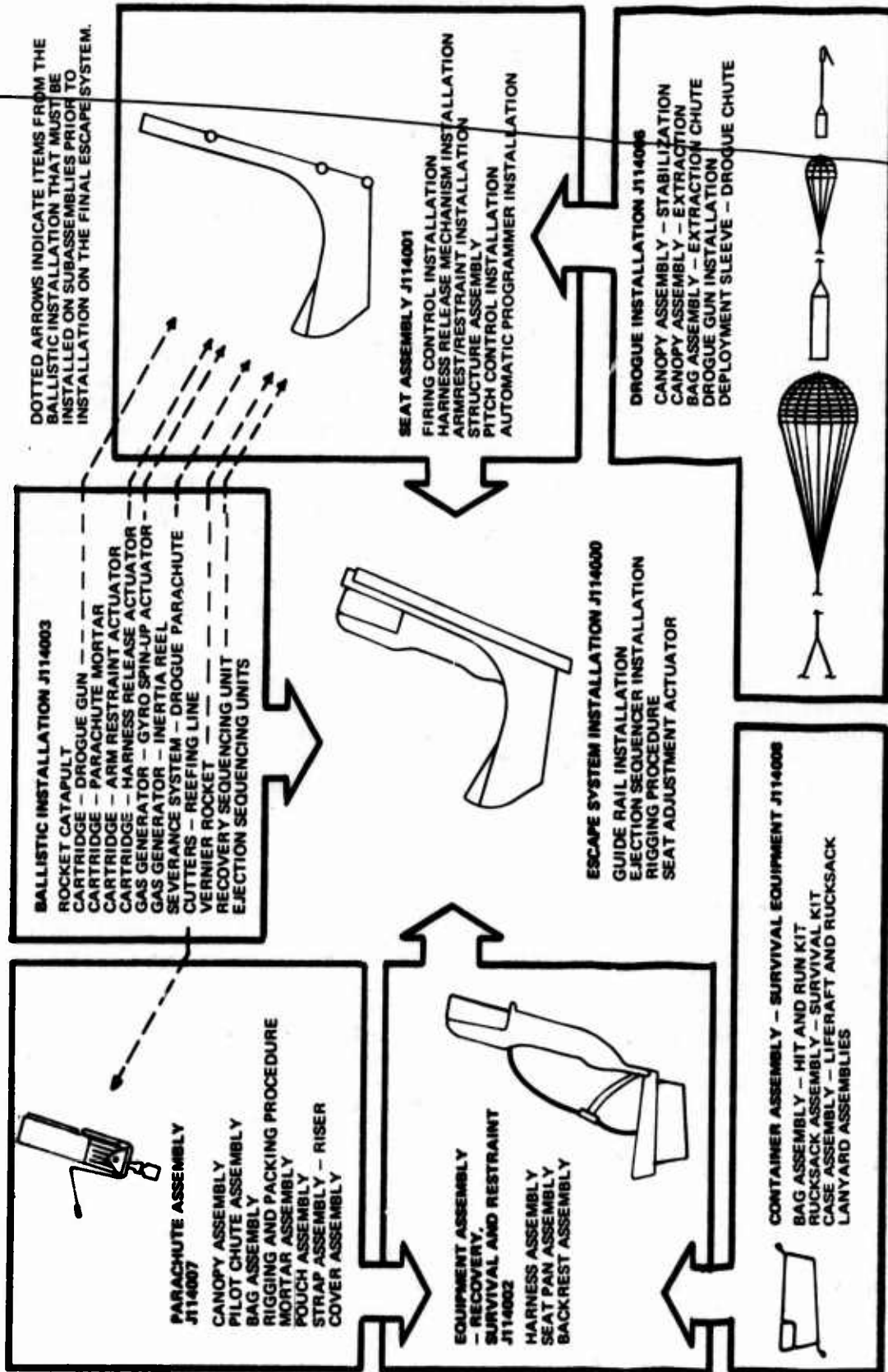


FIGURE 11. ADVANCED CONCEPT EJECTION SEAT MAJOR ASSEMBLIES

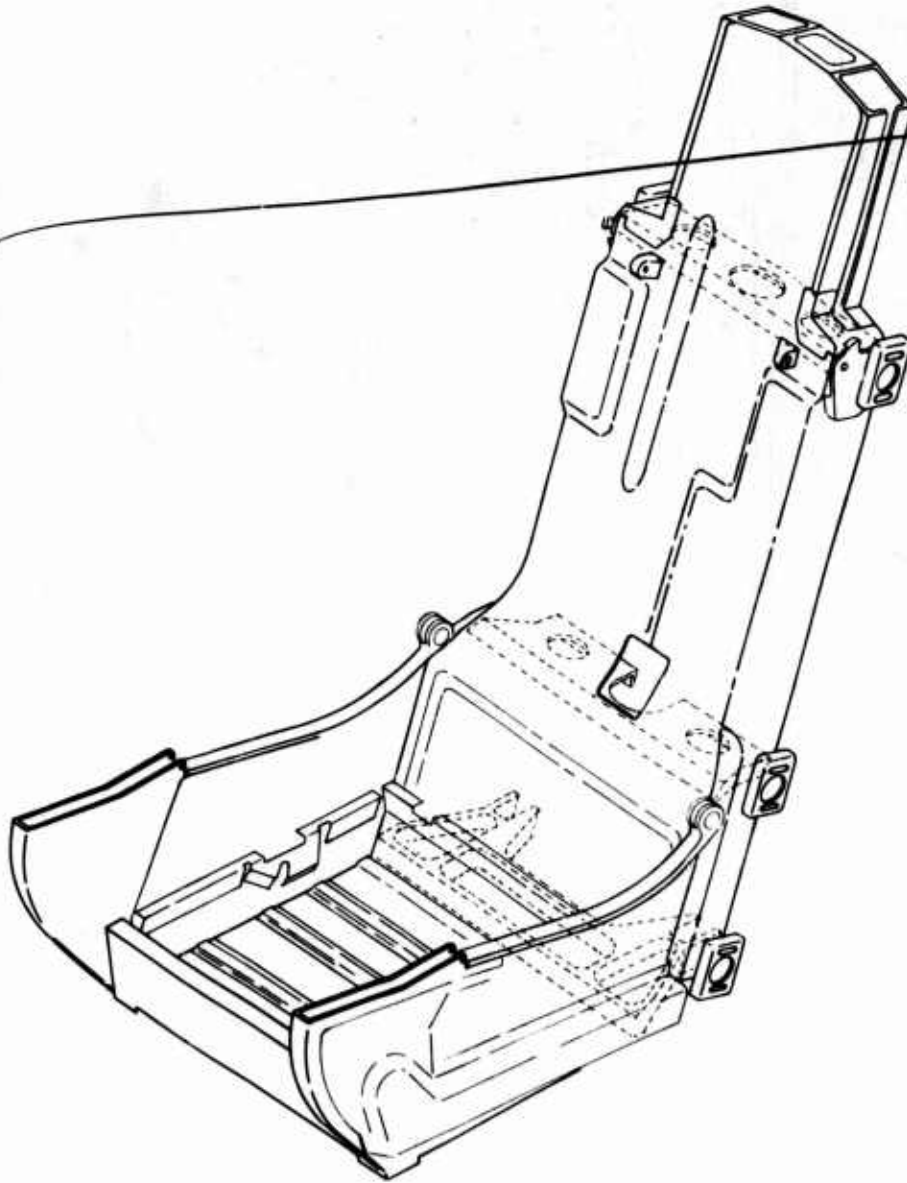


FIGURE 12. ACES SEAT STRUCTURE

Figures 13, 14, and 15 define the manner in which loads were applied to the ACES system for structural design purposes. A detailed load definition and stress analysis of the seat system is provided in Reference 7.

LOAD	PARAGRAPH OF MIL-S-9479A	DESCRIPTION
A	3.6.2.1	ROCKET CATAPULT
B	3.6.2.2	FRONT EDGE
C	3.6.2.3	ARMREST
D	3.6.2.4	EJECTION CONTROL
E	3.6.2.5	HEADREST

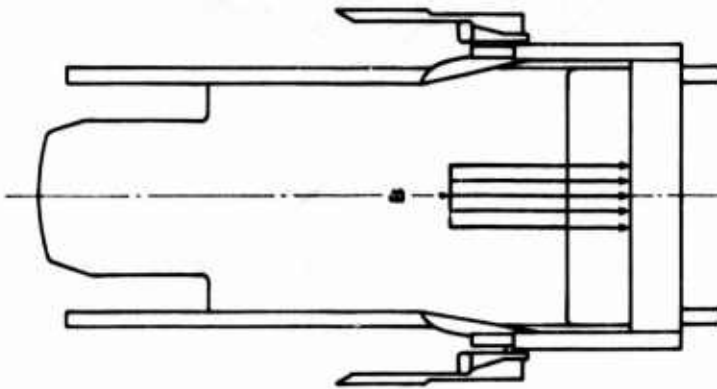
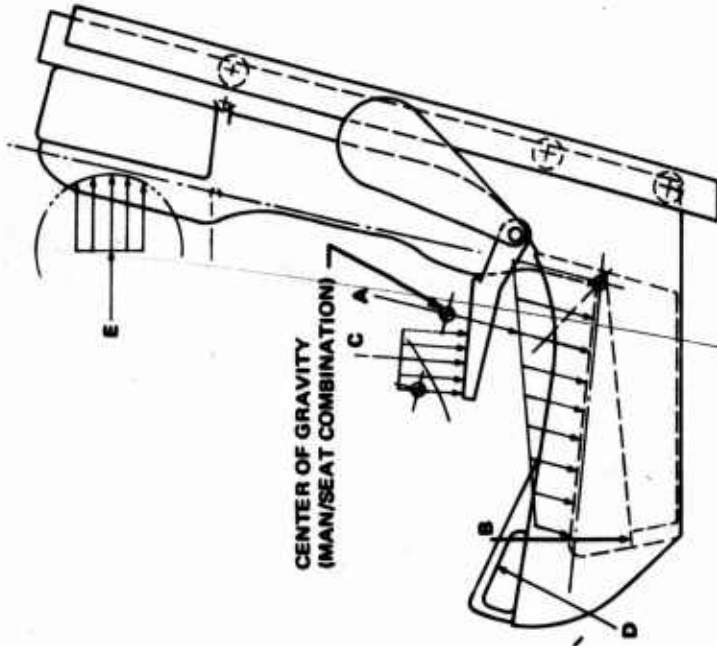
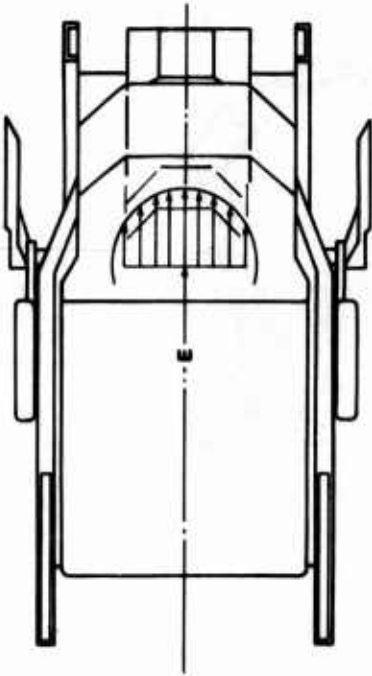


FIGURE 13. SEAT LOAD DATA

LOAD	PARAGRAPH OF MIL-S-9479A	DESCRIPTION
F	3.6.2.6.1.1	CRASH-RESTRAINT SUBSYSTEM
G	3.6.2.6.1.2	CRASH-SEAT INSTALLATION
H(1)	3.6.2.6.2	SIDE CRASH-RESTRAINT SUBSYSTEM
H(2)	3.6.2.6.2	SIDE CRASH-SEAT INSTALLATION
I	3.6.2.6.3a	VERTICAL CRASH-RESTRAINT SUBSYSTEM
J	3.6.2.6.3b	VERTICAL CRASH-SEAT BUCKET
K	3.6.2.7	EJECTION AIRLOAD

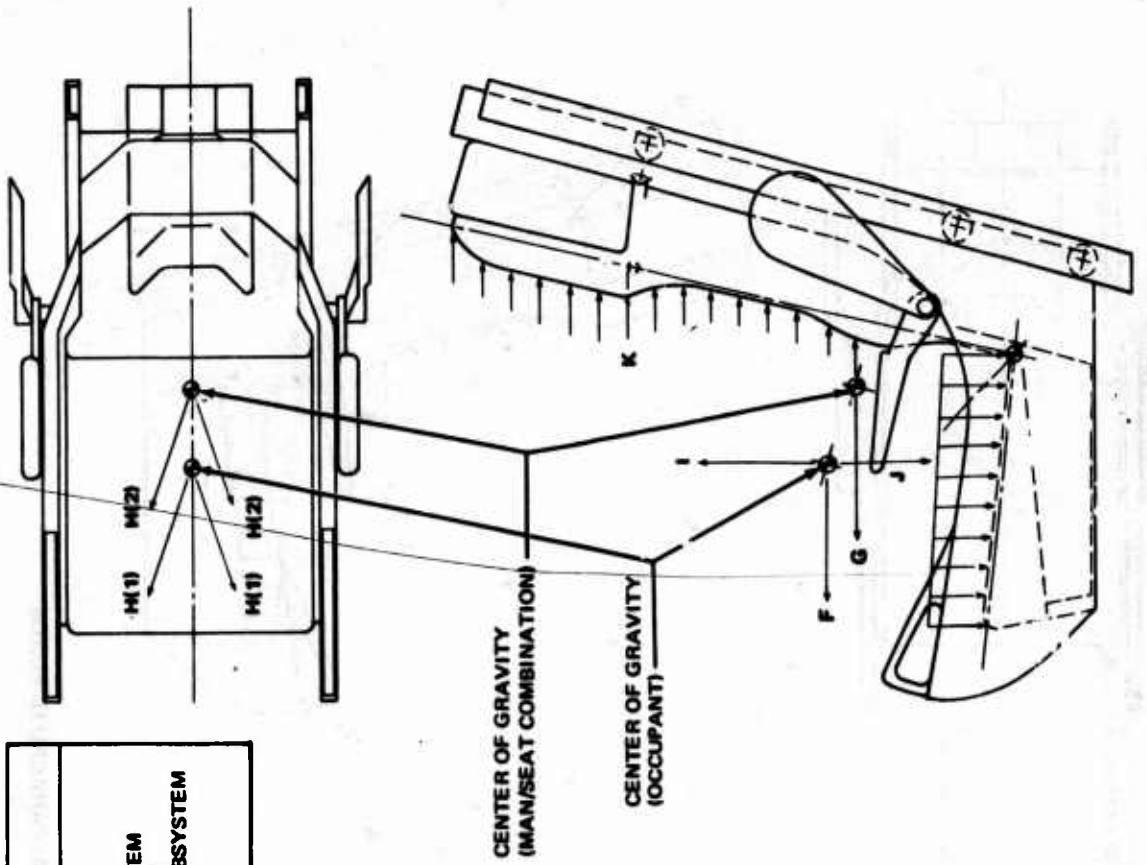


FIGURE 14. CRASH AND AERODYNAMIC SEAT LOADS

LOAD	PARAGRAPH OF MIL-S-9479A	DESCRIPTION
L	3.6.2.6.3.c	VERTICAL CRASH, SEAT INSTALLATION
M	3.6.2.6.4	BACK CRASH
N	NOT SPECIFIED	PARACHUTE LOAD
P	NOT SPECIFIED	PARACHUTE LOAD YAW CONDITION

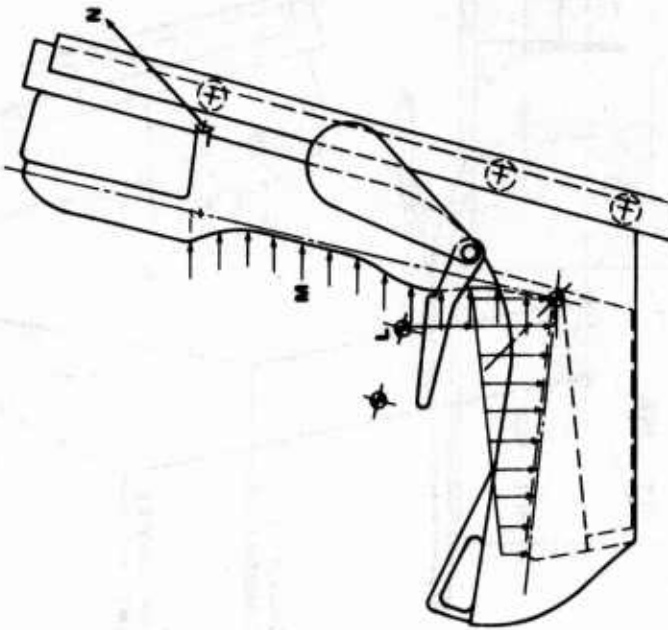
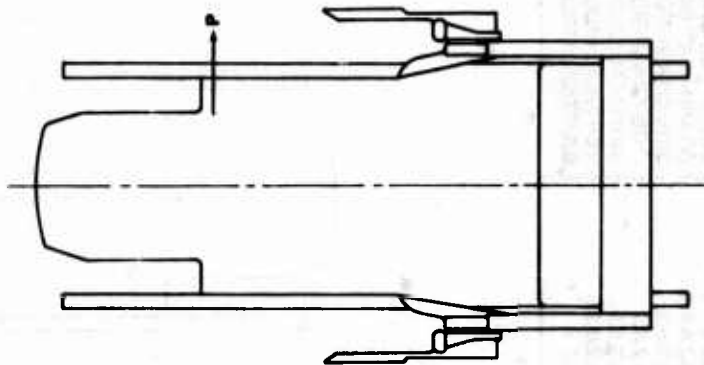
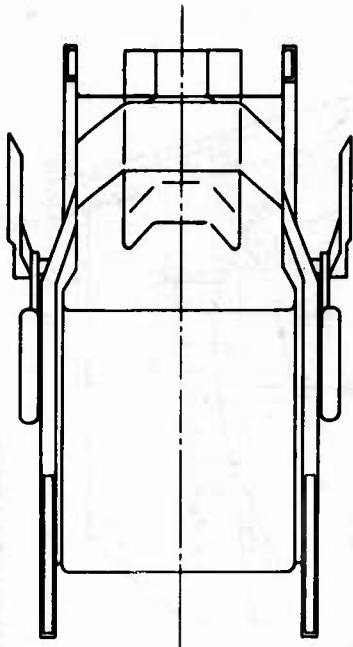


FIGURE 15. CRASH AND PARACHUTE LOADS

CONTROLS

The seat assembly incorporates the following controls:

Control	Function	Location
Ejection (2)	Initiates Automatic Ejection Sequence	Seat (R and LH Sides)
Man/Seat Release	Manually Releases Crewman and Seat if Automatic System Fails	Seat (RH Side)
Seat Adjustment	Adjusts Vertical Seat Position in Cockpit	Seat (RH Side)
Survival Kit Deployment	Selects Automatic or Manual Deployment Mode	Seat (RH Side)
Backrest Release	Jettisons Backrest after Man/Seat Separation (Pilot's Option)	Backrest (LH Side)
Inertia Reel	Locks or Unlocks Inertia Reel Strap	Backrest (LH Side)
Armrest (2)	Raises or Lowers Armrests	Seat (R and LH Sides)
Emergency Oxygen	Activates Emergency O ₂ if Automatic System Fails	Backrest (RH Side)
Seat Pan Release	Disconnects Seat Pan from Seat for Access to Survival Kit	Seat Pan (Front Edge)

The location of the above-listed controls is illustrated in Figure 16.

SEAT-MOUNTED MECHANISM

The mechanism for the man/seat release system and arm restraints is incorporated in the seat structure.

The man/seat release system, Figure 17, consists of two upper and two lower release pins, each attached to separate bellcranks. The upper and lower bellcranks on each side of the seat are connected by cables and the lower cranks by a tension rod. The manual release control handle is attached to the lower left-hand bellcrank via a cable, and the parachute mortar disconnect is connected to the lower right-hand bellcrank. The mechanism is actuated automatically by an electrically initiated thruster that rotates the lower left-hand bellcrank. Manual actuation is accomplished by pulling the control located on the right-hand seat side. Regardless of the

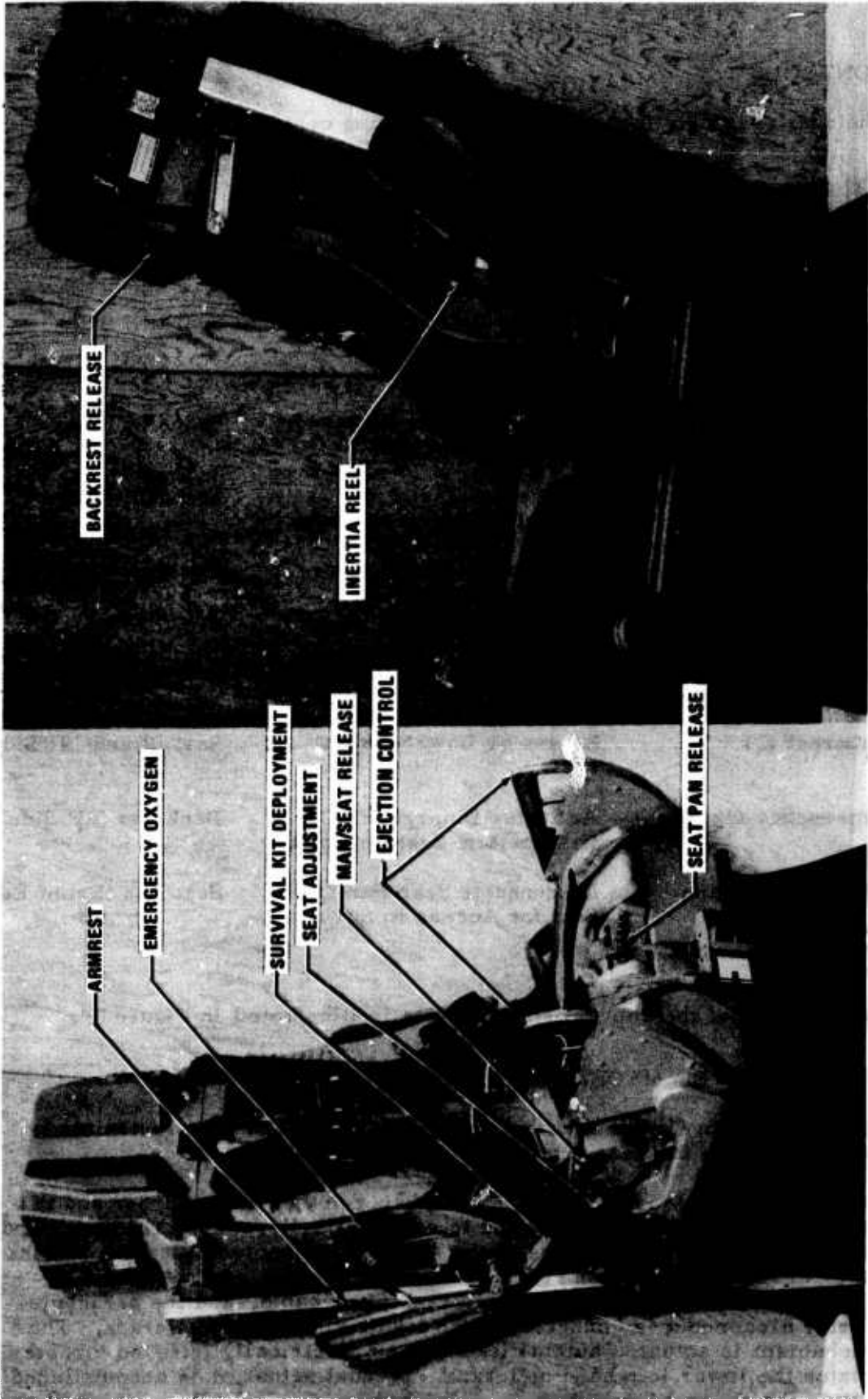


FIGURE 16. SEAT-MOUNTED CONTROLS

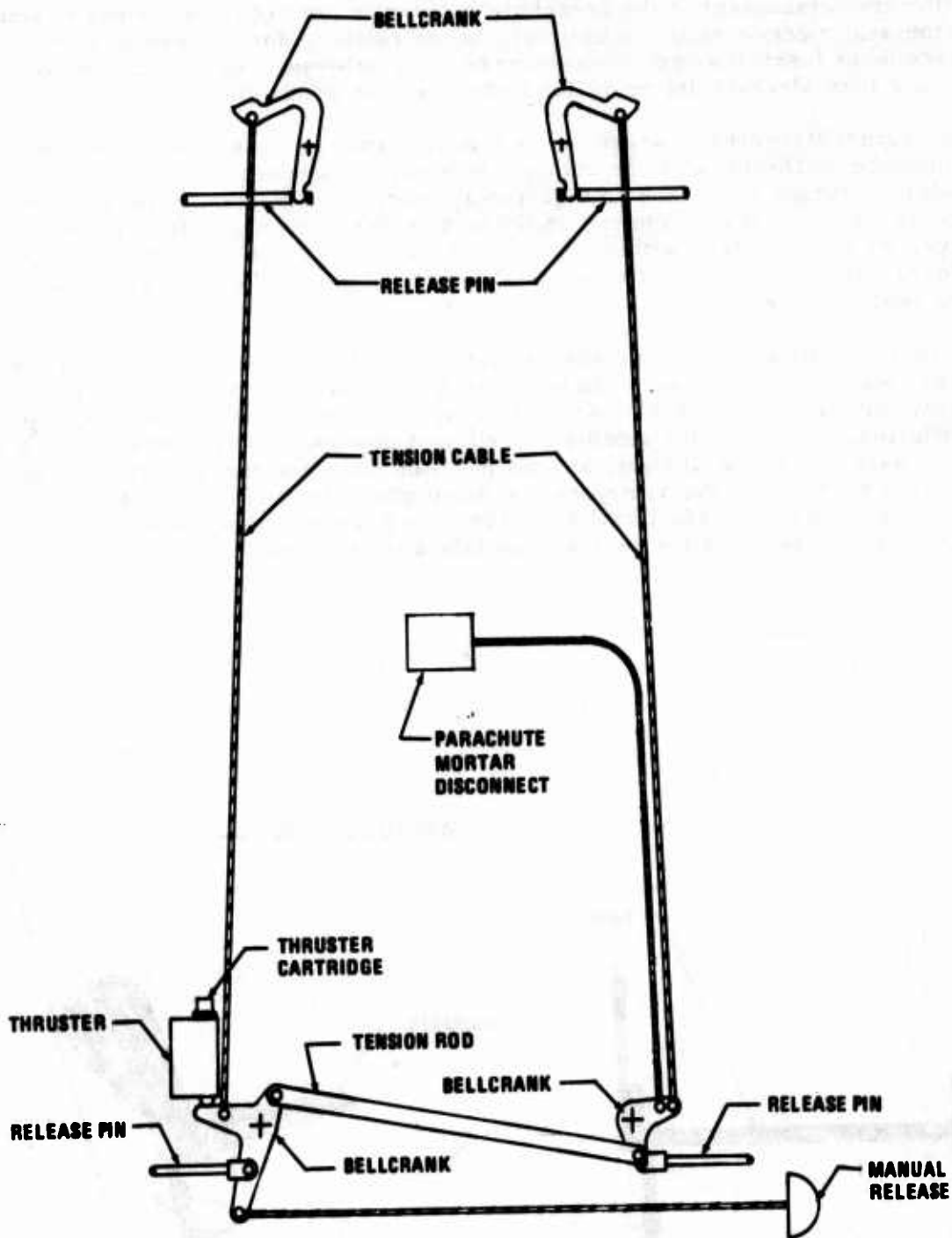


FIGURE 17. MAN/SEAT RELEASE SYSTEM

operational mode, the mortar is always disconnected from seat structure. Although detachment of the parachute mortar is not required for the normal automatic ejection mode, a simpler, more reliable design results if the disconnect functions each time the man/seat release system is actuated, rather than blocking its operation under certain conditions.

The armrest/restraint assembly is incorporated in the seat as shown in Figure 18. The installation comprises a pair of armrests and restraint paddles, torque tube, and an electrically initiated thruster. The armrests and restraint paddles, located on the seat sides, are connected by the torque tube, which is housed within the seat structure forward of the middle slide block. The thruster is attached to the torque tube on the left-hand side of the seat.

Normally, the armrest/restraint assemblies are stowed upright along the seat sides. The armrests can be rotated downward individually but the restraint paddles remain stowed. During ejection, prior to rocket catapult initiation, the restraint paddles are rotated downward by the thruster. If the armrests are in the upright, stowed position when the thruster fires, they remain stowed. If the armrests are down when the thruster fires, they rotate downward an additional 45 degrees to prevent entrapment of the crewman's elbow between the restraint paddle and armrest.

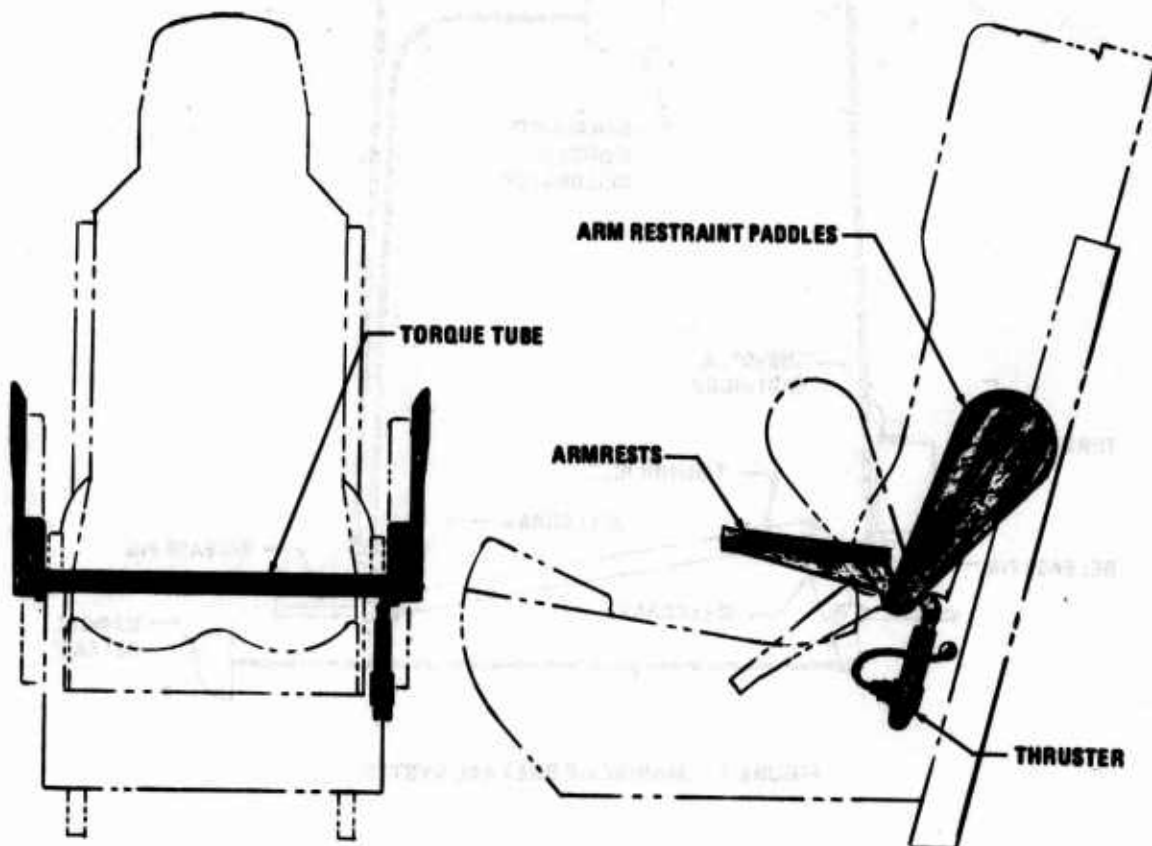


FIGURE 18. ARMREST/RESTRAINT SYSTEM

SECTION IV

INITIATION SUBSYSTEM

The ejection initiation subsystem provides a completely redundant system for firing the rocket catapult, in accordance with the requirements of MIL-S-9479A. This subsystem includes the ejection firing controls, pressure plate assemblies, initiation sequencers, and associated linkage, Figure 19.

Ejection initiation is accomplished by pulling one or both of the firing control handles. A continuous pull first unlocks the interconnected handles and then rotates them up and aft where they lock in place. The handle lock is designed to preclude accidental control actuation — a pull on the forward edge of the handle will not dislodge it from its stowed position. When the ejection control handles are raised to the fired position, they augment the leg restraint provided by the extended seat sides.

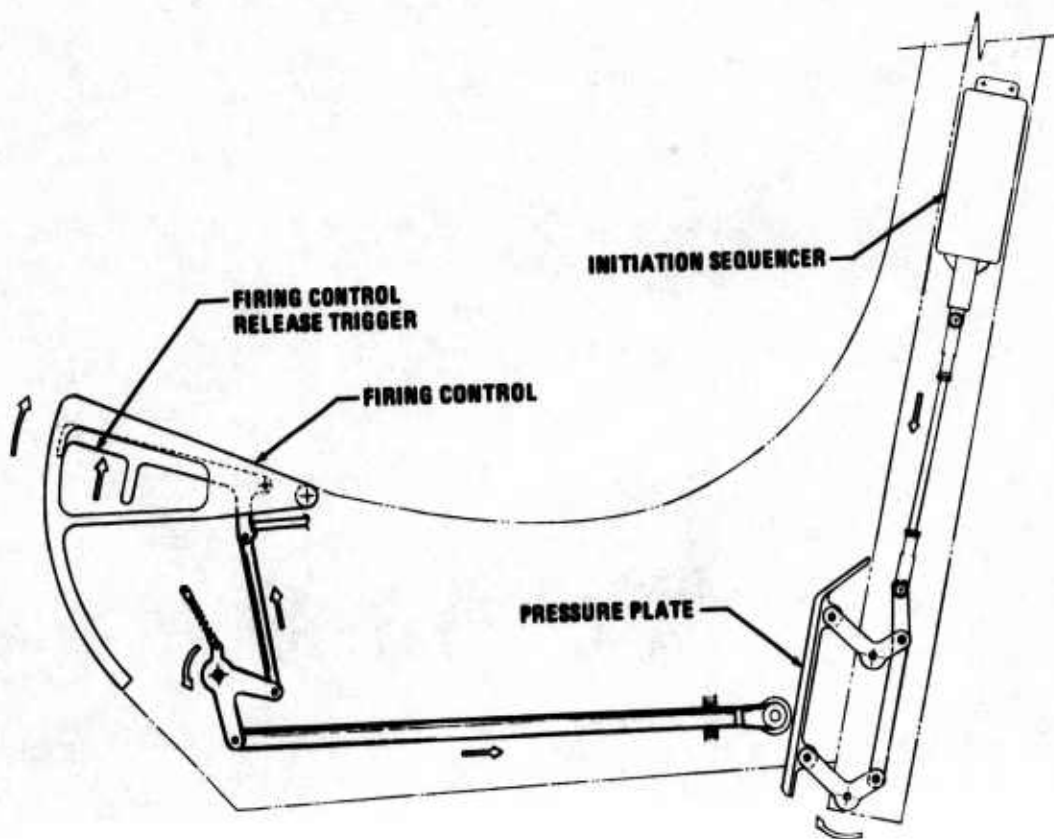


FIGURE 19. INITIATION SUBSYSTEM

Pushrods attached to the control handles extend aft along the seat sides protected by a plastic fairing. The ends of the pushrods engage pressure plates located on each side of the guide rails. The pressure plate contact surface is 6.62 inches long to assure positive engagement over the total range of vertical seat adjustment. Movement of the pressure plates actuates a sear-type mechanism in each initiation sequencer, Figure 20, via a tension rod. Actuation of the sear releases a precocked spring that spins up alternators in each unit to 12,000 rpm. Within 12 msec the alternators generate sufficient electrical power to initiate all pre-ejection functions, and fire the rocket catapult via a 0.3-second electronic delay. A functional block diagram of the initiation subsystem is shown in Figure 21.

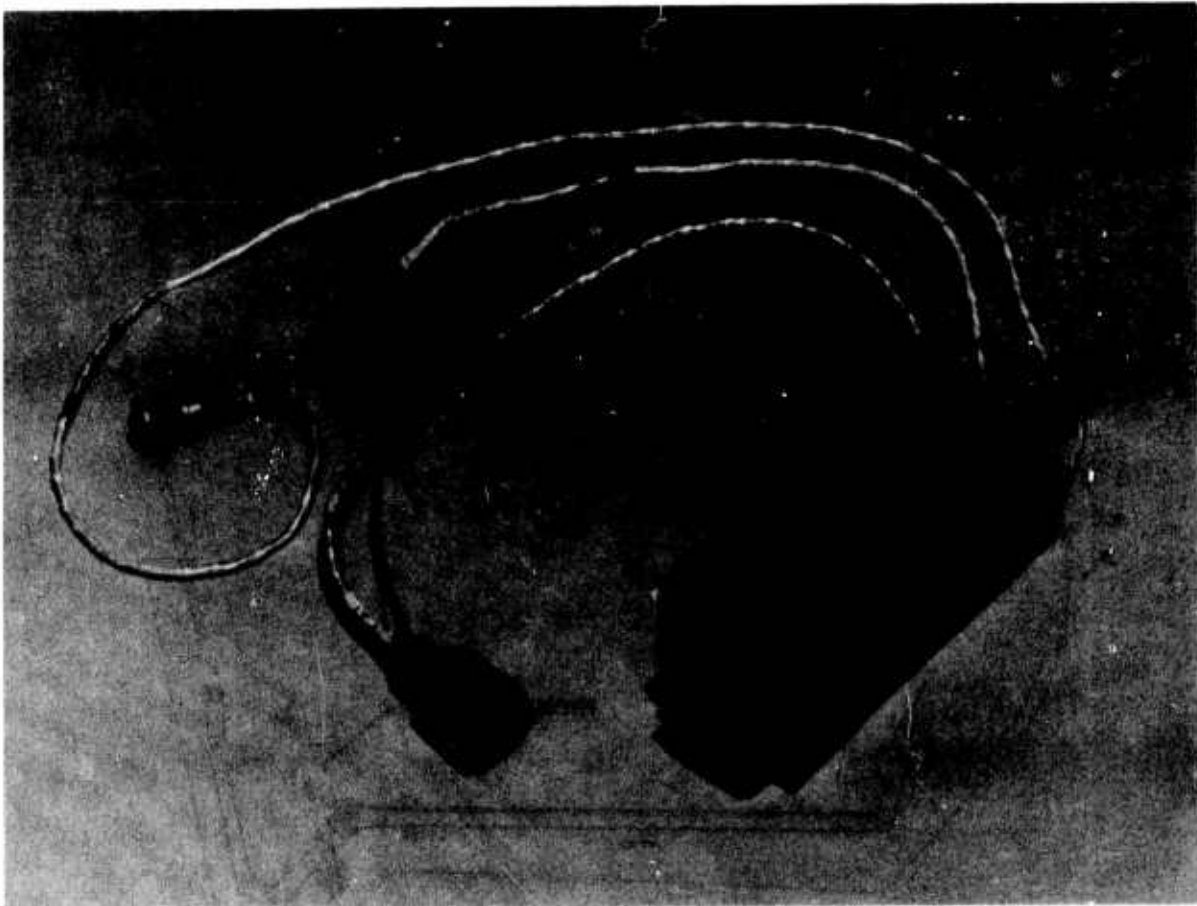


FIGURE 20. INITIATION SEQUENCER

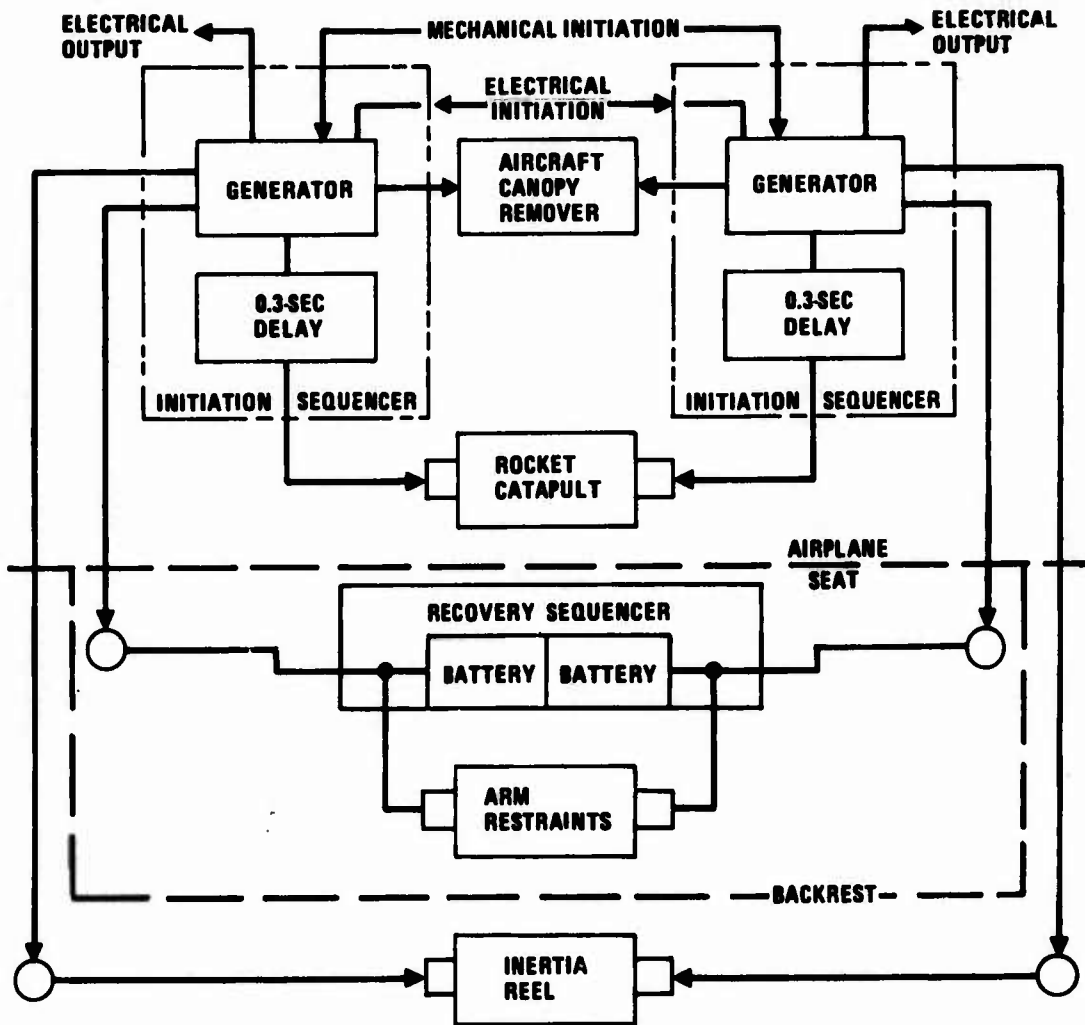


FIGURE 21. INITIATION SUBSYSTEM SCHEMATIC

SECTION V

PROPULSION SUBSYSTEM

The main propulsion source for ACES is the XM-39 rocket catapult furnished by Frankford Arsenal, Figure 22. The assembly consists of a catapult section and sustainer rocket motor, with the catapult (booster tube) inside the motor. Both the catapult cartridge and motor incorporate a polybutadiene-type propellant. Two electrically initiated squibs are installed on the booster tube base plate, which incorporates mounting provisions for the seat adjustment actuator. A threaded stud and two indexing pins are provided on the top face of the rocket motor for attachment of the assembly to the upper beam of the seat structure.

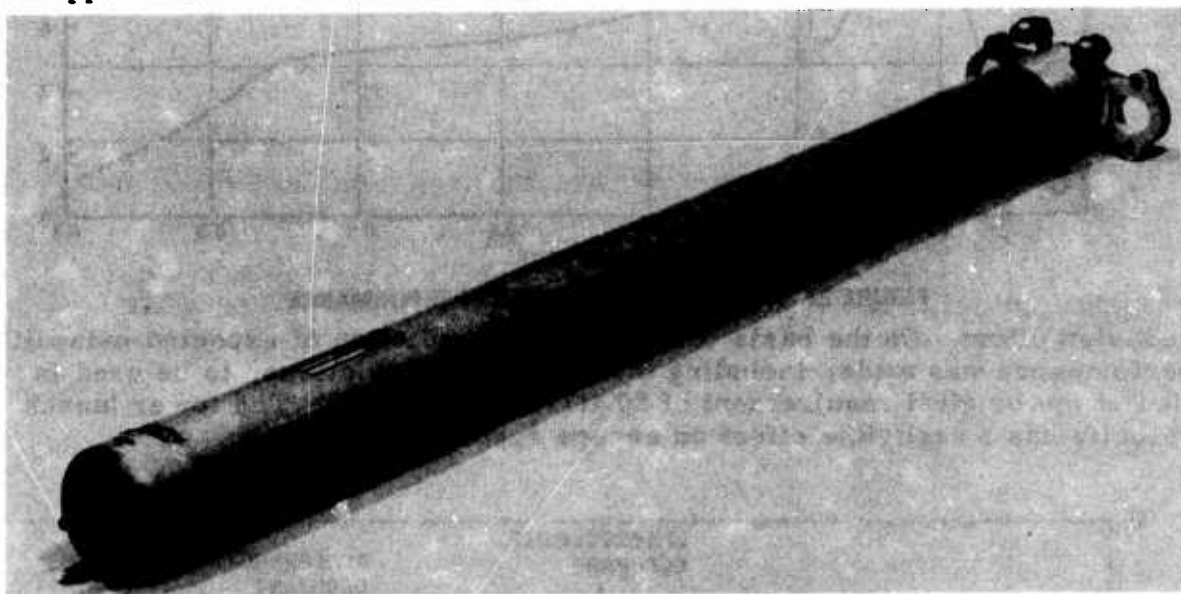


FIGURE 22. XM-39 ROCKET CATAPULT ASSEMBLY

When the squibs are fired, the resulting hot gas output ignites the catapult (launch) cartridge contained in the lower end of the booster tube. The cartridge pressurizes the tube and propels the seat up the guide rails. As the seat nears the top of the guide rails, hot gases are ported to a rocket ignition element, located within the motor, and the motor propellant ignites. The rocket motor gases are exhausted to the atmosphere through a nozzle that provides a thrust vector of 60 degrees relative to the motor axis. A typical thrust-time history for the XM-39 rocket catapult is shown in Figure 23

During development ejection tests, the 50-ft/sec seat launch velocity specified by Douglas was not achieved, although tests by Frankford on their sled device provided the required velocity. Following a study of the seat ejection test data, in addition to tests of the seat system to measure friction levels, it was concluded that (1) the ACES system did not exhibit higher friction forces than other seats, and (2) the Frankford Arsenal rocket catapult test setup did not simulate the actual seat ejection conditions. Further analysis indicated that it would be very difficult to provide a higher launch velocity, and not exceed Dynamic Response Index (DRI) limits, without a major

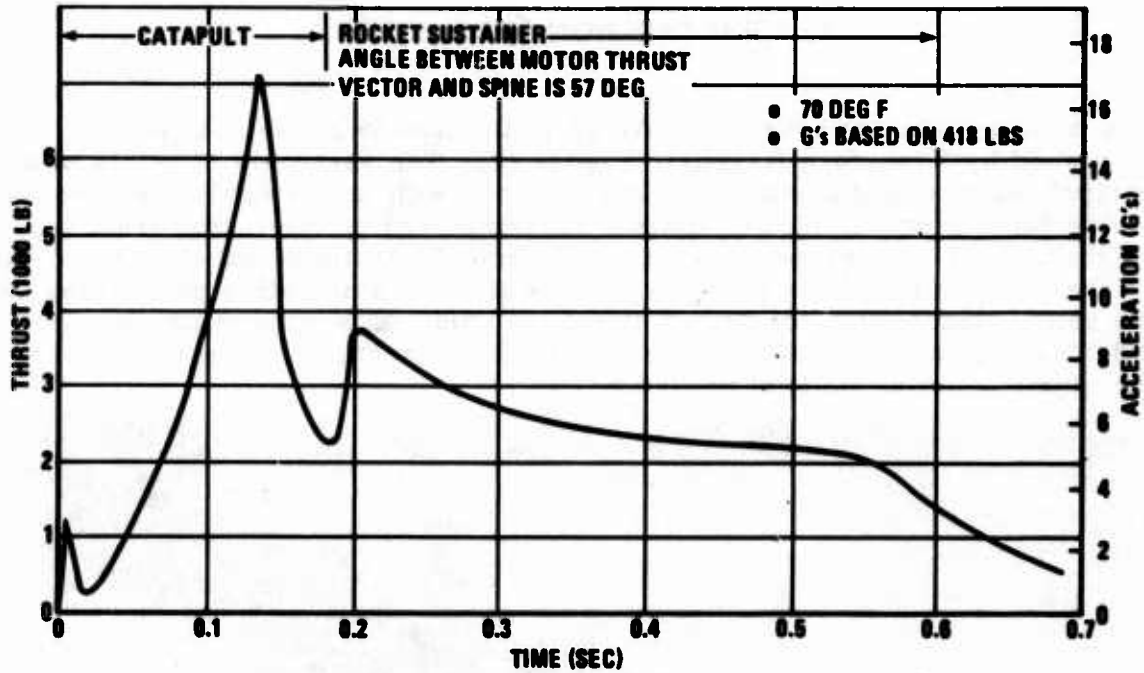


FIGURE 23. XM-39 ROCKET CATAPULT PERFORMANCE

redesign effort. On the basis of test data, a prediction of expected catapult performance was made, including three standard deviations, to be used in lieu of the original requirement of 50 ft/sec, Figure 24. The lower launch velocity has a negligible effect on escape system performance.

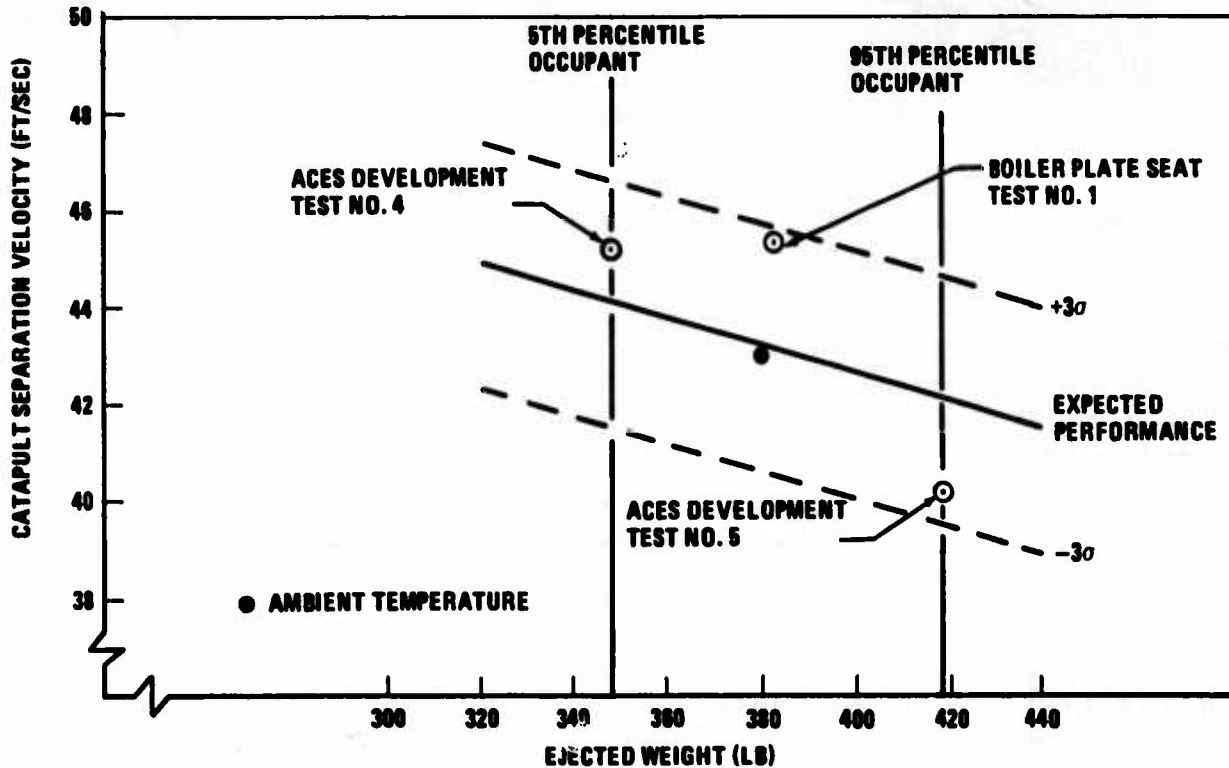


FIGURE 24. ACES CATAPULT SEPARATION VELOCITY PERFORMANCE FOR STATIC EJECTIONS

A bending problem was encountered with the booster tube during static and track seat ejection tests. The bending occurred just above the upper end of the launch cartridge case and appeared to be the result of bending loads imposed during ejection and excessive localized heating of the tube. Initially, a phenolic spacer was inserted in the tube above the cartridge to attenuate the heat effects and, finally, following a structural failure in a track test, the booster tube was reworked to provide greater wall thickness in the affected area.

SECTION VI

ENVIRONMENTAL SENSOR SUBSYSTEM

The multimode timing system requires that the velocity and altitude of the seat be established prior to or during the initial stage of the ejection sequence. This function is accomplished by the environmental sensor subsystem, which consists of two sensing units installed on the upper part of the seat structure. Each unit incorporates an erectable pitot and static and dynamic pressure transducers incased in a housing, Figure.25. The devices are interconnected by an electrical cable.

Two sensors are used to improve system reliability. If a Mode 1 environment is sensed erroneously in a high-speed ejection, because of pitot blanketing, the recovery parachute may be subjected to an unsafe condition. This could result in structural failure of the parachute or an excessive g-load on the crewman.

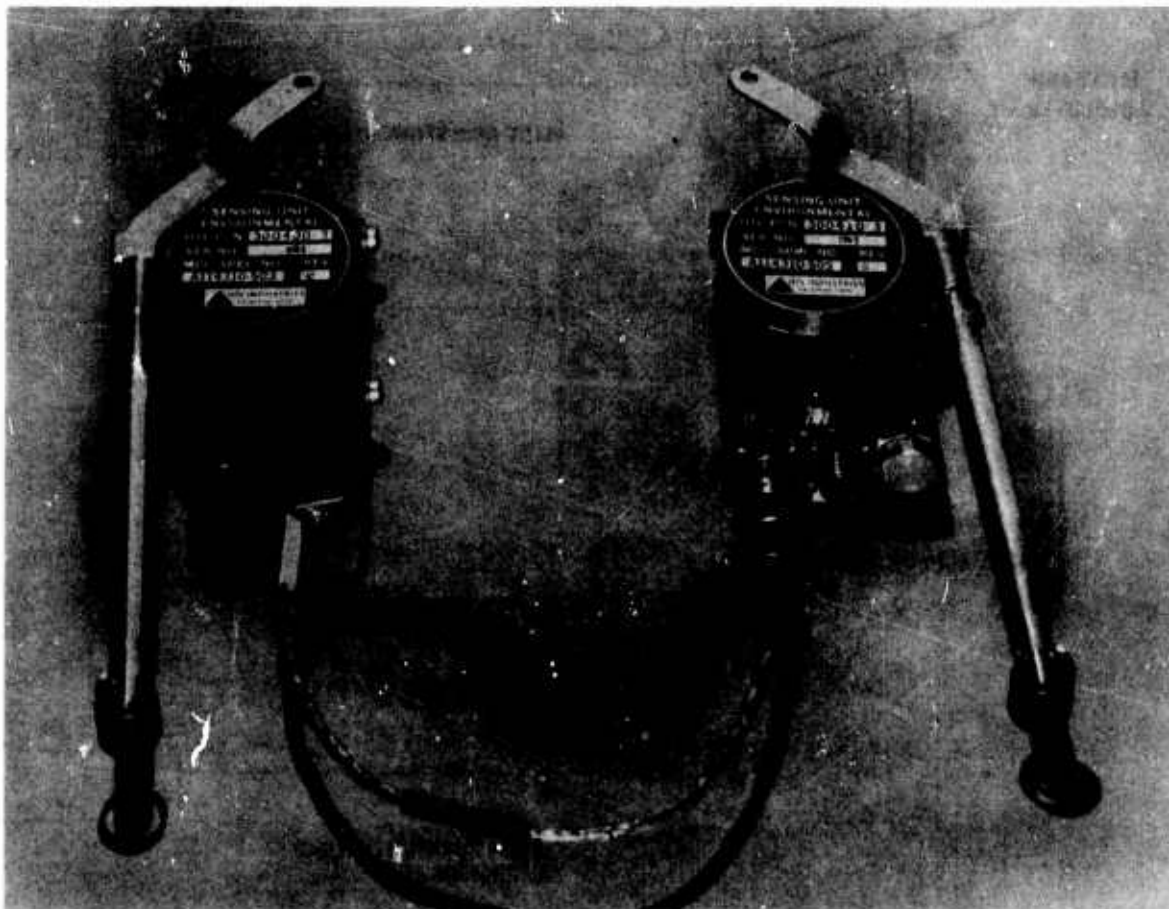


FIGURE 25. ENVIRONMENTAL SENSORS

The sensors are installed on the aft side of the seat structure in the area above the upper slide blocks, Figure 26. The pitot arms nest into slots in the sides of the structure, retained by a pair of latches. This protects the sensors from damage on seat installations where through-the-canopy ejection is required. When the pitot arms are released, after approximately 13 inches of seat travel (from midposition), they rotate upward until the pitot arm is approximately 20 degrees above the horizontal. An over-travel capability allows the pitots to rotate an additional 55 degrees to eliminate the possibility of a hangup if snagged by the parachute risers.

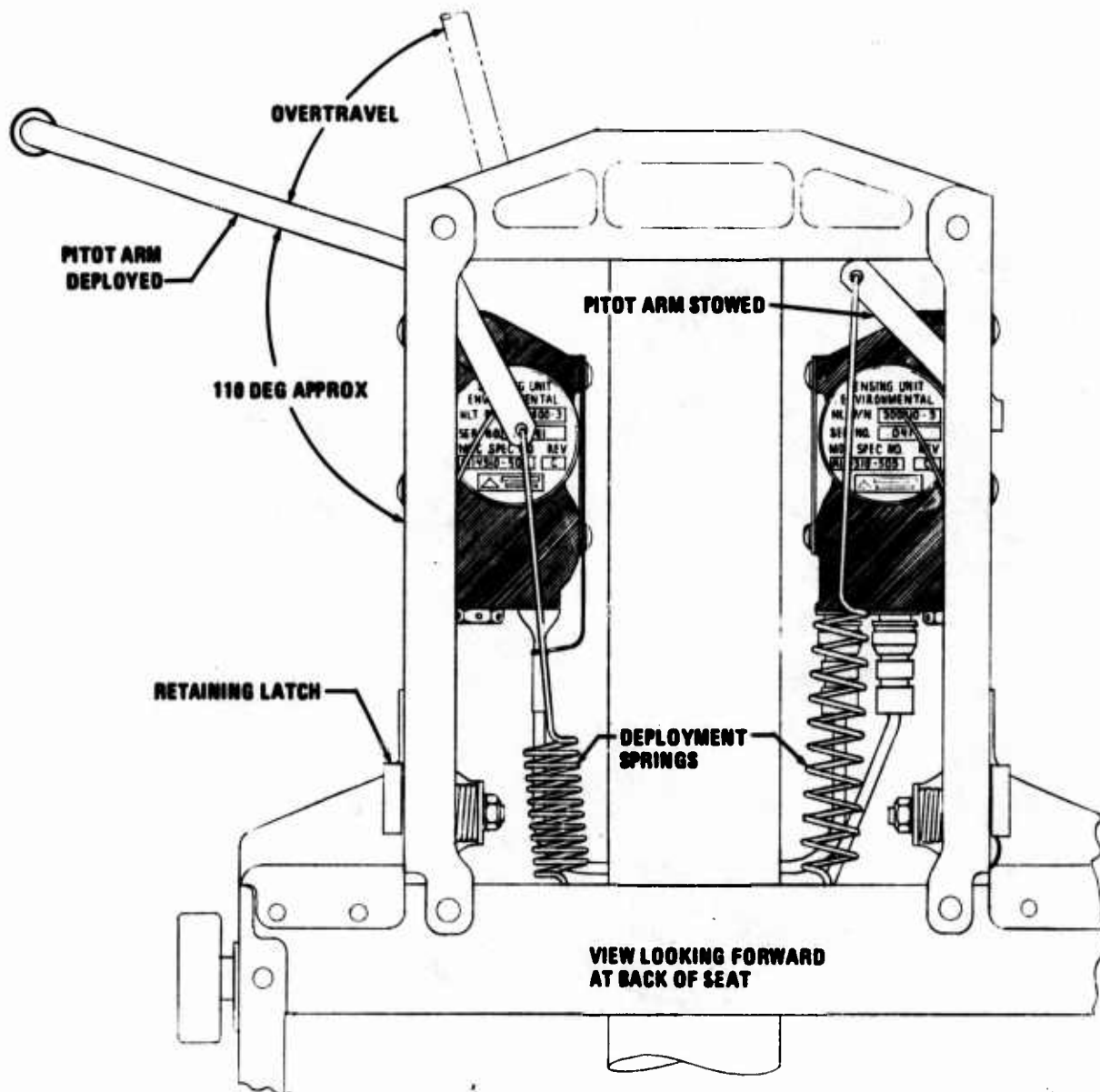


FIGURE 26. ENVIRONMENTAL SENSOR INSTALLATION

Each sensor housing contains a static port, switches, and bellows for the sensing of static and total pressure, Figure 27. The velocity switch is normally closed and this indicates a Mode 1 condition. When the dynamic pressure at the pitot head is equivalent to $275 + 25$ KEAS at sea level, the total pressure bellows extends sufficiently to open the switch, thus indicating a Mode 2 condition to the recovery sequencer. A smaller bellows that measures static pressure is coupled to the total pressure bellows to alter the velocity at which switching occurs as a function of altitude. The specified operational limits for the velocity switches are illustrated in Figure 28. The compensating bellows extends as the static pressure decreases, causing the velocity switches to close at a lower velocity as the altitude increases. As the speed approaches zero, the velocity switches are in the Mode 1 position at a nominal altitude up to 12,000 feet.

As discussed in Section II, the static port of the sensor, being located behind the seat, senses base pressure. This alters the altitude where the system changes from Mode 3 to Mode 2 as a function of seat velocity at ejection, Figure 6.

An electrical schematic of the environmental sensor subsystem is shown in Figure 29. To provide a valid Mode 1 indication to the recovery sequencer, both velocity switches (S_1 and S_3) must be in their normally closed position and the altitude switches (S_2 and S_4) open. If either S_1 or S_3 opens prior to initiation of the parachute mortar, a Mode 2 recovery sequence is provided. Once the Mode 2 sequence is initiated, the system cannot revert to Mode 1, irrespective of subsequent S_1/S_3 switch positions. This feature protects the parachute from being deployed too early in the recovery sequence. The altitude switches (S_2 and S_4) are normally open and both must be closed to provide a Mode 3 signal.

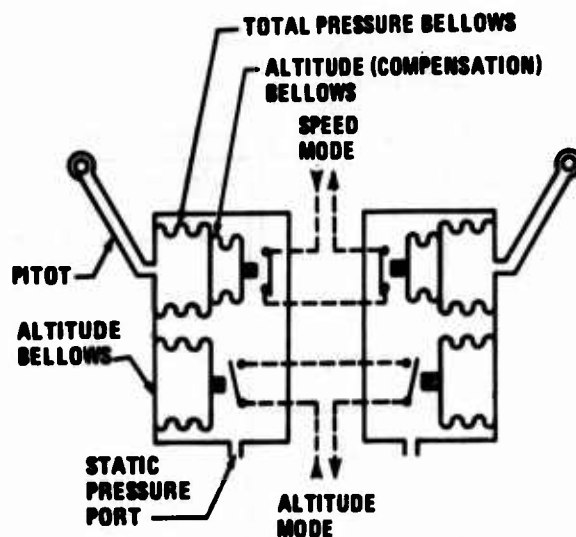


FIGURE 27. ENVIRONMENTAL SENSOR SCHEMATIC

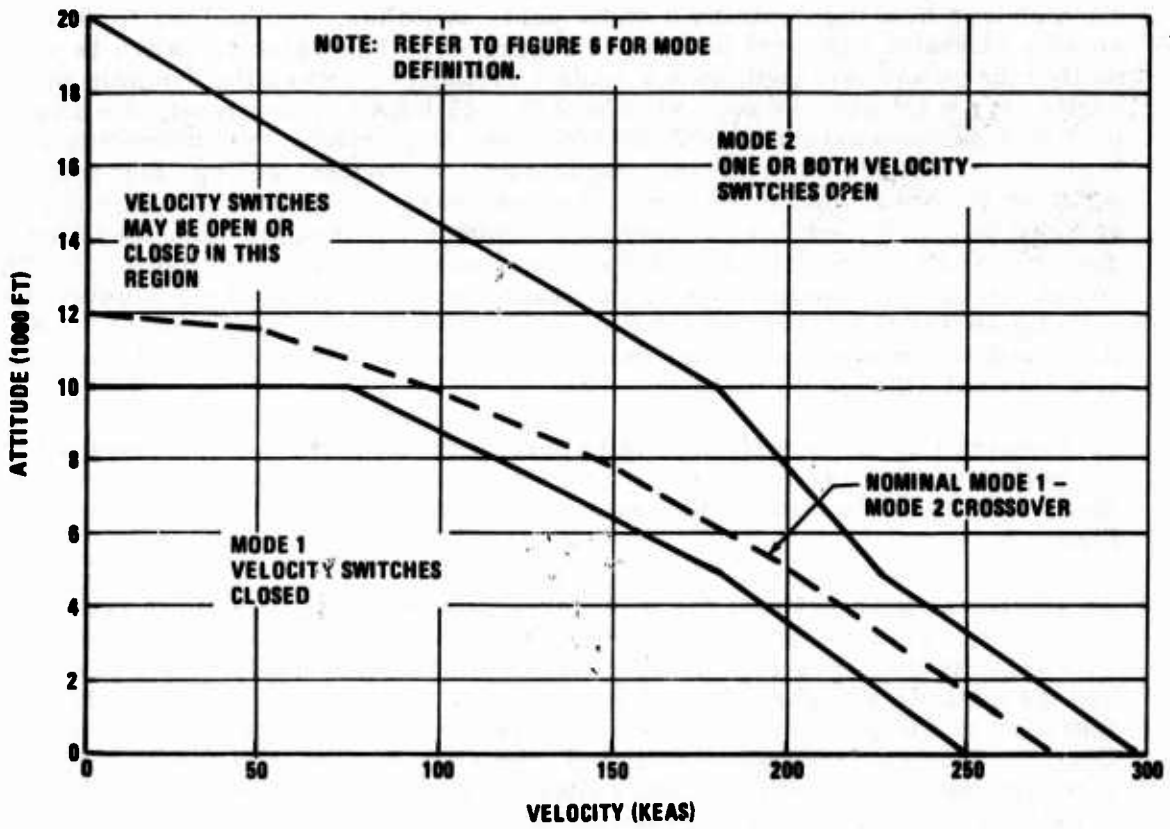


FIGURE 28. VELOCITY SWITCH OPERATIONAL LIMITS

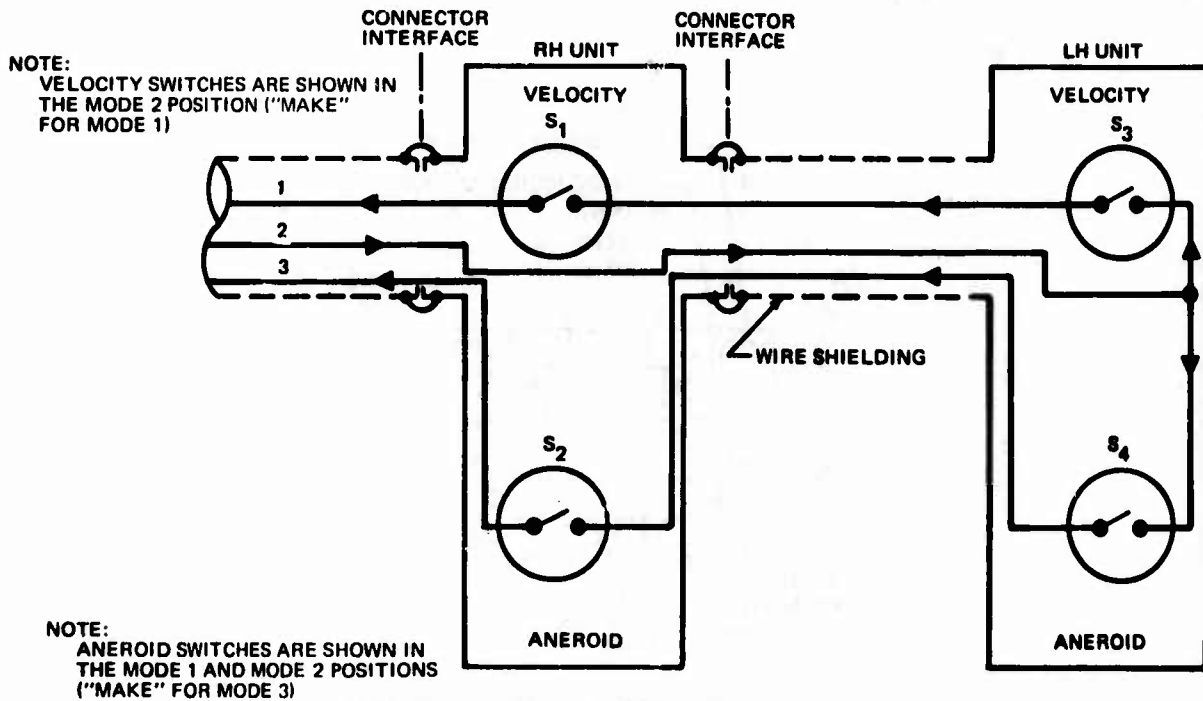


FIGURE 29. ENVIRONMENTAL SENSOR SWITCHING MATRIX

SECTION VII

AUTOMATIC PROGRAMMER SUBSYSTEM

The ACES uses an electroexplosive sequencing subsystem to control the initiation of all ejection and recovery functions. The subsystem is powered by electrical energy from two sources: (1) miniature alternators supplying alternating current with a fast-rise time, and (2) thermal batteries which, upon initiation, furnish direct current at approximately 28 volts.

One complete programmer subsystem includes the following components:

1. Two Initiation Sequencers
2. One Recovery Sequencer
3. One wiring harness for the inertia reel

The initiation sequencers, Figure 20, are mounted on the guide rails, the recovery sequencer, Figure 30, is mounted on the seat structure, and the wiring harness on the backrest assembly. For a two-seat installation, an additional wiring harness is required to transmit an electrical signal between the seats. The Automatic Programmer Subsystem is shown schematically, for a two-seat arrangement, in Figure 31.

An electroexplosive sequencing system was selected over an equivalent pyrotechnic system for the following reasons:

1. **Timing accuracy:** Electronic time delays can provide an accuracy of ± 3 percent at any temperature and ± 5 percent over the temperature range of -65 to $+200^{\circ}\text{F}$. State-of-the-art pyrotechnic delays exhibit time variations of ± 10 percent at any one temperature and ± 15 percent over the required temperature range.
2. **Weight:** The electronic mode-select logic and event-sequencing time delays are lighter than an equivalent pyrotechnic system.
3. **System checkout:** As opposed to pyrotechnic systems, electronic sequencing systems can be nondestructively tested for proper delay and logic operation. An electronic time-delay value can be altered with little or no requalification required.
4. **Signal transmission medium:** Because of its inherent flexibility, electrical wiring is routed more easily between the seat subsystems than gas lines or Shielded Mild Detonating Cord (SMDC), which is encased in stainless steel tubing. Flexibility is required between the seat and aircraft to permit vertical adjustment of the seat. A certain degree of flexibility also is required between the recovery sequencer and some pyrotechnic devices that move relative to the seat structure.

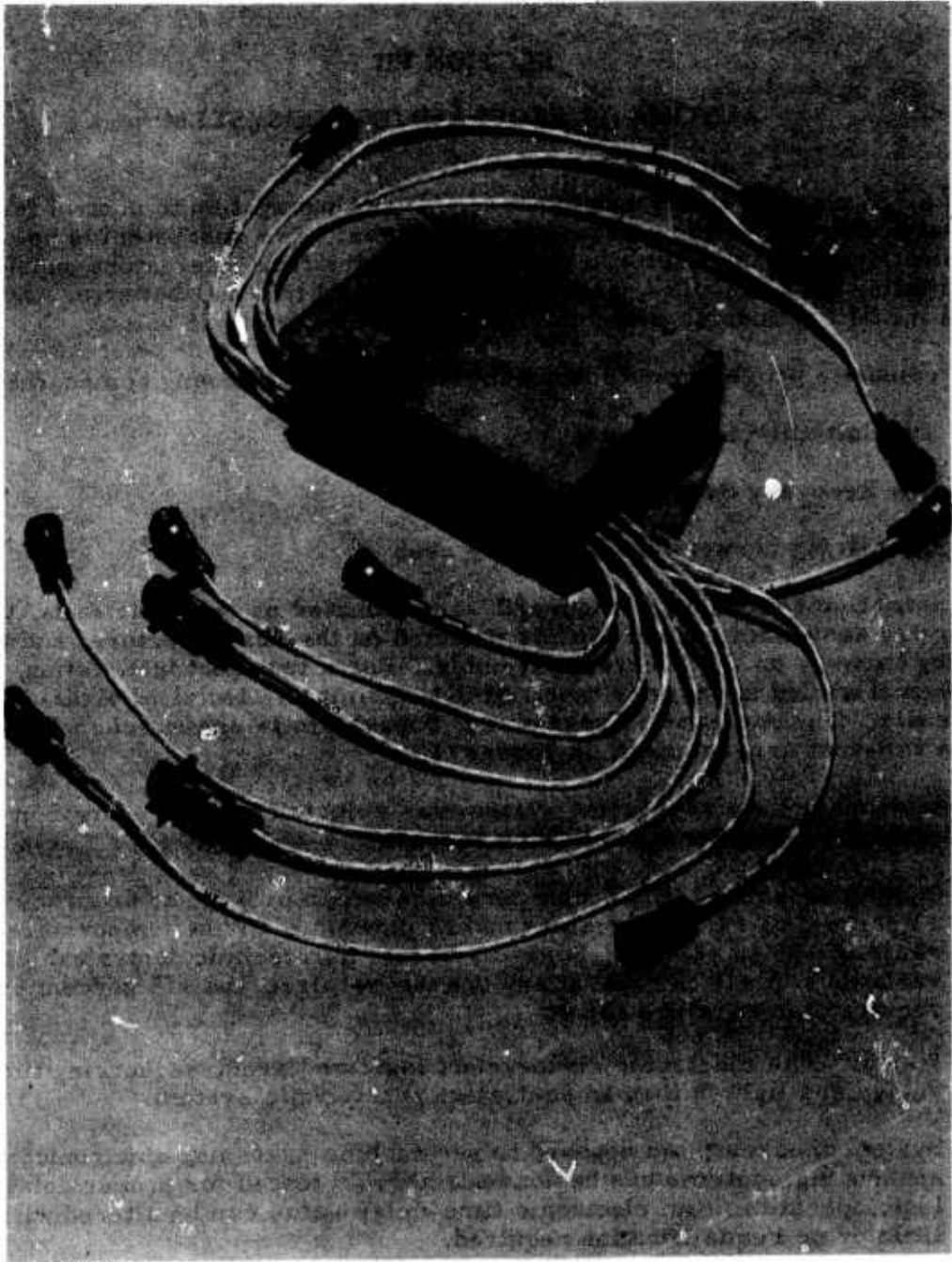


FIGURE 30. RECOVERY SEQUENCER

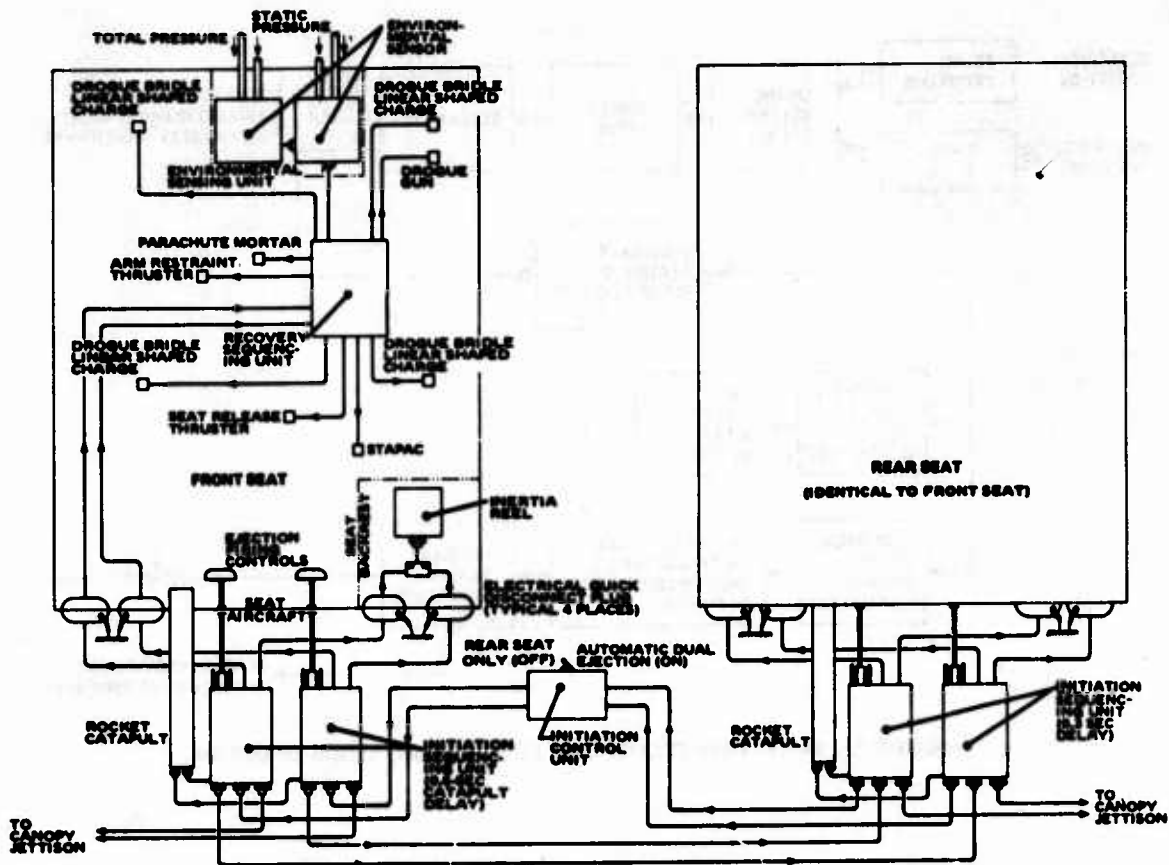


FIGURE 31. AUTOMATIC PROGRAMMER SUBSYSTEM

INITIATION SEQUENCER

Ejection initiation is provided by either of two redundant sequencer units, mounted on the guide rails, that can be activated mechanically by the seat-mounted firing controls or by an electrical pulse from a second-seat sequencer. Referring to Figure 32, a force of 39 ± 7 pounds applied over a distance of 0.38 inch is required to actuate the sear that unlatches the spring release system. The spring release mechanism also may be unlatched by a thruster, which is fired electrically with a recommended current of 5 amperes. When the alternator drive spring is released, it spins the alternator to approximately 12,000 rpm in 10-12 msec.

The alternator incorporates a permanent magnet armature and three field windings. Two of the field windings are employed to initiate as many as five pre-ejection functions within 15-20 msec, each having a recommended firing current of 5 amperes, Figure 33. The third field winding is connected through a rectifying bridge circuit to two storage capacitors. The energy stored in the first capacitor powers a 0.3-second solid-state electronic time delay which, when expended, releases the energy stored in the second capacitor to fire the rocket catapult squib. A resistor is installed in series in the rocket catapult squib circuit and the voltage developed across it, when current flows to fire the squib, initiates the 160-msec delay in the recovery sequencer, Figure 34.

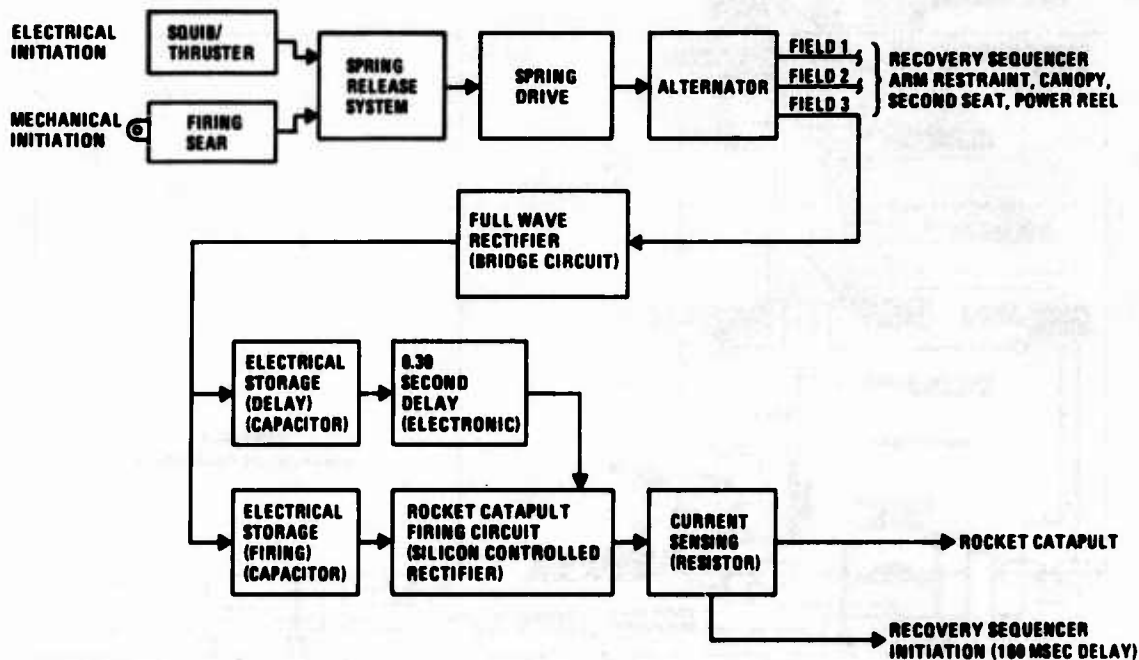


FIGURE 32. INITIATION SEQUENCER FUNCTIONAL BLOCK DIAGRAM

Electrical energy is transmitted from the sequencing unit to the ejection seat through two cables, each equipped with quick-disconnect electrical connectors. One connector is mated with a receptacle on the seat and the other with a receptacle on the backrest assembly. As the seat ejects, these cables are disconnected by lanyards built into the cable assemblies. Electrical energy to initiate the rocket catapult is also transmitted via a cable and connector that is integral with the ejection sequencing unit.

The sequencing unit has three receptacles mounted on its upper surface. Two of these are for output power to initiate the canopy removal system and a second-seat sequencer. The third receptacle accepts power to electrically initiate the unit by an outside source. All electrical cables and connectors are shielded.

Each unit has a provision for insertion of a safety pin that prevents the unit from being mechanically or electrically initiated. Units containing different time delays for rocket catapult ignition incorporate different mounting configurations to preclude incorrect installation. Each sequencer is housed in an aluminum case designed to exclude any radio frequency (RF) energy which might induce accidental squib initiation or circuit damage.

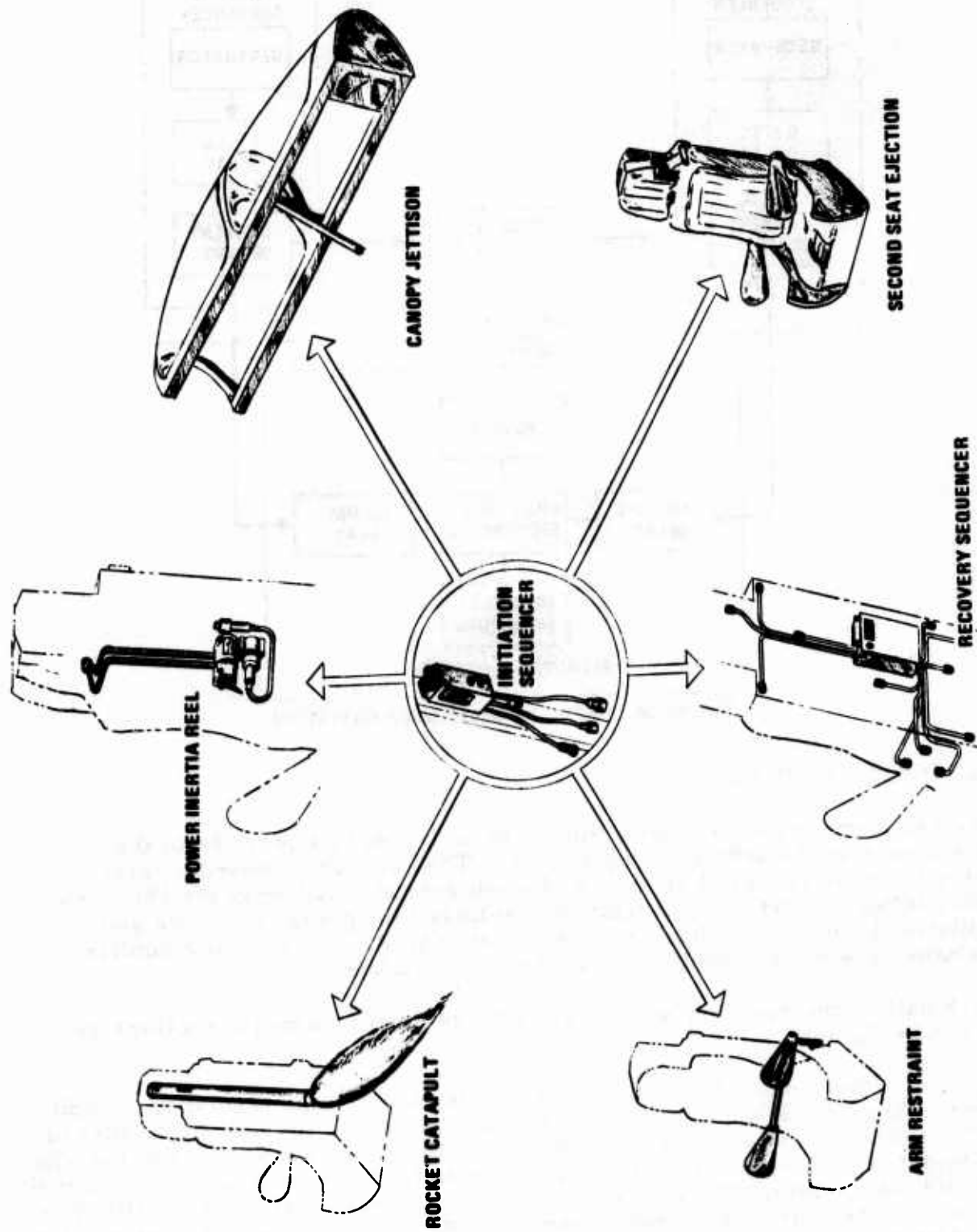


FIGURE 33. PROGRAMMER-INITIATED PRE-EJECTION FUNCTIONS

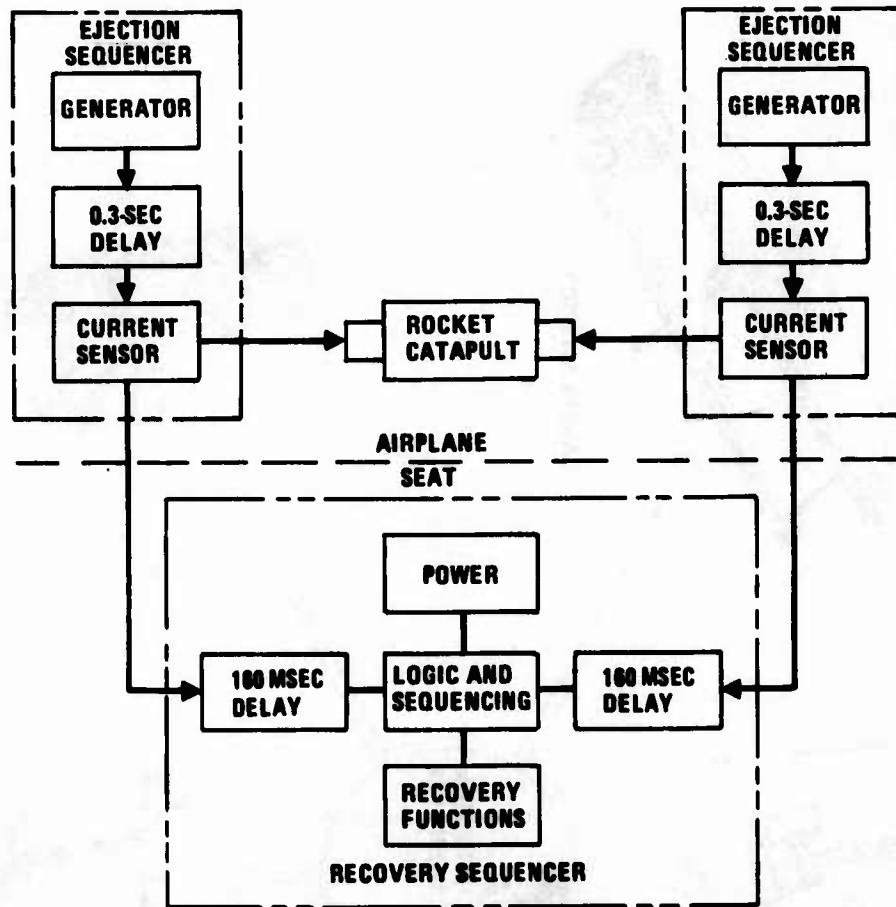


FIGURE 34. RECOVERY SEQUENCER INITIATION

RECOVERY SEQUENCER

The recovery sequencer power supply is activated by a pulse from the alternators in the initiation sequencers. The recovery sequencer interrogates the environmental sensors and when activated following the 160-msec delay (after rocket catapult ignition), selects the appropriate mode and initiates the corresponding recovery functions, Figure 35. All circuitry, including the power supply, is completely redundant.

Each half of the recovery sequencer is made up of four major sections as shown in Figure 36.

The power section contains thermal batteries and voltage regulation circuits. Each of the four thermal batteries, which are electrically activated, measures 0.75 inch in diameter and 1.5 inches in length. When activated, a pyrotechnic material is consumed within the battery, which creates sufficient heat to melt a solid electrolyte. When the electrolyte is in a molten state, the battery is capable of delivering maximum power output. The output drops to zero when the battery cools sufficiently to re-solidify the electrolyte. The battery requires 150-200 msec to develop maximum output power and has a life of approximately 10 seconds. From the time the batteries are activated by the alternators, approximately 460 msec elapses before full power is required.

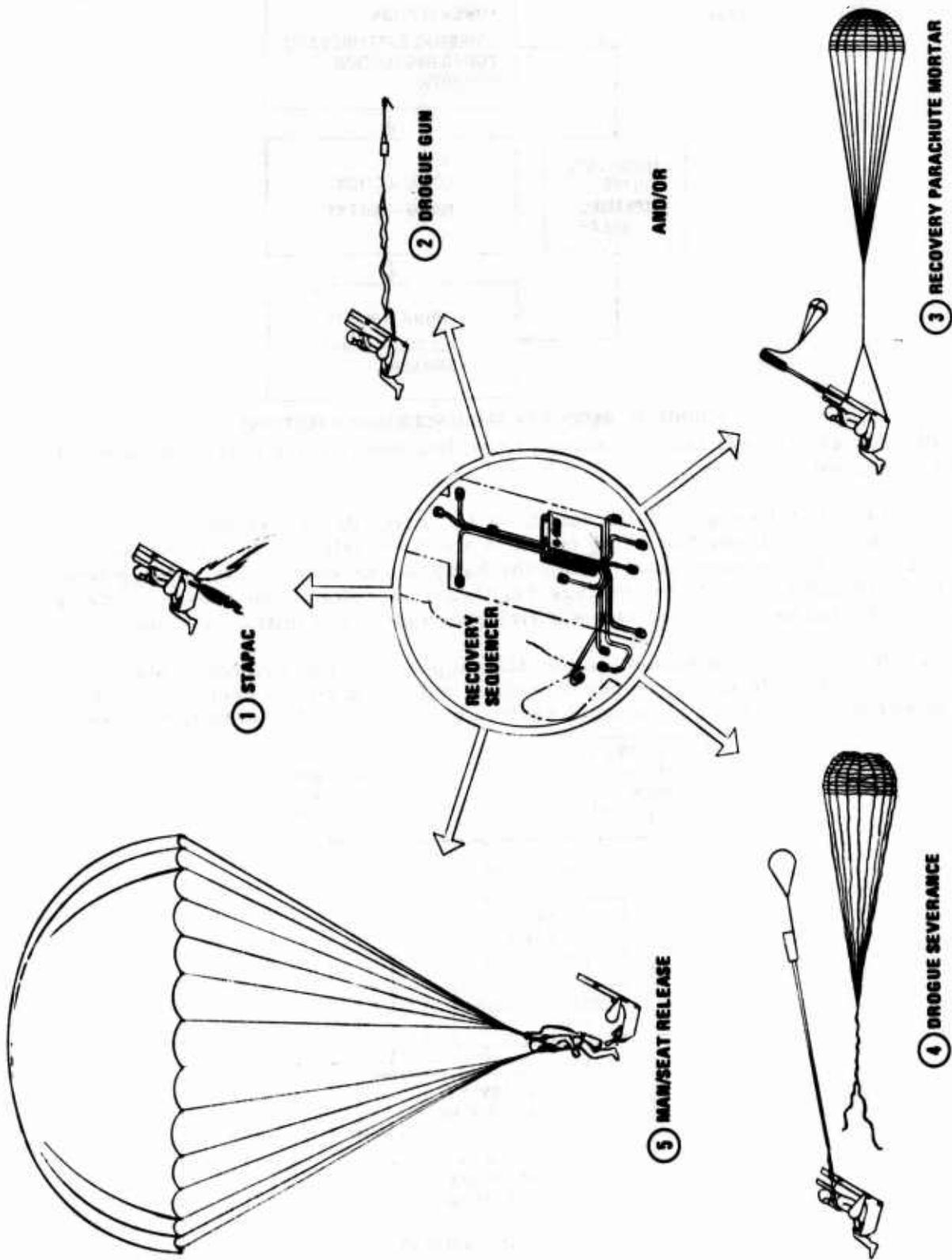


FIGURE 35. PROGRAMMER-INITIATED RECOVERY FUNCTIONS

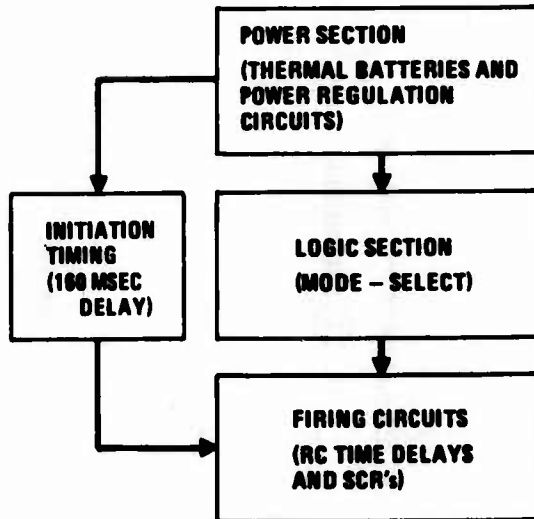


FIGURE 36. RECOVERY SEQUENCER MAJOR SECTIONS

The battery is required to continue providing power for a maximum time of 2.9 seconds.

The initiation timing circuit contains a 160-msec delay element, which is employed to activate the firing circuits and time delays. The 160-msec delay circuit receives power from the batteries as soon as the voltage level is sufficient to initiate the voltage regulation circuits. The 160-msec delay is activated by the rocket catapult firing circuit in the initiation sequencer.

The logic section evaluates information supplied by the environmental sensors and selects the proper functions and sequence for recovery of the crewman, Figure 37. The logic section consists of solid-state filters and

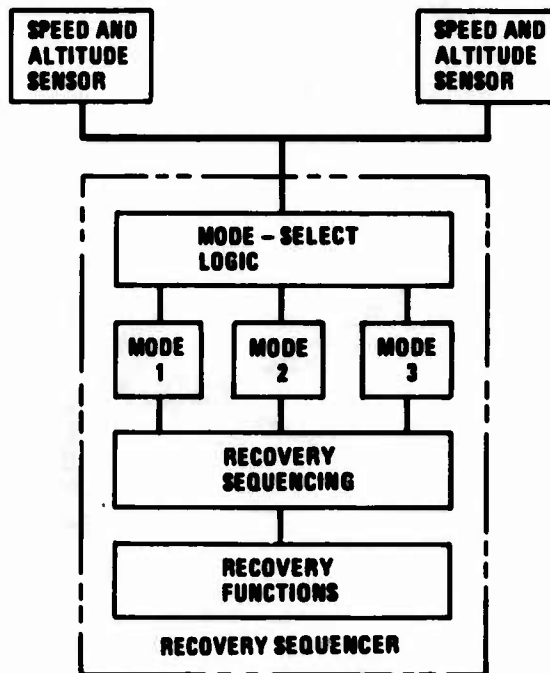


FIGURE 37. RECOVERY SEQUENCER OPERATION

logic circuitry which monitor the speed and altitude switches and control firing circuits and solid-state switches to sequence internal components and recovery functions.

The firing circuit section comprises solid-state resistor-capacitor (RC) timing circuits that trigger silicon-controlled rectifiers (SCR's), Figure 38. The SCR's act as high-current switches to fire subsystem squibs. The RC timing circuit operates by applying a regulated voltage across a resistor and capacitor (R_1 and C_1 in Figure 38) in series. As current flows through R_1 , the voltage across C_1 , measured at the gate, follows the characteristic voltage curve. When the voltage at the gate reaches a critical level, referred to as the intrinsic voltage, the unijunction breaks down permitting all the energy stored in C_1 to flow through it and R_2 to ground. This current flow generates a voltage pulse at the base/output that turns on the SCR allowing current to flow in the squib circuit. Resistor, R_1 , and capacitor, C_1 , are preselected to provide a charging curve that will reach the unijunction breakdown voltage at the design time delay, t .

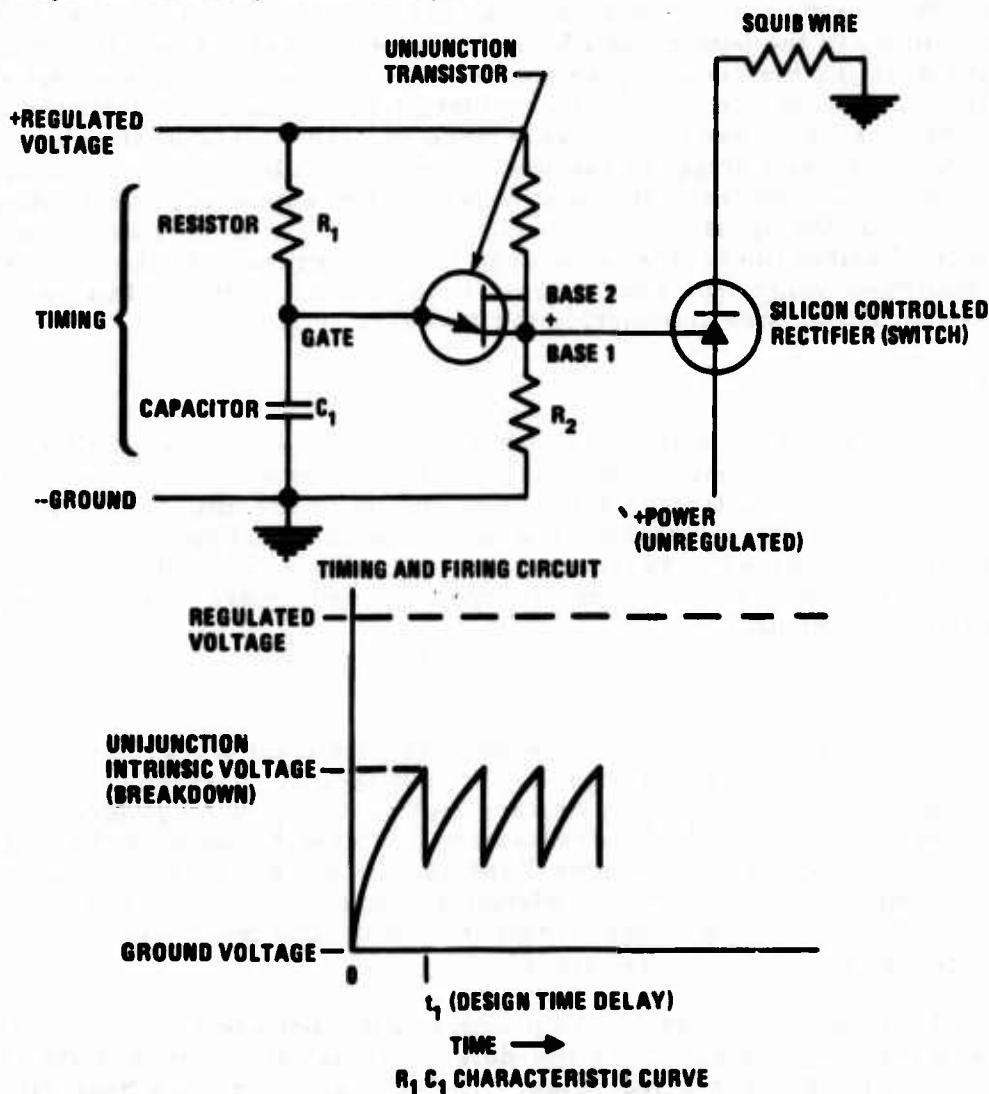


FIGURE 38. TYPICAL R_1 , C_1 TIMING AND FIRING CIRCUIT WITH CHARACTERISTIC OPERATING CURVE

A block diagram for one-half of the recovery sequencer is shown in Figure , the other half being identical in function. A typical operational sequence begins when battery A is activated by the initiation sequencers. This occurs at the same time the pre-ejection functions are initiated. Power is applied to the logic section and the 160-msec delay circuit as soon as the battery begins to function (80-125 msec). When the rocket catapult is fired, 300 msec after ejection initiation, a signal from the initiation sequencer activates the 160-msec delay. At the end of the delay, voltage is applied to initiate and power the 40-msec delay and 850-msec delay. At this time, power also is applied to fire the STAPAC and to begin charging a bank of storage capacitors. Operation of the recovery sequencer up to this time is the same regardless of the speed or altitude at ejection. Recovery functions are provided for three modes and are discussed in the following paragraphs.

Mode 1

In Mode 1, the sensor switches are in the low-speed and high-altitude positions. Battery B is initiated as soon as the storage circuit charges to the firing voltage of the battery squib, with the result that battery B augments battery A during the recovery sequence. The 40-msec delay element expends, initiating the parachute mortar firing circuit which, in turn, initiates the mortar squib, the 120-msec drogue severance and 2100-msec seat release delays. The 120-msec delay triggers the lower Drogue Bridle Severance firing circuit which, in turn, initiates a 30-msec delay. When expended, the 30-msec delay initiates the upper Drogue Bridle Severance firing circuit, which fires the upper flexible linear shaped charge (FLSC) cutters. At the completion of the 2100-msec delay, the seat release firing circuit initiates the man/seat release thruster, thus completing the recovery sequence.

Mode 2

In Mode 2, the sensor switches are in the high-speed and low-altitude positions. The altitude-controlled functions are the same as in Mode 1. The speed switch signal activates the drogue gun firing circuit, firing the drogue gun. Drogue gun firing actuates the Mode 2 latching circuit which, in turn, irreversibly disables the 40-msec delay. The 850-msec delay (6) then initiates the parachute mortar firing circuit. The remainder of the sequence is the same as in Mode 1.

Mode 3

A Mode 3 condition can be encountered in two different ways. During a high-speed ejection at altitudes below 15,000 feet, a short-duration Mode 3 condition can be encountered. At very high altitudes, a long-duration Mode 3 condition can occur in which case battery B is used because of the length of time required for the drogue-stabilized seat to descend to 15,000 feet. The primary battery, A, may be completely expended by the time the seat falls to 15,000 feet where firing of the parachute mortar and initiation of the remaining recovery functions are required.

For a short-duration Mode 3, the position of the altitude switch initiates firing of the drogue gun. The time-delay reset is also activated and continuously zeros the 850-msec delay. The 40-msec delay has been disabled irreversibly as a result of the drogue gun firing. The circuit is now in a

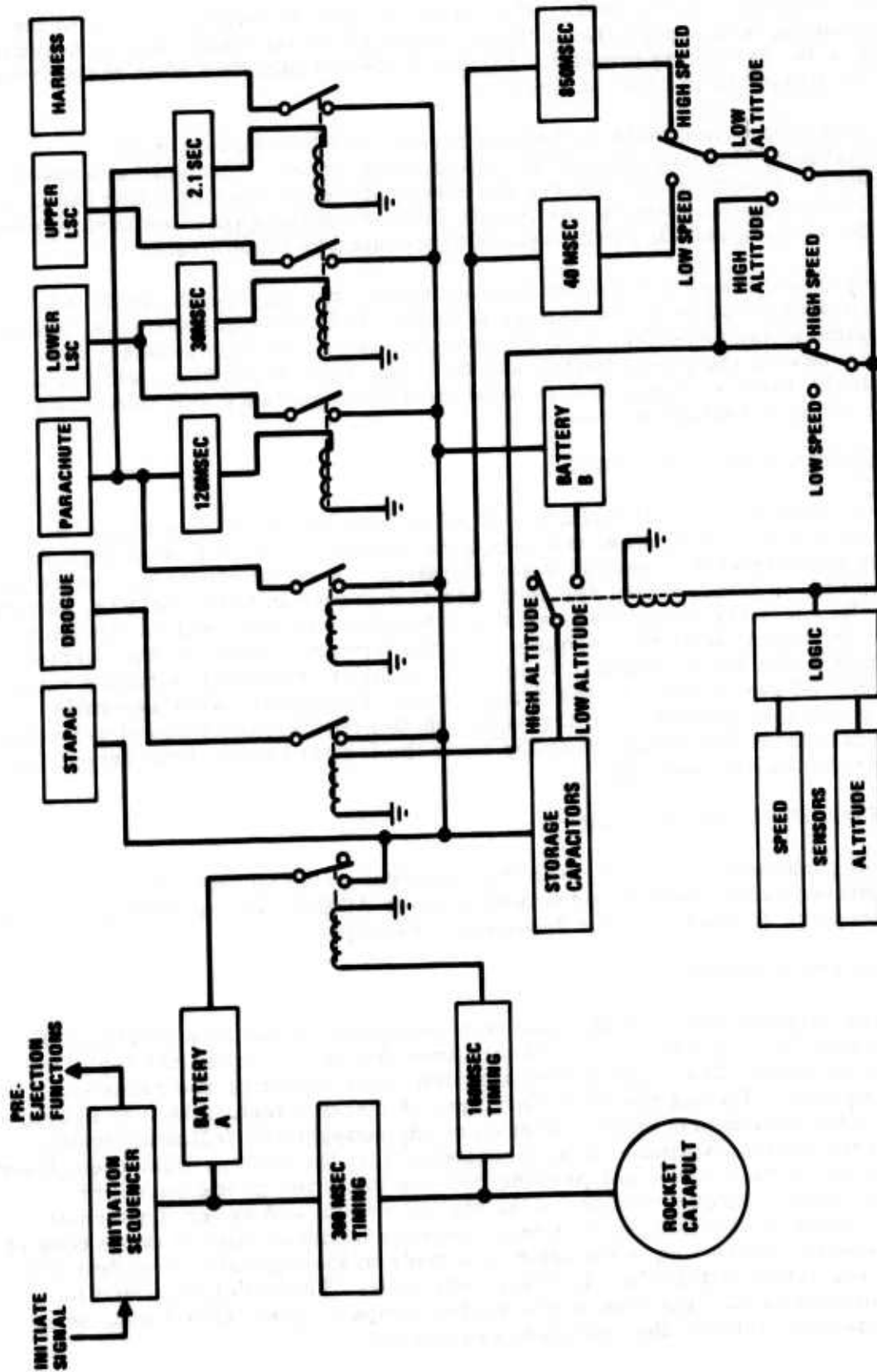


FIGURE 39. RECOVERY SEQUENCER FUNCTIONAL DIAGRAM

holding condition and is reactivated when the altitude switch reverts to the low position, which permits initiation of the 850-msec delay and subsequent firing of the parachute mortar. Battery B also is initiated when the altitude switch changes to the low position.

For a long-duration Mode 3, battery A cools and its electrolyte is re-solidified, thus it is incapable of supplying power. The entire recovery sequencer is dormant except for the energy stored in the capacitor bank. A small amount of current is continually drained off the capacitor bank to monitor the altitude switch as the seat is descending to 15,000 feet.

When the altitude switch indicates low altitude, the energy stored in the capacitors is applied to the battery B squib. Following battery rise, power is applied to the 850-msec and 40-msec delays and the mode-select logic. In most cases, the speed switch will be in the Mode 2 position, which will inhibit the 40-msec delay and provide the 850-msec delay and subsequent firing of the parachute mortar.

INITIATION CONTROL UNIT

In a two-seat (tandem) installation of ACES, the initiation sequencers in the front seat contain a 0.6-second delay; the sequencers in the aft cockpit incorporate the normal 0.3-second delay elements. A set of electrical cables also is required to interconnect the initiation sequencers in both cockpits, Figure 31. The cable set comprises two separate cables to transmit an initiation signal from each initiation sequencer in the forward cockpit to the corresponding units in the aft cockpit and a cable assembly to transmit initiation signals from the aft seat system to the forward one. The latter cable assembly incorporates an initiation control unit, which provides an option of defeating transmission of the signal from the aft to the forward seat, thus permitting ejection of the aft seat only.

DEVELOPMENT PROBLEMS

Several problems associated with the automatic programmer subsystem were encountered during development testing of the ACES. The problems and their solutions are discussed in the following paragraphs.

1. Striker Initiation

The original design of the recovery sequencer required a mechanical input from a striker-actuated cam when the seat reached the top of the guide rails. The input closed a switch, thus initiating the recovery sequence. During the first development ejection test, a failure to actuate the switch precluded initiation of any subsystems following ignition of the rocket catapult. It was concluded that the striker design employed on the system would not provide reliable initiation of the recovery sequence. After a review of the striker design and several alternative methods of providing a recovery sequence initiation signal at the time of catapult separation, a decision was made to incorporate redundant 160-msec delays within the recovery sequencer. These delays would be initiated by current flow in the rocket catapult squib circuit and, when expended, initiate the recovery sequencer.

2. Electrical Connectors

During the second development ejection test, the harness release thruster failed to operate. An investigation established that one of the electrical pins in the initiator was bent and had penetrated the rubber insulation portion of the mating electrical connector, thus producing an open circuit to the bridgewire.

During the preliminary design phase of the program, a decision was made to use only one of the two available bridgewires in certain initiators because the power output of the thermal batteries (as a function of time) had not been firmly established. Each subsystem was evaluated, on a relative basis, to ascertain its functional importance in terms of achieving a successful ejection and recovery. It was decided to use only one bridgewire in initiators for the harness release thruster, STAPAC, and FLSC elements in the drogue severance system. Subsequently, the recovery sequencer was redesigned to include totally redundant firing circuits with accompanying redundant power sources.

The following systems and procedural revisions were made to prevent further recurrence of failures caused by improper connector installation and to improve reliability:

- a. External Faraday caps were employed for squib protection in place of internal shunting springs, which could cause pin deformation upon their removal.
- b. A pin-straightening tool was used to check each initiator for proper pin and keyway alignment immediately prior to connector installation.
- c. The recovery sequencer was modified to provide for dual bridgewire initiation of all pyrotechnic subsystems.
- d. It has been proposed that the production configuration of the programmer subsystem incorporate an electrical continuity check-out capability for all electroexplosive devices on the seat.

3. Environmental Sensor Outputs

The recovery sequence in the third development ejection test was abnormal. Subsequent investigation revealed that pulses, caused by switch chatter, were emanating from the environmental sensor velocity circuits as a result of the normal shock and vibration occurring during the ejection. During a review of the recovery sequencer logic circuitry, the supplier stated that the velocity input logic was sensitive to switch actions of 1 microsecond duration or more.

Because of the difficulties associated with the redesign of the environmental sensors, to provide a unit insensitive to the anticipated shock and vibration levels, it was decided to solve the problem by circuit design in the recovery sequencer.

Compensation for intermittent switch operation in the environmental sensor was made by the addition of a filter circuit in the recovery sequencer at the input from the velocity sensor.

The filter, in order to make an output indicating Mode 2, requires an open circuit (initially closed) for 10 msec.

4. Improper Recovery Sequence

Abnormal recovery sequences were experienced on development ejection tests No. 4, 5, and 6, although modifications had been made to the recovery sequencer logic to eliminate such occurrences. Following test No. 6, the recovery sequencer circuitry was reviewed jointly by the supplier and Douglas Aircraft Company, and a decision made to redesign the logic and firing circuits. The magnitude of the proposed circuit changes was sufficient to cause an 8-month delay in the development and qualification seat ejection test program.

The previous and present firing circuit design is shown in Figure 40. In addition to other circuit simplification, nearly all one-shot multivibrators, believed to be the source of erroneous signals, were eliminated. The previous and present logic circuitry designs are compared in Figure 41. The system complexity was reduced by the elimination of eight inverters. The firing system and logic circuitry redesign eliminated a total of 36 electronic components as outlined in Table II.

In addition to a simpler, more reliable logic and firing system, other changes were made to isolate portions of the redundant circuitry and to provide redundancy for improved reliability. Modifications also were made in the connector-shield and case-shield termination design to improve RFI integrity.

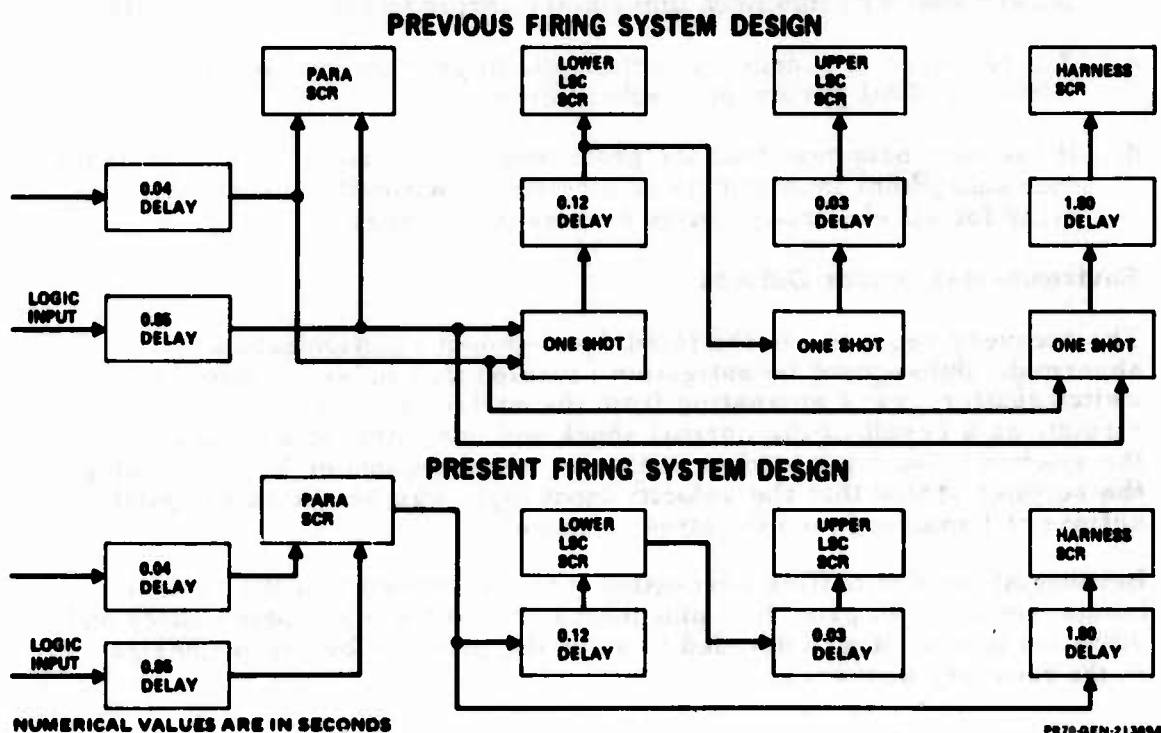


FIGURE 40. RECOVERY SEQUENCER FIRING SYSTEM REVISION

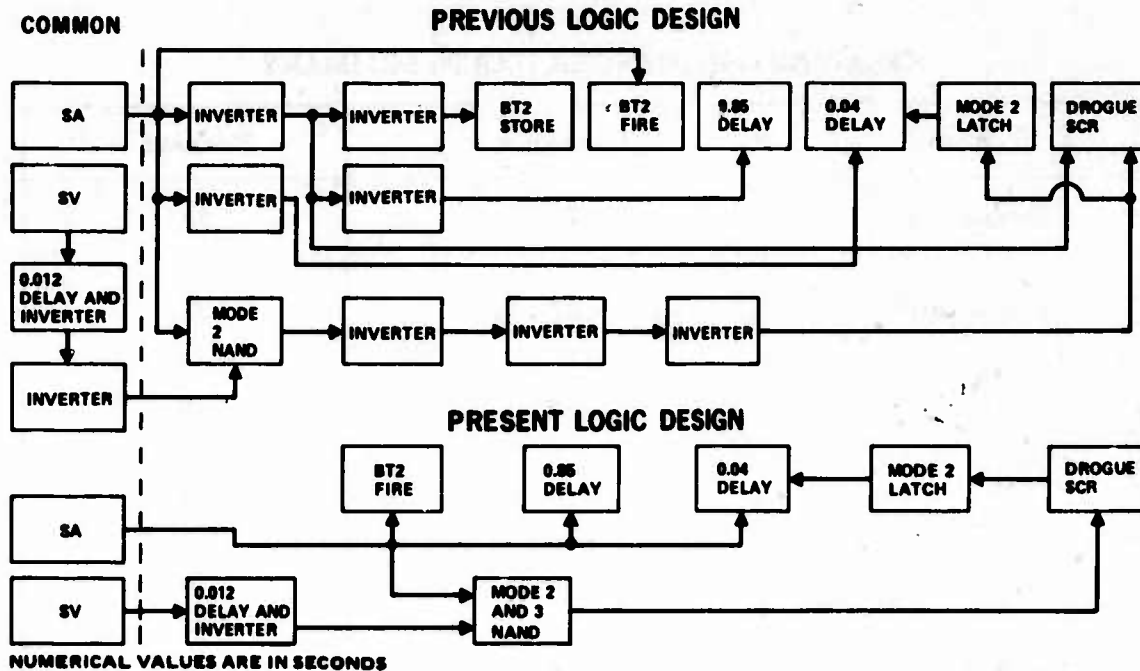


FIGURE 41. RECOVERY SEQUENCER LOGIC REVISION

PR70-GEN-213608

Following premature initiation of the 160-msec delay circuit in development ejection test No. 7, the two remaining one-shot multivibrators were eliminated. The expended-unit visual indicator, believed to be the cause of the premature initiation, was also deleted.

Redesign of the recovery sequencer reduced the number of components by 20 percent, improved reliability, reduced weight, and improved RFI integrity while preserving the basic concept of easily altered RC time delays.

SQUIB ISOLATION

In the eighth qualification ejection test, the arm restraint thruster on the forward seat did not function. Investigation revealed that one of the initiation sequencers on this seat had not operated because of a hairline break in the printed wiring on the circuit board in the electrical initiation circuit. It was determined that the thermal battery squib (in the recovery sequencer), in parallel with the arm restraint thruster squib, had assumed a low impedance when initiated and had shunted all the current normally available to fire the arm restraint thruster. This problem also was experienced in the first inflight ejection test in which one of the initiation sequencers did not function because it had been connected incorrectly to the aircraft power supply. In all cases where both initiation sequencing units have functioned, the arm restraint thruster operated properly. It is theorized that when both initiation sequencers function, the arm restraint thruster squib is fired reliably, even with the battery squib shorted, as both of the redundant bridgewires are heating the primer simultaneously.

Future circuit designs incorporating parallel-circuit squib firing will incorporate isolating resistors in each bridgewire circuit to limit the current.

TABLE II
RECOVERY SEQUENCER PARTS SUMMARY

Item	Previous	Present
Resistors	79	57
Capacitors	33	31
Transistors	14	6
IC's	3	0
SCR's	9	9
UJT's	6	6
Zeners	2	4
Diodes	<u>32</u>	<u>29</u>
TOTAL	178	142

SECTION VIII
ELECTROEXPLOSIVE DEVICES

The ACES employs 22 separate pyrotechnic devices for each seat installation. Three of these devices, two reefing line cutters and the vernier rocket, are initiated mechanically and one device, the sustainer portion of the rocket-catapult, is initiated by ported high-temperature pyrotechnic combustion products. All the remaining devices are initiated by electrical squibs as shown in Table III.

FIRING CHARACTERISTICS

The electrical squibs in the ACES are of the hot bridgewire type and are qualified to a 1-amp, 1-watt, no-fire level as required by Government range-safety requirements. With all explosive devices, the design objective is to provide the least sensitive unit that will function reliably throughout the temperature range. For the ACES, the design objective was to establish the no-fire sensitivity as close as possible to 2 amperes while maintaining a maximum function time of 8 msec when the unit is subjected to 3.5 amperes.

Table IV lists the firing properties of each of the three initiators used in the system. The SOS initiator, P/N S01-10217-21, is employed to initiate all seat subsystems external to the automatic programmer. This squib incorporates dual bridgewire ignition with a common return line, Figure 42. Each of the dual bridgewires is fired by one of the redundant circuits within the recovery sequencer or, in the case of the power haulback reel, by one of the redundant initiator sequencers. The common return configuration was selected over the other two dual bridgewire configurations to minimize RFI sensitivity. The initiation sequencer thrusters and recovery sequencer ther-

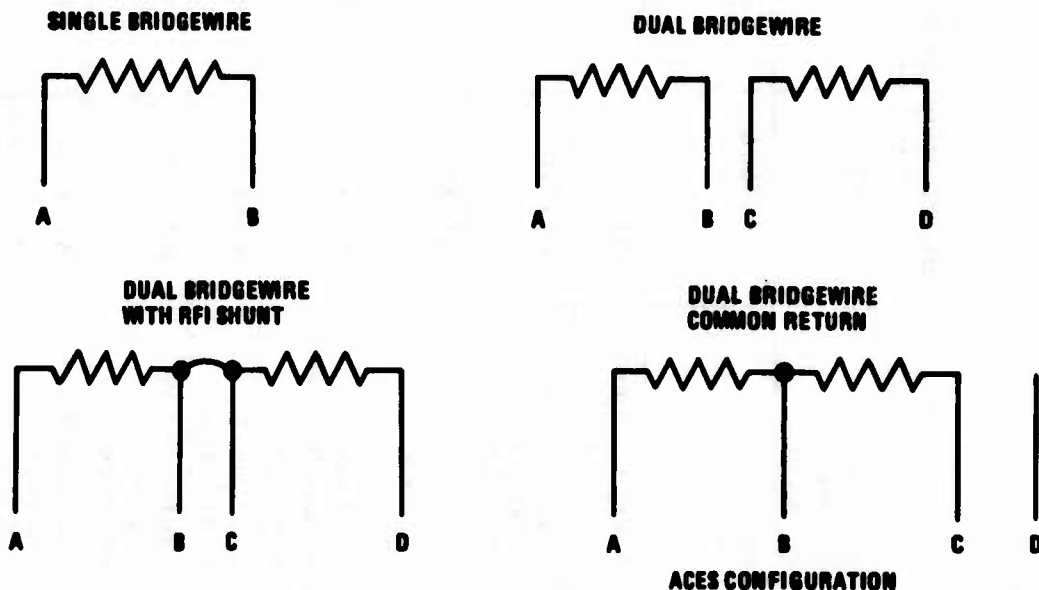


FIGURE 42. ELECTRICAL INITIATOR BRIDGEWIRE CONFIGURATIONS

TABLE III
SEAT SYSTEM ELECTROEXPLOSIVE DEVICES

	Device	Specification	Number of Devices	Output Function	Ignition Element	Static Electricity Protection	Radio Frequency (RFI) Protection
1	Initiation Thruster and Squib	A114306	2	Thrust	Atlas Chemical Initiator	External Preferential Spark Gap	Case Shielding
2	Thermal Battery	A114306	4	Electrical Energy	Network Electronics Initiator	Preferential Spark Gap within Battery	Case Shielding
3	Rocket Catapult-Launch Stage	A114300	1	Thrust	Dual SOS Initiators	Inherent in Initiator	Shielded Wire/Connectors
4	Drogue Bridle Severance Unit (FLSC)	A114302	4	Cutting Jet	SOS Initiator	Inherent in Initiator	Shielded Wire/Connectors
5	Power Inertia Reel Gas Generator	A114303	1	Gas Pressure	SOS Initiator	Inherent in Initiator	Shielded Wire/Connectors
6	Man/Seat Release Thruster Cartridge	A114304	1	Gas Pressure	SOS Initiator	Inherent in Initiator	Shielded Wire/Connectors
7	Gyro Spin-Up Gas Generator	A114308	1	Gas Pressure	SOS Initiator	Inherent in Initiator	Shielded Wire/Connectors
8	Arm Restraint Thruster Cartridge	A114309	1	Gas Pressure	SOS Initiator	Inherent in Initiator	Shielded Wire/Connectors
9	Parachute Mortar Cartridge	A114311	1	Gas Pressure	SOS Initiator	Inherent in Initiator	Shielded Wire/Connectors
10	Drogue Gun Cartridge	A114312	1	Gas Pressure	SOS Initiator	Inherent in Initiator	Shielded Wire/Connectors

**TABLE IV
INITIATOR CHARACTERISTICS**

Initiator	All-Fire Level			No-Fire Level			Bridge Resistance (Ohms)
	Number of Units Tested	Temp (Deg F)	Amps	Number of Units Tested	Temp (Deg F)	Amps	
Space Ordnance Systems (SOS) P/N S01-10217-21	60	-260	2.628	60	-260	2.032	1.05 ± 0.10
	30	300	2.132	30	300	1.514	
Atlas Chemical Industries, Inc. P/N 1 MT 1108	49	-65	3.17	53	160	1.24	1.00 ± 0.10
Network Electronics, Inc. P/N NEI-11	20	70	2.05	50	70	1.34	1.00 ± 0.10

mal batteries employ a single bridgewire circuit as each receives a single initiation signal. Capacitive discharge characteristics of the S01-10217-21 initiator, at ambient temperature, are given below and initiator function times are given in Table V.

Capacitance (Microfarads)	Firing Voltage (Volts)
608*	17.4
114*	29.0

*Reliability = 0.999 at the 0.90 confidence level.

EXTERNAL ELECTROMAGNETIC FIELDS

The Automatic Programmer Subsystem including electroexplosive devices has been designed to preclude inadvertent actuation or dudding from external radiation. The system meets the requirements of MIL-STD-833(USAF). Additional design guidance was obtained from MIL-P-24014(WEP) and supporting document NAVWEPS OD30393, which outlines design concepts to protect systems from the effects of radio frequency interference. The concept selected for the automatic programmer employs the use of compartmentalized, shielded circuitry interconnected by completely shielded electrical wiring.

The enclosures for the electronic and electrical components are fabricated of aluminum and sealed electrically and environmentally. Interconnecting wires are shielded by two layers of served, overlapped metal ribbon. Each layer is wrapped in a different direction, providing a minimum of 200 percent shielding along the wire. All squib electrical connectors are engaged by a threaded, RF attenuating coupling, and each is fitted with a specially designed backshell to provide an environmental and RF-tight transition from cable to connector. Additionally, the bayonet-type electrical connectors employ grounding fingers for increased RF attenuation.

STATIC ELECTRICITY

Douglas Specification A114306 requires that each squib installation be protected from inadvertent actuation by static electricity. As a demonstration of this protection, each squib must be capable of being subjected to a discharge of 25,000 volts between the shorted pins of the bridgewire and the case without ignition. Figure 43 illustrates the method used to prevent ignition caused by spark discharge through the ignition charge material. A preferential spark gap is provided that allows harmless discharge of the electrical energy. SOS initiators, which employ the spark gap concept, are subjected, on a 100-percent basis, to a discharge test before leaving the manufacturer's facility. The squibs within the thermal batteries are similarly pretested, and testing by lot sampling is used to verify compliance. The thruster unit squib in each initiation sequencer is protected by a preferential spark gap placed in the circuitry leading to the initiator.

TABLE V
S01-10217-21 INITIATOR FUNCTION TIMES

Temperature	Voltage or Current Applied	Function Time (msec)				Sample Size
		Min	Mean	Max	σ	
Ambient	3.5 amps	2.2	2.4	2.7	0.153	505
-260°F	5.0 amps	1.5	2.3	3.4	0.422	44
-260°F	22.0 volts	-	0.5	-	-	1
300°F	3.5 amps	1.7	2.24	2.7	0.262	48
300°F	22.0 amps	-	0.4	-	-	2
Ambient	22.0 amps	0.2	0.3	0.4	-	7

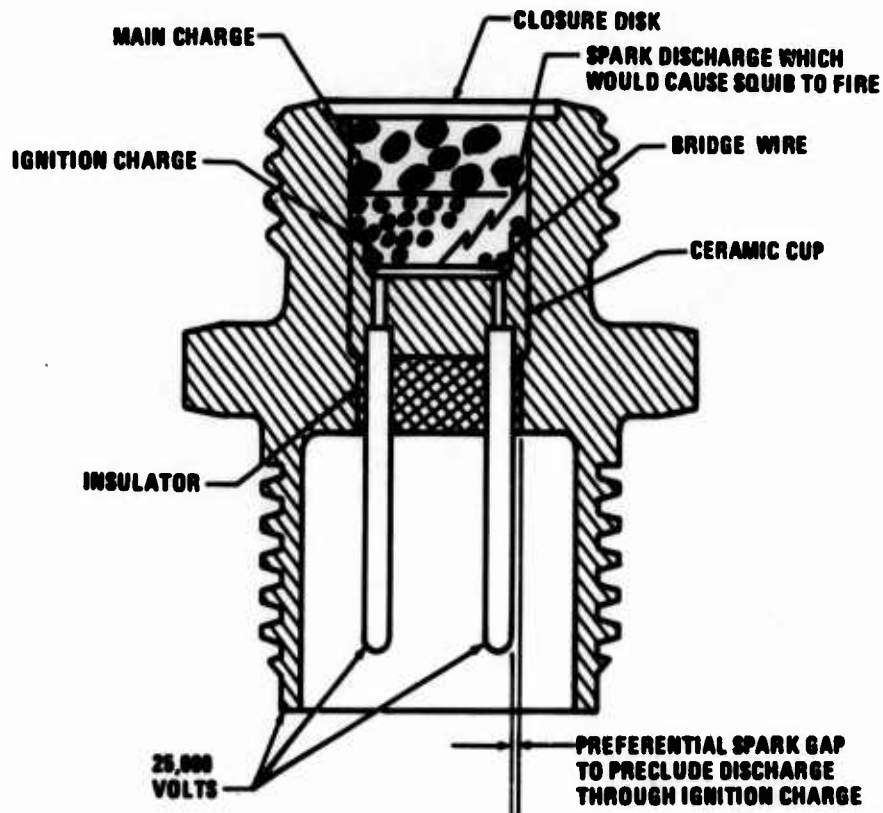


FIGURE 43. STATIC ELECTRICITY DISCHARGE PROTECTION

SECTION IX

STABILIZATION SUBSYSTEM

Stabilization of the ACES is provided by a gyro-controlled vernier rocket motor (STAPAC) and a drogue parachute. The STAPAC unit, which stabilizes the occupied seat during the initial portion of the trajectory, compensates primarily for adverse pitching moments resulting from misalignment of the rocket catapult sustainer motor thrust vector and the system center of gravity (cg). The drogue provides yaw and pitch stability as well as drag to augment seat system deceleration in high-speed ejections. An additional function of the drogue is to stabilize the seat-crewman combination during descent following a high-altitude ejection.

STAPAC

The STAPAC stabilization assembly consists of a rocket motor, rate gyroscope, gyro spin-up actuator, and a cable arrangement that transfers precessional motion of the gyroscope to the vernier rocket motor, Figure 44.

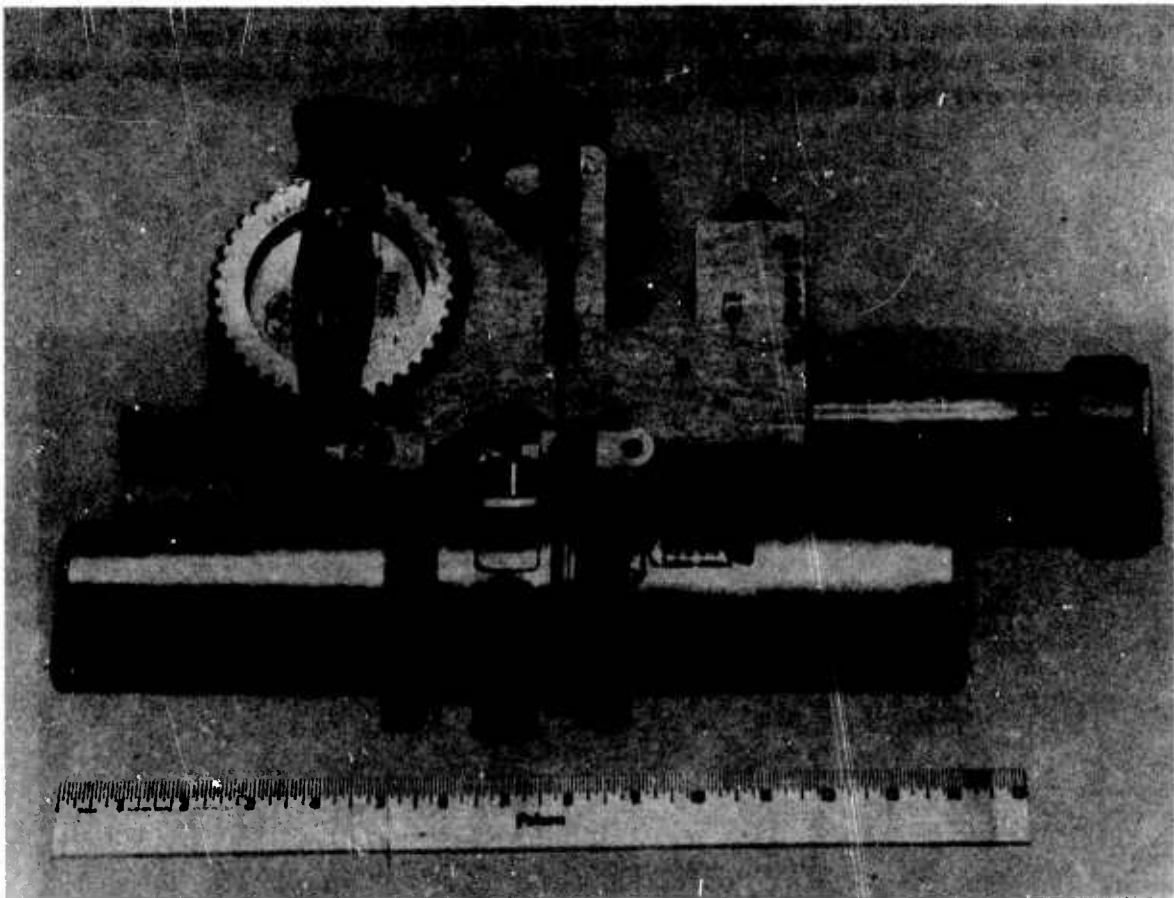


FIGURE 44. GYRO-CONTROLLED VERNIER ROCKET (STAPAC)

The vernier rocket motor, Figure 45., is constructed with cylindrically shaped propellant cases mounted on either side of a center section containing a firing mechanism, nozzle, grooved sector and two shoulders machined to mate with a ball bearing installed on the spin-up actuator housing. The vernier rocket motor develops a thrust of 725 to 740 pounds with a total impulse of approximately 360 pound-seconds, Figure 46.

The gyroscope includes a rotor and gimbal and is mounted on the spin-up actuator housing. Gear teeth on the periphery of the rotor are designed to engage similar teeth on the piston/rack assembly, which is part of the spin-up actuator. As the gyroscope is only gimballed about a single axis, it is only sensitive to pitch rate of the seat and not to seat position. The rate gyro is mounted on the ejection seat with the rotor spin axis and quadrature (sensing) axis oriented in a manner to sense only pitching motion of the ejection seat. The rotor inertia and spin velocity are sufficient to provide the required precessional torque to rotate the vernier rocket motor.

The spin-up actuator comprises a housing and a piston/rack assembly that incorporates gear teeth to mate with those on the periphery of the rotor. Prior to its actuation, the piston/rack assembly provides caging of the gimbal. The uncaging and spin-up functions are accomplished by gas pressure from an electrically initiated cartridge installed in the actuator. A shear pin is installed between the piston/rack and actuator housing to provide positive gyro caging and uniform operation.

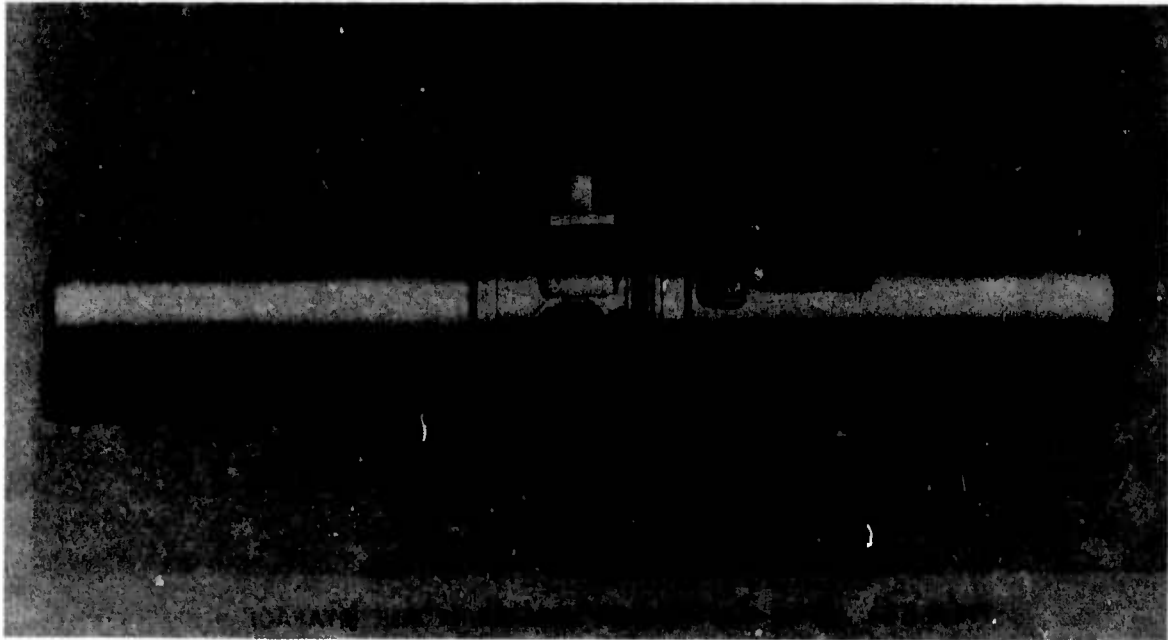


FIGURE 45. VERNIER ROCKET MOTOR

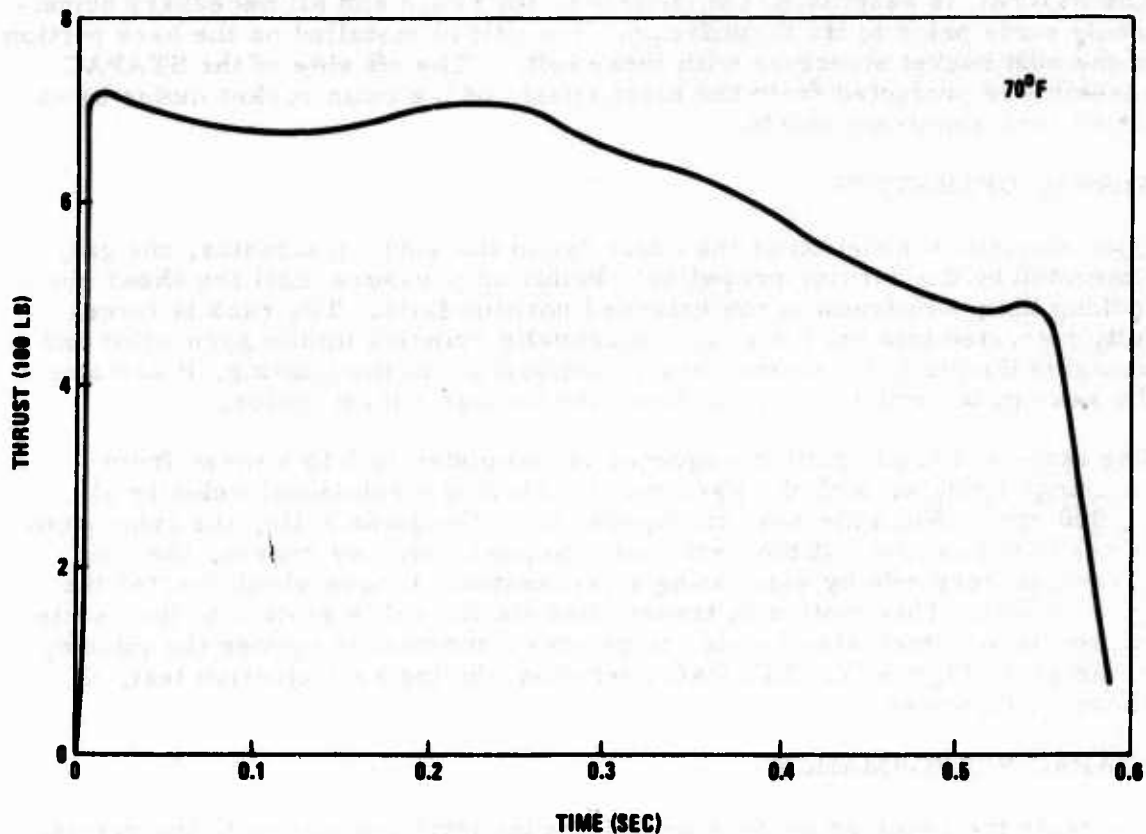


FIGURE 46. VERNIER ROCKET PERFORMANCE

Precessional motion of the gyroscope is transmitted to the vernier rocket by a cable arrangement consisting of four cable assemblies, three sectors and two tension adjusters. The sectors are designed to provide a motion ratio of 3 to 2 between the vernier rocket and the gyroscope; the gyroscope has a maximum precessional angle of ± 30 degrees and the vernier rocket ± 45 degrees. A negator spring, used to bias the output signal of the gyro, is installed on the actuator housing with its free end attached to one of the tension adjusters.

A sear-puller device is used to mechanically fire the vernier rocket motor. The sear-puller is a sliding collar that fits around the piston/rack and attaches to the rocket firing mechanism. When the actuator is initiated, the sear-puller device is actuated as the piston/rack is thrust into the spin-up actuator housing. A roll pin installed in the piston/rack assembly prevents rebounding of the sear puller into the gyro rotor.

All pivoting joints on the STAPAC unit, except the rotor spindle, incorporate ball bearings to minimize friction.

The STAPAC is assembled completely on the bench and all necessary adjustments made prior to its installation. The unit is installed on the back portion of the seat bucket structure with three bolts. The aft side of the STAPAC assembly is protected from the blast effects of the main rocket motor by an 0.080-inch aluminum shield.

STAPAC OPERATION

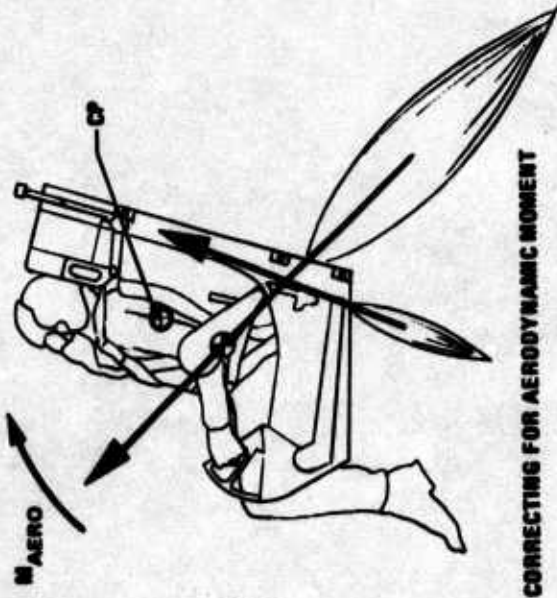
Upon electrical initiation of the cartridge in the spin-up actuator, the gas, generated by the burning propellant, builds up pressure until the shear pin locking the piston/rack in the extended position fails. The rack is forcefully retracted into the housing, sequentially spinning up the gyro rotor and uncaging the gimbal. As the rack is retracted into the housing, it actuates the sear puller which, in turn, fires the vernier rocket motor.

The spin-up/rocket ignition sequence is completed in 5 to 6 msec from cartridge ignition, with the gyro rotor achieving a rotational velocity of 11,000 rpm. When the seat disengages from the guide rails, the subsystem is ready to function. If the seat starts to pitch, for any reason, the rate gyroscope responds by generating a precessional torque which rotates the gyro gimbal. This motion is transmitted via the cable system to the vernier rocket motor which also rotates to provide a moment to oppose the pitching of the seat, Figure 47. STAPAC operation, during seat ejection test, is shown in Figure 48.

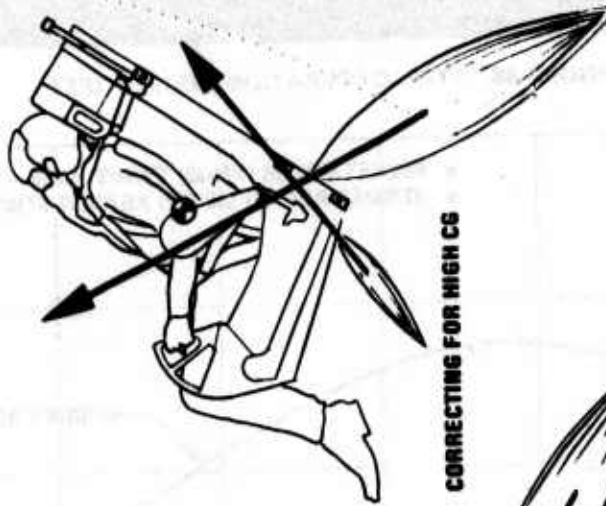
STAPAC PERFORMANCE

To obtain the required performance from the pitch control unit, the vernier rocket must be able to create a moment greater than the disturbing moment of the rocket catapult sustainer motor. This excess torque is required to attenuate the rotation of the seat after the STAPAC system has achieved control. The STAPAC unit has a finite response time and, therefore, must be capable of correcting for seat pitch-rate overshoot. Figure 49 is a plot showing the relative moment-producing capability of the XM-39 rocket motor when the thrust line is displaced 2 inches from the seat system dynamic cg, and when the vernier rocket is rotated 45 degrees from the position where its thrust line passes through the dynamic cg. The graph shows that the angular travel, thrust level, and impulse of the vernier rocket are sufficient to produce moments equal to or greater than those of the main rocket during its entire burntime.

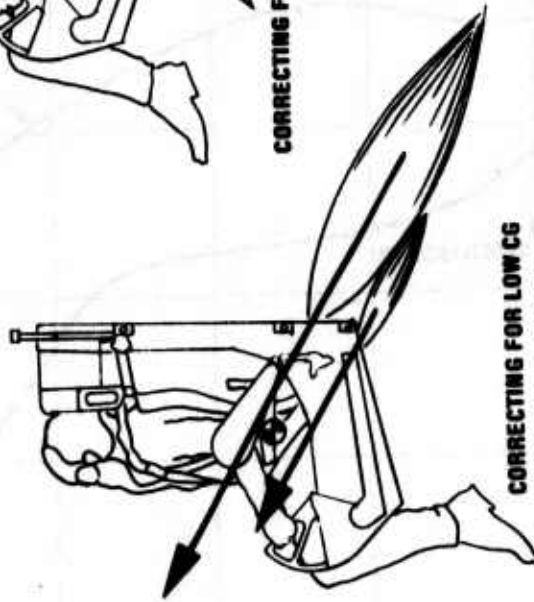
To compensate for the adverse effects of forward pitching on the seat recovery performance (thrust line above cg), a spring is employed to bias the signal output of the gyroscope. The spring used in the ACES STAPAC is a negator, which exhibits constant force at infinite deflection. The spring is employed to induce a torque about the gimbal axis equal to 3 rpm aft pitch of the seat system, Figure 50. In this plot, the seat is oscillating about a constant aft pitch slope equal to 3 rpm, and the amplitude and period of oscillation are influenced by such factors as STAPAC friction, vernier rocket torque, pitch axis inertia of the seat, and the relative moment-producing capability of the vernier and main rocket motors.



CORRECTING FOR AERODYNAMIC MOMENT



CORRECTING FOR HIGH CG



CORRECTING FOR LOW CG

FIGURE 47. STAPAC OPERATION



FIGURE 48. STAPAC OPERATION DURING TEST

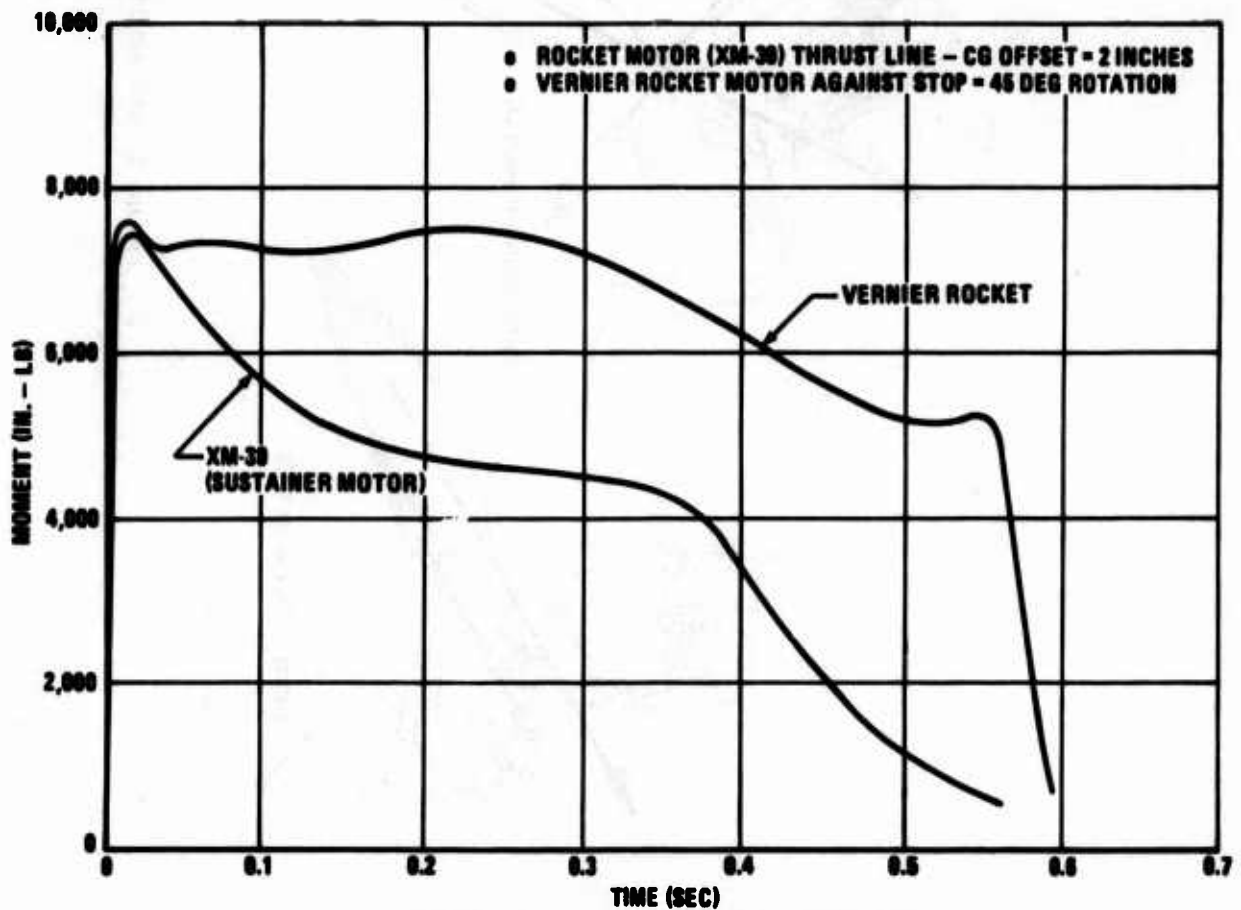


FIGURE 49. ROCKET MOTOR PITCHING MOMENTS

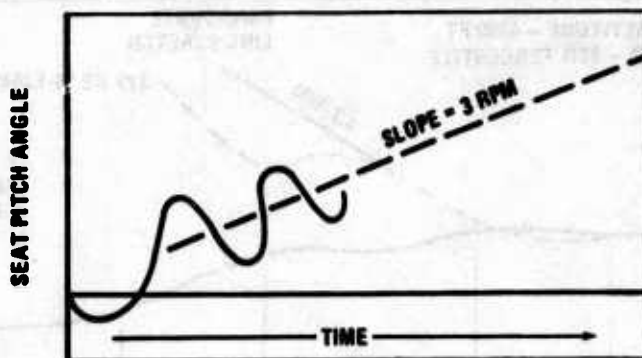


FIGURE 50. PITCH ANGLE VS TIME (WITH BIASING SPRING)

In Figure 51, a computed seat pitch-angle history comparison is shown for an unstabilized seat and one incorporating the STAPAC unit. It is noted that in both of the stabilized-seat cases, the low pitch rate at main rocket burn-out is indicative of excellent control.

The gyro-controlled vernier rocket must provide pitch stability for all Mode 1 ejection conditions up to the time the recovery parachute starts to apply a drag force on the occupied seat. This covers the speed range from 0 to 300 KEAS at sea level. Pitch angle vs time data are plotted in Figure 52 for a zero-speed and a 227-KEAS ejection test performed at 4200 feet alti-

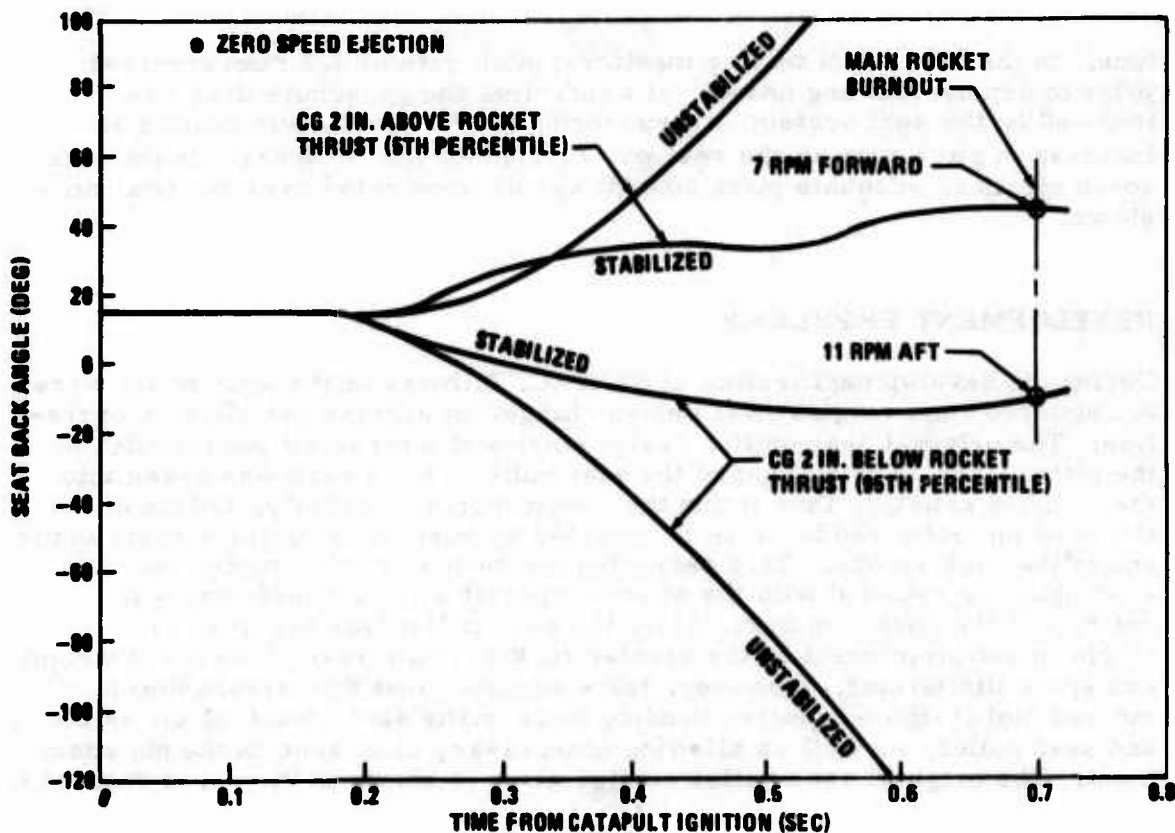


FIGURE 51. COMPUTED PITCH STABILIZATION PERFORMANCE

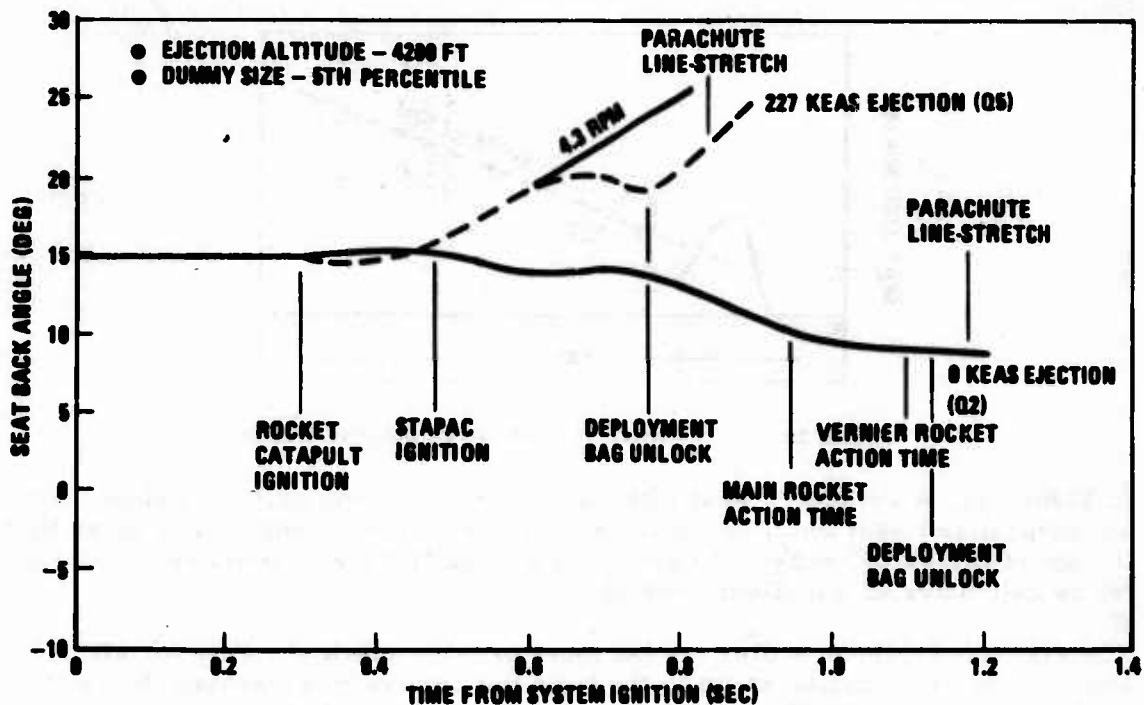


FIGURE 52. PITCH STABILIZATION FOR MODE 1 EJECTIONS

tude. In the 227-KEAS test, a maximum pitch rate of 4.3 rpm occurred prior to deployment bag unlock, at which time the parachute drag was imposed on the seat system, overpowering the STAPAC, and causing an increase in pitch rate as the seat was reoriented for recovery. In the zero-speed ejection, adequate pitch control was demonstrated over the total time shown.

DEVELOPMENT PROBLEMS

During the development testing of STAPAC, failures of the sear puller were encountered requiring several design changes to achieve satisfactory operation. The original sear-puller design employed a threaded pin installed in the piston/rack, which engaged the sear puller as the rack was drawn into the actuator housing, thus firing the rocket motor. Initially, failure of the threaded pin occurred because it impacted against the actuator housing at the end of the rack stroke. This permitted the vernier rocket motor sear and sear puller to rebound with the attendant possibility of interfering with rotation of the rocket motor. Also, the sear puller was designed for a single-shear attachment to the vernier rocket motor sear, because of weight and space limitations. However, tests indicated that this arrangement induced higher-than-expected bending loads in the sear attaching clevis pin and sear puller, as well as allowing unnecessary clearance in the pin attachment. The original sear-puller configuration is shown in View A of Figure 53.

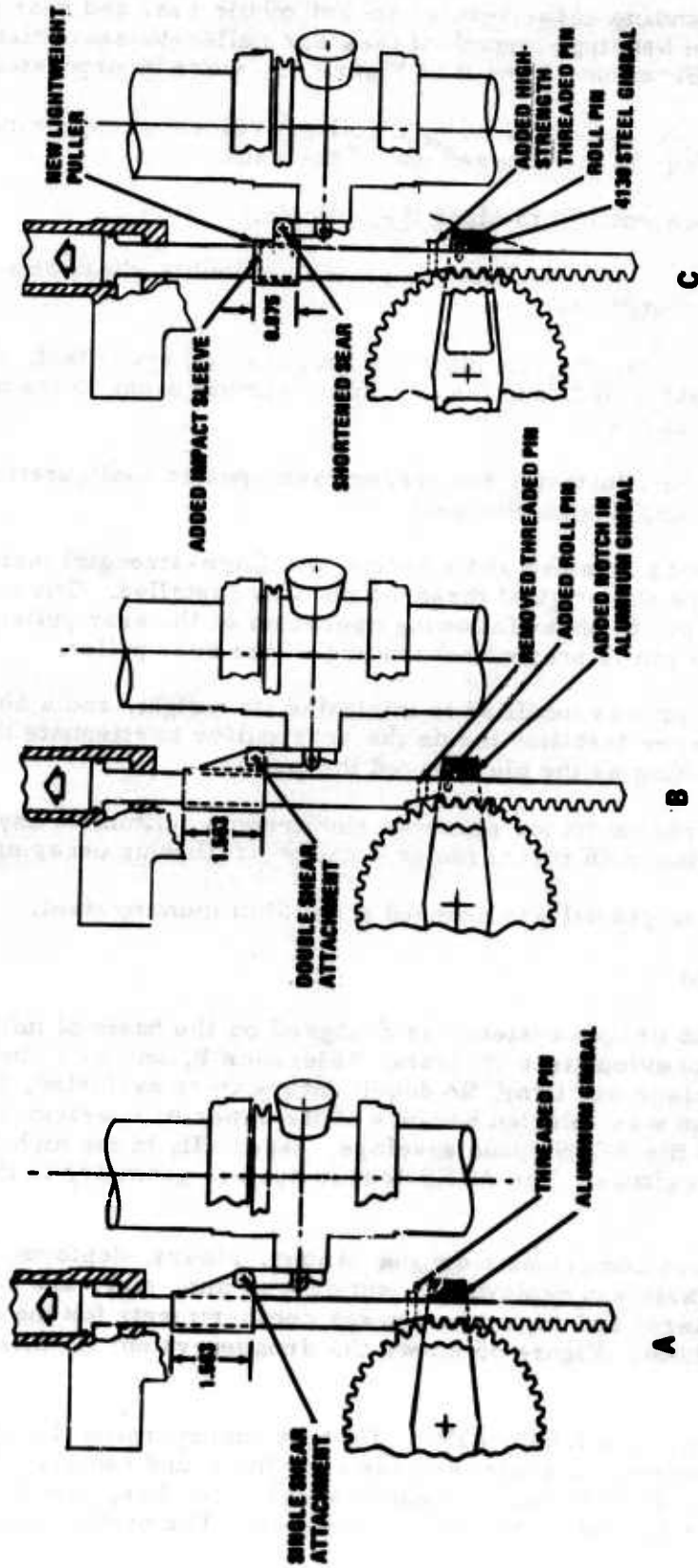


FIGURE 53. STAPAC FIRING MECHANISM REVISIONS (ALTERNATE)

To eliminate rebounding of the vernier rocket motor sear and sear puller, and to increase the bending strength of the sear puller-to-sear attachment, the following modifications, View B of Figure 53, were incorporated:

1. The threaded pin was replaced by a roll pin relocated approximately 0.75 inch closer to the exposed end of the rack.
2. The gimbal was notched to clear the roll pin.
3. The sear puller was redesigned to provide a double shear attachment of the rocket motor sear.

With this configuration, the roll pin failed in shear on every test, whether or not the sear was extracted, and the aluminum gimbal broke in the notched area in nearly all cases.

View C of Figure 53 illustrates the present sear-puller configuration, which included the following design changes:

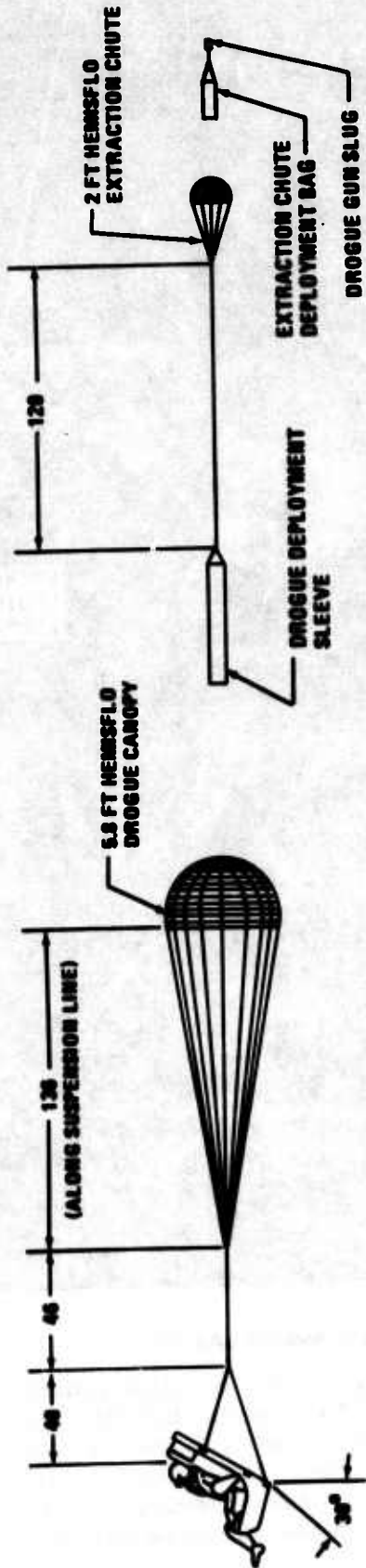
1. The roll pin was retained and a second pin (high-strength) installed in the rack where the original threaded pin was installed. The concept was to allow this pin to shear following operation of the sear puller, and to allow the roll pin to prevent rebounding of the sear puller.
2. The sear puller was modified to minimize its weight, and a 6061-T6 aluminum sleeve installed inside the sear puller to attenuate the effects of impact loading as the pin engaged the puller.
3. The vernier rocket motor sear was shortened to eliminate any possibility of it interfering with rocket motor rotation, following uncaging of the gyro.
4. The gyroscope gimbal was changed from aluminum to steel.

DROGUE SYSTEM

The present ACES drogue system was designed on the basis of information obtained from a previous test program, Reference 8, and on a study in which ribless guide surface and Hemisflo decelerators were evaluated, Reference 5. A hemisflo drogue was selected because of its superior operational characteristics throughout the ACES speed envelope, especially in the high-transonic and supersonic regimes. The ACES drogue system geometry is illustrated in Figure 54.

The drogue system comprises a drogue canopy, risers, deployment sleeve; extraction parachute and deployment bag; drogue gun, slug, and cartridge; FLSC bridle cutters; and separate stowage compartments for the drogue and extraction chute. Figure 55 shows the drogue system installed on the seat.

The drogue canopy is a 5.8-foot Hemisflo type incorporating 16 gores constructed of 650-pound horizontal ribbons and 400-pound radials. The 16 suspension lines, 1500-pound coreless braided nylon line, are divided into four groups and attached to the bridle assembly. The bridle, made from



NOTE:
 DIMENSIONS ARE IN INCHES
 UNLESS OTHERWISE NOTED

FIGURE 54. DROGUE PARACHUTE SYSTEM

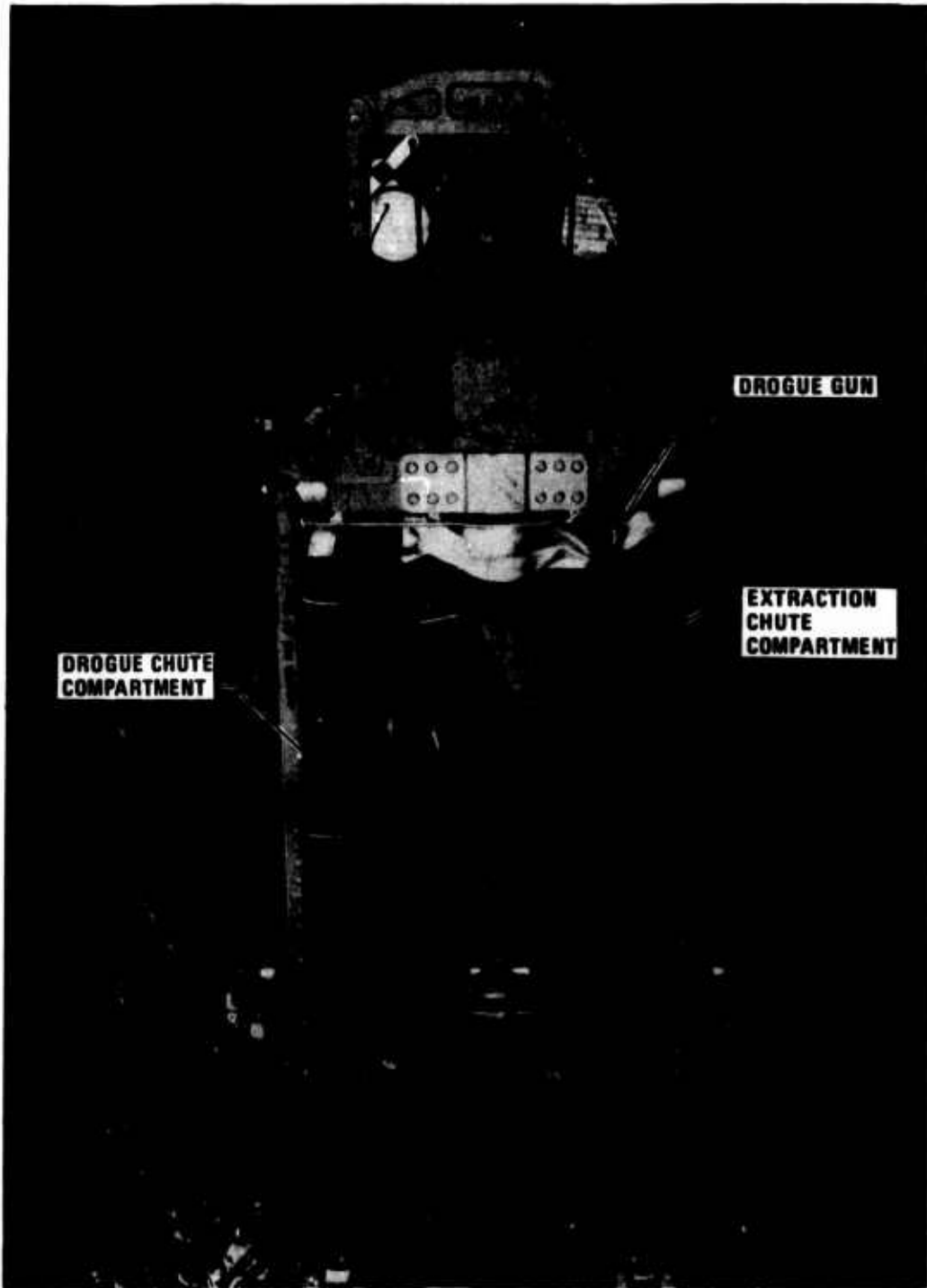


FIGURE 55. DROGUE INSTALLATION

6000-pound nylon webbing, has four loop-ends, for attachment of the suspension lines, a solid portion, and four loop-ends that attach to the seat. The lower bridle segments, that attach to the seat, are encased in a silicone-impregnated fiberglass fabric sleeve to provide thermal protection from the rocket catapult motor plume. The lower bridle segments are fastened to the seat by 100-pound nylon tie-cords, which are covered with a Teflon tubing, Figure 55.

The drogue is stowed in a cotton sleeve to assure an orderly, line-first deployment. The apex of the drogue canopy is attached to the top of the sleeve with a 50-pound cotton cord, and a restrictor band is employed to provide additional retention of the apex to the top of the sleeve, Figure 56. Release of the restrictor band is accomplished by a nylon line that is routed through a grommet in the sleeve, and down to the bottom of the sleeve where

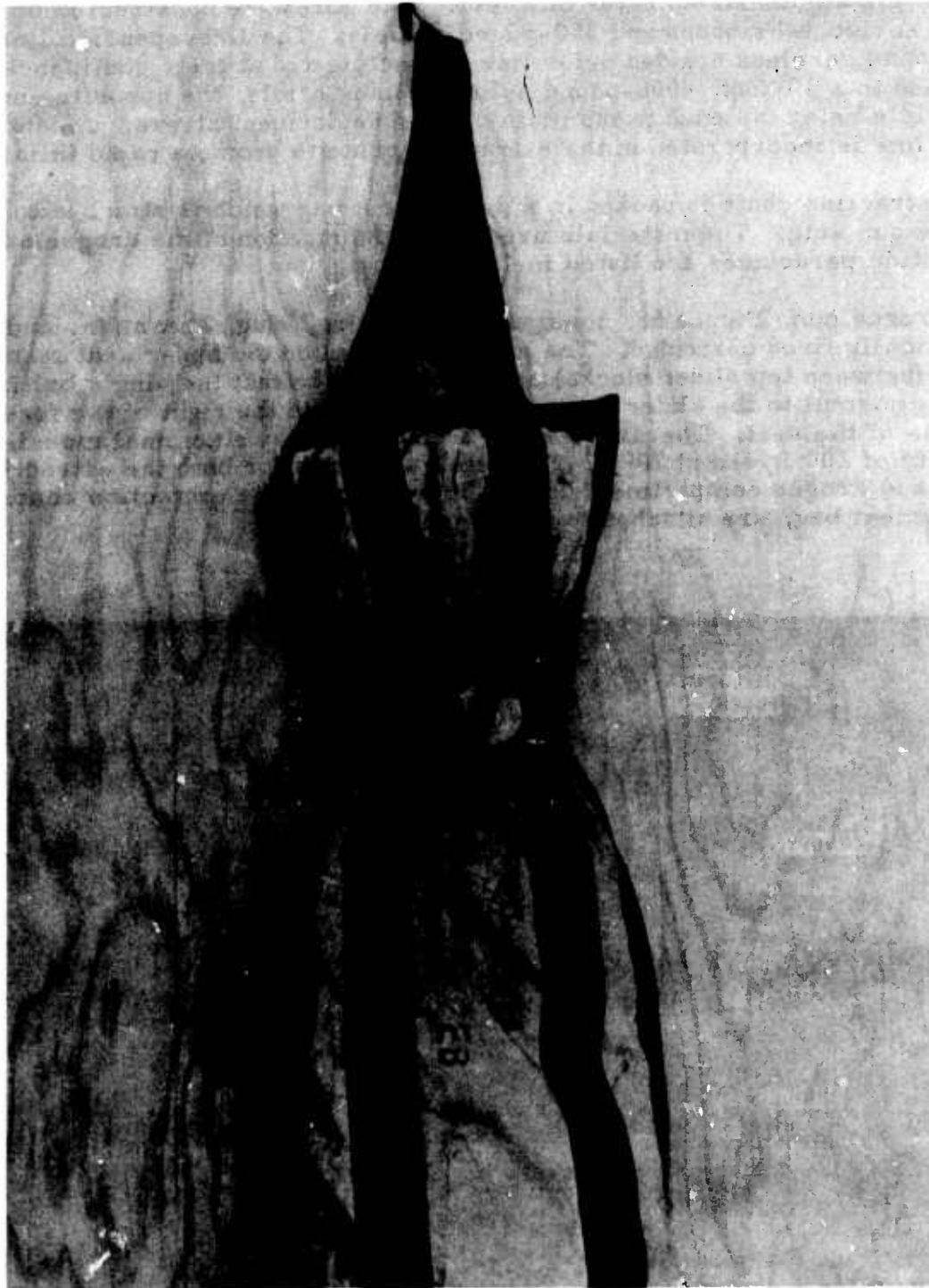


FIGURE 56. RESTRICTOR BAND INSTALLATION

it is attached to a suspension line. The restrictor band is designed to prevent the drogue apex from moving to the bottom of the sleeve prematurely as a result of extraction chute opening forces. Premature downward motion of the drogue within the sleeve can result in exposure of the drogue canopy to the air stream before the suspension lines have deployed.

The extraction chute, Figure 57, is a hemisflo design incorporating 12 gores and having a nominal diameter of 2 feet. The gores are constructed of 400-pound horizontal ribbons and 250-pound radials. The 12 suspension lines, 400-pound coreless braided nylon line, are collected at their confluence and attached to a 10-foot, 4000-pound nylon webbing bridle, the opposite end of the bridle being fastened to the main drogue deployment sleeve. An anti-squid line is incorporated in the extraction chute to promote rapid inflation.

The extraction chute is packed in a deployment bag which is attached to the drogue gun slug. The materials used in the fabrication of the drogue and extraction parachutes are listed in Table VI.

The drogue gun, Figure 58, consists of a housing, slug, shear pin, and electrically fired cartridge. The gun is mounted on the upper seat structural beam (between top slider blocks) and is oriented so that the slug's ballistic path is normal to the slider plane and 30 degrees to the right of the fore-and-aft axis of the seat. The slug weighs 1 pound and has a nominal muzzle velocity of 200 ft/sec at 70°F. The latch assembly for both the extraction chute and drogue compartment doors, in addition to the extraction chute deployment bag, are attached to the drogue gun slug.

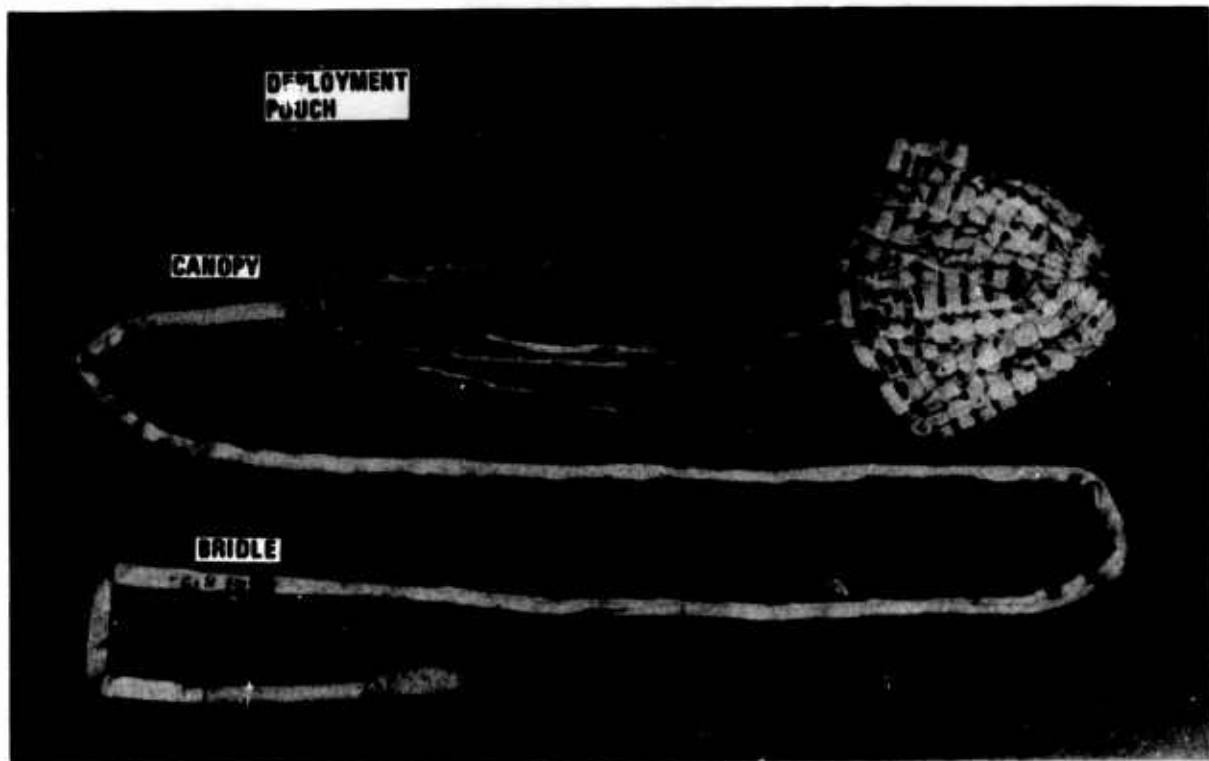


FIGURE 57. EXTRACTION CHUTE ASSEMBLY

TABLE VI
DROGUE SYSTEM PHYSICAL DATA

	Drogue	Extraction Chute
Diameter, D_o	5.8 ft	2.0 ft
No. of Gores	16	12
Suspension Lines	MIL-C-7515, TY V, 1500 lb (140 in.)	MIL-C-7515, TY I, 400 lb (30 in.)
Horizontal Ribbons	MIL-T-5608, TY I, Class E, 1.25 in., 650 lb	MIL-T-5038, TY III, 0.75 in., 400 lb
Radial Ribbons	MIL-T-5038, TY III, 0.75 in., 400 lb	MIL-T-5038, TY III, 0.5 in., 250 lb
Vertical Ribbons	MIL-T-5608, TY II, Class C, 0.38 in., 58 lb	MIL-T-5038, TY III, 0.38 in., 200 lb
Skirt Band	MIL-T-5038, TY III, 1 in., 525 lb	MIL-T-5038, TY III, 0.75 in., 400 lb
Vent Band	MIL-W-27657, TY I, 0.75 in., 3000 lb	MIL-C-7515, TY II, 550 lb
Vent Lines	MIL-C-7515, TY V, 1500 lb	MIL-C-7515, TY I, 400 lb
Vent Cap	MIL-C-7020, TY I, 1.1 oz (treated to reduce porosity)	Not Applicable
Anti-Squid Line	Not Applicable	MIL-C-7515, TY V, 1500 lb
No. of Radials per Main Seam	3	2
Porosity	19 percent	18.5 percent
Bridle	MIL-W-4088, TY XVIII, 1 in., 6000 lb	MIL-W-5625, 1 in., 4000 lb

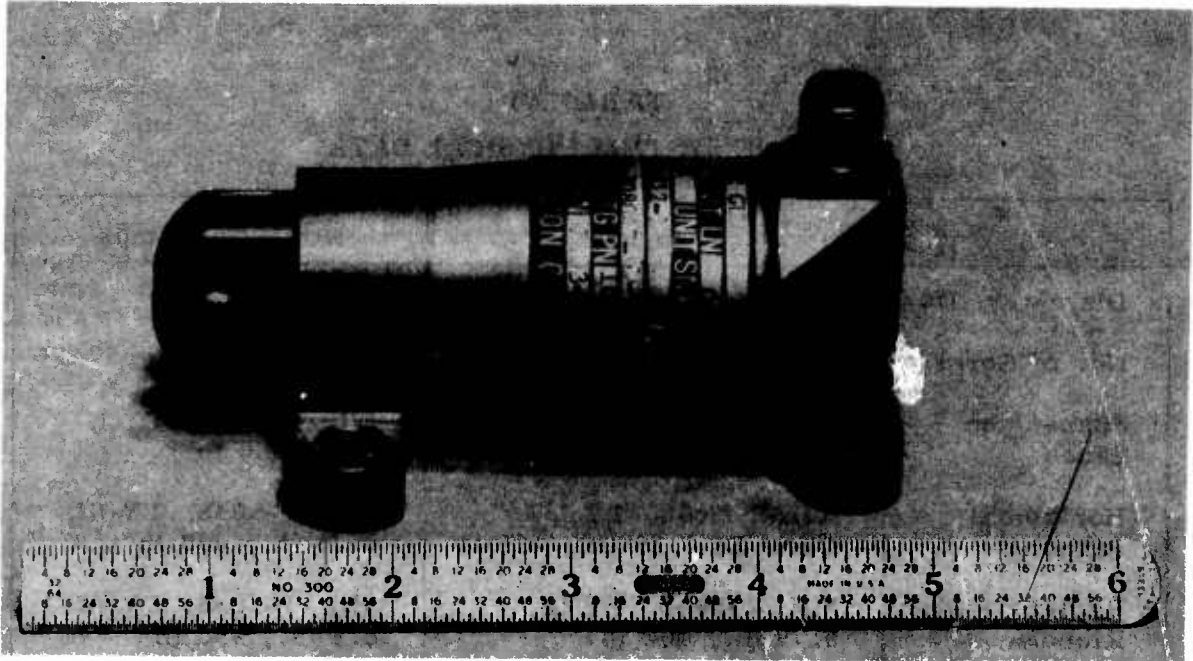


FIGURE 58. DROGUE GUN

The drogue bridle is attached to the upper and lower slider block shafts, and four electrically initiated FLSC cutter devices are installed adjacent to the webbing, Figure 59. The cutters sever the drogue bridle upon receipt of an electrical signal from the Recovery Sequencing Unit.

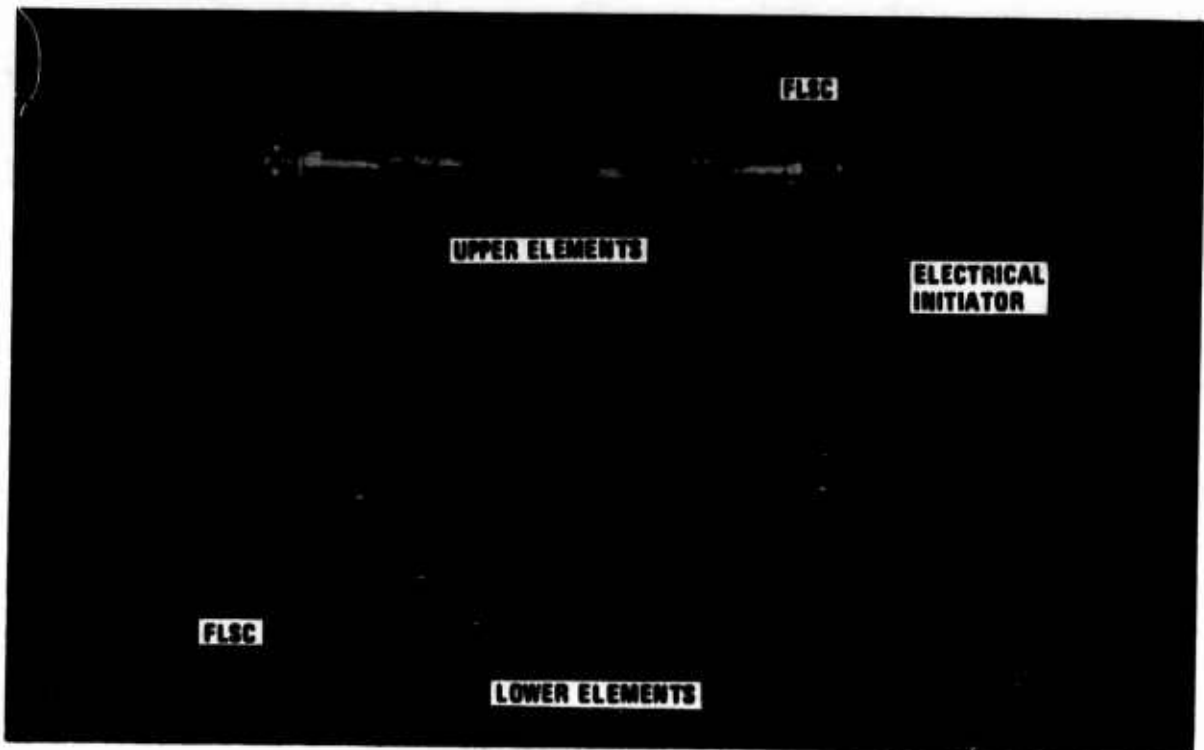


FIGURE 59. DROGUE BRIDLE CUTTERS

DROGUE OPERATION AND PERFORMANCE

During ejection, as the seat nears the top of the guide rails, redundant electrical signals from the recovery sequencer fire the drogue gun cartridge, if the seat is in a Mode 2 or Mode 3 environment. The 1-pound slug is propelled aft at an angle of 30 degrees from the fore-and-aft axis of the seat, simultaneously unlatching the extraction chute and drogue compartment doors. As the extraction chute is pulled from its compartment by the slug, the cover is blown aft and the 10-foot bridle begins to pay out. When the deployment bag strips off, the extraction chute inflates, transmitting load to the drogue sleeve. The drogue suspension lines pay out first, followed by release of the restrictor band, sleeve strip-off, and drogue inflation. The sequence of operation is shown in Figure 60.

To satisfy the seat system stability requirements, the drogue must be effective in time to prevent any large angular deviations of the seat as it enters the air stream. Therefore, the time-to-effectiveness is a significant factor in the performance of the drogue system, especially with ejection at higher speeds where the magnitudes of the aerodynamic moments on the seat are large and STAPAC is less effective. Drogue performance is shown in Figure 61 using data obtained from seat ejection tests. The extraction chute's operating time is shown to be relatively constant from 400 to 600 KEAS, attributable to the high drogue gun slug velocity and small diameter of the extraction chute. The anti-squid line is presumed to contribute to the uniform operation. A slight increase in time to full inflation of the extraction chute occurs below 400 KEAS. The time from drogue-gun-fire to full inflation of the drogue is well within the predicted value of 0.3 second at 600 KEAS, Reference 3.

The stabilization provided by the drogue system is illustrated in Figure 62, in which seat back angle is plotted as a function of time. In the 438-KEAS test, the seat pitches forward as it leaves the guide rails, seeking an aerodynamic trim attitude forward of the launch attitude. By the time the forward pitching is arrested, the seat rotates approximately 35 degrees. As the seat rotates aft, it overshoots the 30-degree design trim angle, Figure 54, and the parachute mortar fires when the back angle is approximately 40 degrees. In the 578-KEAS test, the aft tip-off is necessarily more severe than on the 438-KEAS test and, by the time the seat pitches forward 7 degrees, the drogue reverses the rotation. The seat rotates aft 5 degrees beyond the trim attitude, with the seat-back at approximately 28 degrees at parachute mortar fire.

The size of the present drogue was based on the requirement to decelerate the seat and 95th percentile occupant from 600 KEAS to a velocity of 320 KEAS at recovery parachute line-stretch in 0.51 second at 16,000 feet, Reference 5. The 0.51-second parachute time-delay was used to make the original ACES Mode 2 performance predictions and was incorporated as a specification requirement for the recovery sequencer. The 320-KEAS line-stretch velocity was considered to be within the capability of the reefed C-9 parachute on the basis of whirl tower tests in which canopies with a 5-percent reefed drag area were successfully tested at vehicle release velocities of 330 KEAS, using 300-pound torso dummies. Reefed inflation forces of approximately 6000 pounds were calculated for the ACES recovery parachute using reefed-fill times measured in the whirl tower tests. Loads of this magnitude were believed within the structural capability of a reefed C-9 canopy.

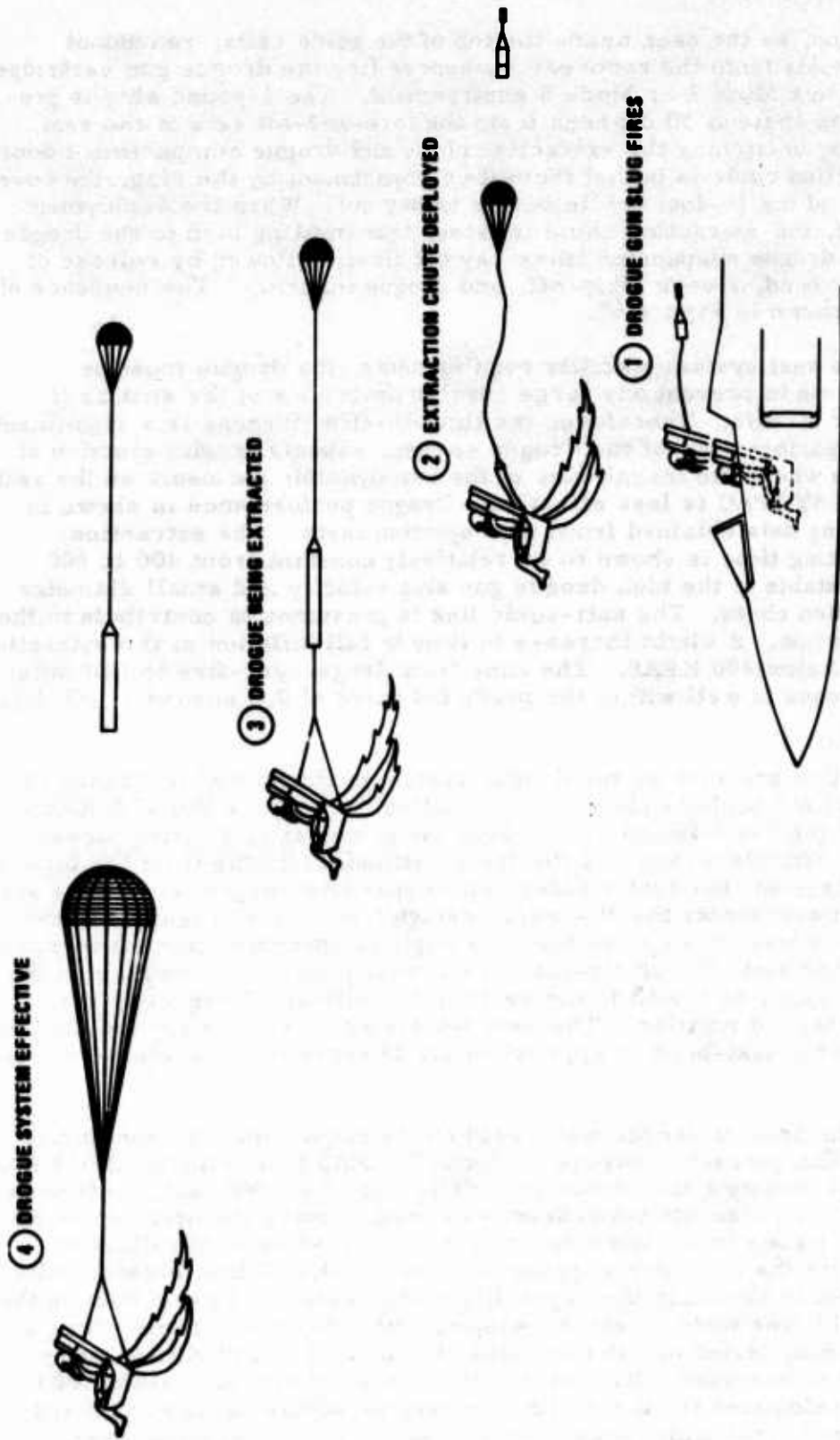


FIGURE 80. DROGUE SYSTEM OPERATION

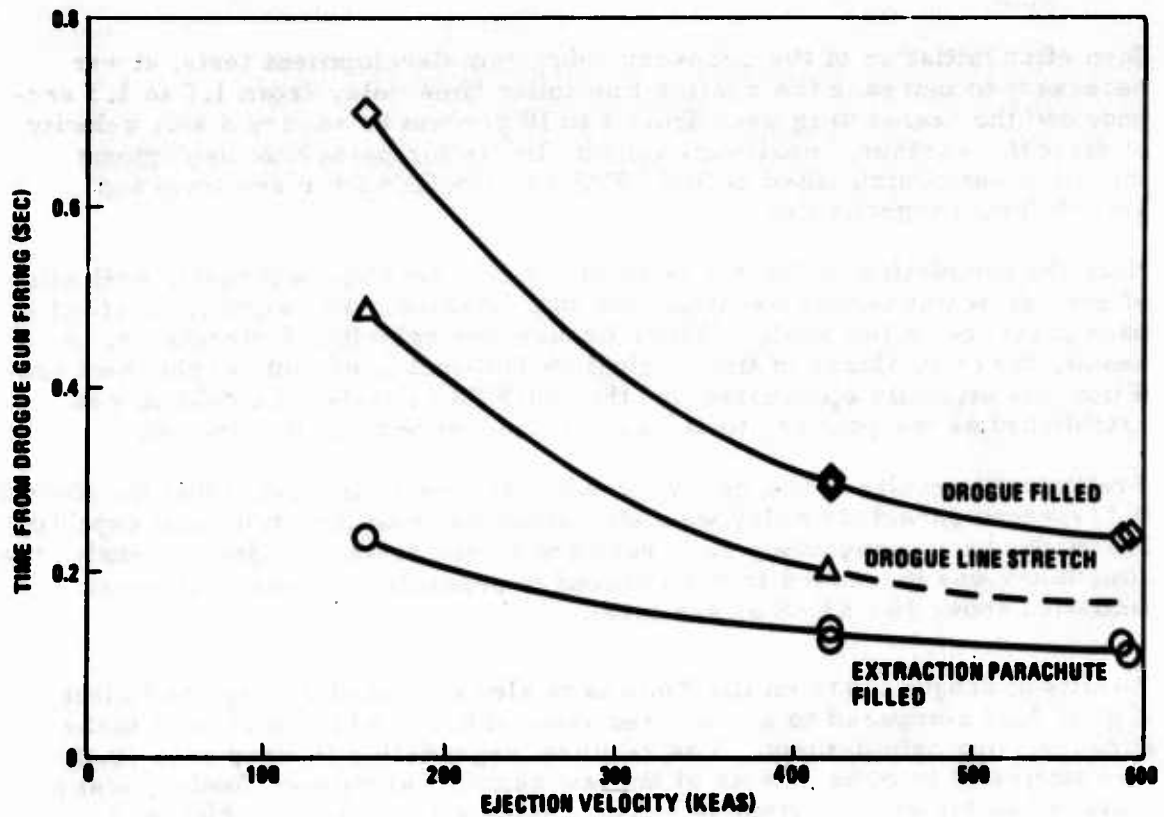


FIGURE 61. DROGUE OPERATIONAL TIMES

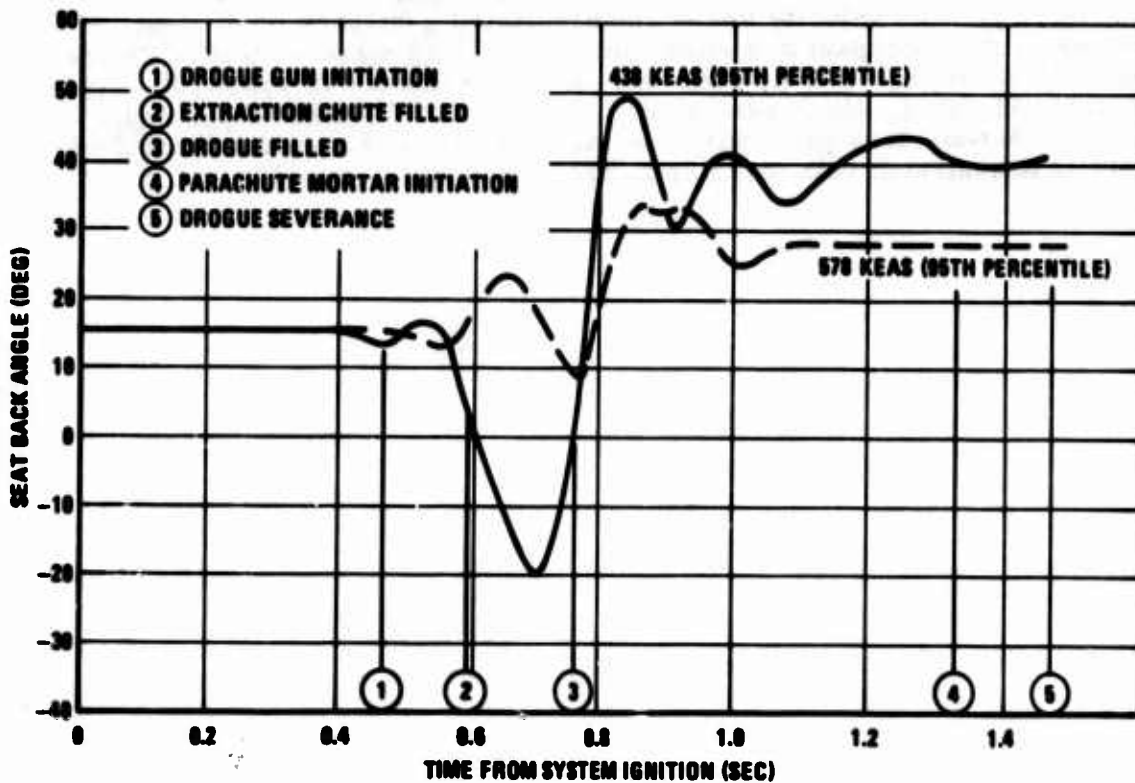


FIGURE 62. PITCH STABILIZATION FOR MODE 2 EJECTIONS

Soon after initiation of the recovery subsystem development tests, it was necessary to increase the reefing line cutter time delay from 1.0 to 1.3 seconds and the reefed drag area from 4 to 10 percent to assure a safe velocity at disreef. Further, maximum velocity limits for parachute deployment initiation were established at 300 KEAS and 175 KEAS for sea level and 16,000 feet, respectively.

Near the completion of the recovery subsystem development tests, evaluation of environmental sensor dynamic test data disclosed the significant effect of base pressure on the Mode 2/Mode 3 crossover velocity, Reference 9. As a result, the criticalness of the original 16,000-foot parachute deployment condition was virtually eliminated and the 300-KEAS sea-level condition was established as the primary deceleration requirement for the drogue.

Preliminary results of the recovery subsystem tests indicated that the Mode 2 0.51-second parachute delay was not compatible with the structural capability of the recovery parachute. As a result of a seat system trajectory study, the time delay was increased to 0.85 second to preclude recovery subsystem initiation above 300 KEAS at sea level.

Results of drogue tests on the Tomahawk sled indicated a drag coefficient (C_d) of 0.22 compared to a predicted value of 0.36, which was used in the drogue-sizing calculations. The resultant degradation in drag area (C_dS) was attributed to wake effects of the test setup, a simulated (boilerplate) seat installed on top of the Tomahawk sled. Using a C_d of 0.33, which was considered a more realistic value for the drogue behind the actual ejection seat, the adequacy of the 0.85-second delay was re-evaluated and determined to be satisfactory. The velocity decay and associated g-history of the seat and 95th percentile occupant are shown for a 578-KEAS ejection test in Figure 63. The velocity at the time the recovery parachute mortar is initiated is approximately 298 KEAS, which results in a velocity of 250 KEAS at parachute line stretch. Satisfactory parachute operation was demonstrated in bomb drop tests at line-stretch velocities up to 272 KEAS, Reference 10.

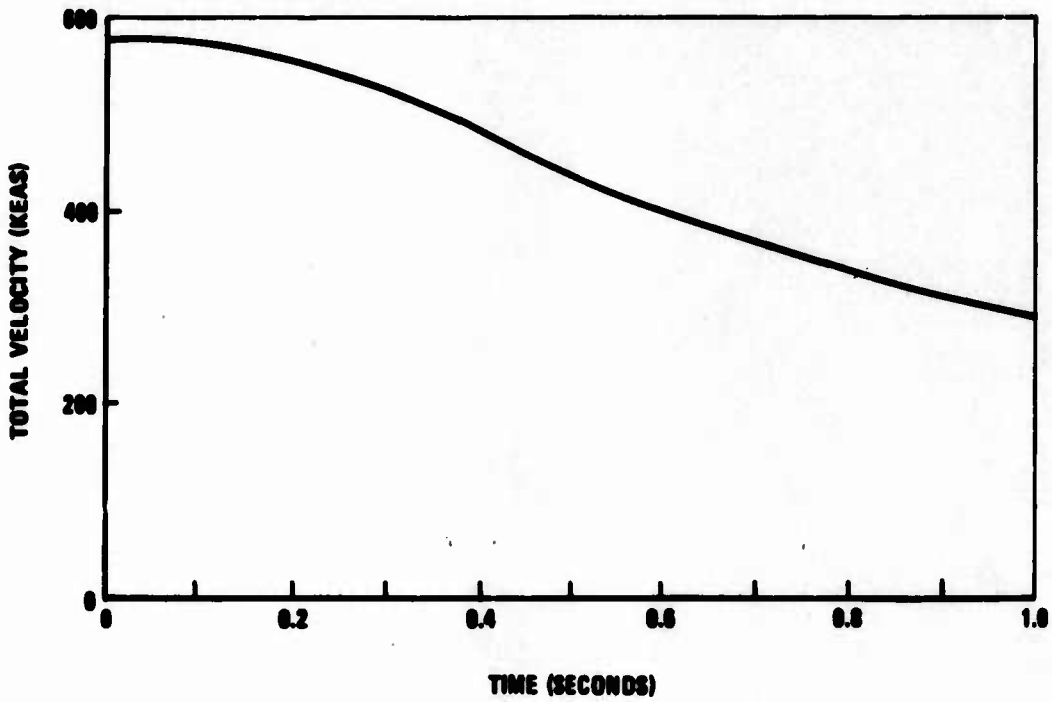
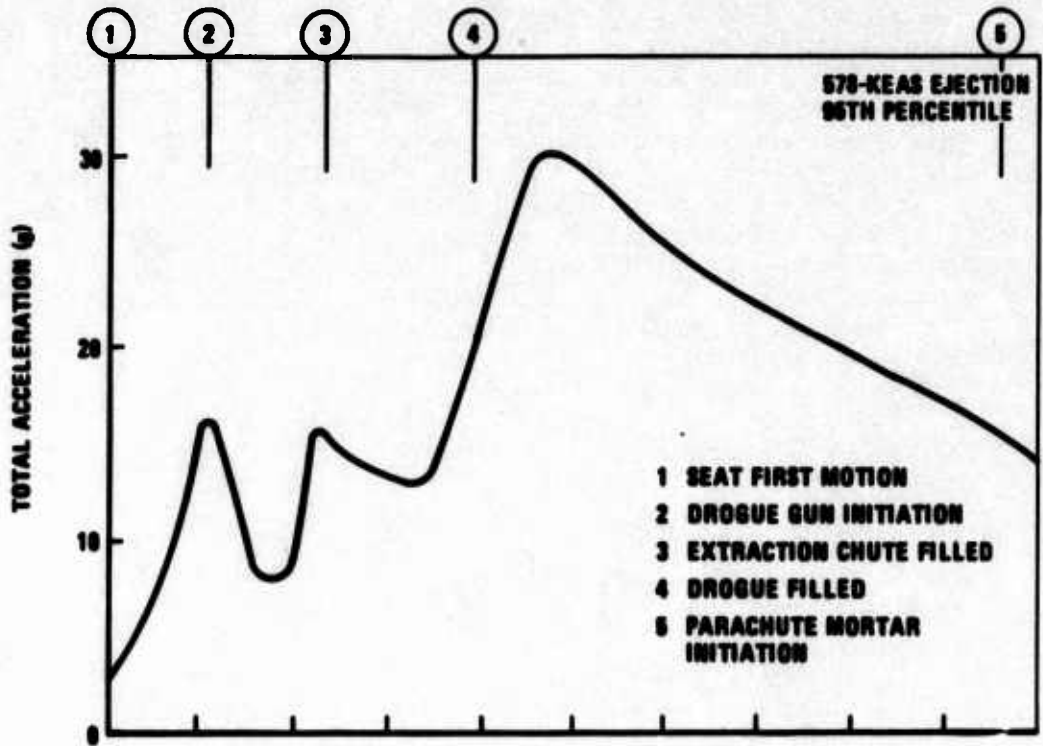


FIGURE 63. DROGUE PERFORMANCE

SECTION X

RECOVERY SUBSYSTEM

A reefed, mortar-deployed, 28-foot, flat-circular parachute is employed as the ACES recovery subsystem, Figure 64. The principal components of this subsystem are a canopy assembly, deployment bag, pilot chute, mortar, reefing line cutters, and cover assembly.

The parachute canopy is a conventional 28-foot flat-circular design, Air Force type C-9. The apex area of the canopy is reinforced with three concentric 1-inch-wide nylon tapes, each having a breaking strength of 525 pounds. In addition, two reefing line cutter pockets (at lines No. 7 and 21) and 30 reefing rings are installed on the skirt of the canopy, with backup arming lanyards stitched to lines No. 7 and 21. The reefing line, MIL-C-7515, Type III nylon line, is 156 inches in length, providing a reefed drag area equivalent to 10 percent of the canopy surface area.

The canopy is packed in a deployment bag that incorporates longitudinal tunnels for stowage of the suspension lines, Figure 65. Flaps on the open end of the bag retain the canopy until the suspension lines have deployed. A 0.090-inch aluminum doubler is incorporated in the top section of the bag to carry the mortar thrust load. Pilot chute attachment is provided by a triangular-shaped, reinforced fabric panel attached at the top of the bag and extending its full length. Retainer flaps, released at the end of the mortar stroke, cover the ends of the longitudinal tunnels to prevent line spillage resulting from mortar-induced accelerations.

A four-vane pilot chute having a nominal diameter of 36.1 inches is used to assist deployment of the parachute. The pilot chute is stowed in a pouch that is attached to the seat structure. The pilot chute is extracted through a 3.5-inch slit in the top of the pouch. The pilot chute and pouch are shown in Figure 66.

The mortar consists of an inner and outer tube that are assembled with a shear pin, Figure 67. The lower end of the inner tube incorporates an integrally machined fitting, which is the upper half of a disconnect; the lower half attaches to the seat structure. The upper end of the outer tube incorporates an extension that allows attachment of the mortar assembly to the deployment bag. A bell-shaped fitting, installed on the lower end of the outer tube, disperses the cartridge residual propellant fragments away from the deployment bag when the mortar tubes separate. A pair of machined fingers, attached to the outer tube, are used to maintain alignment of the reefing line cutters during and following parachute packing. The mortar has a stroke of 17 inches and provides a nominal velocity of 59 ft/sec at the time the tubes separate.

The reefing line cutter, Figure 68, incorporates a 1.3-second delay element and is designed to cut MIL-C-7515, Type III nylon line. Two cutters are installed on the parachute canopy at lines No. 7 and 21.

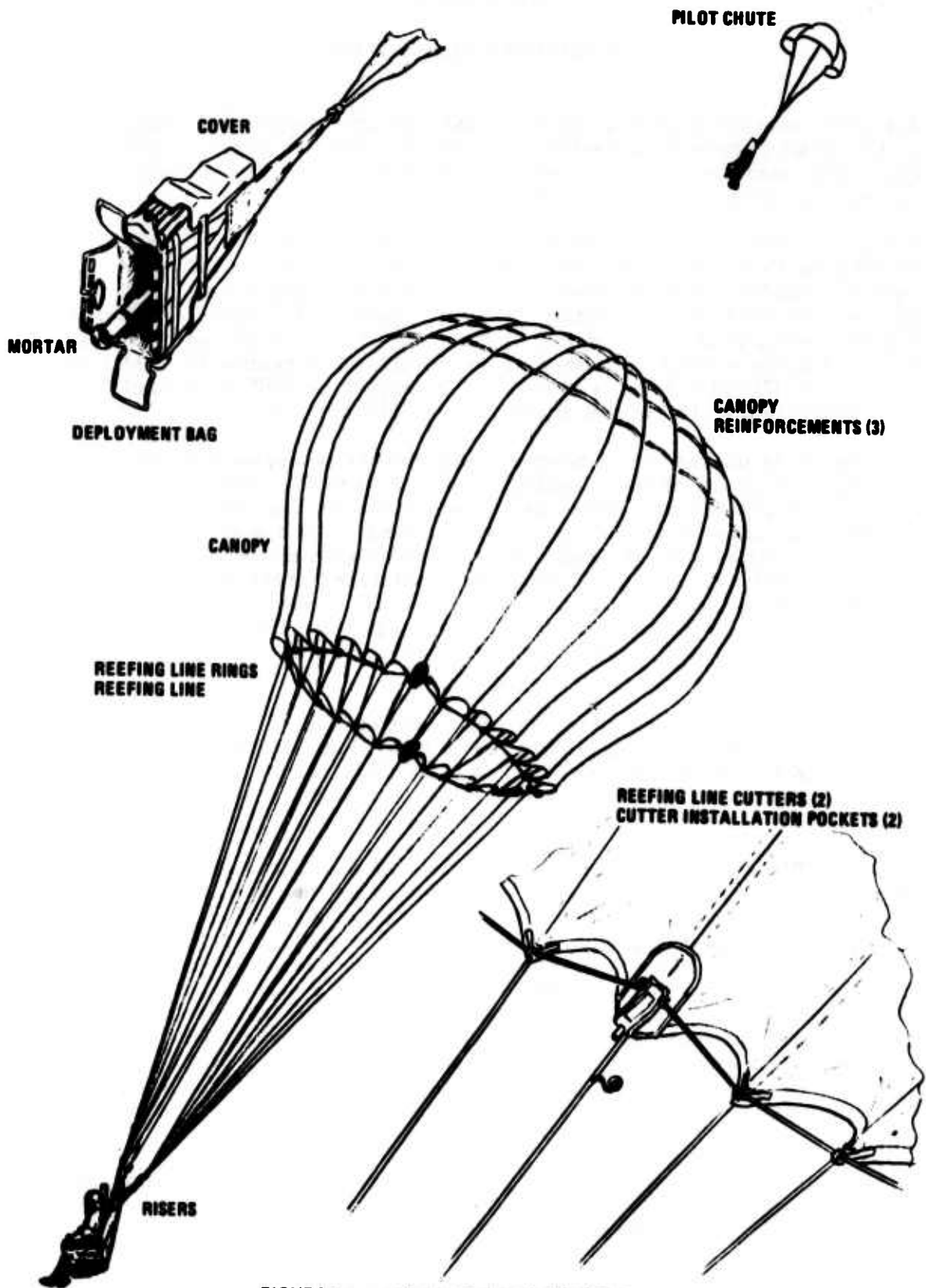


FIGURE 64. ACES RECOVERY SUBSYSTEM



FIGURE 65. DEPLOYMENT BAG

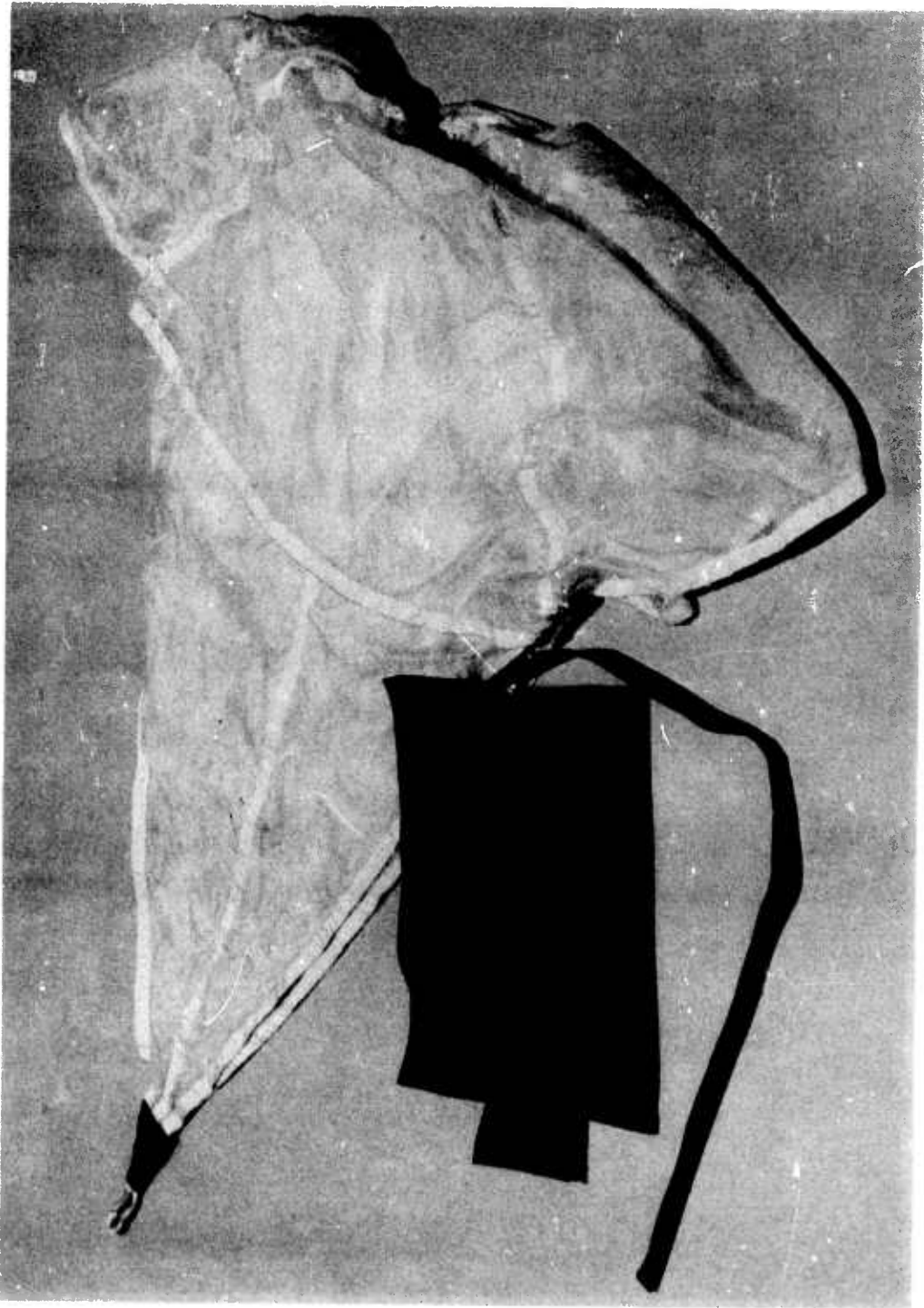


FIGURE 66. PILOT CHUTE AND POUCH

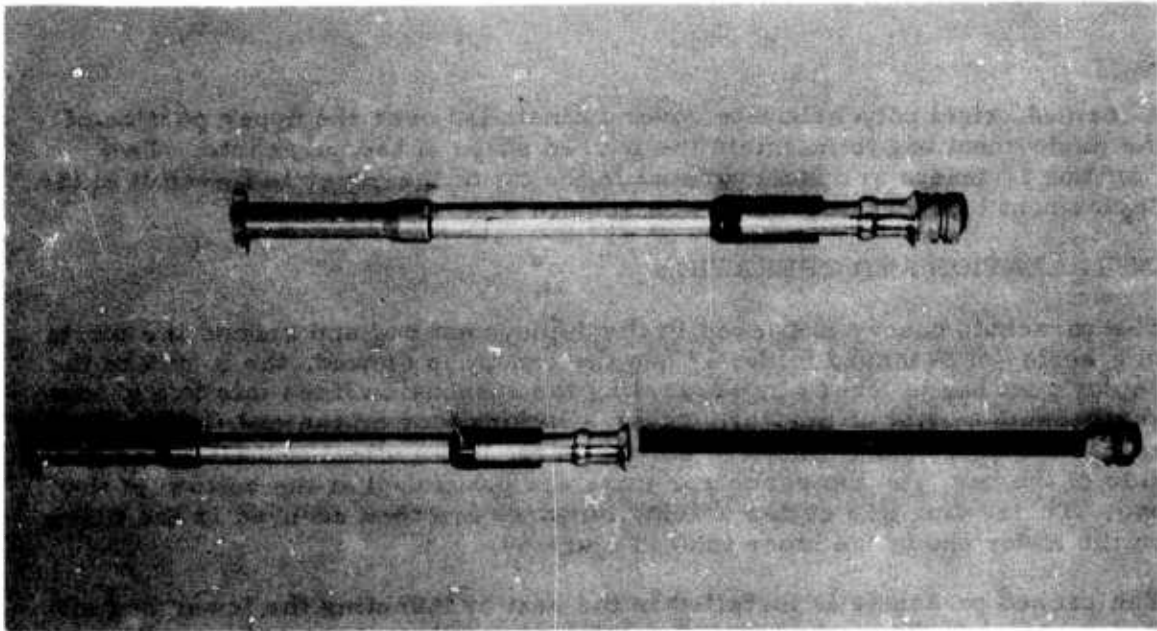


FIGURE 67. MORTAR ASSEMBLY

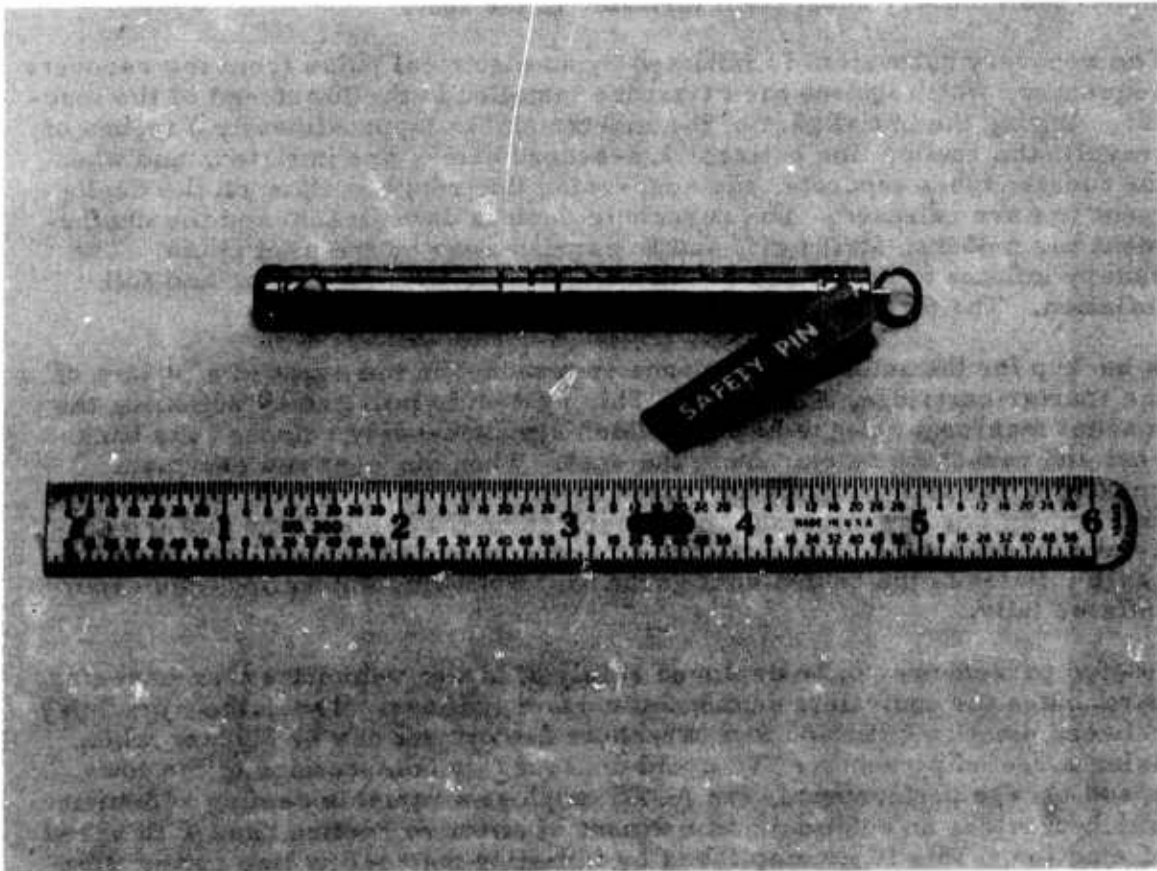


FIGURE 68. REEFING LINE CUTTER

A formed, rigid polycarbonate cover is installed over the upper portion of the deployment bag to maintain the packed shape of the parachute. Two CamLoc fasteners are incorporated in the top of the cover to fasten it to the deployment bag. The cover can be seen in Figure 69.

INSTALLATION AND OPERATION

The parachute canopy is packed in the deployment bag and around the mortar in a series of S-shaped folds. When the canopy is stowed, the mouth of the deployment bag is locked by separating the suspension lines into two groups and passing a bight of line through each locking loop on the end flaps. The remaining suspension lines are stowed in the longitudinal tunnels on each side of the bag, and the connector links are positioned at the bottom of the bag. The reefing line cutter arming lanyards are then secured to the fitting on the lower end of the inner tube, Figure 69.

The packed parachute is installed in the seat by inserting the lower end of the mortar into the seat-mounted portion of the disconnect and engaging the disconnect locking pin. After attaching the pilot chute pouch to the seat back, the parachute risers on the aft side of the bag are connected to the seat, and the remaining risers are routed up the forward side of the deployment bag and over ledges on the backrest. Finally, the lanyard on the pilot chute pouch is attached to a pip-pin located on the top beam of the seat structure. Figure 70 shows the recovery subsystem installed in the seat.

The recovery subsystem is initiated by an electrical pulse from the recovery sequencer, which ignites the cartridge installed in the lower end of the mortar. During the initial part of the mortar stroke (approximately 6 inches of travel), the reefing line cutters' 1.3-second delays are initiated, and when the mortar tubes separate, the suspension line retainer flaps on the deployment bag are released. The parachute deploys downstream and the deployment bag unlocks, strips off, and is carried away by the pilot chute. The canopy inflates to the reefed condition, followed by a disreefing and full inflation. The foregoing sequence is illustrated in Figure 71.

A backup for the automatic sequence is provided in the event of a failure of the mortar cartridge, Figure 10. This system is initiated by actuating the manual man/seat release handle, which simultaneously releases the backrest and parachute mortar from the seat. When the seat and crewman separate, the pilot chute is extracted from its pouch, inflates, and tows the deployment bag downstream. At line-stretch, the reefing line cutters are armed by the backup lanyards, the deployment bag strips off, and the parachute inflates to the reefed configuration. Following disreefing, the canopy inflates fully.

Reefed parachutes can be deployed safely at higher velocities than unreefed parachutes for equivalent suspended mass conditions. Thus, the time delay between ejection initiation and parachute deployment can be shorter when using a reefed parachute. To avoid unnecessary compromise of the low-speed escape performance, the ACES employs a variable reefing scheme, which provides an automatic adjustment of effective reefing time with speed of ejection. This is accomplished by initiating the reefing line cutter time-delay when the parachute is projected from the seat. This results in shorter effective reefing times (time from reefed inflation to disreefing) at low



FIGURE 69. PARACHUTE ASSEMBLY

ejection velocities than at high velocities, Figure 72. The variation of effective reefing with velocity is shown to be appreciably greater in Mode 1 than in Mode 2, because the parachute deployment time is relatively constant for all Mode 2 ejection velocities.

One of the most important factors in determining the effectiveness of the escape system is the distance traveled between ejection initiation and recovery of the crewman. Obviously, the shorter the distance traveled between these events, the greater the escape system capability in effecting recovery of the crewman. Therefore, an optimum recovery sequence is one in which the maximum tolerable g-load is maintained on the seat system from ejection to recovery. The use of a reefed parachute, which can be deployed earlier in the ejection sequence than an unreefed parachute, is one approach to minimizing distance traveled. The distance traveled during ACES qualification ejection tests is plotted in Figure 73.

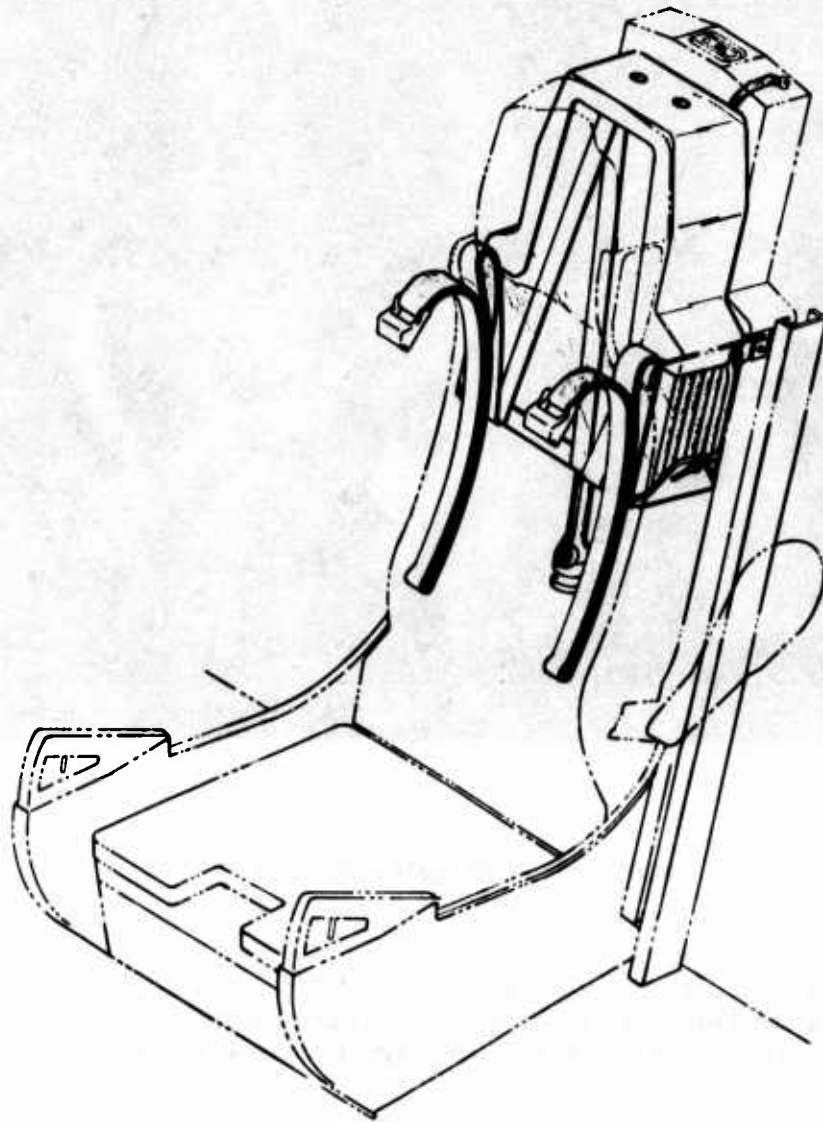
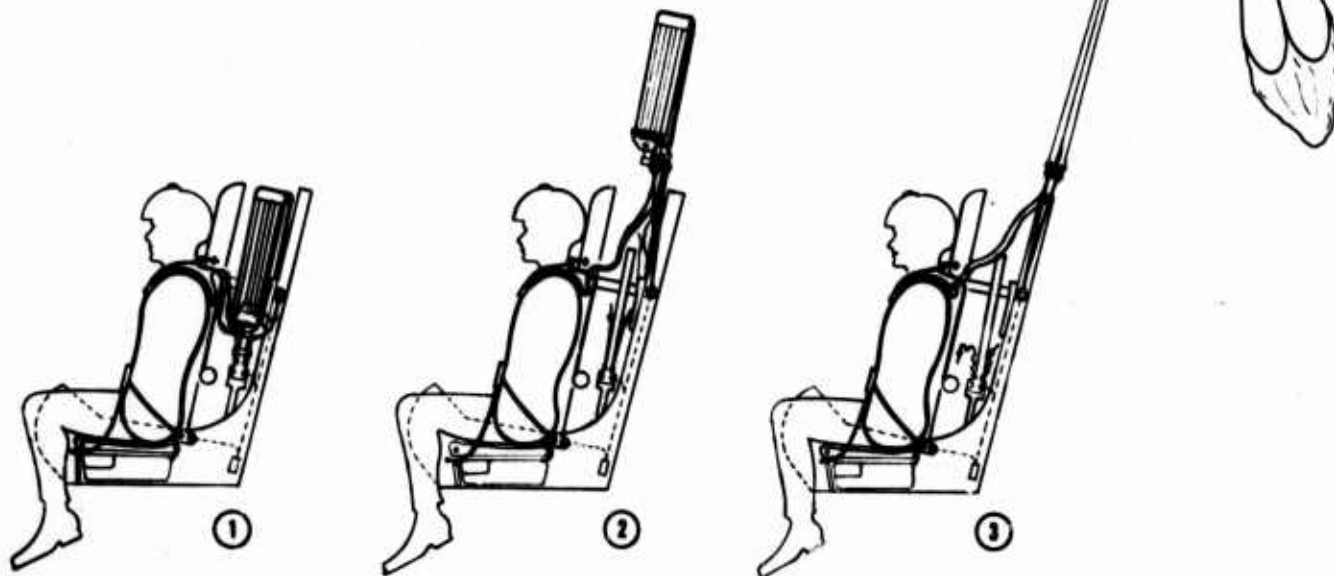


FIGURE 70. PARACHUTE INSTALLATION

- ① ● PARACHUTE MORTAR INITIATED
● REEFING LINE CUTTERS INITIATED
● (AFTER APPROXIMATELY 6 INCHES OF STROKE)
- ② ● PARACHUTE SUSPENSION LINES START TO DEPLOY
● PILOT CHUTE IS EXTRACTED FROM POUCH
- ③ ● PARACHUTE SUSPENSION LINES CONTINUE TO DEPLOY
● PILOT CHUTE STARTS TO INFLATE
- ④ ● PARACHUTE CANOPY EMERGES FROM DEPLOYMENT BAG
● DEPLOYMENT BAG STRIPS OFF
- ⑤ ● PARACHUTE INFLATES TO REEFED CONDITION
- ⑥ ● PARACHUTE DISREEFS AND FULLY INFLATES
● MAN/SEAT RELEASE MECHANISM ACTUATES DISCONNECTING THE:
 - A. BACKREST
 - B. PARACHUTE MORTAR AND
 - C. PARACHUTE RISERS FROM SEAT STRUCTURE
 - MAN AND SEAT SEPARATE
 - DEPLOYMENT OF SURVIVAL KIT CONTENTS INITIATED
● (IF SELECTOR PRE-POSITIONED IN AUTOMATIC MODE)



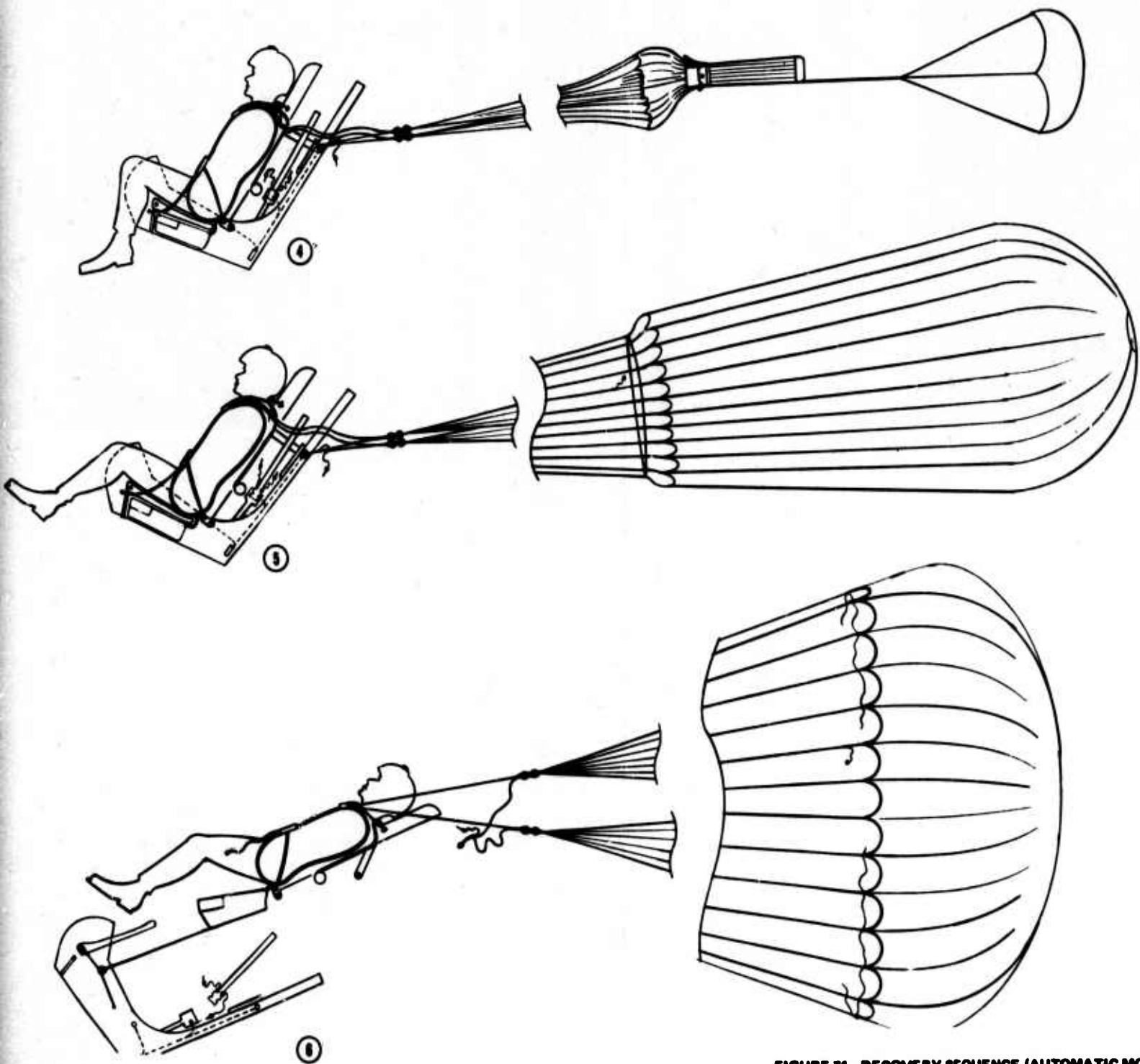


FIGURE 71. RECOVERY SEQUENCE (AUTOMATIC MODE)

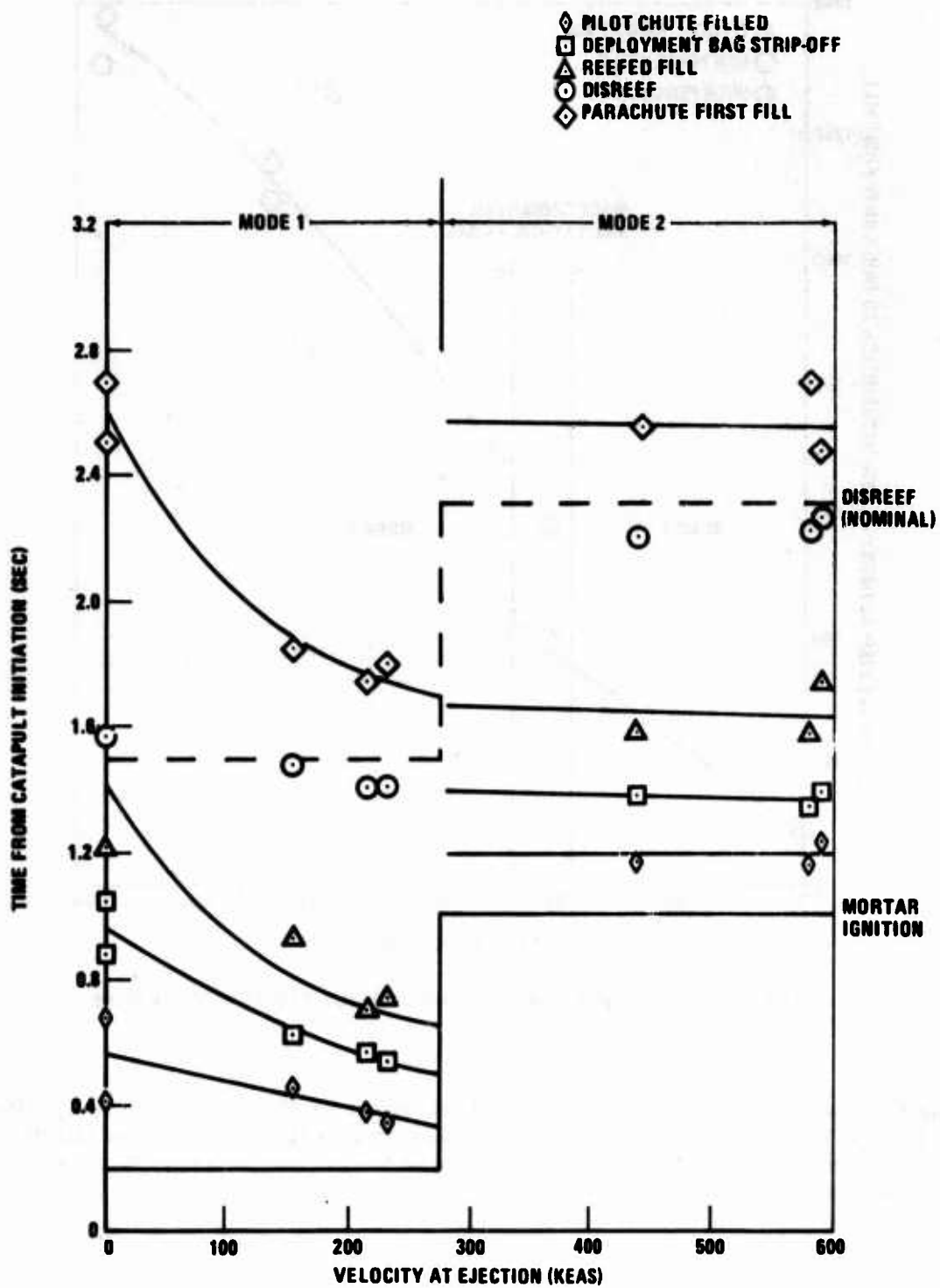


FIGURE 72. PARACHUTE OPERATION OVER THE EJECTION VELOCITY RANGE

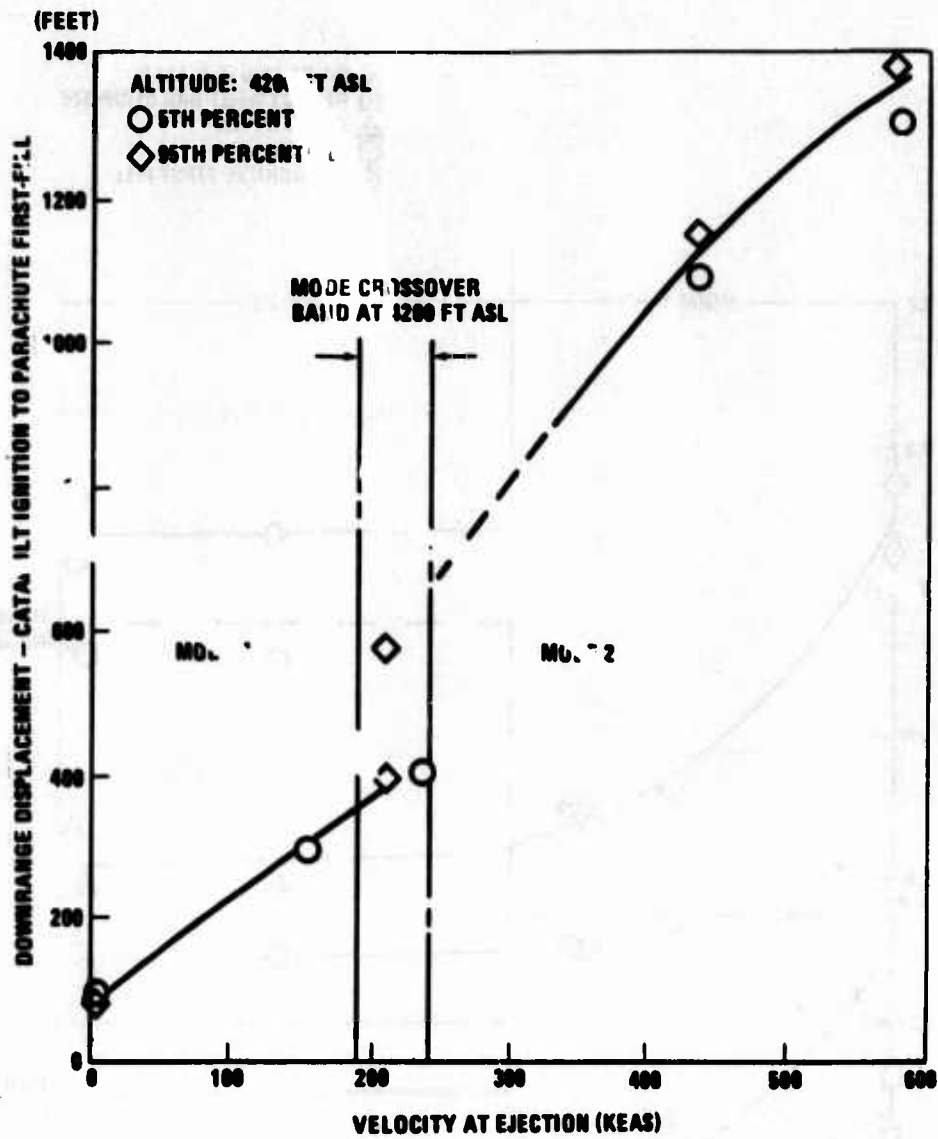


FIGURE 73. DISTANCE TRAVELED AT VARIOUS EJECTION VELOCITIES

The forces transmitted to the seat and occupant by the parachute are plotted in Figure 74. The data used to define parachute reefed and full inflation loads were obtained during the qualification tests (bomb drops) of the recovery subsystem.

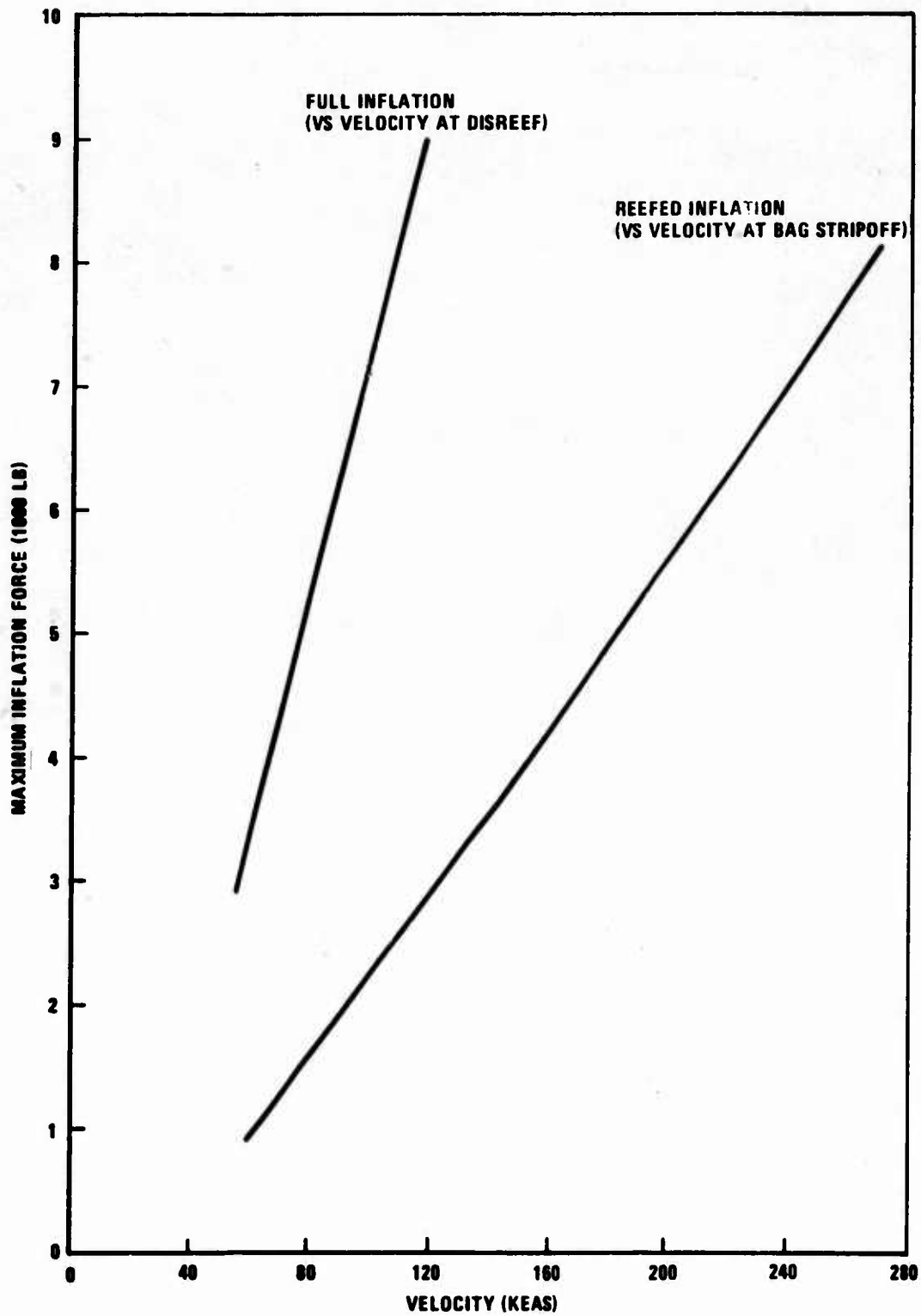


FIGURE 74. MAXIMUM REEFED AND FULL INFLATION FORCES

SECTION XI

CREW SUPPORT AND RESTRAINT SUBSYSTEM

This subsystem includes all the components required for support and protective restraint of the crewman during normal flight, during ejection, and under crash landing conditions. The basic components of this subsystem are a backrest assembly and restraint harness, Figure 75.

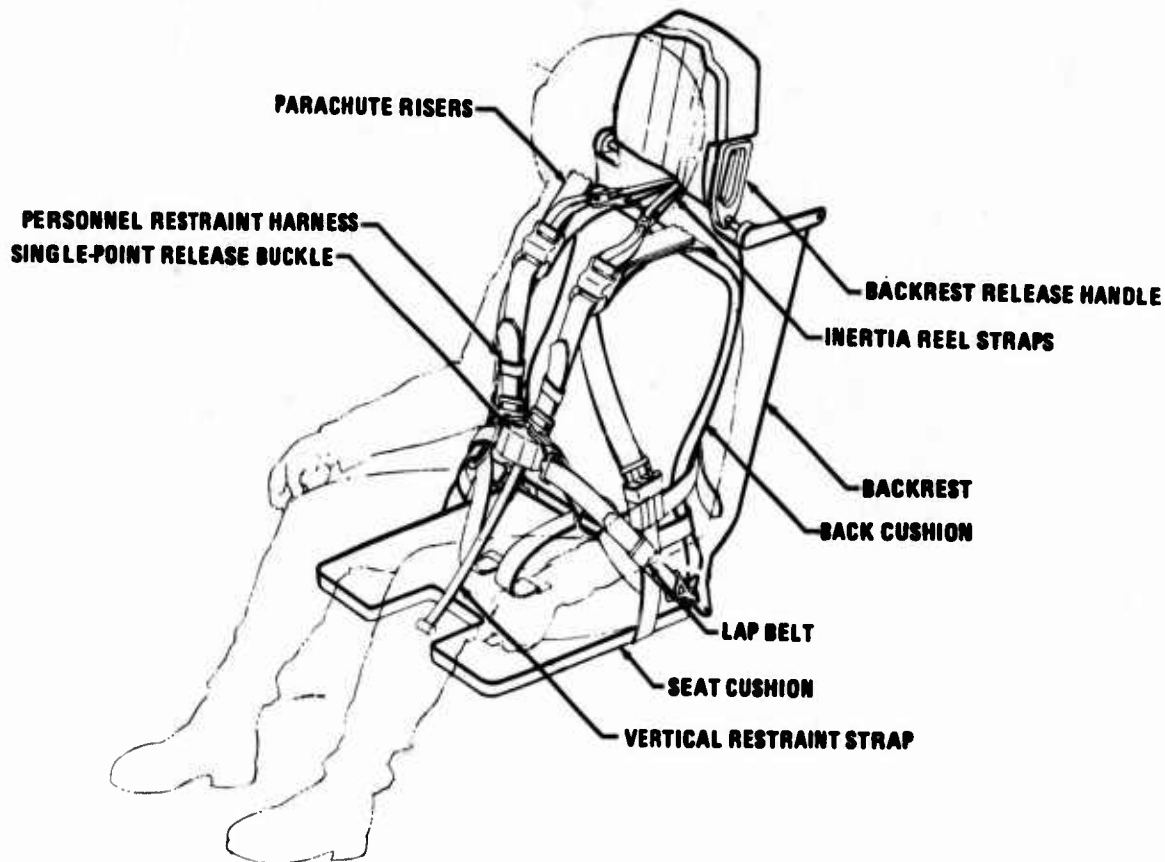


FIGURE 75. CREW SUPPORT AND RESTRAINT SUBSYSTEM

BACKREST

The backrest structure consists of two parallel tee extrusions joined at the top by a machined beam and at the bottom by a channel section. The headrest portion of the backrest is a box structure riveted to the machined beam. Fittings incorporated at the bottom outboard edges of the backrest structure are used to pick up lap belt loads. Links are attached to the outboard edges of the machined beam to transfer crash and drogue loads to the seat structure. An aluminum sheetmetal skin covers the forward surface of the backrest structure to provide a shear panel. An additional plastic cover, which is contoured for lumbar support, is also attached to the front surface of the structure. Polyurethane foam pads, shaped to provide proper support of the crewman's helmeted head, are cemented to the forward face of the headrest, Figure 76.

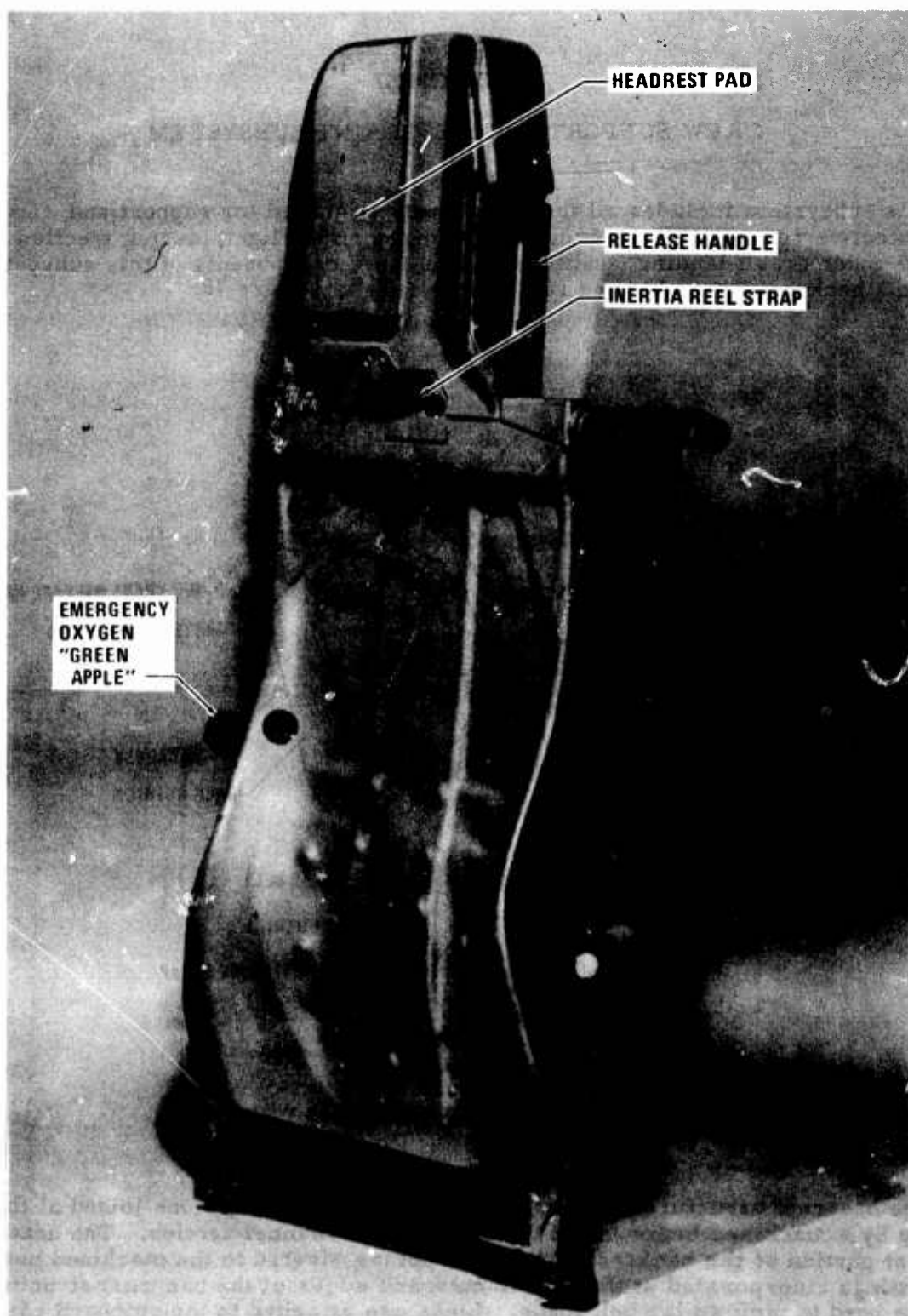


FIGURE 76. BACKREST ASSEMBLY -- FORWARD SIDE

A dual-strap, power haul-back inertia reel is installed on the lower aft side of the backrest, with the straps routed up and over a pair of nylon rollers located in a cut-out area of the machined beam. The inertia reel manual control is located on the lower left-hand side of the backrest. An emergency oxygen supply stored in a 22-cu. in. MS22069-3 cylinder assembly, except that a shorter hose is employed, also is installed on the aft side of the backrest in the area above the inertia reel. Figure 77 shows the installation of the above-described equipment. The emergency oxygen is activated automatically during ejection by the downward travel of the arm restraint paddles. Manual actuation is accomplished by pulling the "green apple" located on the right-hand side of the backrest.

To permit the crewman to jettison the backrest prior to parachute landing, a release system is incorporated that is actuated by a handle located on the left-hand side of the headrest, Figure 78. A latch positively locks the handle in place, preventing inadvertent actuation of the release mechanism. Backrest release is accomplished by squeezing the trigger and rotating the handle downward, all in one motion.

RESTRAINT HARNESS

The restraint harness provides the required torso restraint during crash landing, ejection, and flight maneuvers. A quick-release buckle allows rapid doffing of the harness for ground emergencies where immediate egress is essential for safety. Parachute canopy release fittings also are included to permit manual jettisoning of the parachute following landing. The general arrangement of the harness is illustrated in Figure 79.

The primary structural members of the harness are the saddle/body strap and cross back straps. During a manual operation of the parachute, the leg straps carry a relatively-high percentage of the load, but during a normal recovery sequence, the major loading in the lower portion of the harness is shared by the two lapbelt segments. Upward displacement of the crewman as a result of negative g's is limited by the vertical restraint strap. The upper end of this strap is attached to the quick-release buckle and the lower end, which incorporates a plastic (epoxy) knob, is retained between the seat pan and the front edge of the seat bucket structure. During ejection, the lower end of the strap is released when man/seat separation occurs.

The restraint harness incorporates seat and back cushions that retain the various straps. A plastic stiffener (ABS), conforming to the contour of the backrest, is installed in the aft portion of the back cushion to prevent it from collapsing under the weight of the harness straps and hardware. The rigidity provided by the stiffener also facilitates donning of the harness. The seat cushion employs a combination of a closed-cell sponge material (ensolite) and foam rubber for shock attenuation (spinal axis loading, G_z) and comfort.

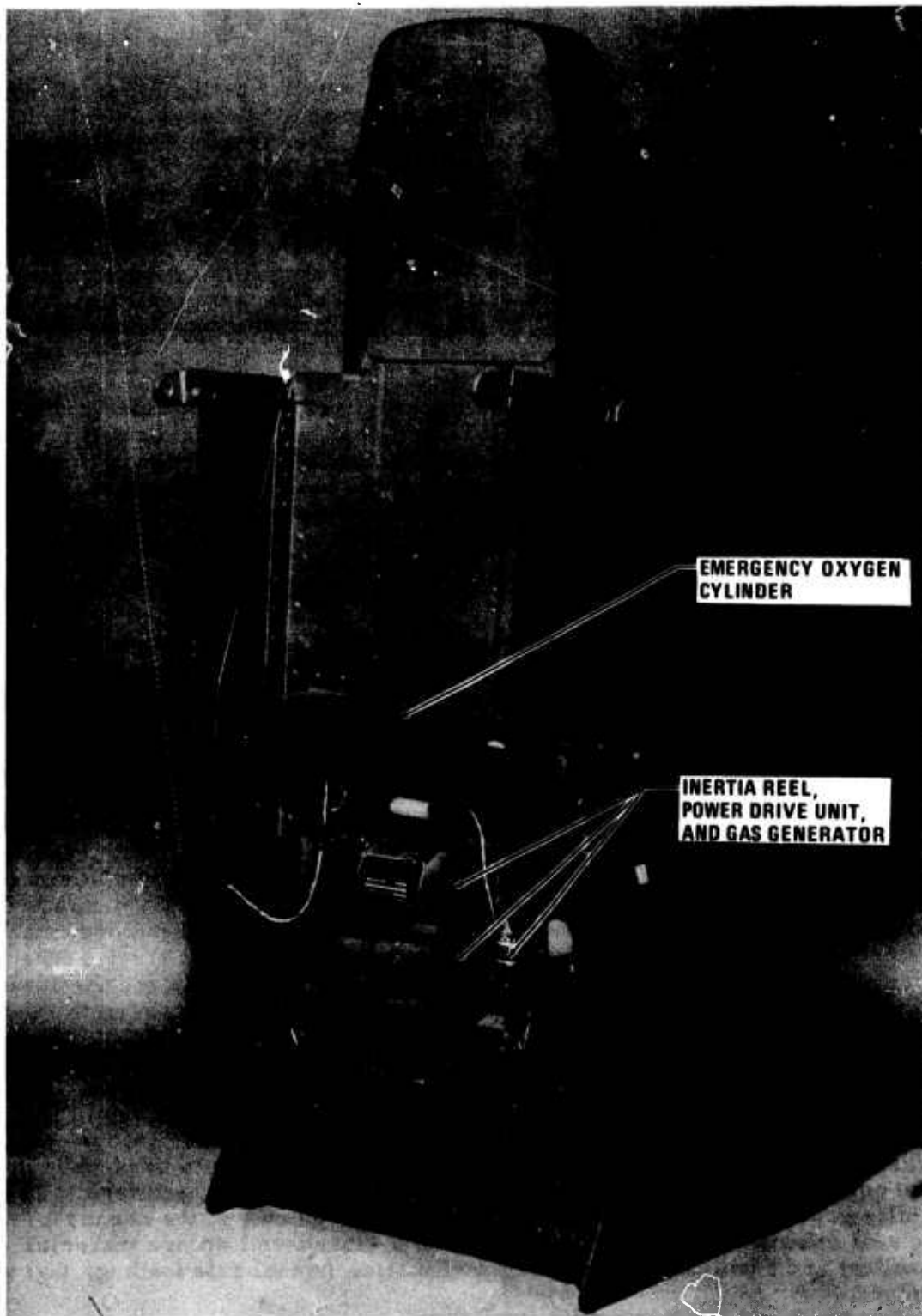


FIGURE 77. BACKREST ASSEMBLY – AFT SIDE

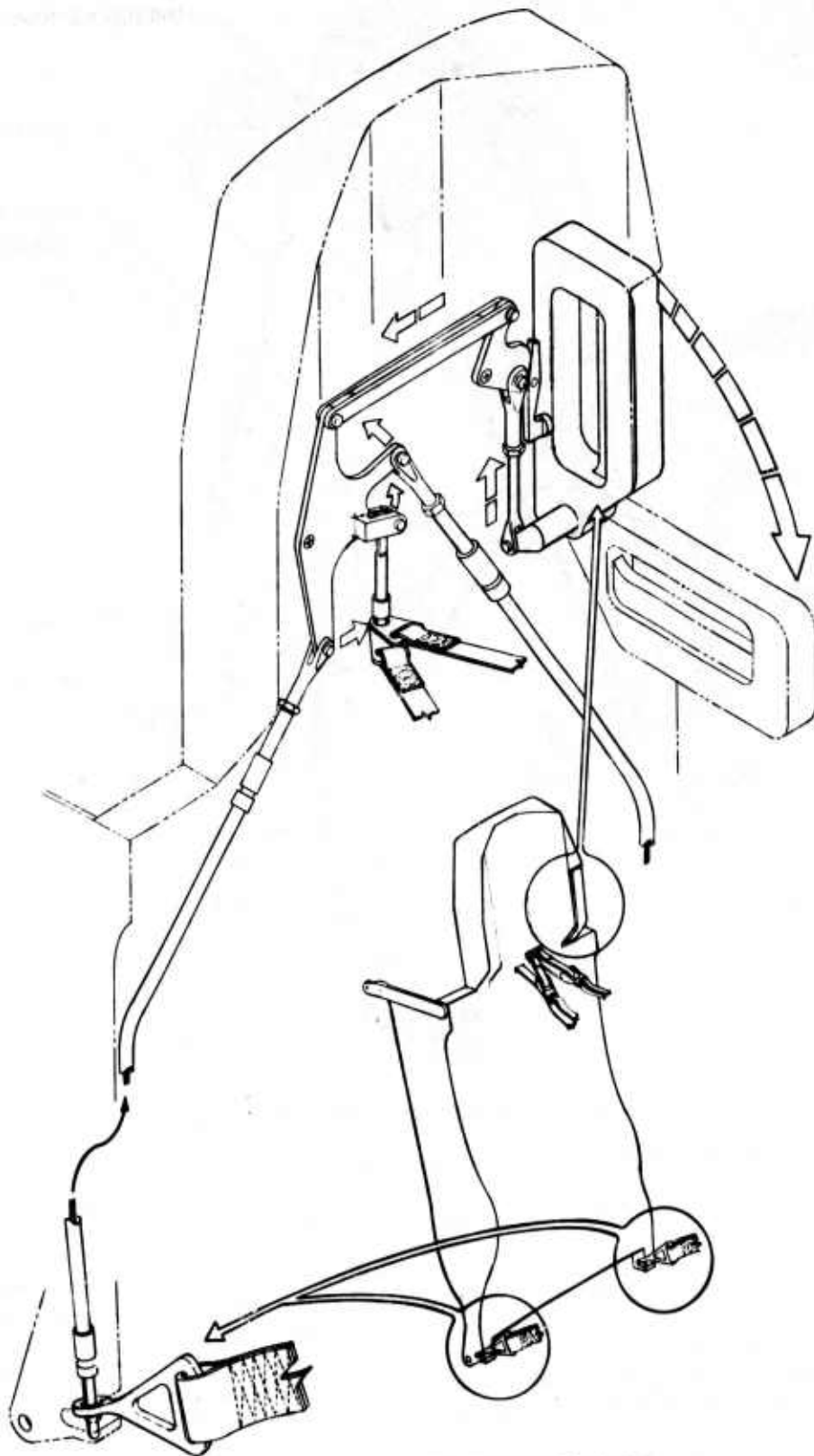


FIGURE 78. BACKREST RELEASE SYSTEM

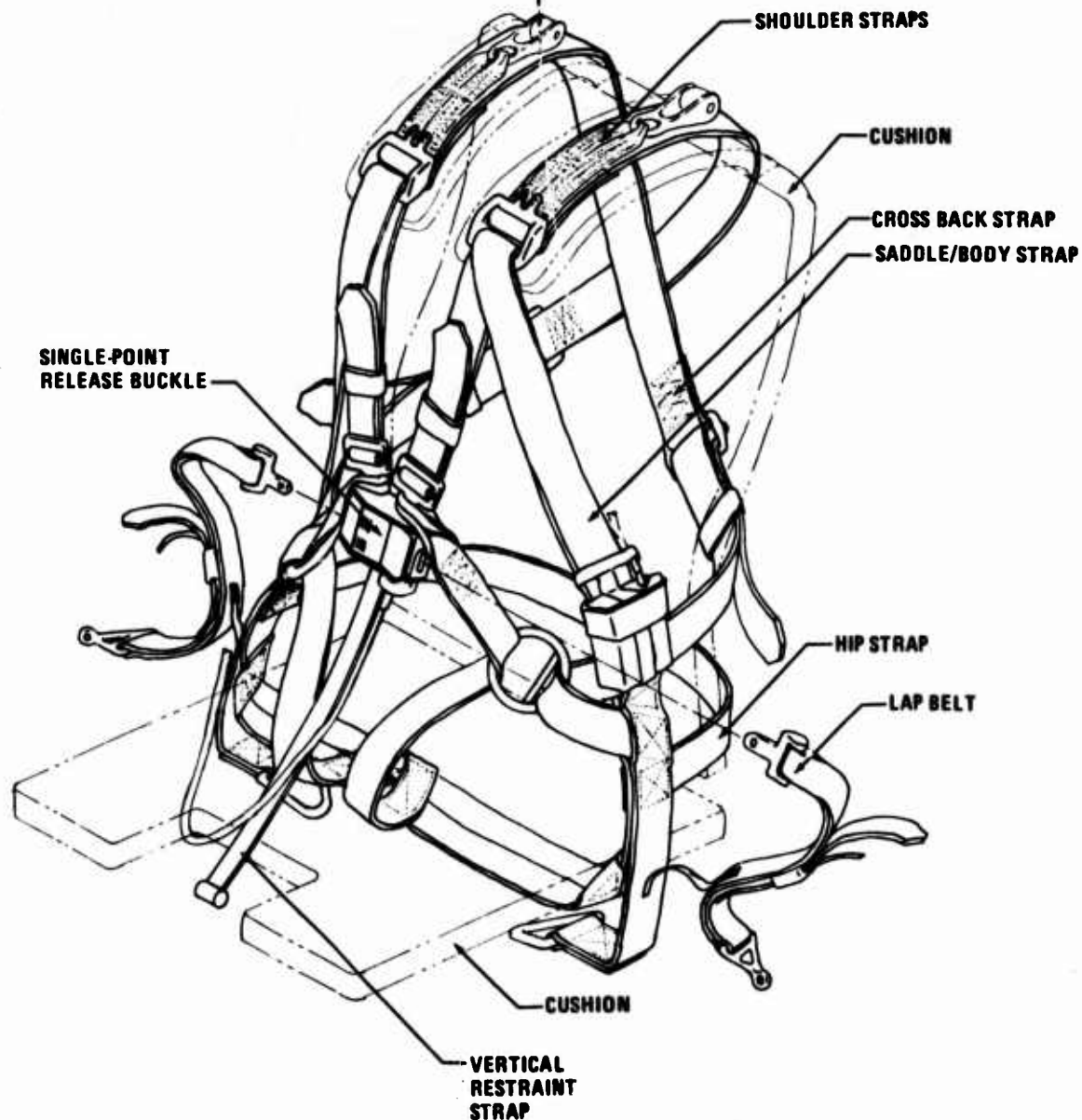


FIGURE 79. SINGLE-POINT RELEASE HARNESS

The quick-release buckle performs two functions when actuated:

1. It releases all the harness straps constraining the crewman in the seat.
2. It disconnects the distal end of the oxygen mask hose from the CRU-60/P connector, which is located on the right-hand sling strap. An adapter containing a releasing mechanism is connected to the mask hose port of the CRU-60/P and, in turn, the mask hose is bayoneted into the adapter. Actuation of the quick-release buckle transmits mechanical motion to the adapter releasing mechanism via a sheathed cable.

Figure 80 shows the crewman in the restraint harness and Figure 81 is a view of the oxygen disconnect adapter.



FIGURE 80. CREWMAN WEARING HARNESS



FIGURE 81. OXYGEN HOSE DISCONNECT

SECTION XII

SURVIVAL AND PERSONAL EQUIPMENT

SURVIVAL KIT

The survival kit for the ACES is a non-rigid package containing all survival equipment except emergency oxygen. The "soft" survival kit concept is employed to reduce the weight, complexity, and cost attendant to contemporary, rigid-type kits. The ACES survival kit stows in the seat bucket under a rigid, contoured seat pan and is not required to support any down loads resulting from ejection, flight, or crash conditions. The container configuration provides for both automatic and manual deployment of the kit contents and inflation of the liferaft.

The assembled kit, Figure 82, is comprised of two units:

1. The outer container (main kit), which contains the liferaft and rucksack, and provisions for its attachment to the crewman's restraint harness.
2. The hit-and-run kit (HARK), which attaches to the forward portion of the outer container.

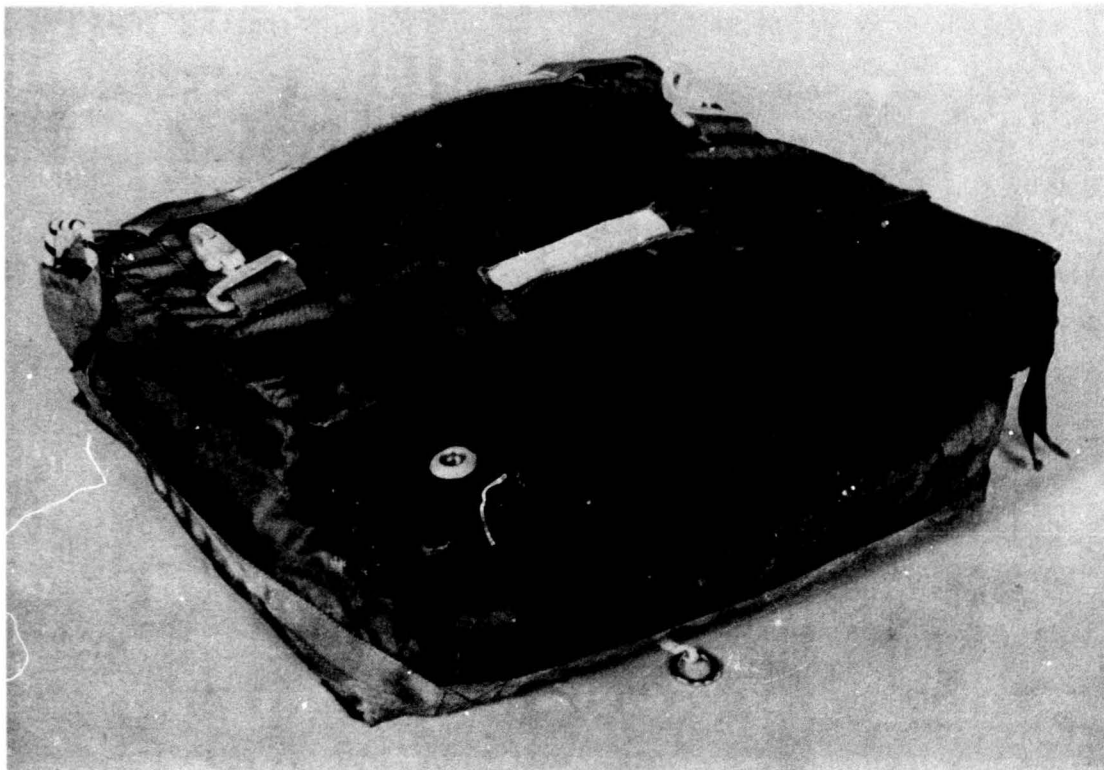


FIGURE 82. SURVIVAL KIT ASSEMBLY

OUTER CONTAINER

The outer container is fabricated from MIL-C-7219 nylon cloth and is reinforced with nylon webbing. A pocket housing the manual D-ring is located on the aft, right-hand corner of the container and snaps for attaching the container to the restraint harness are installed on the upper surface of the container. The outer container also incorporates a series of elastic loops to retain the automatic ripcord, a 6-foot length of nylon cord. One end of the cord is attached to the two pins that lock the container flaps, and a metal ring is attached to the other end. A nylon webbing bridle arrangement is incorporated on the inside of the container to which the liferaft and rucksack dropline is attached, Figure 83. The liferaft is stowed in the upper portion of the kit followed by the rucksack, as shown in Figure 84. Details of the manual and automatic ripcord installations are shown in Figures 85 and 86.

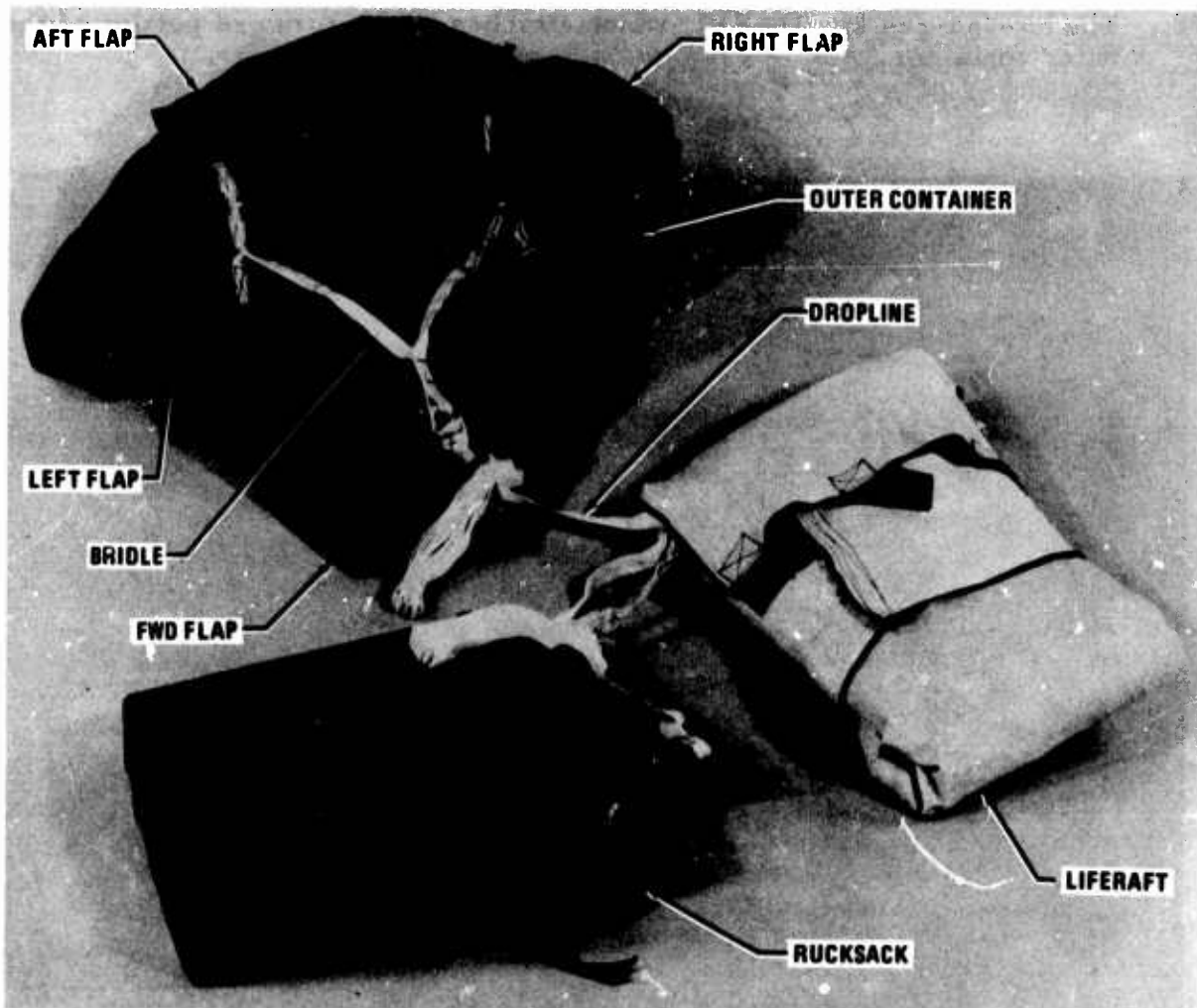


FIGURE 83. DROPLINE ATTACHED TO RUCKSACK AND CASE

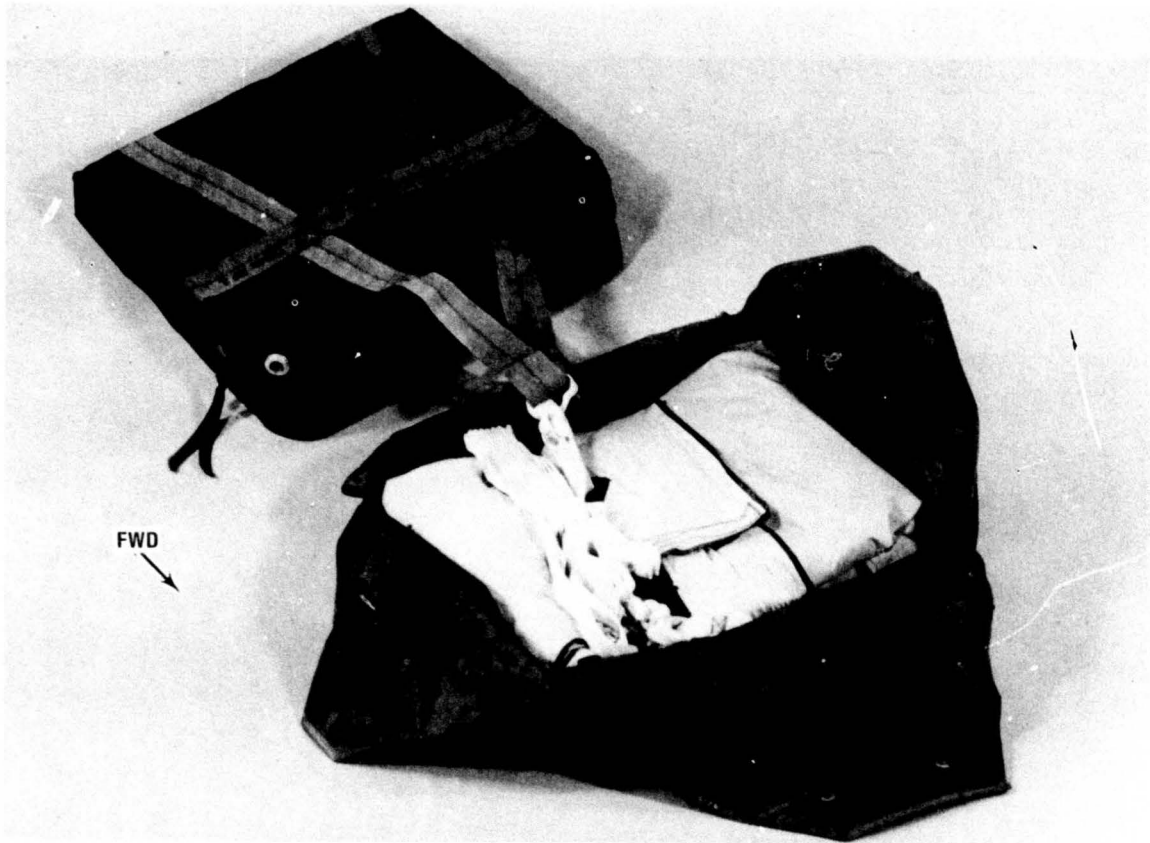


FIGURE 84. RAFT STOWED IN CASE WITH DROPLINE



FIGURE 85. RIPCORDER PINS THROUGH RING ASSEMBLY AND CORD LOOPS

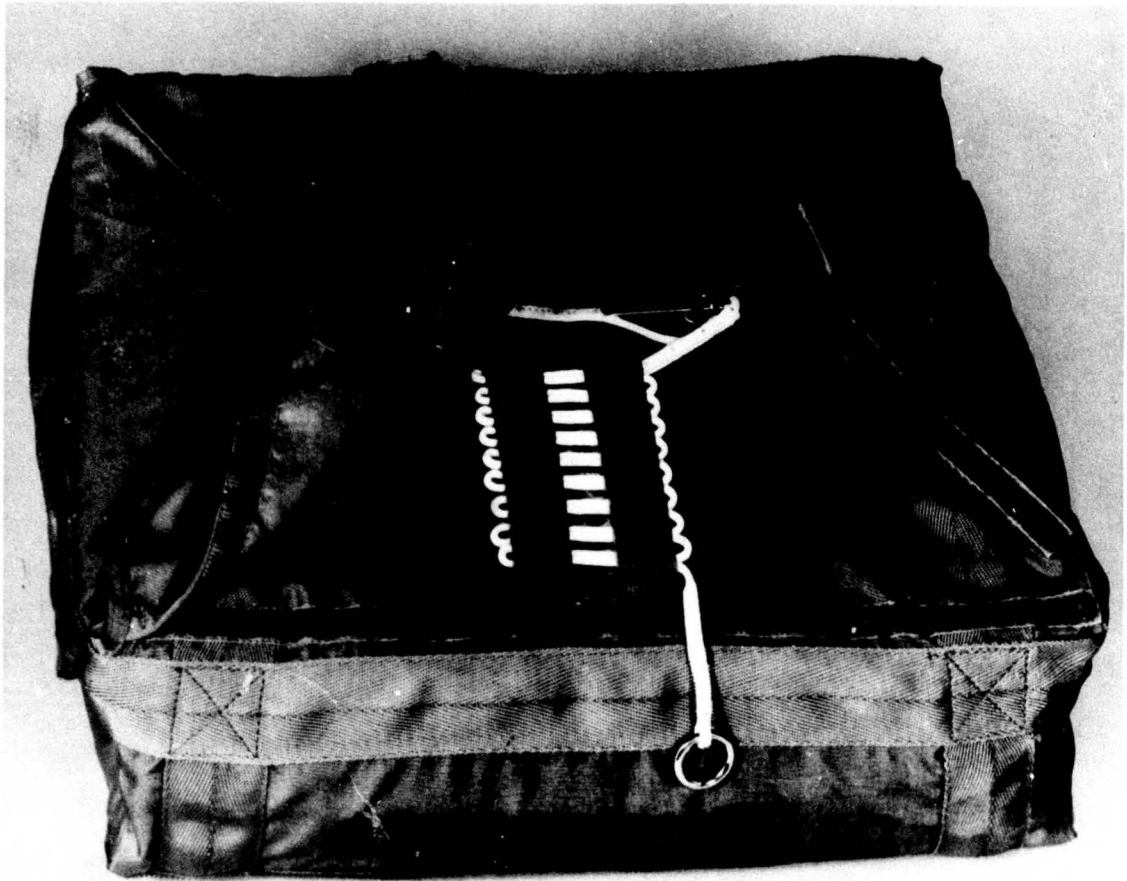


FIGURE 86. AUTOMATIC RIPCORD STOWED

The rucksack, Figure 87, is fabricated from chloroprene-coated nylon cloth and incorporates a waterproof zipper and a check valve. The rucksack is reinforced with nylon webbing to distribute and react the inertia loads resulting from the container falling to the end of the dropline. The rucksack and liferaft are attached to each other and to the outer container with the conventional length dropline used with U.S. Air Force rigid survival kits.

HARK

The HARK is fabricated from chloroprene-coated nylon cloth and incorporates a waterproof zipper and check valve, Figure 88. The kit contents are arranged on a web strap in such a manner that they can be worn around the waist as a belt after their removal from the waterproof kit, Figure 89. The HARK is retained to the outer container by velcro tape and by two pins that are inserted through webbing loops extending from the outer container through slots in the pin protector flaps. The pins are part of a handle assembly that, when pulled, first extracts the pins and then, as the pull is continued, separates the HARK from the survival kit outer container, Figure 90.

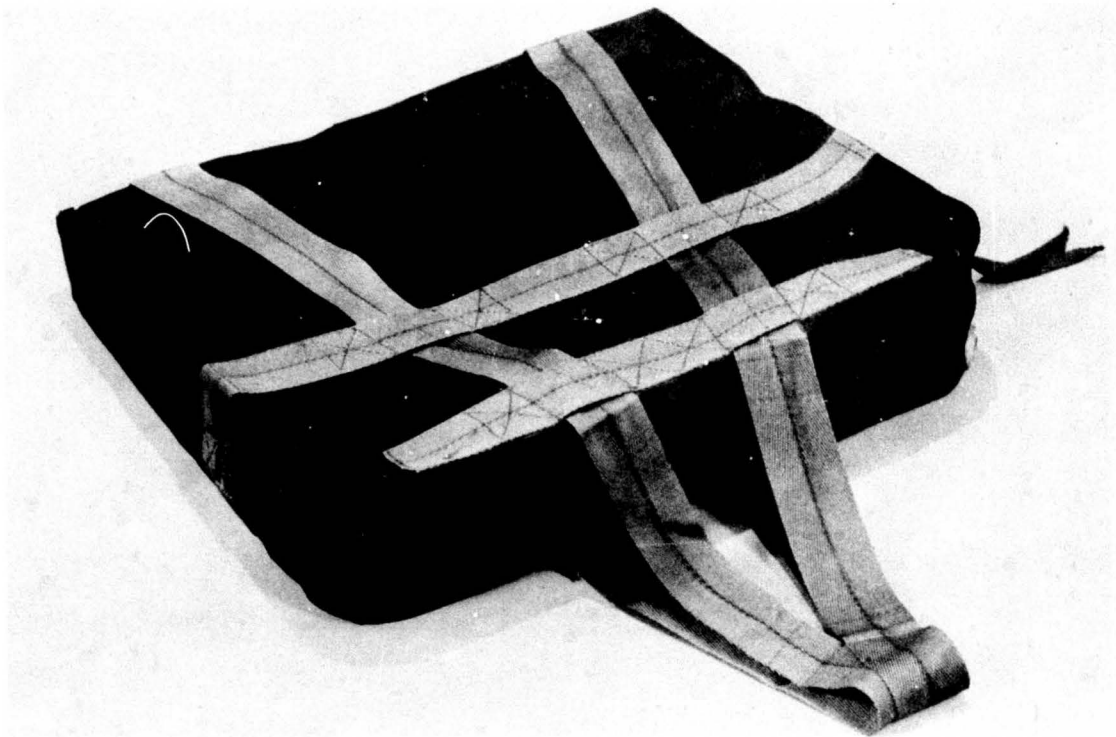


FIGURE 87. RUCKSACK

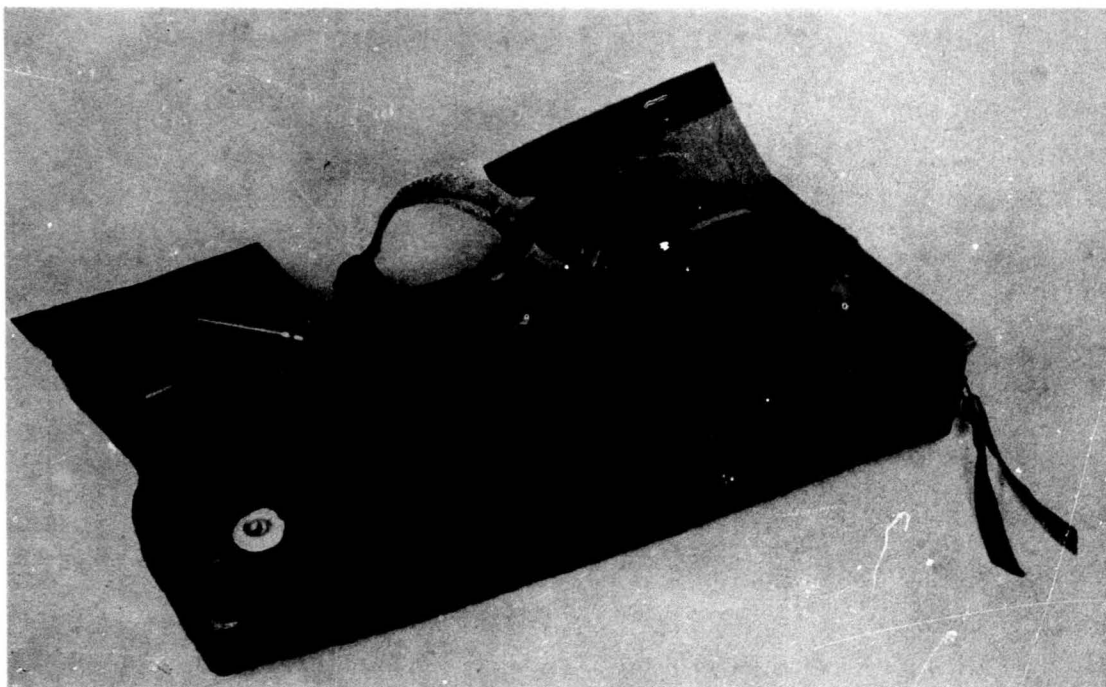


FIGURE 88. HIT-AND-RUN KIT

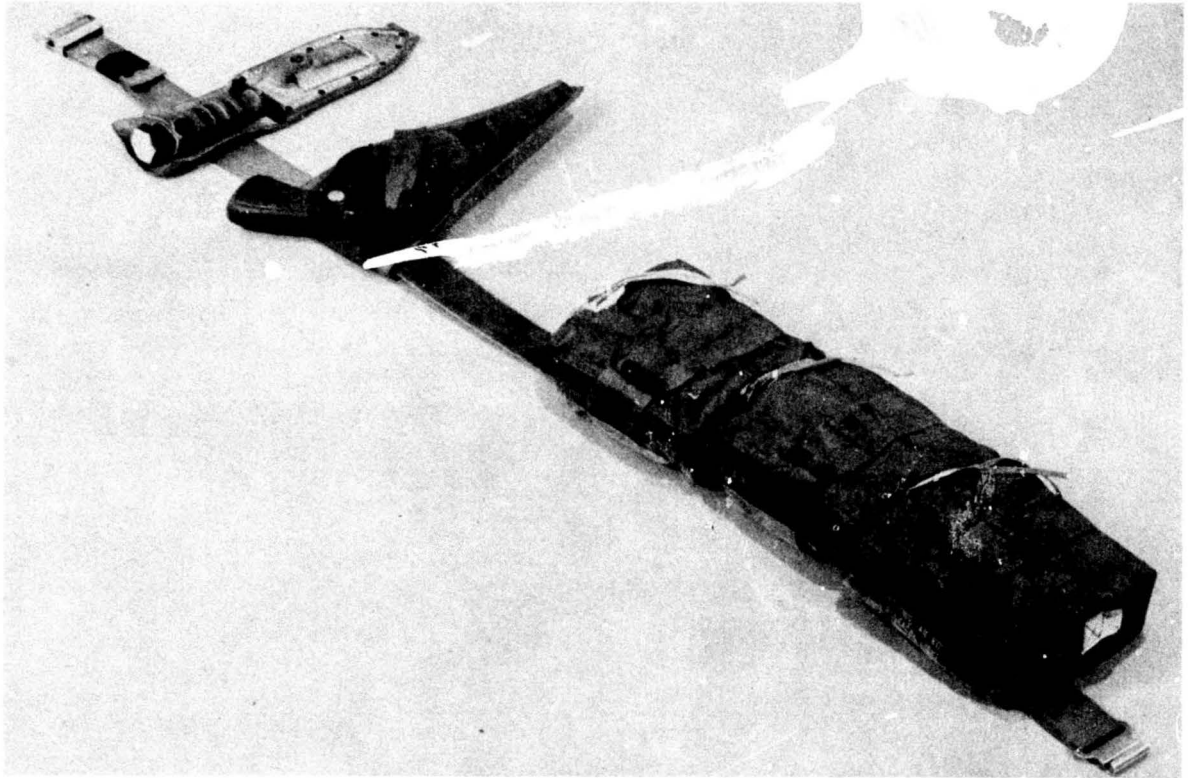


FIGURE 89. HIT-AND-RUN KIT CONTENTS

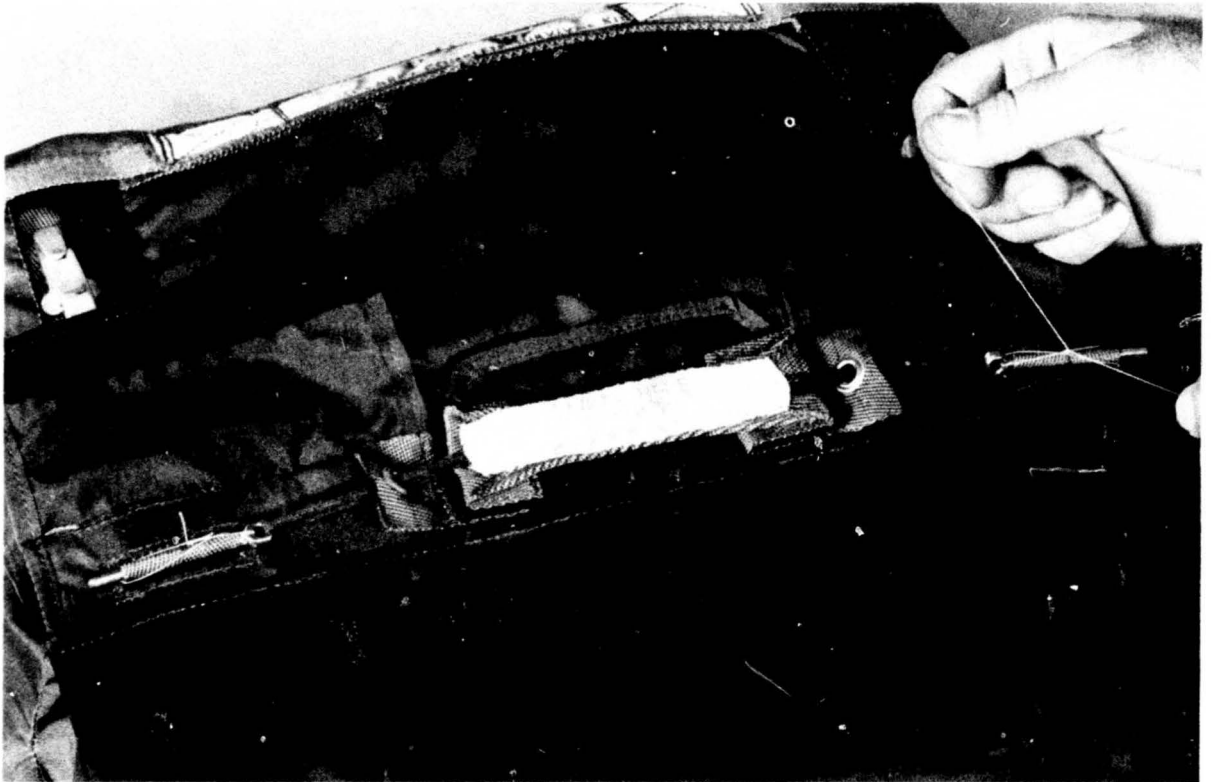


FIGURE 90. HARK PINS SAFETY TIED

The kit is designed to accommodate the survival equipment listed in Table VII. It is relatively important that additional items not be packed in the kit unless items of equivalent volume and/or shape are removed. This is to prevent growth of the kit envelope and attendant installation problems. In addition, excessive friction between the survival kit and seat bucket, resulting from an oversize kit, may cause a delay in man/seat separation, especially if the ejection occurs at zero or very low airspeeds.

To install the survival kit in the seat, a cable assembly, attached to the deployment selector, is routed through the metal ring in the end of the automatic ripcord and then fastened to the right-hand seat pan retaining pin, Figure 91.

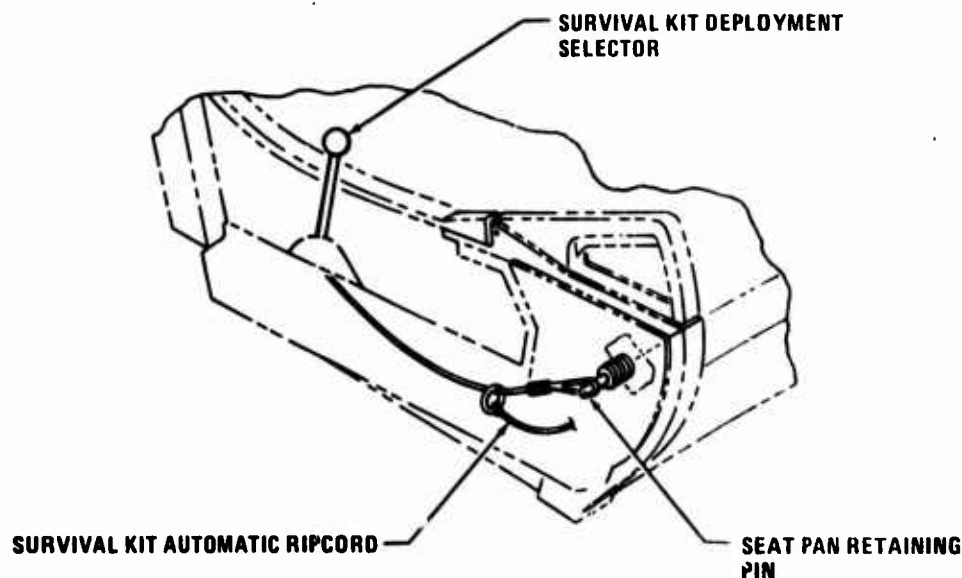


FIGURE 91. SURVIVAL KIT INSTALLATION

If the deployment selector is set to the automatic position at the time of ejection, the survival kit operational sequence is as illustrated in Figure 92. In the event the deployment selector is set to the nonautomatic position, the crewman can initiate deployment of the rucksack and liferaft, during parachute descent, by pulling the D-ring located on the aft, right-hand corner of the outer container.

LOCATOR BEACON

The URT-33 locator beacon is located in a fabric pocket on the restraint harness' left-hand sling strap. This location allows easy access to the on-off switch in the event the crewman desires to deactivate the unit at any time. The switch actuation lanyard and the antenna are routed up the parachute riser inside a protective tunnel. The switch actuation lanyard is attached to a cord loop stitched to one of the parachute suspension lines. Figure 93 illustrates details of the installation and operation.

**TABLE VII
ACES SURVIVAL EQUIPMENT**

Qty	Name	FSN
Liferaft Items		
1	Liferaft, type LRU-6/P	4220-869-2738
1	Inflation assembly, type FLU-2/P	4220-756-0474 LS
1	Liferaft retainer	4220-761-8185
HARK Items		
1	Radio, type ACR-RT-10 (including battery)	5821-912-4480 LS
1	Light marker, distress SDU-5/E	6230-067-5209
1	Signal kit, personal distress	1370-921-6172-LY35
1	First aid kit, tropical	6545-782-6412
1	Tourniquet	6515-333-0565
1	Compass, lensatic	6605-846-7618
1	Knife, pocket	7340-162-2205
1	Plastic water container	8465-634-4499
4	Fire starters, type M-2	1370-219-8566
1	Knife, survival, 5-inch blade	7340-098-4327
1	Revolver, .38 cal., 4-inch	Smith & Wesson #10
23	Cartridges, .38 cal. revolver	
1	Battery, (spare) RT-10 radio	6135-930-0810
Rucksack Items		
1	Raft repair kit (2 plugs)	4220-693-1471
2	Signal, smoke and illumination, Mk 13, Mod 0	1370-309-5027-L275
1	Mirror, Mk-3, MIL-M-18371 Type 1 (Metal Equivalent preferred)	6350-NSL

TABLE VII (Continued)

Qty	Name	FSN
1	Sea Marker Packet	6850-285-4324
1	Match box, water proof, w/matches	8465-265-4925
1	Whistle, police, plastic	8465-254-8803
1	Radiac Meter (IM-179)	6665-975-5167
1	Goggles, sun, Type MA-1	8465-530-4083
1	Boots, mukluk	8430-275-5732
Pr		
1	Insect repellent, stick form 6-12 or equal	Commercial
1	Sun ointment	8510-162-5658
1	Snake bite kit, suction	6545-952-5325
2	Soap bars, toilet, miniature	Commercial
2	Food packets, survival, general purpose	8970-082-5665
1	Shark deterrent	6850-281-6926
20	Wire, Comm. Brass	9525-596-3498
Ft		
1	Saw, hand, fingerrip, Type MB-2	5110-570-6896
1	Hood, winter, MIL-H-25754	8415-543-7130
1	Gloves, inserts	8415-269-0500
Pr		
1	File, flat, 6-inch, Type B	5110-236-6532
1	Tool kit, survival, Type SRU-18/P	4240-065-6713
6	6-ft Plastic sheet	Commercial
Ft		

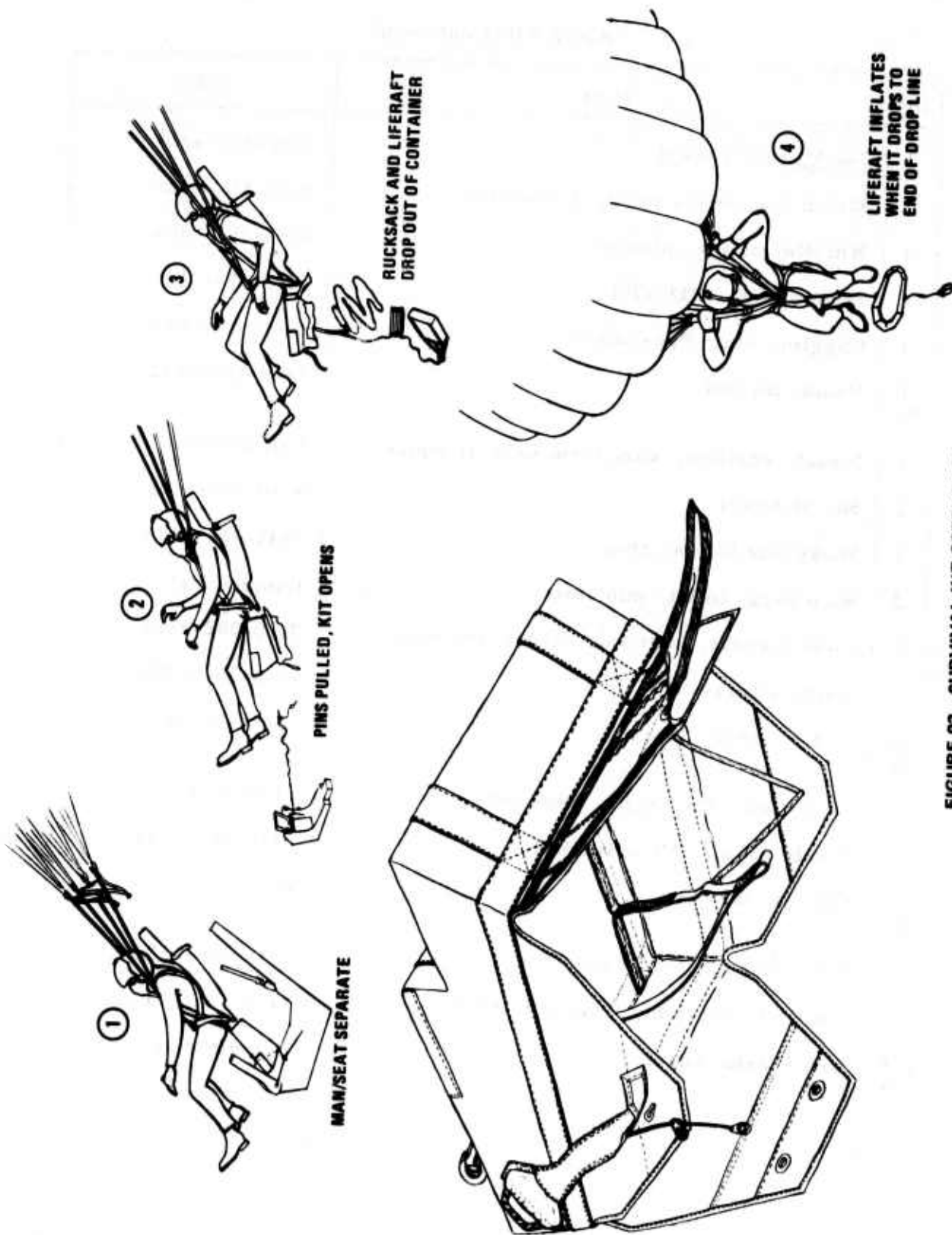


FIGURE 92. SURVIVAL KIT OPERATION

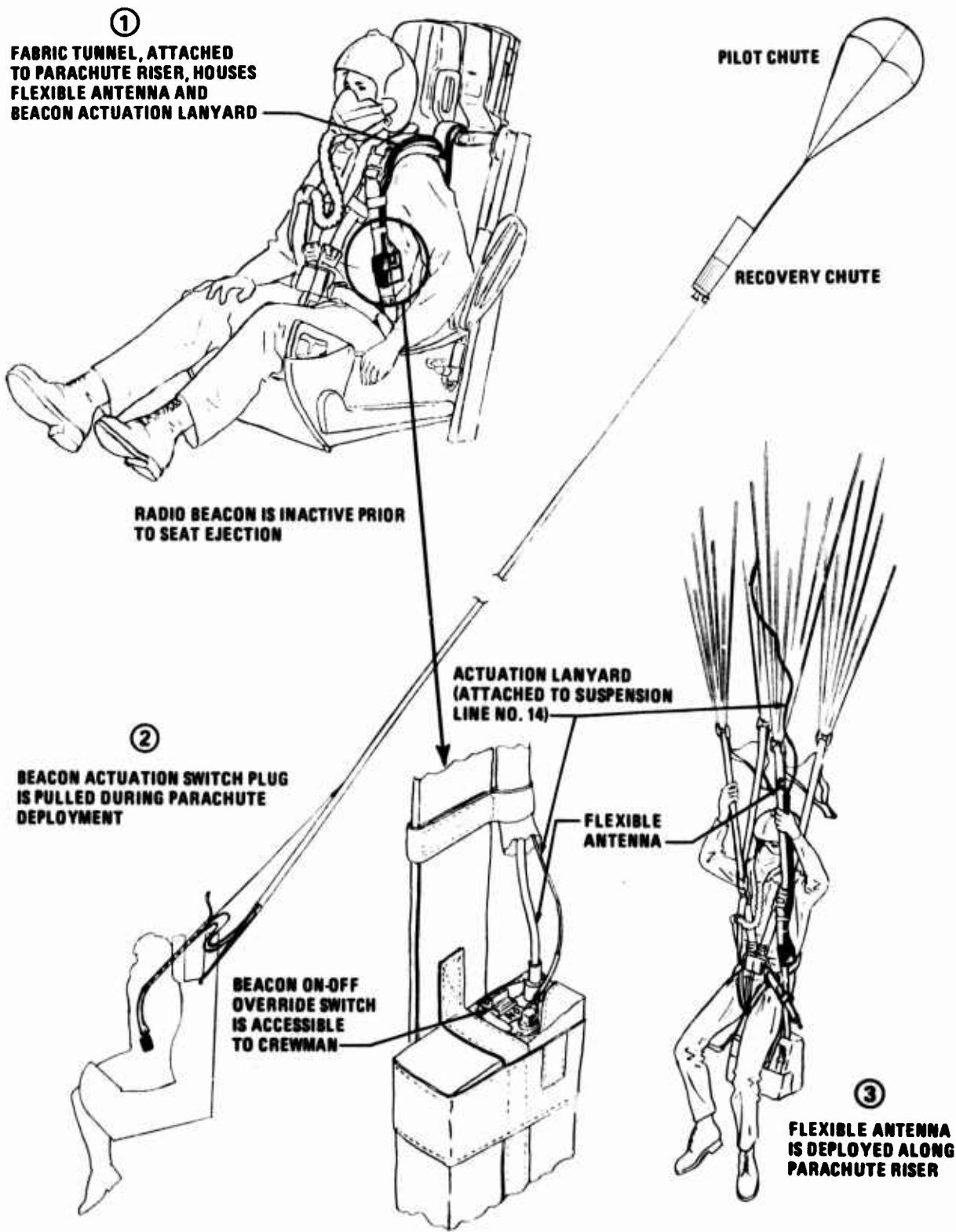


FIGURE 93. AN/URT-33 RADIO BEACON INSTALLATION

SECTION XIII

WEIGHT SUMMARY

A summary of ACES weights is included in Table VIII. The weight distribution results in an ejected mass center of gravity as illustrated in Figure 94. Static cg/rocket thrust line nominal offsets also are given for the 5th and 95th percentile crewman.

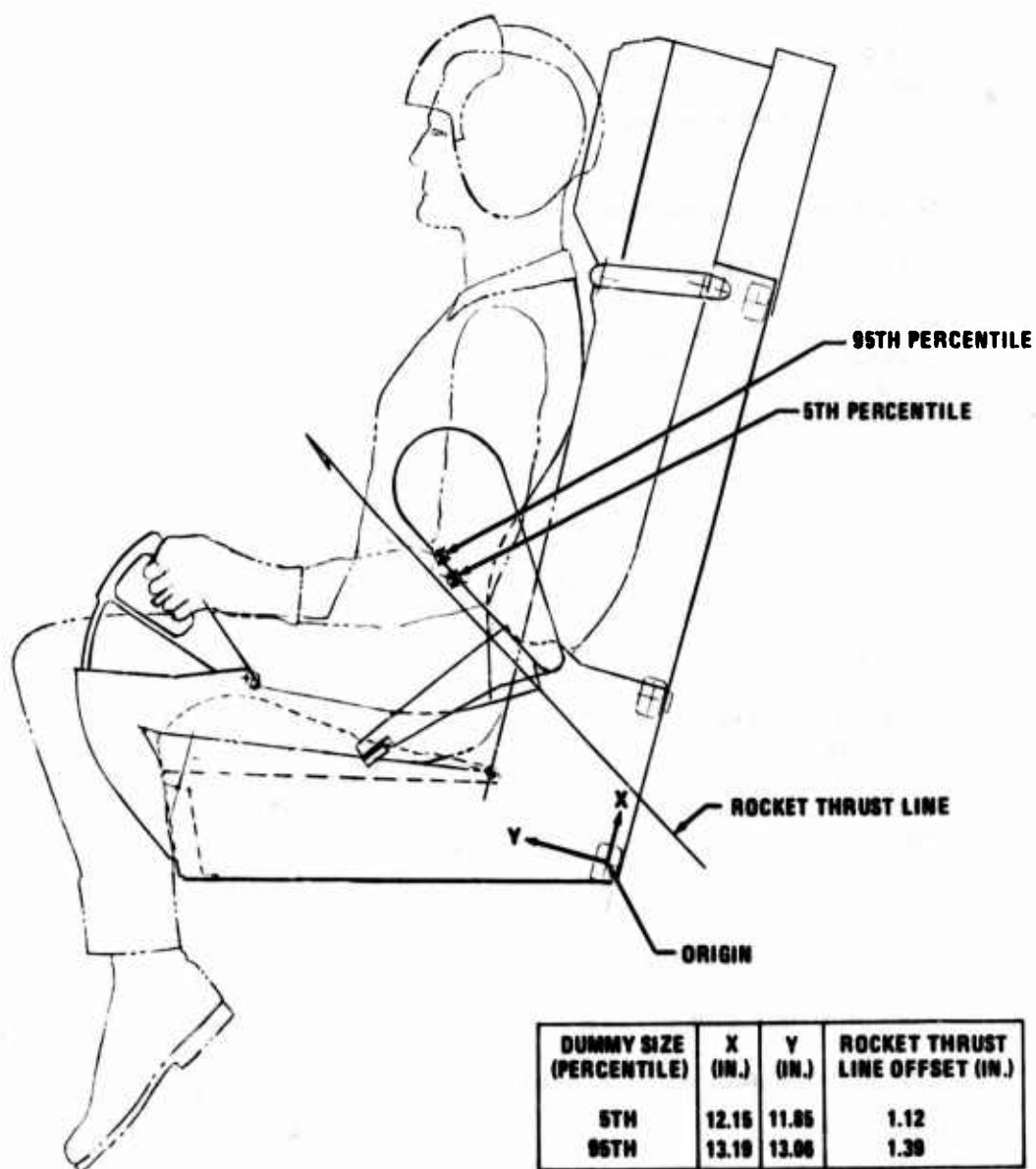


FIGURE 94. ACES CENTER OF GRAVITY LOCATIONS

TABLE VIII
ACES WEIGHT SUMMARY

Item	Weight (pounds)	
	Installed	Ejectable
Seat Assembly	94.1	94.1
Structure and Bolt-ons	40.4	
Ejection Controls	10.2	
Environmental Sensors	3.3	
Arm Restraints and Armrests	6.4	
Recovery Sequencer	5.5	
STAPAC	11.5	
Drogue	12.8	
Man/Seat Release System	4.0	
Backrest Assembly	25.3	25.3
Structure, Linkage, etc.	17.0	
Inertia Reel	5.9	
Emergency Oxygen	2.4	
Parachute Assembly	20.3	20.3
Canopy and Pilot Chute	12.0	
Deployment Bag	2.2	
Mortar Assembly	2.2	
Cover, Riser and Pilot Chute Pouch	3.4	
Pyrotechnics	0.5	
Survival Kit Assembly	33.4	33.4
Outer Container, Ripcords, etc.	1.7	
Rucksack and Dropline	2.2	
HARK Containers and Belt	1.7	
Equipment Items	27.8	
Harness Assembly	13.1	13.1
Harness Structure	5.3	
Lapbelts	2.2	
Quick-Release Buckle	1.2	
Back Pad	3.0	
Seat Pad	1.4	
Rocket Catapult	21.4	17.9
Booster Tube and Cartridge	3.5	
Motor	11.9	
Rocket Propellant	6.0	
Initiation Sequencers and Linkage	8.9	--
Guide Rails	23.1	--
Adjustment Actuator	5.6	--
TOTAL	245.2	204.1

SECTION XIV TEST PROGRAM

Development and qualification of the ACES system included extensive testing of components, subsystems and of the complete seat system. Formal reports have been prepared and published on all qualification tests in addition to the seat system development ejection tests. Results of other tests have been included in progress reports furnished to the Life Support SPO.

The ACES test program was carried out in accordance with a master test plan, Reference 11. Each series of tests was conducted in compliance with a specific test procedure, which covered test requirements in greater detail than the test plan. System testing was accomplished at various localities, including Long Beach, California; El Centro, California and Alamogordo, New Mexico. Subsystem and component testing was also performed at these locations, as well as at various subcontractor's facilities.

COMPONENT DEVELOPMENT TESTS

Gyro Spin-up Actuator

A series of 18 bench test firings were conducted on the gyro spin-up actuator to assure conformance with design criteria over the total temperature range and to optimize performance. A summary of the test results is shown in Table IX. To achieve the required performance, a 15 percent increase in the gas generator energy was necessary. In addition, minor redesign of the housing end cap and a material change in the gyro gimbal (aluminum to steel) were required for structural purposes. As mentioned in Section IX, problems also were encountered with the vernier rocket sear pin-puller mechanism, requiring several design changes to achieve satisfactory operation.

Automatic Oxygen Hose Disconnect Adapter

Tests were conducted on the automatic oxygen hose disconnect adapter to verify that it functioned in accordance with the design requirements. Functional operation and service life tests were conducted on the complete system, which included the harness quick-release buckle and the adapter attached to the CRU-60/P connector. A total of 1000 operational cycles was performed without failure.

Pressure drop and leakage tests were conducted on the oxygen adapter fitted to a CRU-60/P connector, and the results met the requirements of MIL-C-38271A, paragraphs 3.6.2, 3.6.5, and 3.6.7, Reference 12.

Several human subjects, attired in full flight gear and representing 5th through 95th percentile body sizes, evaluated the oxygen adapter system subjectively while restrained in an ACES seat. Assessments were made relative to operation, comfort, and compatibility with the seat and restraint system. These evaluations were considered successful and the oxygen adapter deemed compatible with the seat.

TABLE IX
GYRO SPIN-UP ACTUATOR DEVELOPMENT TESTS

Test No.	Conditions			Results					Remarks
	Temp (°F)	Initial Volume (in ³)	Cartridge-Universal Propulsion P/N	Time to Spin-Up (sec)	Max Rotor Velocity (rpm)	Velocity at 0.5 Sec (rpm)	Max Pressure (psi)		
1	90	1.33	1004-1	0.01	9,833	N/A	7,345		
2	84	1.33	1004-1	N/A	9,524	8,940	7,287		
3	85	1.16	1004-1	0.01	9,870	9,186	7,550	Failed end cap.	
4	78	0.98	1004-1	0.007	10,400	9,857	8,028	Failed end cap.	
5	80	0.98	1004-1	0.008	10,594	8,921	8,534		
6	78	1.00	1004-1	0.008	10,056	9,416	7,917		
7	74	0.83	1004-1	0.007	9,902	9,247	8,744	Failed actuator housing mounting support.	
8	76	1.00	1004-3	0.008	10,842	10,120	9,700		
9	76	1.00	1004-3	0.006	10,955	10,196	10,172		
10	70	1.00	1004-3	0.007	10,790	N/A	10,330		
11	-69	1.00	1004-3	0.006	12,012	10,912	12,950	Failed gimbal and actuator housing gimbal support.	
12	-66	1.00	1004-3	0.006	N/A	N/A	14,057	Failed gimbal.	
13	-65	1.33	1004-3	0.007	11,667	11,143	7,997	Failed gimbal and actuator housing mounting support.	
14	66	1.33	1004-3	*	10,807	*	*	*Partial instrumentation failure precluded acquisition of data.	
15	72	1.33	1004-3	0.006	11,064	10,030	9,097		
16	-64	1.33	1004-3	0.005	11,451	10,754	9,805		
17	200	1.33	1004-3	0.006	9,806	9,314	8,061		
18	200	1.33	1004-3	0.005	10,650	*	8,173		

The oxygen adapter was incorporated on all the ACES dynamic ejection tests, and wind blast integrity proved satisfactory at ejection speeds up to 590 KEAS.

SUBSYSTEM DEVELOPMENT TESTS

Restraint Harness

The restraint harness, which includes the quick-release buckle, was subjected to a series of drop tests from a tower and from an airplane at the DOD JPTFC, El Centro, California. Six drop tests were conducted from a tower wherein the harness was fitted to a 301-pound torso-shaped dummy and dropped from a height of 16.5 feet. A cable attached to the dummy, via a pair of webbing risers, stops its fall which results in a force similar to that of a parachute opening shock. Instrumentation consisted of load cells in each riser assembly and accelerometers and a telemetry transmitter installed in the neck cavity of the dummy. The first five tests were successful, with minor damage or webbing slippage occurring in three cases. On the sixth test, the drop height was increased to 17.5 feet to intentionally induce a failure of the harness. The harness failed where the right-hand sling strap passes through the canopy release fitting. As the sixth test was not required by the test procedure, this phase of the testing was considered successful. The results are tabulated in Table X.

The tower drops were followed by a series of five drop tests from a C-130 airplane at a speed of 150 KIAS and an altitude of 1000 feet. The first four tests were completed without damage to the harness. On the fifth test, the harness sling strap failed in tension where it passes through the right-hand canopy release fitting; however, the dummy was retained in the harness throughout the recovery and landing impact. Test results are given in Table XI. As the test conditions were deemed to be unrealistically severe for the restraint harness, structural integrity was considered adequate. In the ACES system, the only time the harness serves in the capacity of a conventional harness is (1) following recovery when the seat is released from the crewman, or (2) if the parachute fails to initiate automatically. In both cases, anticipated parachute loads are well below those measured in the tower and air drop tests.

Pitch Stabilization Unit (STAPAC)

Three tests of the vernier rocket pitch stabilization subsystem (STAPAC) were conducted. The object of the tests was to verify functional operation and response of the gyro-control vernier rocket under various pitch-rate conditions. The subsystem was tested on a fixture that was free to rotate ± 40 degrees about a fixed axis. The fixture was capable of simulating seat pitch rates for a range of cg/main rocket thrustline offsets of ± 2 inches. The fixture was also capable of simulating man/seat moments of inertia of 5th through 95th percentile personnel. Simulated conditions for the three tests were as follows.

TABLE X.
RESTRAINT HARNESS DROP TOWER TESTS

Test No.	Date	Maximum Riser Load (lb)			Acceleration (G)			Remarks
		Right	Left	Total	Vertical	Lateral	Longitudinal	
1	9-3-70	4480	4100	8500	19.5	2.5	18.7	Slight damage to right-hand sling strap near canopy release. One-half inch webbing slippage in front body strap adjuster.
2	9-3-70	4550	4175	8675	18.0	2.2	20.0	No damage. Approximately 0.5-inch webbing slippage in front body strap adjusters.
3	9-3-70	4625	3650	7500	21.0	0.4	10.6	Additional damage to right-hand sling strap near canopy release. Approximately 0.5-inch webbing slippage in front body strap adjusters.
4	9-4-70	4200	3700	7900	20.0	4.5	11.0	No damage
5	9-4-70	4350	4150	8500	16.5	3.0	16.9	No damage
6	10-21-70	---	---	7098	---	---	---	Harness failed at previously damaged area. This was an intentional destructive test. Drop was made from a height of 17 ft 6 in.

NOTE: All tests made using same harness assembly, serial No. 6.
Total riser load is galvanometer summation.
All drops made from a height of 16 ft. 6 in., except as noted
All drops made using a 301-pound dummy.

TABLE XI.
RESTRAINT HARNESS AIRDROP TESTS

Test No.	Date	Maximum Riser Load (lb)			Acceleration (G)			Remarks
		Right	Left	Total	Vertical	Lateral	Longitudinal	
1	9-9-70	3500	3775	7200	14.5	2.2	7.2	No damage or webbing slippage
2	9-11-70	3650	---	7000*	20.0	---	23.5	No damage or webbing slippage TM antenna was damaged * calculated from accelerometer data.
3	9-16-70	3120	3580	7550	17.0	0.0	21.0	No damage or webbing slippage
4	9-18-70	3900	4200	7650	21.5	7.5	4.5	No damage or webbing slippage
5	9-23-70	1400	1380	2250	9.5	20.2	14.0	Harness sling strap failed at point where it passes through R. H. canopy release fitting. Dummy was retained by harness and recovered successfully.

NOTE: All tests made using same harness assembly, serial No. 7
 Total riser load is galvanometer summation, except as noted
 All drops made at airspeed of 150 KIAS and an altitude of 1000 ft
 All drops made using a 299-pound dummy

Test No. 1 - 50 percent crewman, rocket thrustline offset 0 inches

Test No. 2 - 95 percent crewman, rocket thrustline offset 2 inches below man/seat cg.

Test No. 3 - 5 percent crewman, rocket thrustline offset 2 inches above man/seat cg.

Tests No. 1 and 3 were completed successfully. In Test No. 2, the vernier rocket exploded shortly after ignition. The rocket failure was attributed to a faulty bond of the rocket grain to the casing. Test No. 2 was not re-run because the efficacy of a design change in the vernier rocket, to provide an adequate grain-to-case bond, was demonstrated in Test No. 3, as well as in tests by the supplier on six units that had been subjected to extreme temperature cycling prior to firing.

Drogue Parachute and Environmental Sensors

Static and dynamic tests were conducted on the drogue subsystem to evaluate function and performance. Four static tests of the drogue parachute installation were made to measure drogue gun slug velocities and to verify proper deployment of the system from the stowage compartment. The tests were made from an actual seat structure, which was retained in an upright attitude. Except for minor problems experienced with the stowage compartment latch bar, requiring a design change, all design criteria were met. The drogue gun muzzle velocity was determined to be 227 feet per second.

A series of five of eight scheduled tests were made on the Tomahawk sled at Holloman AFB to evaluate deployment and inflation behavior, opening forces and drag characteristics. The results of these tests are tabulated in Table XII. Drag coefficients were lower than the 0.36 predicted value (approximately 0.21), albeit canopy inflated shapes appeared normal for a Hemisflo design. The low drag coefficients were attributed to wake effects caused by the boiler-plate, simulated ACES installation on top of the sled from which the drogue was deployed. Although deployment data was considered valid, it was decided to discontinue testing as the aerodynamic wake behind the sled/vehicle combination was not believed representative. This contention was supported by results of subsequent seat ejection tests in which drag coefficients of the order of 0.36 were obtained. During the course of the test program modifications were incorporated in (1) the drogue to reduce geometric porosity and increase trail distance, (2) in the extraction chute to improve inflation times by addition of a center line, and (3) in the drogue deployment sleeve to improve structural integrity and prevent premature deployment of the drogue canopy and suspension lines. Typical drogue performance for tests conducted on the Tomahawk sled is shown in Figure 95.

Coincident with the drogue dynamic tests, evaluations were made on the environmental sensors. Information was obtained relative to total and static pressure, transducer response time, and switch positions versus velocity. On test No. 4 in which the pitot was erected at a sled velocity of 508 KEAS, the velocity switches changed from Mode 1 to Mode 2 in 30 msec from the time the release mechanism on the boilerplate seat was initiated. The total-pressure oscillograph trace revealed that the unit sensed the change from zero to the ambient pressure at 508 KEAS 4 msec, which is more than adequate for reliable mode selection in the time available.

TABLE XII
ACES DROGUE SYSTEM TEST RESULTS (TOMAHAWK)

Test No.	Test Date	Velocity At Drogue System Initiation $t = 0$			Event Times - Sec							Peak Opening Force			Average Force Data			Average Drag Coefficient C _{D0}	Calculated X Factor	Barometric Conditions
		KEAS	Ft/Sec	Mach	Drogue Gun Muzzle Flash	Drogue Deploy Line Initiation	Extraction Chute Line Stretch	Drogue Bag Stripoff	Drogue Line Stretch	Drogue Full Open	Drogue Fill Time Sec	Lb	Lb	Dynamic Pressure Lb/Ft ²	Velocity Mach	Lb	Lb			
1	7-7-70	495	923	0.802	0.004	0.069	0.113	0.190	0.260	0.522	0.262	3800	3416	643	0.721	0.201	0.978	90°F 25,905 in Hg		
2	7-14-70	584	1092	0.947	0.004	- - -	- - -	- - -	0.270	1.42	1.150	3900	3723	735	0.758	0.192	0.989	91°F 25,930 in Hg		
3	8-14-70	503	935	0.817	- - -	- - -	- - -	- - -	0.270	0.450	0.180	4000	3587	676	0.736	0.201	1.014	85°F 25,865 in Hg		
4	8-21-70	508	948	0.825	- - -	- - -	- - -	- - -	0.250	0.365	0.115	4800	4140	694	0.737	0.225	1.025	89°F 25,850 in Hg		
5	10-31-70	500	927	0.831	- - -	- - -	- - -	- - -	0.250	0.960	0.710	3300	- - -	- - -	- - -	0.201	- - -	58°F 25,865 in Hg		

NOTE: Parachute drag coefficient, C_{D0}, based on nominal diameter. Surface area, S₀, equal to 26.4 square feet.

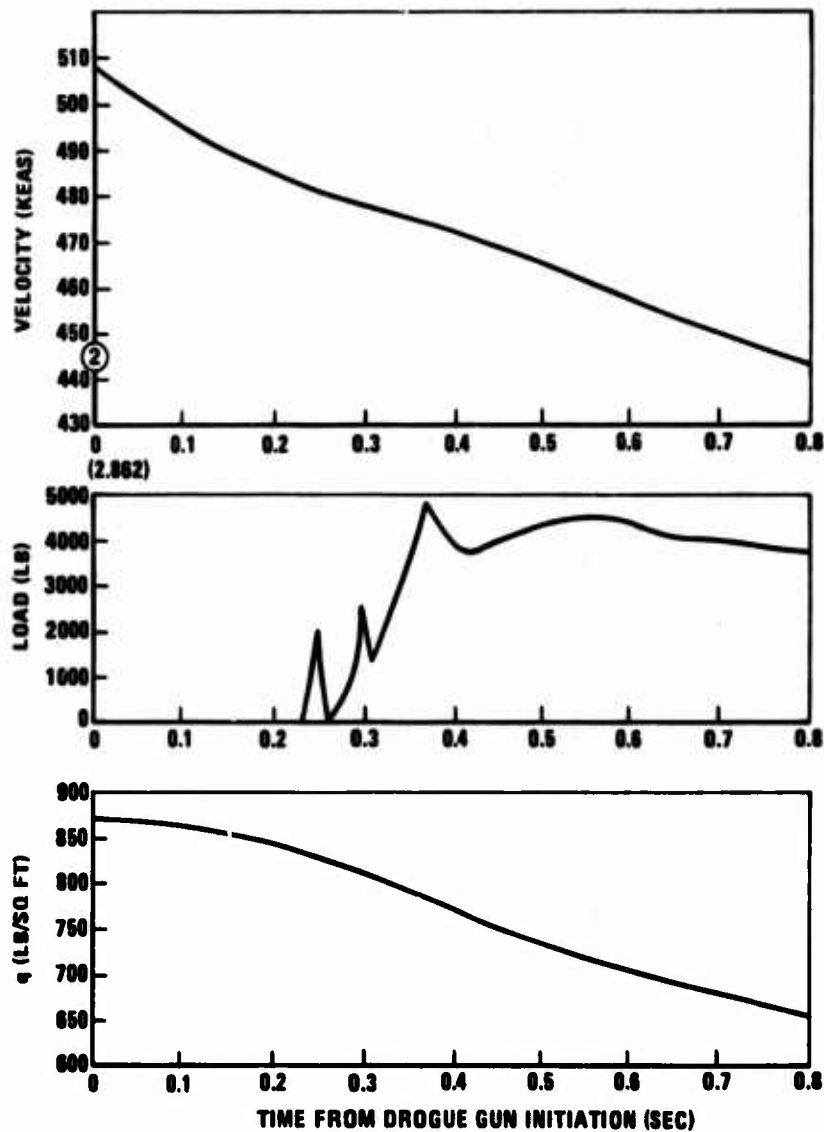


FIGURE 95. DROGUE PERFORMANCE (TOMAHAWK TEST NO. 4)

Of equal importance is the base pressure, which is the static pressure measured adjacent to the transducer static pressure ports. If the base pressure effect is of sufficient magnitude, it can alter the normal Mode 2 - Mode 3 crossover velocity, which is a function of the total and static pressure altitude. Figure 96 plots the base pressure coefficient for a range of dynamic pressures using data obtained from the first and second Tomahawk sled runs. As the base pressure coefficient is relatively constant with altitude, a mean value of 0.4 has been used to estimate the base pressure behind the seat for all speeds and altitudes within the ACES escape envelope, Reference 9.

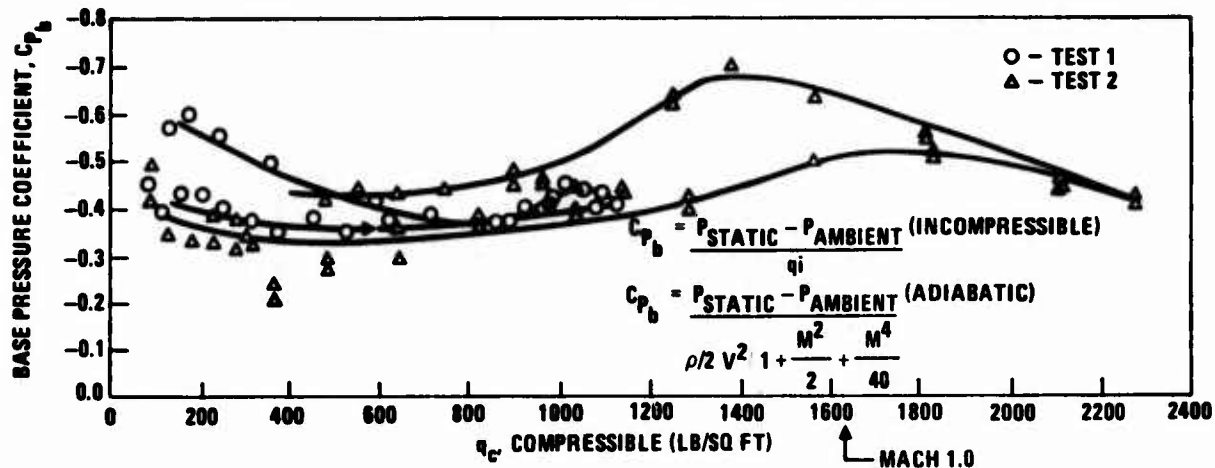


FIGURE 96. BASE PRESSURE COEFFICIENT VS DYNAMIC PRESSURE

Recovery Parachute

The ACES recovery subsystem was subjected to a series of 29 development drop tests using a 425-pound bomb-type vehicle. The objective of these tests was to demonstrate adequate structural integrity of the parachute system, to optimize the reefing configuration and to obtain time-force histories of parachute operation over a range of speeds from 125 to 300 KEAS and altitudes from 1500 to 17,000 feet.

During the early part of the test program, it became evident that the C9 canopy required apex reinforcement to sustain the forces imposed by the 425-pound suspended mass. In addition, the reefing line length was increased from 86 to 156 inches, in two stages, to provide a balance between reefed opening and full inflation forces. The 156-inch reefing line resulted in a reefed drag area ratio, $(CDS)_R / (CDS)_O$, of 10 percent. To further reduce full inflation forces, the reefing line cutter time delay was increased from 1.0 to 1.3 seconds to allow greater deceleration during the reefed portion of the parachute operation. The results of the final 15 tests of the development program, wherein all parachutes incorporated 10 percent reefing and 1.3-second delay cutters, are listed in Table XIII. Satisfactory performance was demonstrated at speeds up to 290 KEAS (at mortar initiation) at 5300 feet and at 179 KEAS at 17,000 feet.

Survival Kit

A series of tests were conducted on the survival kit assembly to determine the suitability of the survival equipment package with respect to (1) watertightness, (2) dropline deployment of the liferaft and rucksack, including raft inflation, (3) operation of the automatic and nonautomatic features, and (4) separation from the seat.

The equipment container and rucksack were submerged separately in water and checked for water leakage. The rucksack, containing 29.5 pounds of equipment, was dropped from a height of 40 feet and snatched at the end of a 30-foot nylon dropline prior to submergence. Both units provided acceptable protection against water leakage.

TABLE XIII
ACES RECOVERY SUBSYSTEM DEVELOPMENT TESTS - 10 PERCENT REEFING

Test No.	Test Date	Events												Remarks					
		Parachute Mortar Initiation			Pilot Chute Full Inflation			Parachute Deployment Bag Strippoff		Reefed Inflation		Max. Reefed Load (Lb)			Disreef		Full Inflation		Max. Full Infl. Load (Lb)
		Alt	Time	Vel.	Time	Vel	Time	Vel	Time	Vel	Time	Vel	Time		Vel	Time	Vel	Time	Vel
15	4/9/70		1,540	0	229	0.376	204	0.461	197	0.699	169	1.29	84	1.59	49	560	No Damage		
16	4/15/70		1,412	0	214	0.350	204	0.491	198	0.533	192	1.35	118	1.89	57	7300	No Damage		
17	4/20/70		1,377	0	230	0.335	202	0.415	197	0.849	156	1.35	97	1.68	49	8400	No Damage		
18	4/23/70		1,470	0	248	0.374	212	0.424	203	0.683	161	1.35	60	1.60	34	7850	Ruptured one gore - normal rate of descent (R/D)		
19	4/29/70		1,340	0	248	0.408	207	0.459	199	0.868	124	1.33	64	1.67	30	6600	No Damage		
20	5/1/70		1,670	0	241	0.239	214	0.300	206	0.682	141	1.08	79	1.57	30	7550	One reefing line cutter did not fire		
21	5/5/70		1,390	0	277	---	---	0.386	258	1.20	130	1.33	103	1.60	62	---	No TM used. Four suspension lines broken		
22	5/11/70		1,130	0	269	0.296	255	0.375	248	0.689	195	1.27	96	1.54	57	7000	Both reefing line cutter pockets damaged.		
23	5/13/70		1,330	0	283	0.309	278	0.391	268	0.600	233	0.795	187	---	---	9700	Major damage - canopy did not remain inflated. Early disreef		
24	6/25/70		17,200	0	143	0.418	140	0.542	136	0.668	130	1.35	79	1.65	52	8200	No Damage		
25	6/29/70		17,300	0	186	0.376	180	0.397	179	0.564	170	1.34	91	1.61	62	9200	Two gores ruptured. One reefing line cutter not initiated. R/D o.k.		
26	7/2/70		14,700	0	146	0.420	143	0.550	140	0.623	137	1.42	73	1.71	46	7600	No Damage		
27	7/7/70		17,000	0	179	0.222	177	0.434	176	0.609	176	1.40	81	1.63	56	9200	No Damage		
28	7/10/70		5,300	0	290	0.259	290	0.431	280	0.500	273	1.29	99	1.56	56	8000	Both reefing line cutter pockets damaged		
29	7/23/70		5,200	0	316	0.232	305	0.350	293	0.530	267	1.29	159	4.33	23	4400	Four suspension lines broken during reefed inflation. Canopy damaged at full infl. - R/D excessive		

NOTE: Altitude is in feet
Time is in seconds
Velocity is in KEAS
All tests made with a 425 ±5-lb bomb
Reefing line cutter time delay = 1.3 secs

The ripcord pins on the equipment container closure flaps were pull tested using the manual D-handle and the automatic deployment lanyard. Four static pull tests were made with the manual and automatic controls. Recorded pull forces were all well within the 25 ±5-pound design limit.

Four tests were made in which the liferaft and rucksack were deployed from the equipment container. The equipment container, weighing 31 pounds with survival equipment installed, was suspended 35 feet above the ground by the harness attach fittings. The automatic deployment ripcord lanyard on the equipment container was pulled to unlock the container and allow the liferaft and rucksack to free fall from the container and be snubbed by the nylon dropline. Liferaft and rucksack deployment, including liferaft inflation, was satisfactory in each test.

Several live subjects were used to initiate deployment of the liferaft and rucksack while suspended above the ground in a simulated parachute descent condition. The subjects, representing the extremes in size and reach, wore the ACES restraint harness, which was suspended from the parachute riser fittings. All subjects were able to reach and pull the manual D-handle on the equipment container.

Survival kit deployment from the seat was made under simulated ejection conditions. Man/seat separation was simulated by hoisting a 95th percentile dummy from the seat through an attachment to the restraint harness parachute riser fittings. The seat was fixed to the ground but free to rotate in the pitching plane. Two tests were conducted, one with the selector mechanism on the seat set for manual and the other for automatic liferaft and rucksack deployment. The survival kit separated from the seat without difficulty and the deployment mechanism operated properly in both the manual and automatic deployment positions.

Telescoping Guide Rails

Two dynamic load tests of the telescoping guide rail installation were conducted to verify functional operation, structural integrity, and adequacy of the energy absorption stop device. The tests consisted of ejecting a boilerplate-type seat, utilizing a GFE M3A1 ballistic catapult, from a set of telescoping guide rails mounted on a static test stand. The M3A1 catapult was used to provide the same seat end velocity at the top of the rails as the ACES system rocket catapult. The boilerplate seat simulated the ACES system mass and moment of inertia with a 5th percentile dummy in one test and 95th percentile dummy in the other. Results of these tests showed that the telescoping guide rails functioned as designed.

Guide Rail Friction Testing

As a result of difficulties encountered in not meeting the originally specified 50 ft/sec catapult end velocity, a test was performed to determine if the friction coefficients between the seat guideblocks and the telescoping portion of the guide rails were excessive. Four tests were performed. In all tests, the seat was propelled up the guide rails by application of hydraulic pressure to a modified XM-39 rocket catapult. A moment of 7300 ft/lb, roughly equivalent to that experienced at a time when 17 g of catapult load would be

experienced, was induced on the seat throughout the entire catapult stroke by a beam and weight assembly.

The first two tests were conducted employing slippers used during a previous test and a set of guide rails used for nine previous ejection tests. The average C_f (coefficient of friction) for guide rail-to-guide rail friction was found to be 0.24 and 0.28 respectively. Design C_f was anticipated to be in the range of 0.17 to 0.20. Average slipper-to-guide rail coefficients were 0.14 and 0.15 respectively; the design value was 0.15.

Tests 3 and 4 were performed using new sideblocks and the same guide rail system as for tests 1 and 2 except that all surfaces were inspected and lubricated, where required, to return the system to a near-new status. Guide rail-to-guide rail coefficients were not available on test 3 but averaged 0.21 on test 4. Slideblock-to-guide rail C_f was 0.15 to 0.11 respectively. Although, for these tests, guide rail-to-guide rail friction coefficients were slightly higher than anticipated, it has been determined that this would have only a small effect on the end velocity. It was further noted that there were no unusual binding or interference problems uncovered, even though the moments throughout the entire stroke were much higher than encountered during a normal ejection.

SYSTEM DEVELOPMENT TESTS

Boilerplate Seat Tests

Two boilerplate seat ejection tests were conducted to evaluate the efficiency of changes incorporated in the ACES seat structure, rocket catapult-to-seat attachment, adjustment actuator, and in the XM-39 rocket catapult. Secondary objectives included obtaining rocket catapult pressure data and a yaw history of the ejected mass.

Test conditions were as follows:

	<u>Test No. 1</u>	<u>Test No. 2</u>
Static cg (X) - inch	11.67	13.26
(Y) - inch	0.038 RT	0.026 LF
(Z) - inch	11.83	12.02
Static cg Offset - inch	0.16	0.29
Ejected Mass - pounds	382	345
Moment of Inertia (I_{yaw}) - slug - ft ²	8.3	7.3
(I_{pitch}) - slug - ft ²	-	19.4

In Test No. 1, the rocket booster tube developed a hotspot and bending occurred after approximately 1 foot of seat travel in the guide rails. Seat velocity at catapult separation was 45 fps. The seat was very stable and exhibited no perceptible yaw.

In Test No. 2, the seat was stable in pitch but exhibited some rotation in the yaw plane, approximately 45-degrees counter-clockwise at rocket burnout. No structural damage was noted to the rocket catapult, catapult-seat attachment, or seat adjustment actuator (full extended position). Catapult booster pressure was recorded and the maximum pressure was 8220 psi.

Ground Functional

Man/Seat Release Mechanism - Two series of tests were conducted on the man/seat release mechanism to measure the manual handle detent pull-out, pin first-motion, and sustained pin motion forces. In the first test series the parachute was installed to impose the most severe static friction condition on the mechanism. In the second series the parachute was omitted to simulate a failure of the mechanism following a normal automatic parachute deployment. Pull forces, tabulated below, were considered within acceptable limits.

Test Series	Average Handle Force (pounds)		
	Detent Pull-Out	Pin First Movement	Pin Sustained Motion
1	27.3	43.4	30.5
2	32.5	30.4	18.3

One additional test was conducted on the man/seat release mechanism, prior to the first development seat ejection test, to verify proper functioning of the mechanism when activated in the automatic mode. The seat was loaded to simulate a 5-g parachute drag force, which imposed the maximum anticipated friction load on the mechanism. Positive man/seat release was demonstrated following initiation of the thruster cartridge.

Backrest Release Mechanism - Tests were conducted on the backrest release mechanism to verify that a crewman could reach and operate the release handle and that the backrest would fall away without a hangup. Several human subjects, representing the 5th through 95th percentile in stature, specifically in functional reach, were suspended from a cable in the restraint harness with the backrest attached. All subjects were able to actuate the release handle without difficulty and the backrest dropped away without incident.

Ejection Firing Controls - Tests were conducted to determine the force required to actuate the ejection firing controls. Using a Hunter force indicator, pull tests were made on a single control and on both controls to obtain comparative data. The force required to unlatch the controls was the maximum force recorded and this ranged between 65 and 70 pounds when pulling one control. When pulling both controls simultaneously, the maximum unlatch force was 60 pounds.

The firing controls actuation force, although exceeding the 20 ±3 pounds specified in MIL-S-9479A, is considered well within practical limits for the specific geometry of the ACES system. Subjective evaluations of the firing control subsystem by contractor and ASD personnel indicated that the operation of the mechanism is smooth and does not require excessive pull force.

Emergency Oxygen Green Apple - A test was conducted on the emergency oxygen green apple automatic actuating mechanism to verify proper operation.

With the backrest installed, the actuating linkage was adjusted to remove all slack from the system. The arm restraint paddles were manually rotated forward to the actuated position, but the green apple was not pulled sufficiently to activate the oxygen supply. This was determined to be the result of excessive green apple cable length. A new oxygen cylinder assembly with a shorter green apple cable was installed, and the test was repeated with satisfactory results.

Seat System Static and Dynamic Ejection Tests

Nine static (zero-zero) and three dynamic (220 to 590 KEAS) development ejection tests were conducted on the ACES system, Reference 13. The objective of these tests was to verify the functional operation and predicted performance of the ACES system. A summary of each test is presented below and the test results are tabulated in Table XIV. All static tests were conducted at the Long Beach Municipal Airport and the dynamic tests at Holloman AFB, Alamogordo, New Mexico.

Test No. 1 (Zero KEAS) - This test, 11 March 1970, employed a 5th percentile dummy resulting in an ejected mass of 346 pounds. The system static cg was located 1.21 inches above the rocket catapult thrust line, which was considered a nominal (design) offset.

A failure to activate the switch in the recovery sequencer precluded initiation of any subsystems following ignition of the rocket catapult. The occupied seat attained a height of 150 feet and contacted the ground 300 feet in front of the test stand, Figure 97. It was also noted that the velocity of the seat

EVENT	TIME (SEC)	X (FT)	Y (FT)	Z (FT)	VELOCITY (FT/SEC)
1 EJECTION SEAT FIRST MOTION	0.0	0	0	7	18
2 CATAPULT SEPARATION	0.14	-1	0	10	44
3 MAIN ROCKET BURNOUT	0.51	10	0	31	92
4 ROCKET ACTION TIME	0.77	24	3	52	94
5 GROUND CONTACT (SEAT)	6.90	295	101	3	90

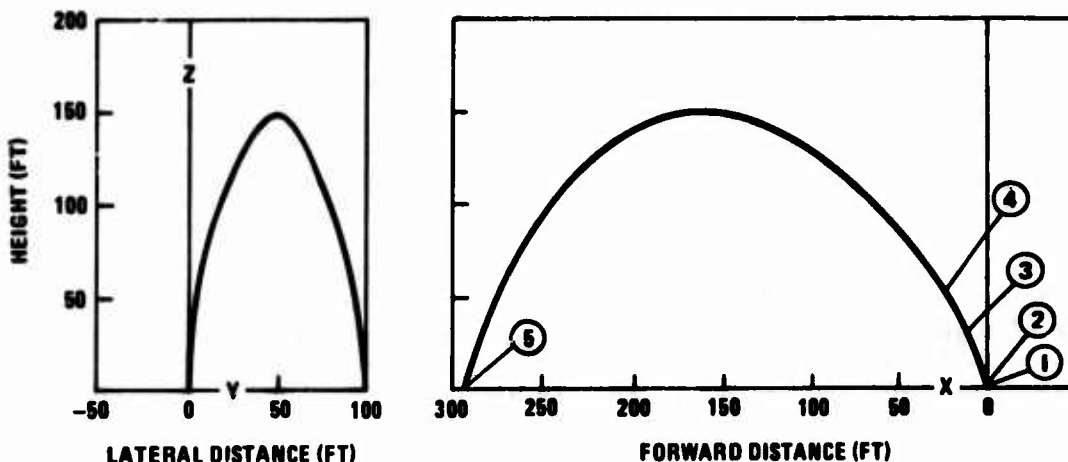


FIGURE 97. TRAJECTORY AND EVENT DATA FOR ACES DEVELOPMENT TEST NO. 1

TABLE XIV

SUMMARY OF EVENT TIMES FOR ACES DEVELOPMENT EJECTION TESTS

Test Number	1	2	3	4	5	6	7	8	9	10	11	12
Test Date	11 Mar 70	7 Apr 70	30 Apr 70	14 May 70	23 June 70	17 July 70	24 Mar 71	15 Apr 71	21 Apr 71	14 May 71	21 May 71	22 June 71
Velocity at Ejection (KEAS)	0	0	0	0	0	0	0	0	0	410	220	590
TIME FROM SYSTEM IGNITION (SECONDS)												
Event	1	2	3	4	5	6	7	8	9	10	11	12
System Initiation	0.0	0.0	0.0	0.0	0.0	0.0	0.0	0.0	0.0	0.0	0.0	0.0
Arm Restraint First Motion	(4)	0.038	0.035	0.037	0.029	0.024	0.039	0.034	0.048	(7)	(7)	(7)
Arm Restraint in Position	(4)	0.277	0.064	0.261	0.280	0.274	0.355	0.315	0.320	(7)	(7)	(7)
First Seat Motion	0.336	0.373	0.320	0.345	0.355	0.325	0.353	0.364	0.365	0.359	0.320	0.328
Environmental Sensor Pitot Release	(4)	0.398	0.420	0.428	0.444	0.338	(4)	(7)	0.442	(4)	(4)	(4)
Environmental Sensor Pitot In Position	(4)	0.438	0.456	0.456	0.476	0.375	(4)	0.480	0.476	(4)	(4)	(4)
Drogue Gun Fires	(5)	(5)	1.05(1)	(5)	(5)	(5)	(5)	(5)	(5)	0.452	(5)	0.451
STAPAC Ignition	(3)	0.471	0.484	0.487	0.484	0.493	0.278(1)	0.485	0.491	0.460	0.489	0.455
Catapult Separation	0.480	0.463	0.475	0.485	0.494	0.461	0.497	0.519	0.504	0.480	0.493	0.450
Extraction Parachute Filled	(5)	(5)	(4)	(5)	(5)	(5)	(5)	(5)	(5)	0.584	(5)	0.560
Drogue Parachute Filled	(5)	(5)	(4)	(5)	(5)	(5)	(5)	(5)	(5)	0.766	(5)	0.670
Main Rocket Action Time	1.11	0.88	0.996	0.965	0.998	(1)	1.02	1.04	1.02	0.92	0.98	0.94
Vernier Rocket Action Time	(3)	1.03	1.10	1.07	1.07	1.09	0.85	1.09	1.07	1.03	1.06	0.98
Parachute Pack First Motion	(3)	1.14(1)	1.02	0.516	0.511	0.995(1)	0.317(1)	0.532	0.518	1.28	0.527	1.27
Lower Drogue Bridle Severance	(3)	0.896(1)	1.11	0.638	0.626	1.10	(7)	0.643	0.640	1.39	0.648	1.38
Upper Drogue Bridle Severance	(3)	0.926(1)	1.13	0.665	0.535(1)	1.0(1)	0.462	0.666	0.671	1.42	(7)	1.41
Deployment Bag Pilot Chute Filled	(3)	(4)	(4)	1.41	0.966	(4)	1.02	0.93	1.14	2.05	0.81	1.42
Deployment Bag Unlock	(3)	1.71	1.76	1.18	1.13	(1)	1.09	1.16	1.12	(7)	0.934	1.56
Deployment Bag Stripoff	(3)	2.09	(4)	1.46	1.45	(1)	1.29	1.42	1.37	2.54	1.01	1.62
Parachute Reefed Fill	(3)	(6)	(6)	(6)	(6)	(1)	(6)	(6)	(6)	(1)	1.52	1.87
Parachute Disreefed	(3)	2.17	(7)	(7)	1.80	(7)	(7)	(7)	1.9	(1)	1.88	2.46
Parachute First Filled	(3)	3.74	5.51	3.61	4.04	(1)	2.9	3.20	3.1	3.2	2.25(1)	2.86
Seat Release	(3)	(4)	2.73	2.35	2.37	2.65	2.46	2.60	2.66	3.29	2.73	3.28
Man/Seat Separation	(3)	(4)	4.53	(4)	3.87	(1)	4.4	4.1	(1)	(1)	(1)	4.90
Parachute Final Fill	(3)	5.24	5.51	5.32	4.04	(1)	5.0	4.7	4.7	5.61	(1)	4.75
Ground Contact	7.2	14.3	8.88	11.4	8.18	4.28	10.2	7.0	9.6	5.61	4.75	4.90

NOTES:

1. Malfunction - See discussion of individual test
2. Estimated
3. Recovery sequencer was not initiated on this test
4. Not recorded
5. Normally does not occur
6. Did not occur in this test - not a malfunction
7. Not observed

at the end of the guide rails was 44 ft/sec in lieu of the required 50 ft/sec. The recovery sequencer was modified prior to subsequent testing by replacing the striker-actuated switch with a 160 msec delay circuit initiated by the rocket catapult firing signal from either one of the ejection sequencers.

Test No. 2 (Zero KEAS) - This test was conducted on 7 April 1970 and employed a 5th percentile dummy, resulting in an ejected mass of 343 pounds. The system static cg was located 1.03 inches above the thrust line.

Problems were encountered with recovery event sequencing and with the electrical circuit to the harness release thruster, the latter preventing separation of the seat and dummy. The seat achieved a height of 200 feet, Figure 98, with full parachute inflation at 200 ft. The dummy remained in the seat to ground contact. Prior to proceeding with the third test, a minor wiring change was made in the recovery sequencer to provide a compatible circuit with the environmental sensors. The harness release thruster problem resulted from a bent connector pin. For subsequent tests, a pin straightening tool was used to preclude recurrence of the problem experienced in this test.

EVENT	TIME (SEC)	X (FT)	Y (FT)	Z (FT)	VELOCITY (FT/SEC)
1 EJECTION SEAT FIRST MOTION	0.33	0	0	7	11
2 CATAPULT SEPARATION	0.46	-1	0	10	38
3 ROCKET ACTION TIME	0.88	15	4	44	129
4 VERNIER ROCKET BURNOUT	0.91	17	4	47	130
5 PARACHUTE DEPLOYMENT BAG STRIPOFF	2.09	83	89	156	49
6 PARACHUTE DISREEFED	2.17	87	90	161	47
7 PARACHUTE INFLATED	3.74	141	68	200	42
8 TERMINAL RATE OF DESCENT	5.24	120	87	162	28
9 GROUND CONTACT (DUMMY)	14.30	67	-66	2	35

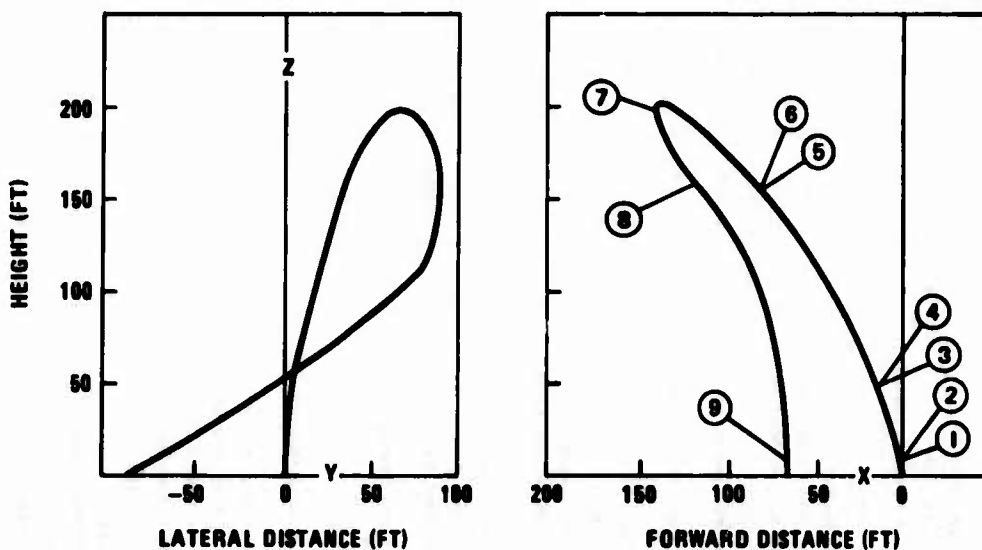


FIGURE 98. TRAJECTORY AND EVENT DATA FOR ACES DEVELOPMENT TEST NO. 2

Test No. 3 (Zero KEAS) - This test was conducted on 30 April 1970 and employed a 95th percentile dummy, resulting in an ejected mass of 414 pounds. The system static cg was located 1.39 inches above the rocket catapult thrust line.

Successful recovery of the dummy was achieved with full parachute inflation occurring at an altitude of 82 feet, Figure 99. Malfunctions were encountered in system sequencing and in parachute operation, and a structural failure occurred in the rocket catapult, which resulted in a portion of the catapult locking mechanism being ejected. The damage did not appear to affect performance of the catapult.

Because the system performed a Mode 2 recovery sequence, except that the drogue was not initiated, it was concluded that microsecond-level pulses emanating from the environmental sensors were responsible for the incorrect mode selection. A filter circuit was incorporated in the recovery sequencer to assure that the logic circuitry would not react to signals of shorter than 10 msec duration.

The parachute deployment and filling were delayed because of a temporary entanglement of the pilot chute and main canopy suspension lines.

EVENT	TIME (SEC)	X (FT)	Y (FT)	Z (FT)	VELOCITY (FT/SEC)
1 EJECTION SEAT FIRST MOTION	0.32	0	0	7	8
2 CATAPULT SEPARATION	0.48	-1	0	10	36
3 MAIN ROCKET BURNOUT	0.83	8	4	34	96
4 VERNIER ROCKET BURNOUT	1.10	17	14	57	90
5 PARACHUTE PACK FIRST MOTION	1.02	14	11	51	95
6 PARACHUTE DEPLOYMENT BAG UNLOCK	1.78	33	30	101	66
7 HARNESS RELEASE INITIATION	2.73	52	70	134	41
8 DUMMY/SEAT SEPARATION	4.53	82	118	116	36
9 PARACHUTE INFLATED	5.51	90	123	82	30
10 GROUND CONTACT (SEAT)	8.00	92	72	2	23

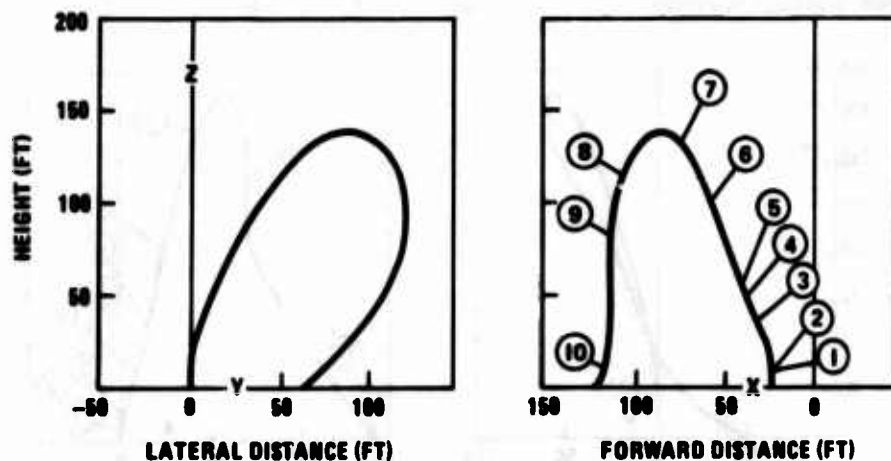


FIGURE 99. TRAJECTORY AND EVENT DATA FOR ACES DEVELOPMENT TEST NO. 3

Test No. 4 (Zero KEAS) - the fourth development ejection test was conducted on 14 May 1970 using a 5th percentile dummy. The ejected mass was 348 pounds and the system static cg was 2.62 inches above the thrust line.

The STAPAC unit compensated for the high cg location by providing good pitch control; the pitch rotation at rocket action time was 5.5 rpm forward. Full parachute inflation (final fill) occurred at a height of 141 feet, Figure 100, but the seat and dummy did not separate because of entanglement of the parachute risers and the environmental sensors. Structural failures of the seat adjustment actuator and rocket catapult (XM-39) booster tube occurred but these did not appear to affect the performance of the seat.

To prevent entanglement of the parachute riser and environmental sensor arm, the aft edge of the pitot duct was relieved, a latch was incorporated on the seat to lock the sensor arms in the erected position, and a v-shaped fabric gusset was stitched between each riser assembly.

The pilot chute installation was modified by attaching the deployment pouch to the forward side of the seat-back skin with velcro tape. The open end of the pouch was reworked to reduce the size of its opening. These modifications were made to obtain earlier and more effective deployment of the pilot chute.

EVENT	TIME (SEC)	X (FT)	Y (FT)	Z (FT)	VELOCITY (FT/SEC)
1 EJECTION SEAT FIRST MOTION	0.35	0	0	7	15
2 CATAPULT SEPARATION	0.40	-1	0	10	42
3 PARACHUTE PACK FIRST MOTION	0.52	0	0	12	48
4 MAIN ROCKET BURNOUT	0.87	9	2	41	105
5 ROCKET ACTION TIME	0.97	12	4	51	111
6 VERNIER ROCKET BURNOUT	1.07	14	7	62	114
7 PARACHUTE DEPLOYMENT BAG STRIPOFF	1.46	23	19	102	99
8 HARNESS RELEASE INITIATION	2.35	40	43	106	65
9 PARACHUTE INFLATED	3.61	58	57	107	15
10 PARACHUTE FINAL FILL	5.32	68	46	141	32
11 GROUND CONTACT (DUMMY)	11.40	142	-45	3	23

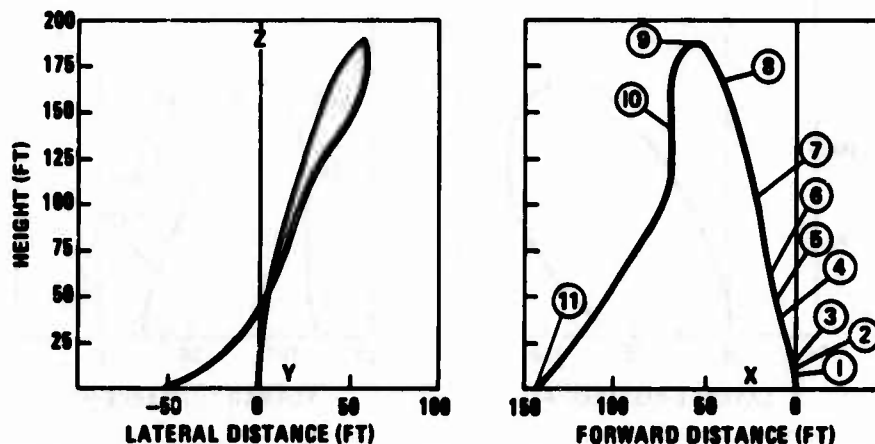


FIGURE 100. TRAJECTORY AND EVENT DATA FOR ACES DEVELOPMENT TEST NO. 4

Test No. 5 (Zero KEAS) - This test was conducted on 23 June 1970 using a 95th percentile dummy, which provided an ejected mass of 419 pounds. The system static cg was 0.34 inch above the thrust line, intended to induce a forward pitching of the man/seat combination.

The test was considered successful with man/seat separation occurring at an altitude of 118 feet followed by full parachute inflation at 113 feet, Figure 101. The STAPAC unit functioned properly to control a forward pitching seat, although the seat appeared to yaw quite severely. A slight delay in separation of the seat was observed, which was attributed to the seat yawing. This resulted in the parachute riser lodging under the left-hand pitot tube, and seat separation was not effected until the parachute developed sufficient drag to break the pitot tube. Prior to the sixth test, 0.063-inch steel cables were attached between the pitot head and seat structure to prevent the parachute risers from becoming lodged beneath the tubes.

A premature severance of the lower drogue bridles was suspected but was not confirmed at this time. Although it did not affect the seat operation, Dorsett Electronics was requested to investigate the suspected discrepancy.

EVENT	TIME (SEC)	X (FT)	Y (FT)	Z (FT)	VELOCITY (FT/SEC)
1 EJECTION SEAT FIRST MOTION	0.36	0	0	7	9
2 CATAPULT SEPARATION	0.49	-1	0	10	36
3 PARACHUTE PACK FIRST MOTION	0.51	-1	0	10	40
4 MAIN ROCKET ACTION TIME	1.00	13	7	44	96
5 VERNIER ROCKET ACTION TIME	1.07	18	10	50	97
6 PARACHUTE DEPLOYMENT BAG STRIPOFF	1.45	29	25	78	81
7 PARACHUTE DISREEFED	1.80	40	40	97	71
8 HARNESS RELEASE INITIATION	2.37	58	60	118	52
9 DUMMY/SEAT SEPARATION	3.07	91	95	118	29
10 PARACHUTE INFLATED	4.04	93	96	113	30
11 GROUND CONTACT (DUMMY)	8.18	91	61	3	26

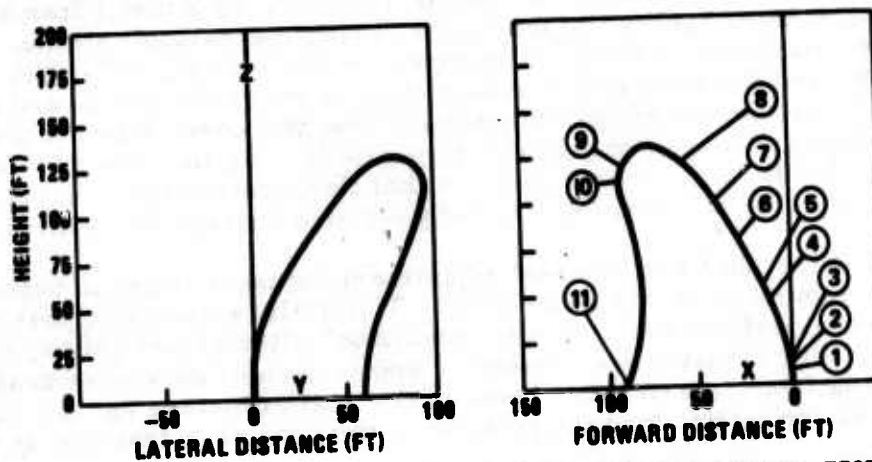


FIGURE 101. TRAJECTORY AND EVENT DATA FOR ACES DEVELOPMENT TEST NO. 5

Test No. 6 (Zero KEAS) - The sixth development test was conducted on 16 July 1970 using a 5th percentile dummy, resulting in a 346-pound ejected mass. The system static cg was located 2.31 inches above the rocket catapult thrust line, which was intended to induce aft pitching of the seat.

The rocket catapult sustainer stage failed to ignite and, as a result, the seat did not achieve sufficient height to permit recovery of the dummy. A malfunction in the recovery subsystem sequencing also was noted. The STAPAC system demonstrated its capability to stabilize the seat system under an extremely adverse situation. The resultant trajectory is shown in Figure 102.

EVENT	TIME (SEC)	X (FT)	Y (FT)	Z (FT)	VELOCITY (FT/SEC)
1 EJECTION SEAT FIRE	0.33	0	0	7	16
2 PARACHUTE PARACHUTE DEPLOYMENT	1.00	-4	0	3	45
3 HARNESS RELEASE	2.05	1	-8	3	11
4 GROUND IMPACT (SEAT)	4.28	11	-13	3	40

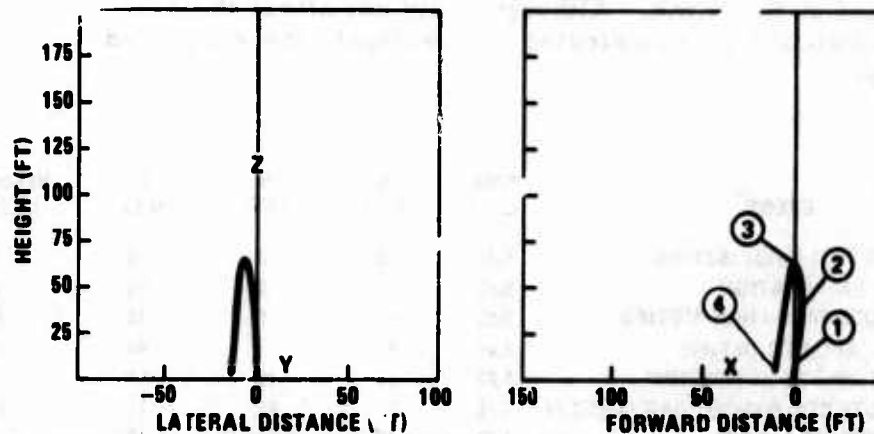


FIGURE 102. TRAJECTORY AND EVENT DATA FOR ACES DEVELOPMENT TEST NO. 6

The rocket motor failed to ignite after separation from the catapult tube. The motor nozzle is isolated from catapult pressure by a metal flame barrier to prevent premature ignition of the motor during the catapult stroke. Near the end of the stroke the barrier is stripped off the rocket, within the catapult tube, and the hot gases are permitted to enter the nozzle and ignite the motor. Post-test investigation revealed that the cover failed to properly strip-off and was damaged sufficiently to partially plug the free flow of hot gas to the rocket motor. It was believed that this restriction of hot gases to the motor precluded adequate heat and pressure buildup for ignition.

The vertical drive shafts of the seat adjustment actuator failed in bending as the seat was propelled up the guide rails. This failure did not appear to affect subsequent seat performance. It was concluded, after investigation, that the failure of the seat actuator was caused by application of excessive bending loads resulting from interference between the seat structure and the catapult launch tube during initial forward rotation of the seat as it traveled up the guide rails.

Following STAPAC ignition, an abnormal recovery sequence was observed. Parachute mortar first-motion occurred 0.995-second after rocket catapult ignition, which is in agreement with a Mode-2 timing sequence. Upper drogue bridle severance was observed at 1.00 second, in lieu of the anticipated 0.150 second, following initiation of the parachute mortar. Seat release was observed 2.65 seconds after parachute mortar ignition. This event is believed to have occurred prior to the prescribed 1.8 seconds following mortar initiation.

The improper sequence described above was duplicated in subsequent testing of the recovery sequencing unit at Dorsett Electronics.

After the sixth development test, several significant modifications were incorporated in the ACES system as follows:

1. The XM-39 rocket catapult, manufactured by Frankford Arsenal, Philadelphia, Pennsylvania was used on all subsequent ejection testing.
2. Based on the erratic performance of the recovery sequencing unit, a complete redesign of the circuitry was undertaken.
3. The seat structure was reworked and the actuator bracket altered, moving the actuator aft, to provide adequate clearance for the rocket catapult.
4. The top beam of the seat structure was altered to allow the sensor pitot arms to rotate to a near vertical position. This would allow a parachute riser, entangled beneath the arm, to release itself. Additional springs were added to index the pitots near the optimum sensing position.

Test No. 7 (Zero KEAS) - This test was conducted on 24 March 1971 using a 5th percentile dummy, resulting in a 355-pound ejected mass. The system static cg was 2.36 inches above the rocket catapult thrust line, which was intended to induce aft pitching of the ejection seat.

The seat exhibited good pitch control, with recovery parachute final inflation occurring at an altitude of 134 feet. Dummy/seat separation was normal, Figure 103. A review of the test films revealed that the recovery events were initiated earlier than intended but times between events were

Premature initiation of the recovery sequencer was caused by a large pulse in the battery circuit produced by the firing of the expended-battery indicator. This, in conjunction with subsequent shorting of the indicator's current-limiting resistor, caused the 160 msec delay circuit to latch up. This effect was simulated by pulsing the battery line with a special laboratory voltage supply. The expended-battery indicator was removed from all recovery sequencing units and the input circuit to the 160 msec delay redesigned to render it less sensitive to noise on the power-supply bus.

Test No. 8 (Zero KEAS) - This test was conducted on 15 April 1971 employing a 95th percentile dummy resulting in an ejected mass of 425 pounds. The system static cg was located 0.09 inch below the rocket catapult thrust line, which was intended to induce forward pitching of the seat.

EVENT	TIME (SEC)	X (FT)	Y (FT)	Z (FT)	VELOCITY (FT/SEC)
1 VERNIER ROCKET IGNITION	0.29	0	0	7	2
2 CATAPULT SEPARATION	0.50	-1	0	10	47
3 ROCKET ACTION TIME	1.02	14	0	55	116
4 PARACHUTE DEPLOYMENT BAG STRIPOFF	1.29	23	0	85	110
5 HARNESS RELEASE INITIATION	2.46	55	0	171	41
6 PARACHUTE INITIAL INFLATION	2.90	64	0	181	23
7 DUMMY/SEAT SEPARATION	4.40	80	0	155	32
8 PARACHUTE FINAL INFLATION	5.00	78	0	134	32
9 GROUND CONTACT	10.2	64	0	3	13

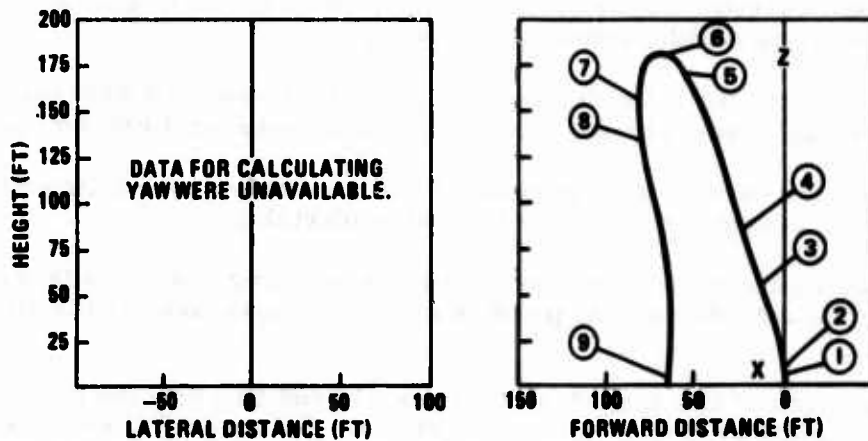


FIGURE 103. TRAJECTORY AND EVENT DATA FOR ACES DEVELOPMENT TEST NO. 7

All seat functions were normal and occurred at the specified times. The pitch stabilization system (STAPAC) provided good rotation and trajectory control, and initial parachute inflation was observed at a height of 122 feet, Figure 104. Dummy/seat separation and parachute final inflation occurred as expected.

Test No. 9 (Zero KEAS) - The ninth static development test was conducted on 21 April 1971 using a 5th percentile dummy, which resulted in an ejected mass of 356 pounds. The system static cg was located 2.38 inches above the rocket catapult thrust line.

All subsystems functioned properly and at the specified time, except that the seat did not separate. The seat system achieved a maximum height of 165 feet, at which point initial parachute inflation occurred, Figure 105.

Harness release was observed 2.66 seconds after ejection, during the parachute transition from reefed to full opening. However, the parachute filling forces were insufficient to effect separation of the seat before ground contact, at 9.6 seconds. There was no physical evidence of mechanical component or system malfunction.

As no reason for the separation failure could be found, and as the failure could not be simulated during repeated laboratory-type testing, no corrective action could be taken.

EVENT	TIME (SEC)	X (FT)	Y (FT)	Z (FT)	VELOCITY (FT/SEC)
1 PARACHUTE PACK PROJECTED	0.53	-1	0	11	38
2 MAIN ROCKET ACTION TIME	1.04	13	8	43	96
3 VERNIER ROCKET ACTION TIME	1.90	15	10	47	95
4 PARACHUTE DEPLOYMENT BAG STRIPOFF	1.42	28	22	71	83
5 HARNESS RELEASE INITIATION	2.00	68	56	119	35
6 PARACHUTE INITIAL INFLATION	3.20	82	80	122	29
7 SEAT JETTISON	4.10	82	40	100	30
8 PARACHUTE FINAL INFLATION	4.70	90	37	78	40
9 GROUND CONTACT (DUMMY)	7.00	78	0	3	28

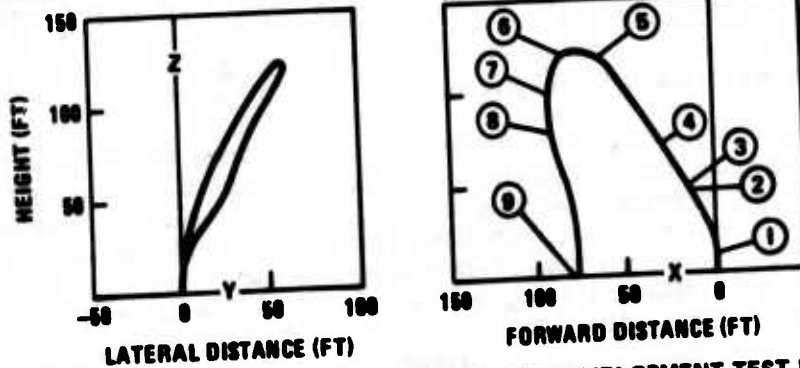


FIGURE 104. TRAJECTORY AND EVENT DATA FOR ACES DEVELOPMENT TEST NO. 8

EVENT	TIME (SEC)	X (FT)	Y (FT)	Z (FT)	VELOCITY (FT/SEC)
1 PARACHUTE PACK PROJECTED	0.52	-1	1	12	43
2 MAIN ROCKET ACTION TIME	1.02	13	4	54	111
3 VERNIER ROCKET ACTION TIME	1.07	18	4	60	113
4 PARACHUTE DEPLOYMENT BAG STRIPOFF	1.37	28	12	91	105
5 PARACHUTE DISREEFED	1.90	46	22	134	74
6 HARNESS RELEASE INITIATION	2.00	65	29	164	22
7 PARACHUTE INITIAL INFLATION	3.10	70	27	165	19
8 PARACHUTE FINAL INFLATION	4.70	80	0	122	40
9 GROUND CONTACT (DUMMY)	9.00	41	101	3	29

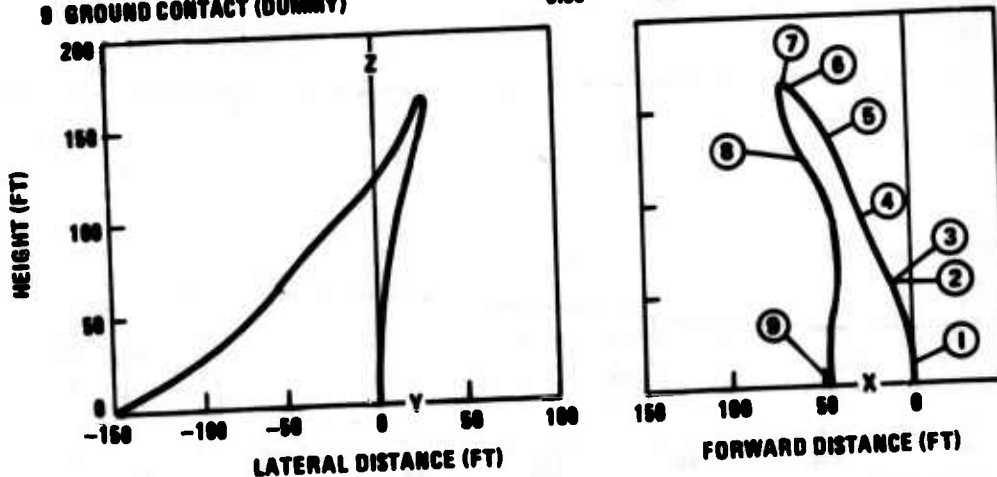


FIGURE 105. TRAJECTORY AND EVENT DATA FOR ACES DEVELOPMENT TEST NO. 9

Test No. 10 (410 KEAS) - The tenth development ejection test was conducted from the aft cockpit station of an F-105 sled on the high-speed track facility at Holloman AFB. The test was conducted on 14 May 1971 using a 5th percentile dummy; ejected mass was 354 pounds. The system static cg was located 1.57 inches above the rocket catapult thrust line.

The system performed as designed, except for (1) failure of the lower drogue bridles, and (2) the main parachute pack projection velocity was lower than required, resulting in excessive deployment time. Parachute first-fill occurred 3.2 seconds after ejection initiation at a height of 60 feet.

The STAPAC stabilization system functioned to assist in initial control of the seat. The lower drogue bridles were weakened by the main rocket flame, and both failed in tension on load application when the seat pitched aft following drogue deployment. As a result, aft pitching was not arrested until the seat back was aligned with the relative windstream.

The parachute was mortar-deployed 1.28 seconds after ejection initiation. It was observed that the projection velocity was substantially lower than that achieved in static ejection tests. This low velocity coupled with an unfavorable seat attitude, resulting from failure of the lower drogue bridles, combined to produce a slower-than-normal deployment of the main canopy. Parachute full inflation occurred at 3.2 seconds at a height of 65 feet above the terrain, Figure 106.

EVENT	TIME (SEC)
1. CATAPULT IGNITION	0.300
2. CATAPULT SEPARATION	0.490
3. DROGUE PARACHUTE FILLED	0.766
4. MAIN ROCKET ACTION TIME	0.92
5. VERNIER ROCKET ACTION TIME	1.03
6. PARACHUTE PACK FIRST MOTION	1.28
7. UPPER DROGUE BRIDLE SEVERANCE	1.42
8. MAIN PARACHUTE DEPLOYMENT BAG STRIPOFF	2.54
9. PARACHUTE FIRST FILLED	3.20
10. HARNESS RELEASE	3.29
11. MAN/SEAT SEPARATION	3.60
12. PARACHUTE FINAL INFLATION	5.61
13. GROUND CONTACT (DUMMY)	5.61

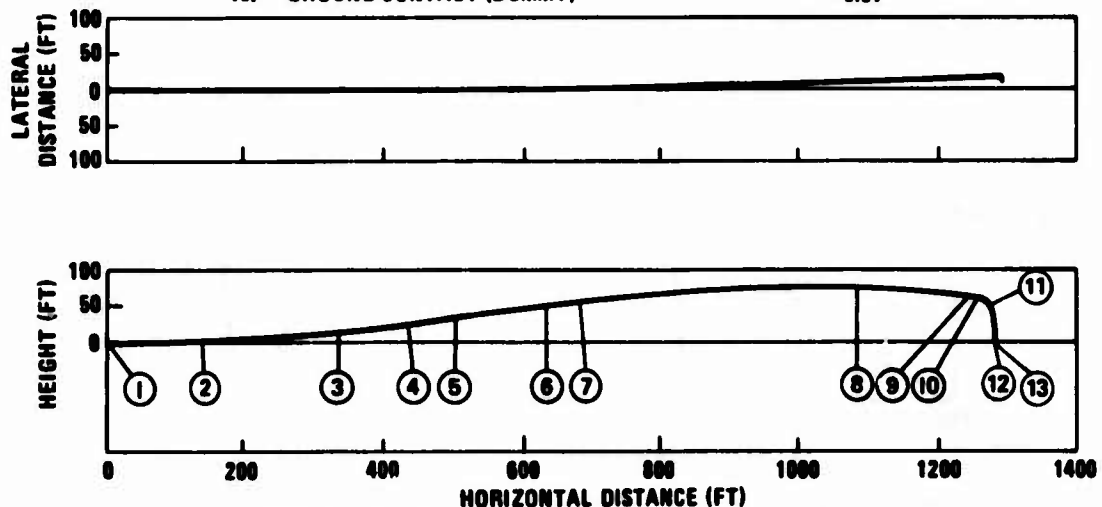


FIGURE 106. TRAJECTORY AND EVENT DATA FOR ACES DEVELOPMENT TEST NO. 10

An investigation was initiated to determine the cause of the low parachute projection velocity, with the mortar cartridge being modified following test No. 11.

As the aluminized Nomex protective covers on the lower drogue bridles did not provide adequate protection from the rocket exhaust, the lower drogue risers were covered with a silicone rubber-impregnated fiberglass sleeve for greater thermal protection.

Sheet metal plates were installed on seat blast shield to deflect the rocket exhaust away from the lower drogue risers, and each of the lower drogue risers was fastened to the back of the seat with three 100-pound nylon tie-cords incased in teflon tubing. This modification was intended to prevent the risers from deploying prematurely and falling into the rocket exhaust plume.

Test No. 11 (220 KEAS) - This test was conducted on 21 May 1971 using a 95th percentile dummy. The ejected weight was 423 pounds and the system static cg was located 1.35 inches above the thrust line.

The system performed a satisfactory Mode 1 sequence; however, the rocket catapult booster tube bent and the recovery parachute sustained multiple suspension line failures during first-fill. Although the seat release mechanism functioned properly, the parachute was unable to develop sufficient drag to effect seat separation. The seat trajectory and event times are shown in Figure 107. The bent rocket catapult booster tube did not adversely affect system performance.

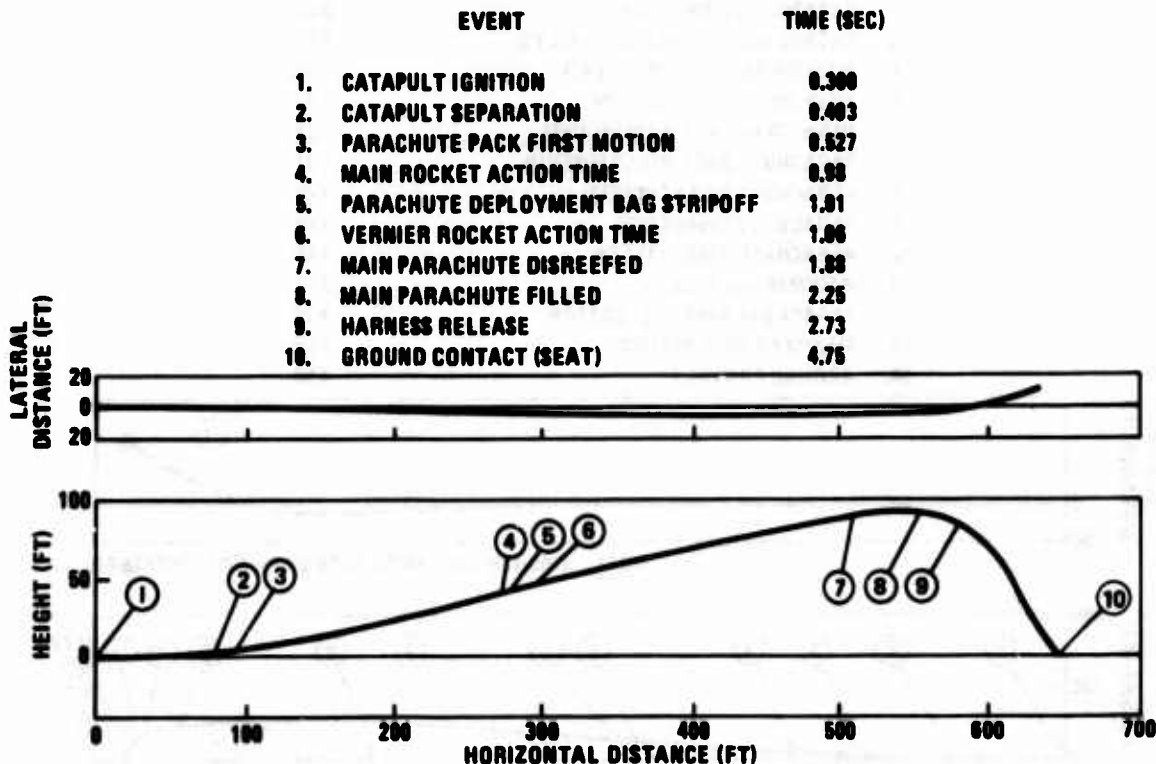


FIGURE 107. TRAJECTORY AND EVENT DATA FOR ACES DEVELOPMENT TEST NO. 11

The parachute problems encountered in tests No. 10 and 11 were considered related to inadequate mortar performance. In both cases the deploying parachute fell into the turbulent seat wake because of insufficient mortar thrust. Prior to proceeding to the next scheduled test, the mortar cartridge was redesigned to increase the nominal pack projection velocity from 35 to 59 ft/sec.

Test No. 12 (590 KEAS) - This test was performed on 22 June 1971 employing a 95th percentile dummy. The ejected weight was 354 pounds with the system static cg located 1.61 inches above the rocket catapult thrust line.

The seat system performed smoothly with all functions occurring at the specified time for a Mode 2 sequence. Following actuation of the seat release mechanism, the seat failed to separate prior to ground impact. The seat trajectory and event-time data are shown in Figure 108.

The booster tube of the rocket catapult sustained a slight amount of bending along its entire length, but this did not influence the seat performance. A structural failure of the drogue deployment sleeve resulted in premature drogue canopy deployment; however, drogue system performance was considered satisfactory. Burning of the skirt area of the recovery parachute also occurred, apparently caused by expulsion of hot propellant fragments from the mortar when the tubes separated. No parachute structural damage was encountered and operation of the recovery subsystem was satisfactory.

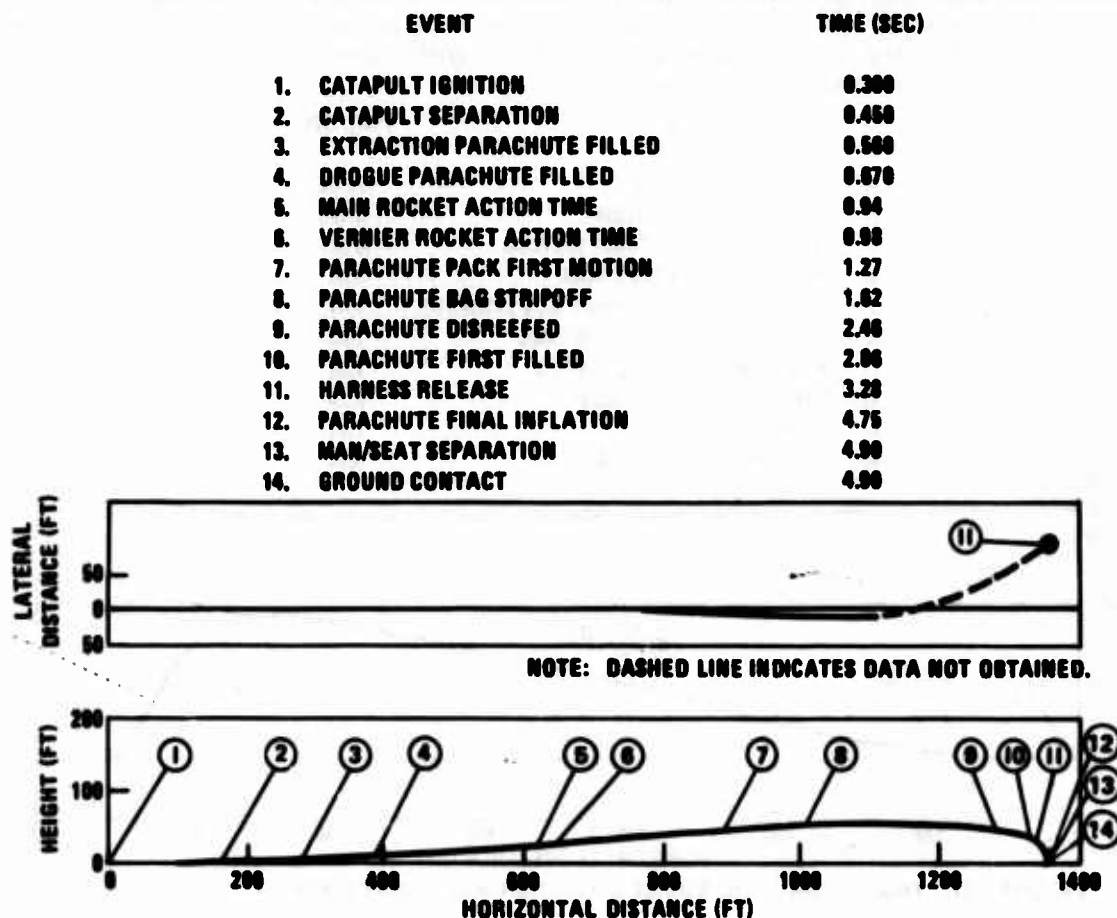


FIGURE 108. TRAJECTORY AND EVENT DATA FOR ACES DEVELOPMENT TEST NO. 12

In a series of tests conducted at Holloman AFB and at Douglas, the dummy/seat separation failure was reproduced under static conditions. The cause of the failure of the seat to release in the 590 KEAS ejection, as well as in the ninth static and, possibly, the 220 KEAS tests, is attributed to; (1) insufficient length of the long-riser segment between the parachute connector links and the dummy's restraint harness, and (2) the tips on the ends of the pins installed in the short-riser segments that attach to seat structure. When the long-riser segments that attach to the seat structure were lengthened 8 inches and the tips of the short-riser pins removed, positive and unimpeded seat separation was demonstrated in seven consecutive laboratory tests using both 5th and 95th percentile dummies.

Prior to proceeding with the qualification ejection tests, the following modifications were made:

- (1) The parachute mortar was modified by adding a flash suppression sleeve to the outer mortar barrel
- (2) The parachute riser that attaches to the crewman's harness was lengthened 8 inches and the indicator tips ground off the riser retaining pins.

COMPONENT QUALIFICATION TESTS

Parachute Mortar and Gyro Spin-Up Actuator

Qualification tests of the parachute mortar and gyro spin-up actuator were conducted by an independent test laboratory, Ogden Technology Laboratories, Incorporated, Fullerton, California. The parachute mortar and gyro spin-up actuator were tested in accordance with MIL-C-25918 and a summary of the tests performed is shown in Table XV. The parachute mortar and gyro spin-up actuator tests are reported in Ogden reports No. F-70182 and F-70181 respectively, References 14 and 15.

The average maximum velocity and the standard mean deviation for the parachute mortar and the gyro spin-up actuator are as follows:

<u>Parachute Mortar Firings</u>	<u>Average Maximum End Velocity (FPS)</u>	<u>Standard Mean Deviation (3σ)</u>
10 tests at ambient temperature	55.7	±14.8
7 tests at 200° F	58.6	±10.5
10 tests at -65° F	61.5	±18.7

TABLE XV.
PARACHUTE MORTAR AND GYRO SPIN-UP ACTUATOR QUALIFICATION TESTS

Type of Test	Parachute Mortar		Gyro Spin-Up Actuator		Control Specification	
	No. Units Tested	Total No. Firings	No. Units Tested	Total No. Firings	MIL-C-25918	MIL-E-5272
Hydrostatic	24		24		4.2.3.8	4.5.7
Demagnetization	24		24		4.2.3.7	4.5.6
Structural Mounting	2		-		4.2.3.5.1	4.5.4.1
Threaded Joint Torque	2		2		4.2.3.9	4.5.8
Vertical Drop	2		1		3.4.8	4.5.11
Shear Pin	25		25		4.2.3.11	4.3.2.9
Vibration	6		6		4.2.3.3	4.5.2.1
High Temperature	6		6		4.2.3.3	4.5.2.2
Humidity	6		6		4.2.3.3	4.5.2.3
Low Temperature	6		6		4.2.3.3	4.5.2.4
Salt Spray	6		6		4.2.3.3	4.5.2.5
Sand and Dust	6		6		4.2.3.3	4.5.2.6
Static Firing at -65°F	19	23	19	26	4.2.3.1	4.5.1.1
Static Firing at 70°F	20	22	20	22	4.2.3.1	4.5.1.1
Static Firing at 200°F	20	21	20	25	4.2.3.1	4.5.1.1
Static Firing (Locked) at 200°F	1	1	3	3		
Static Firing at -65°F	1	1	3	3	4.2.3.1	4.5.1.3

<u>Gyro Spin-up Actuator Firings</u>	<u>Average Maximum Rotor Velocity (RPM)</u>	<u>3 x Standard Deviation (3σ)</u>
14 tests at ambient temperature	11,200	1835
14 tests at 200°F	10,206	1807
15 tests at -65°F	11,456	2720

The mortar cartridge was modified after start of the mortar qualification tests. The 27 firings shown, 23 by Ogden and 4 by the cartridge supplier, were the total test firings with the modified cartridge. The 43 gyro spin-up actuator firings represents the total for which data were available.

Subcontractor-Qualified Components

The major portion of pyrotechnic components were procured from subcontractors who designed and qualified the items to a Douglas Specification Control Drawing (SCD). A list of these items including the qualification report number is given in Table XVI.

Automatic Oxygen Hose Disconnect Adapter

Qualification tests on the disconnect adapter were accomplished during the environmental tests of the seat system, in which the adapter and CRU-60/P connector were assembled to the harness. Operation of the entire disconnect system was satisfactory after exposure to all specified environments. As noted previously, the adapter assembly demonstrated adequate wind blast integrity in seat system sled tests up to 590 KEAS and satisfactory operation during life cycle, leakage and pressure drop tests.

SUBSYSTEM QUALIFICATION TESTS

Recovery Parachute

A series of 68 drop tests were conducted on the ACES Recovery Subsystem at the Joint Parachute Test Facility, El Centro, California. The purpose of these tests was to qualify the recovery parachute subsystem for use with the ACES system, Reference 10. The test results indicated that the recovery subsystem satisfied the ACES system requirements.

The maximum allowable rate of descent was exceeded in three cases because of heavy damage experienced by the parachutes. In two of these cases, the damage was attributed to improper rigging and, in the other, to an out-of-tolerance reefing line cutter time delay. Times from initiation to full parachute inflation were very consistent, with the 2.0 second limit being met in all but one case. In this instance the reefing cutter time delay was longer than permitted by specification.

In tests where moderate-to-heavy damage was experienced, the relatively high forces occurring during full inflation (following disreefing) were the major contributor. Under actual ejection conditions, the magnitude of the reefed-open and full-open forces will be reduced, and damage should be less

**TABLE XVI
SUBCONTRACTOR - QUALIFIED COMPONENTS**

Component	DAC Specification Control Drawing	Supplier	Test Document No.
Rocket Catapult*	A114300	Frankford Arsenal	10700 Rev D
Vernier Rocket	A114301	Talley Industries	H/13119 A
Drogue Severance Cutter	A114302	Teledyne McCormick Selph	TR 700
Inertia Reel and Gas Generator	A114303	Pacific Scientific	TR 1016
Harness Release Thruster and Cartridge	A114304	Universal Propulsion	ER-077 Rev A
Recovery Sequencer	A114306	Dorsett Electronics	ACDL 70-7
Reefing Line Cutter	A114307	Atlas Chemical	TR 1040
Gas Generator, Gyro Spin-Up Actuator	A114308	Universal Propulsion	TR 1023 A
Arm Restraint Thruster and Cartridge	A114309	Universal Propulsion	300408
Environmental Sensor	A114310	HTL Industries	TR 1335
Parachute Mortar Cartridge	A114311	Universal Propulsion	TR 1046
Drogue Gun and Cartridge	A114312	Universal Propulsion	

*The rocket catapult meets the envelope and performance requirements of the noted specification but is a Government-furnished item. The qualification test report was not available at the time this report was published.

severe, because the ejection seat will experience greater velocity decay between mortar initiation and parachute disreefing, Reference 10.

A summary of the drop test results is presented in Table XVII. Tests are grouped by airspeed and average values given for the parameters listed.

Gravity-Launched Seat Tests

A series of 8 of an initially specified 15 seat system drop tests was conducted on the ACES recovery subsystem at the DOD JPTF, El Centro, California, Reference 16. The purpose of these tests was to qualify and demonstrate the operation of the recovery subsystem in the automatic and manual deployment modes. Test results are tabulated in Table XVIII.

Five of the seat drop tests were conducted with the recovery subsystem operating in the normal automatic mode and three tests in the manual backup mode. In all tests, the seat systems were gravity-launched from a C-130 aircraft with the seat-mounted electronic programmer initiating recovery functions. Certain seat subsystems and pyrotechnic components, whose functions were not required for these tests, were inoperative.

Satisfactory recovery subsystem operation was observed in all eight tests. In one case in the manual mode, parachute deployment initiation was delayed because dummy/seat separation did not occur until the seat recovery parachute inflated. However, as soon as the dummy and seat physically separated, the recovery subsystem functioned satisfactorily.

Prior to and during this series of tests, several modifications were incorporated in the mortar assembly to solve a parachute canopy and deployment bag burning problem, which resulted from use of a new, higher-energy mortar cartridge. Following test No. AGL-4, in which the mortar barrel was revised to incorporate a gas deflector cone, parachute burn damage was negligible.

Operation of the survival kit's automatic deployment system was also evaluated in this series of tests. Satisfactory deployment of the rucksack and inflation of the liferaft were demonstrated in all tests. In test No. 5, a delay in the deployment of the equipment, following release of the outer container flaps, was observed. The substitution of wooden blocks, which were used to simulate the shape and weight of actual items, was believed partially responsible for the delayed deployment. It was concluded that a minor modification to the front corners of the outer container would improve reliability of operation.

SYSTEM QUALIFICATION TESTS

Seat Static Structural Tests

An ACES seat system was tested structurally under 13 different loading conditions as shown in Figures 13, 14, and 15 (Section III). Except as noted previously, the loads were applied in accordance with the requirements of MIL-S-9479A. Loads were applied incrementally up to the limit load, then relaxed, and reapplied incrementally to ultimate load (150 percent of limit).

TABLE XVII

SUMMARY OF ACES RECOVERY SUBSYSTEM QUALIFICATION TESTS

Number of Tests	Velocity Range at Parachute Mortar Ignition (KEAS)	Parachute Mortar Fires		Pilot Chute Full Inflation		Parachute Deployment Bag Stripoff		Parachute Reefed Inflation		Maximum Reefed Load		Parachute Disreef		Parachute Full Inflation		Maximum Inflated Load		
		Avg Alt	Avg Vel t	Avg Vel t	Avg Vel t	Avg Vel t	Avg Vel t	Avg t	Avg Vel t	Avg t	Avg Vel t	Avg t	Avg Vel t	Avg t	Avg Vel t	Avg t	Avg Vel t	Avg Lb g
9	53 to 63	3.0	0	57	0.362	61	1.081	66	1.251	65	1.118	3.0	1.422	62	1.999	37	3048	8.0
6	87 to 108	3.1	0	100	0.375	102	0.701	97	0.991	91	2.050	5.3	1.347	68	1.695	41	4724	11.6
5	141 to 151	3.2	0	148	0.406	142	0.607	137	0.890	120	3.584	8.8	1.384	73	1.686	46	4816	12.1
5	188 to 202	3.1	0	194	0.319	189	0.521	179	0.706	161	5.190	13.6	1.386	78	1.704	46	5120	12.6
6	223 to 240	3.0	0	235	0.273	229	0.435	213	0.739	177	5.782	14.9	1.354	92	1.656	54	6130	15.5
8	247 to 291	3.0	0	255	0.234	247	0.442	229	0.690	195	6.232	15.9	1.269	99	1.578	54	7012	17.0
4	272 to 291	3.2	0	282	0.237	274	0.405	260	0.603	234	6.313	16.1	1.357	120	1.339	56	7927	18.9
5	214 to 220	5.0	0	217	0.293	210	0.472	199	0.743	171	6.170	15.9	1.322	87	1.616	51	6880	16.6
5	188 to 199	10.0	0	193	0.377	185	0.510	179	0.763	154	5.795	14.5	1.302	81	1.553	54	7600	18.0
5	126 to 131	16.3	0	128	0.324	126	0.656	121	0.889	113	2.875	7.3	1.493	71	1.776	48	6195	16.0
10	146 to 159	16.5	0	155	0.280	152	0.559	144	0.824	1.280	3.451	9.0	1.264	89	1.520	62	8930	22.0

TABLE XV
SUMMARY OF ACES SYSTEM G

Test Number	1			2			3			4		
Date	28 July 1971			23 Aug 71			27 Aug 71			1 Sept 71		
Dummy Size (Percentile)	5			95			5			95		
Event	Time (Sec)*	Pressure Altitude (Ft)	Velocity (KEAS)	Time (Sec)*	Pressure Altitude (Ft)	Velocity (KEAS)	Time (Sec)*	Pressure Altitude (Ft)	Velocity (KEAS)	Time (Sec)*	Pressure Altitude (Ft)	Velocity (KEAS)
Extraction Chute Open	-7.173	14,992	146.39	N. A.	N. A.	N. A.	-11.303	(E) 15,079	(E) 152.34	-10.626	14,949	(E) 151.6
Seat Launch	-5.348	14,992	150.04	-5.115	15,123	146.72	-5.527	15,079	144.76	-5.083	14,949	146.3
Mortar Fire or Pack Movement	(1) 0.000	14,668	81.68	(2) 0.000	14,785	91.94	(2) 0.000	14,690	81.79	(2) 0.000	14,595	78.9
Pilot Chute Release	0.196	14,660	81.29	0.339	14,780	92.13	0.103	14,680	81.80	0.043	14,590	78.9
Pilot Chute Full Open	0.463	14,647	81.58	0.649	14,712	91.35	0.312	14,656	81.72	0.199	14,578	78.9
Line Stretch	0.659	14,625	83.39	0.724	14,739	90.85	0.376	14,651	81.67	0.398	14,553	78.9
Deployment Bag Release	0.840	14,604	80.21	0.954	14,690	90.40	0.642	14,600	80.06	0.558	14,536	78.9
Reefed Opening	1.021	14,570	78.45	1.226	14,660	89.87	0.860	14,575	76.18	0.909	14,498	80.9
Disreef	1.184	14,531	74.23	1.498	14,617	83.34	1.280	14,531	63.35	1.258	14,465	73.9
Full Open	1.770	14,518	46.10	1.816	14,600	69.39	1.680	14,489	39.36	1.575	14,427	54.9
Dummy/Seat Separation	(3) 2.182	14,486	19.55	(3) 2.292	14,536	24.60	(3) 2.059	14,474	19.78	(3) 1.904	14,391	32.9
Second Full Open	2.760	14,442	17.02	2.863	14,523	19.43	2.854	14,453	14.79	2.452	14,377	16.9
Survival Kit Deployment	2.436	14,476	18.28	2.862	14,531	22.59	2.697	14,458	15.33	3.477	14,349	13.9
Ground Contact	695.264	(E) 458	(E) 11.66	606.439	(E) 287	(E) 9.75	726.086	(E) 303	(E) 12.49	604.675	(E) 439	(E) 13.9

Notes: *From System Initiation
(N. A.) = Not Available
(E) = Estimated

(1) = Mortar Fire
(2) = Parachute Pack Fir vement
(3) = Harness Release (F ulb Firing)
(4) = Actual Phys e ion
(Q) = Questionable btained from Test Drop Data Report

TABLE XVIII

DES SYSTEM GRAVITY-LAUNCH TESTS

4			5			6			7			8		
1 Sept 71			13 Sept 71			15 Sept 71			5 Oct 71			7 Oct 71		
95			5			95			5			95		
Pressure Altitude (Ft)	Velocity (KEAS)	Time (Sec)*	Pressure Altitude (Ft)	Velocity (KEAS)	Time (Sec)*	Pressure Altitude (Ft)	Velocity (KEAS)	Time (Sec)*	Pressure Altitude (Ft)	Velocity (KEAS)	Time (Sec)*	Pressure Altitude (Ft)	Velocity (KEAS)	
14,949	(E) 151.63	-10.920	15,166	143.90	-15.127	15,210	149.50	-15.387	N. A.	N. A.	-15.078	N. A.	N. A.	
14,949	146.32	-5.249	15,171	132.66	-7.125	15,210	144.57	-7.671	14,949	142.06	-7.298	15,079	140.60	
14,595	78.95	(2) 0.000	14,842	82.66	(2) 6.520	13,297	113.77	44.794	3,750	109.98	1.200	14,221	93.03	
14,590	78.93	0.000	14,842	82.66	6.606	13,280	113.21	44.395 (Q)	3,787 (Q)	116.45 (Q)	1.250	14,210	93.19	
14,578	78.84	0.217	14,796	83.16	6.735	13,253	112.47	44.540 (Q)	3,758 (Q)	114.33 (Q)	1.537	14,150	93.96	
14,553	78.60	0.447	14,767	83.39	6.948	13,161	109.86	46.053 (Q)	3,497 (Q)	86.24 (Q)	2.205	14,052	94.16	
14,536	78.77	0.601	14,734	83.35	7.175	13,122	106.37	46.015 (Q)	3,502 (Q)	87.00 (Q)	2.405	14,010	93.12	
14,498	80.81	0.790	14,713	80.89	7.380	13,080	97.39	46.729	3,400	72.03	3.082	13,876	76.75	
14,465	73.89	1.304	14,656	65.92	8.273	12,963	50.99	47.783	3,394	49.73	3.999	13,759	45.12	
14,427	54.63	1.682	14,617	42.87	8.648	12,930	32.30	48.381	3,252	39.55	4.651	13,736	17.39	
14,391	32.79	(3) 2.018 (4) 12.906	14,597 14,301	22.39 15.04	(3) 0.000 (4) 6.229	14,571 13,357	97.96 114.83	(3) 0.000 (4) 44.694	14,333 3,753	90.95 111.71	(3) 0.000 (4) 0.600	14,391 14,306	90.98 91.86	
14,377	16.13	3.001	14,567	13.44	10.921	12,896	12.49	49.657	3,183	20.11	6.167	13,690	11.71	
14,349	13.36	44.218	13,580	14.39	7.600	13,047	83.69	45.921	3,516	88.86	3.162	13,867	74.16	
(E) 439	(E) 13.65	726.378	(E) 391	(E) 15.38	(E) 559.041	(E) 161	(E) 12.21	234.064	199	15.23	603.142	(E) 364	(E) 15.57	

2

The test specimen withstood the 100-percent limit load without yielding and the 150-percent ultimate load without failure under all test conditions, Reference 17. A summary of loading conditions and the loads applied is presented in Table XIX.

Seat System Functional and Environmental Tests

Seat system functional and environmental qualification tests were conducted by Ogden Technology Laboratories, Incorporated, Reference 18. Tests were performed in accordance with the requirements specified in MIL-S-9479A and MIL-E-5272. Table XX lists the environmental test conditions and the

TABLE XIX
ACES STATIC STRUCTURAL TEST CONDITIONS

Test No.	Type Test	Applicable Paragraph MIL-S-9479A	Design Limit Load (Lb)	Ultimate Load (Lb)
1	Front Edge	3.6.2.2	266	399
2	Armrest Structure (Each)	3.6.2.3	135	200
3	Ejection Controls (Each)	3.6.2.4	200	300
4	Headrest Structure	3.6.2.5	330	500
5	Rocket Catapult and Ejection Airload	3.6.2.7	1620 3134	2055 4701
6	Forward Crash Load Seat Installation Restraint Subsystem	3.6.2.6.1	5474 5741	8211 8611
7	Side Crash Load Seat Installation Restraint Subsystem	3.6.2.6.2	5474 5741	8211 8611
8	Vertical Crash Load Restraint Subsystem	3.6.2.6.3	1167	1751
9	Vertical Crash Load Seat Bucket Seat Installation	3.6.2.6.3	2880 2880	4320 4320
10	Back Crash Load	3.6.2.6.4	1000	1500
11	Parachute Riser Load	-	11,040	16,560
12	Parachute Riser Load (Yaw Position)	-	2340	3510
13	Rocket Catapult Load	3.6.2.1	7150	10,725

TABLE XX
SEAT SYSTEM FUNCTIONAL AND ENVIRONMENTAL TEST SUMMARY

Type of Test	Control Specification		Handle Loads (Lb)								
	MIL-S-9479	MIL-E-5272	Survival Kit Deployment Selector		Inertia Reel Shoulder Harness Straps		Single-Point Release Buckle	Ejection Firing Control	Manual Harness Release	Backrest Jettison	Seat Pan Release
			Auto-matic	Man-ual	Lock	Unlock					
Pretest (Ambient)	-	-	10	9	8	7	28	28	44	42	64
High Temperature	4.5.5.1	4.1.2	9	9	6	9	28	24	51	66	106 *
Low Temperature	4.5.5.3	4.2.1	10	8	8	6	26	24	40	16	46
Salt Spray	4.5.5.7	4.6.1	5	7.5	7	5.5	19	28	52	16.5	17.5
Temperature/Altitude	4.5.5.4	4.14.2	8	8	10	8	16	32	35	16	64
Vibration	4.5.5.5	4.7.12	9.5	9	6	2.5	32	16	42	18	20
Humidity	4.5.5.2	4.4.1	10.5	12	9	9.5	17	35.5	47	18	53
Sand and Dust	4.5.5.8	4.11.1	18	17	10	18	13	34	60	19	91

*See discussion of variable seat pan release loads on page 155.

various seat mechanisms that were actuated. Handle pull-forces were measured before and after exposure to each environmental test condition; the maximum force is shown.

Except for the seat pan release loads, all handle pull-forces were within specified values. The variability of the seat pan release loads was attributed to the manner in which the loads were measured. In an attempt to obtain uniform results, a slow steady pull was applied to the seat pan release handle. However, the relatively high static friction of the release pins resulted in high initial loads, dropping abruptly to a very low value after initial movement of the pins. Application of a jerk-type load to the handle easily actuated the release mechanism, but credible force measurements were impractical to obtain. A handle pull force of $30 \pm \begin{matrix} 20 \\ 15 \end{matrix}$ pounds was specified for release of the seat pan.

Upon completion of these tests, the seat system was employed in a 450-KEAS ejection test with successful results.

Seat System Qualification Static and Dynamic Ejection Tests

Following completion of the development seat ejection tests, two static and six dynamic qualification ejection tests were conducted on the ACES system, Reference 19. Two of the dynamic tests were dual ejections, making a total of eight dynamic seat tests. The tests were made from a rocket-propelled F-105 cockpit section on the high-speed track facility at Holloman AFB. The tests were conducted during the period of 7 July through 3 September 1971.

A summary of trajectory and event time data is tabulated in Table XXI and a synopsis of the test results is given in the following paragraphs. All tests were conducted at an essentially nominal static cg as the dummy's chest cavity, normally used for ballasting purposes, was occupied by a telemetry transmitter and associated equipment. For tests with 5th percentile dummies, the system static cg ranged from 1.61 to 1.68 inches above the rocket thrust line and, for tests with the 95th percentile dummies, from 1.26 to 1.50 inches above the thrust line. Nominal cg offsets are 1.12 and 1.37 inches, respectively.

Test No. 1 (212 KEAS) - This test was conducted with a 95th percentile dummy (420-pound ejected mass). Recovery parachute inflation occurred in 2.04 seconds, following system initiation, and at a height of 80 feet, Figure 109.

The test was successful with a proper Mode-1 sequence demonstrated. The following incidents were noted but they did not adversely influence the test results:

1. Rocket catapult launch tube failed in bending after approximately 1 foot of stroke. The bending was restricted to an area weakened by excessive heating.
2. Main parachute canopy and suspension lines received minor burns as a result of the parachute mortar muzzle flash.
3. Main parachute deployment bag pilot chute received minor friction burns from contact with the main canopy suspension lines.

TABLE
SUMMARY OF TRAJECTORY/EVENT TIME DATA

Test Number (Date)	Q1 (7-7-71)			Q2 (7-14-71)			Q3 (7-19-71)			Q4 (Dual) (7-28-71)			
Dummy Size (Percentile)	95			5			95			5 (aft Seat)			
Sled Velocity at Seat First Motion (KEAS)	212			Zero			Zero			151			
	Time (Sec)	Height (Ft)	Velocity (FPS)	Time (Sec)	Height (Ft)	Velocity (FPS)	Time (Sec)	Height (Ft)	Velocity (FPS)	Time (Sec)	Height (Ft)	Velocity (FPS)	Time (Sec)
Ejection Initiation	0.0	0.0	398	0.0	0.0	0.0	0.0	0.0	0.0	0.0	0.0	282	0.0
First Seat Motion	0.343	0.0	393	0.344	0.0	0.0	0.327	0.0	0.0	0.330	0.0	279	0.656
Drogue Gun Fire	NA	-	-	NA	-	-	NA	-	-	0.506	6	287	0.829
STAPAC Ignition	0.459	4	392	0.476	5	NR	0.466	5	NR	0.465	5	278	0.802
Catapult Separation	0.475	5	391	0.470	5	NR	0.461	5	NR	0.461	5	278	0.769
Extraction Parachute Filled	NA	-	-	NA	-	-	NA	-	-	NO	-	-	1.06
Drogue Parachute Filled	NA	-	-	NA	-	-	NA	-	-	NO	-	-	1.53
Main Rocket Action Time	0.930	36	387	0.960	42	89	0.940	42	94	NO	-	-	NA
Vernier Rocket Action Time	1.04	45	355	1.10	53	88	1.09	53	91	0.940	40	312	1.43
Parachute Pack First Motion	0.493	6	387	0.509	5	91	0.506	5	NO	0.497	6	292	1.66
Lower Drogue Bridle Severance	0.609	12	398	0.634	16	90	0.624	16	102	0.619	13	300	1.78
Upper Drogue Bridle Severance	0.639	14	400	0.665	18	90	0.654	18	101	0.648	15	305	1.81
Main Parachute Pilot Chute Filled	0.680	16	403	0.680	20	90	0.710	20	100	0.750	23	317	1.89
Main Parachute Bag Unlock	0.790	25	406	1.13	56	88	1.01	47	93	0.850	32	319	2.05
Main Parachute Bag Stripoff	0.870	31	399	1.18	60	88	1.35	74	84	0.930	39	313	2.20
Parachute Reefed Fill	1.00	42	366	1.52	86	84	1.99	111	62	1.23	64	252	2.57
Parachute Disreef	1.71	75	176	1.88	111	78	NO	-	-	1.78	91	122	2.96
Parachute First Fill	2.04	80	111	3.00	169	48	2.80	136	32	2.15	96	58	3.32
Peak Trajectory	2.11	80	93	4.05	188	21	3.13	139	23	2.19	96	50	2.07
Harness Release	2.54	76	35	2.69	157	58	2.60	133	39	2.66	91	79	3.79
Dummy/Seat Separation	3.50	53	34	4.75	183	18	3.90	129	24	3.90	56	32	NO
Ground Contact	5.54	-	21	11.8	-	26	7.50	-	36	6.60	-	25	4.00

Note:

NA = Not Applicable
NO = Not Observed
NR = No Record

Test No.	Conversion F (FPS to KE)
Q1	0.5389
Q2	0.5401
Q3	0.5375
Q4	0.5398
Q5	0.5429
Q6	0.5419
Q7	0.5419
Q8	0.5437

TABLE XXI

EVENT TIME DATA FOR ACES QUALIFICATION EJECTION TESTS

Q4 (Dual) (7-28-71)			Q5 (8-4-71)			Q6 (8-20-71)			Q7 (8-26-71)			Q8 (Dual) (9-3-71)								
(Aft Seat)			95 (Fwd Seat)			5			5			95			95 (Aft Seat)			5 (Fwd Seat)		
151			149			227			577			578			438			437		
Height (Ft)	Velocity (FPS)	Time (Sec)	Height (Ft)	Velocity (FPS)	Time (Sec)	Height (Ft)	Velocity (FPS)	Time (Sec)	Height (Ft)	Velocity (FPS)	Time (Sec)	Height (Ft)	Velocity (FPS)	Time (Sec)	Height (Ft)	Velocity (FPS)	Time (Sec)	Height (Ft)	Velocity (FPS)	
0.0	282	0.0	0.0	282	0.0	0.0	424	0.0	0.0	1077	0.0	0.0	1080	0.0	0.0	812	0.0	0.0	812	
0.0	279	0.656	0.0	276	0.354	0.0	418	0.348	0.0	1064	0.350	0.0	1067	0.344	0.0	806	0.708	0.0	804	
6	287	0.829	6	266	NA	-	-	0.469	5	1055	0.458	4	1059	0.455	5	803	0.781	4	804	
5	278	0.802	5	266	0.463	5	416	0.477	5	1055	0.468	5	1058	0.462	5	803	0.779	4	804	
5	278	0.769	-	275	0.474	5	416	0.484	5	1054	0.479	5	1058	0.469	5	803	0.813	5	804	
-	-	1.06	13	265	NA	-	-	0.581	10	998	0.580	10	1005	0.578	10	777	0.918	11	789	
-	-	1.53	24	254	NA	-	-	0.713	16	914	0.740	18	NR	0.748	21	739	1.08	20	761	
-	-	NA	-	-	0.930	37	405	0.970	30	690	0.950	30	733	0.942	33	656	1.28	34	693	
40	312	1.43	22	254	1.04	47	367	1.10	34	605	1.08	36	657	1.07	40	594	1.40	42	579	
6	292	1.66	26	243	0.490	5	416	1.32	38	492	1.31	43	549	1.28	51	505	1.59	53	492	
13	300	1.78	28	237	0.610	11	427	1.44	39	457	1.42	46	511	1.39	55	471	1.71	59	456	
15	305	1.81	28	235	0.639	12	429	1.47	38	450	1.45	47	503	1.42	56	459	1.74	61	448	
23	317	1.89	29	232	0.650	13	430	1.55	38	437	1.47	47	498	1.44	57	458	1.78	62	439	
32	319	2.05	30	224	0.760	21	432	1.61	38	429	1.58	49	474	1.58	61	435	1.92	68	413	
39	313	2.20	30	213	0.840	28	425	1.71	38	414	1.65	50	460	1.65	63	425	2.04	72	392	
64	252	2.57	27	175	1.04	47	364	2.06	35	295	1.88	52	395	1.85	66	378	2.27	78	333	
91	122	2.96	21	121	1.71	77	145	2.58	28	NR	2.54	45	NR	2.47	68	184	2.80	82	171	
96	58	3.32	13	62	2.10	80	76	3.00	20	NR	3.00	38	NR	2.82	64	113	3.19	78	100	
96	50	2.07	30	226	2.05	80	89	1.44	39	457	1.93	52	380	2.22	69	244	2.69	82	194	
91	79	3.79	4	23	2.55	75	22	3.50	9	NR	3.43	30	NR	3.22	58	28	3.61	71	24	
56	32	NO	-	-	3.55	46	35	3.80	4	NR	NO	-	-	3.66	52	18	4.02	63	23	
-	25	4.00	-	29	5.50	-	26	4.20	-	NR	4.60	-	NR	5.55	-	23	6.13	-	32	

Test No.	Conversion Factor (FPS to KEAS)
Q1	0.5389
Q2	0.5401
Q3	0.5375
Q4	0.5398
Q5	0.5429
Q6	0.5419
Q7	0.5419
Q8	0.5437

2

"PRECEDING PAGE BLANK-NOT FILMED."

EVENT	TIME (SEC)
1. SEAT FIRST MOTION	0.343
2. CATAPULT SEPARATION	0.475
3. PARACHUTE DEPLOYMENT BAG FIRST MOTION	0.403
4. PARACHUTE DEPLOYMENT BAG STRIPOFF	0.870
5. MAIN ROCKET ACTION TIME	0.93
6. VERNIER ROCKET ACTION TIME	1.04
7. MAIN PARACHUTE DISREEFED	1.71
8. MAIN PARACHUTE FILLED	2.04
9. HARNESS RELEASE	2.54
10. DUMMY/SEAT SEPARATION	3.50
11. GROUND CONTACT	5.5

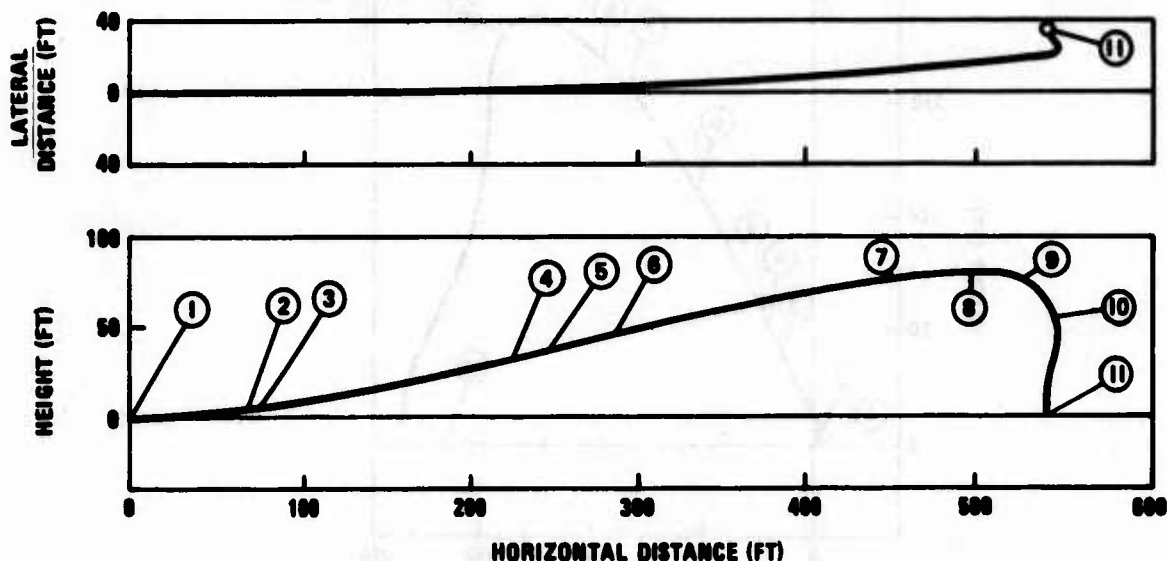


FIGURE 109. TRAJECTORY CURVE, ACES QUALIFICATION SLED TEST NO. 1 - 212 KEAS

4. Post-ejection examination of the drogue gun revealed that the initiator had been fired. Investigation led to the conclusion that it was initiated when the seat assembly contacted the terrain following separation.

Seat pitching and yawing was minimal prior to parachute line stretch. Seat separation followed harness release when sufficient load was developed by the secondary filling of the parachute.

Test No. 2 (Zero KEAS) - This test employed a 5th percentile dummy resulting in an ejected mass of 355 pounds. Recovery parachute inflation occurred in 3.0 seconds, following system initiation, and at a height of 169 feet, Figure 110. The test was successful, although the recovery parachute sustained minor burns in the skirt of the canopy as a result of mortar muzzle flash. Seat pitch control was excellent and all recovery events were initiated at the correct time for a Mode 1 sequence.

Test No. 3 (Zero KEAS) - With a 95th percentile dummy installed (423-pound ejected mass), the seat achieved a maximum height of 139 feet, and full parachute inflation occurred in 2.8 seconds following system initiation, Figure 111. The test was successful with good pitch control demonstrated, and all recovery events were initiated in the correct sequence and at the proper time. Post-test examination of the seat system components disclosed the following:

EVENT	TIME (SEC)
1. SEAT FIRST MOTION	0.344
2. PARACHUTE DEPLOYMENT BAG FIRST MOTION	0.500
3. MAIN ROCKET ACTION TIME	0.90
4. VERNIER ROCKET ACTION TIME	1.10
5. PARACHUTE DEPLOYMENT BAG STRIPOFF	1.10
6. MAIN PARACHUTE DISREEFED	1.90
7. HARNESS RELEASE	2.00
8. MAIN PARACHUTE FILLED	3.00
9. DUMMY/SEAT SEPARATION	4.75
10. GROUND CONTACT	11.8

NOTE: LATERAL (Y) TRAJECTORY COORDINATES WERE NOT OBTAINED DUE TO INSUFFICIENT OPTICAL TRACKING DATA. THE DISCREPANCY BETWEEN HORIZONTAL DISTANCE (X) DESCENT TRAJECTORY AND MEASURED GROUND CONTACT POINT IS ATTRIBUTED TO THE SAME CAUSE. THE DUMMY GROUND CONTACT POINT WAS 60 FEET LEFT OF THE INITIAL CENTER PLANE.

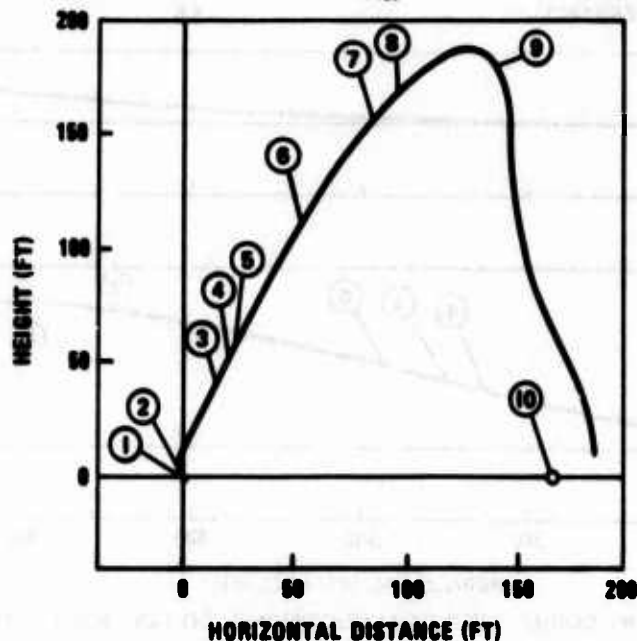
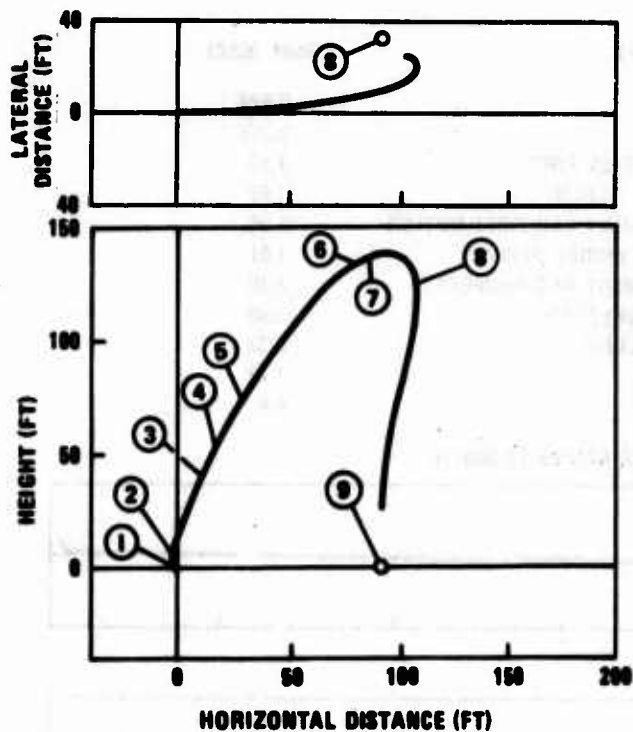


FIGURE 110. TRAJECTORY CURVE, ACES QUALIFICATION SLED TEST NO. 2 - 0 KEAS

1. Rocket catapult launch tube failed in bending after approximately 1 foot of stroke. The bending was restricted to an area weakened by excessive heating.
2. Main parachute canopy received minor burns as a result of the parachute mortar muzzle flash.
3. Seat pitch control was slightly impaired as a result of a mechanical interference between the vernier rocket and the seat assembly blast shield.

Test No. 4 (150 KEAS Nominal) - This was a dual ejection using a 5th percentile dummy in the aft cockpit and a 95th in the forward crew station. Ejected weights for the seat systems were 355 and 423 pounds, respectively. Trajectory and event time data are shown in Figures 112 and 113.



EVENT	TIME (SEC)
1. SEAT FIRST MOTION	0.327
2. PARACHUTE DEPLOYMENT BAG FIRST MOTION	0.506
3. MAIN ROCKET ACTION TIME	0.94
4. VERNIER ROCKET ACTION TIME	1.00
5. PARACHUTE DEPLOYMENT BAG STRIPOFF	1.35
6. HARNESS RELEASE	2.00
7. MAIN PARACHUTE FILLED	2.90
8. DUMMY/SEAT SEPARATION	3.90
9. GROUND CONTACT	7.50

FIGURE 111. TRAJECTORY CURVE, ACES QUALIFICATION SLED TEST NO. 3 - 0 KEAS

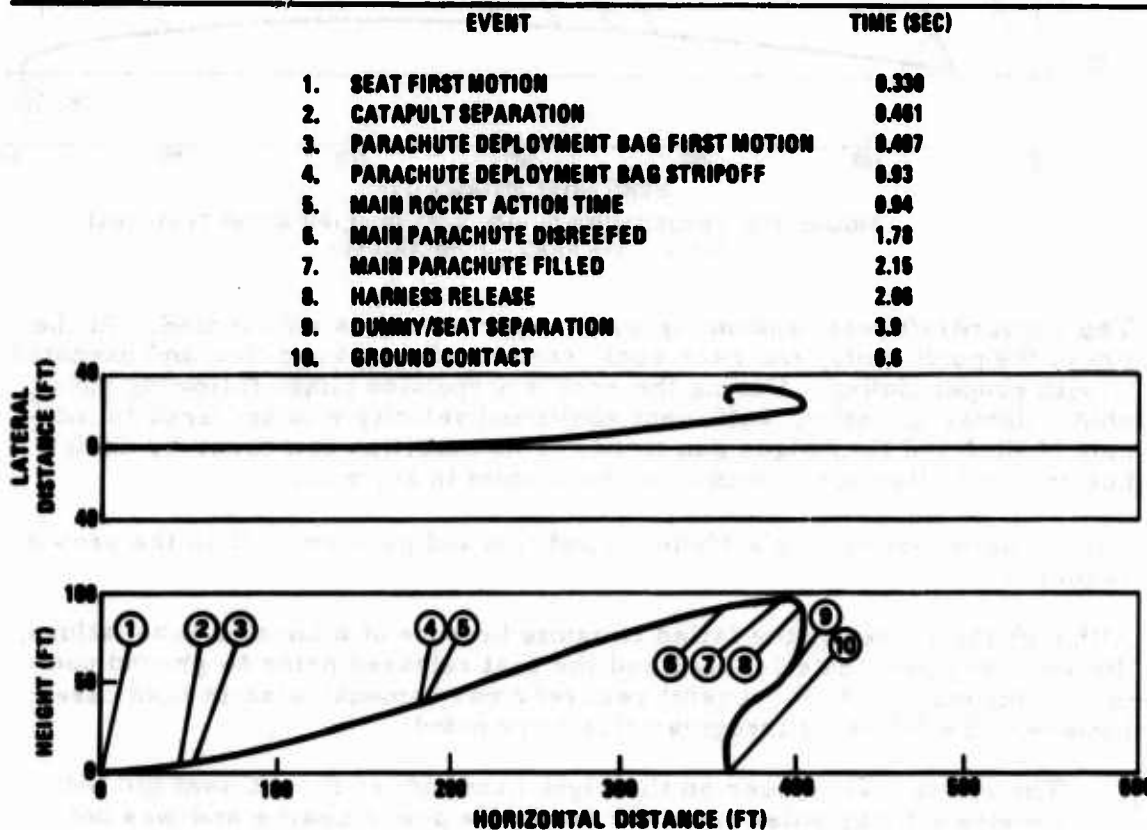


FIGURE 112. TRAJECTORY CURVE, ACES QUALIFICATION SLED TEST NO. 4 - 151 KEAS - AFT SEAT

EVENT	TIME (SEC)
1. SEAT FIRST MOTION	0.856
2. CATAPULT DAMAGED	0.789
3. VERNIER ROCKET ACTION TIME	1.43
4. DROGUE PARACHUTE FILLED	1.53
5. PARACHUTE DEPLOYMENT BAG FIRST MOTION	1.86
6. DROGUE PARACHUTE BRIDLE RELEASE	1.81
7. PARACHUTE DEPLOYMENT BAG STRIPOFF	2.29
8. MAIN PARACHUTE DISREEFED	2.96
9. MAIN PARACHUTE FILLED	3.32
10. HARNESS RELEASE	3.79
11. GROUND CONTACT	4.8

NOTE: ROCKET SUSTAINER FAILED TO IGNITE

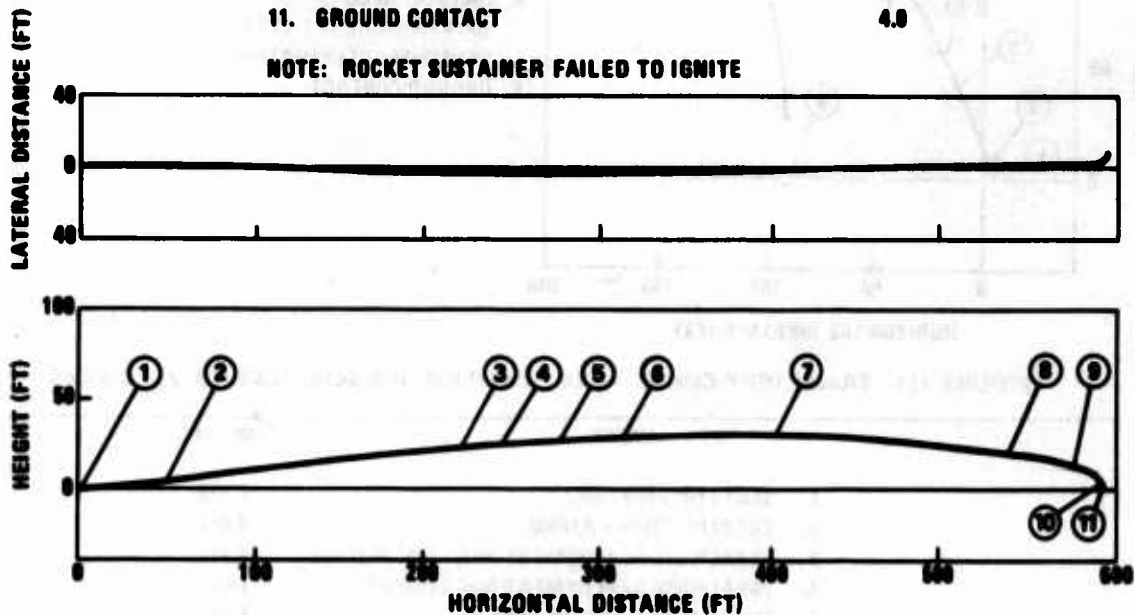


FIGURE 113. TRAJECTORY CURVE, ACES QUALIFICATION SLED TEST NO. 4 - 149 KEAS - FORWARD SEAT

The forward/aft seat sequencing system performed as anticipated. At the top of the guide rails, the rear seat sensed a Mode 1 condition and executed it with proper timing. During the rocket propulsion phase following parachute mortar initiation, sufficient additional velocity was acquired to indicate Mode 2 and the drogue gun fired. This condition can occur by design but does not alter performance of the system in any way.

The forward seat sensed a Mode 2 condition and performed it in the proper sequence.

Although the rocket motor failed to ignite because of a booster tube failure, the recovery parachute inflated and the seat released prior to ground contact of the dummy. * Successful recovery was demonstrated in both cases; however, the following irregularities were noted:

1. The ejection sequencer on the right-hand side of the aft seat did not receive a firing pulse from the trackside power source and was not initiated.

*Physical separation of the seat and dummy was not observed.

2. The ejection sequencer on the right-hand side of the forward seat was found fired, despite the fact that the right-hand aft ejection sequencer did not provide an initiation firing pulse. Analysis of the event times showed that the forward seat was ejected in the proper time sequence, which indicates that the right-hand sequencer fired after ejection initiation. Post-test examination of the ejection sequencer showed the electrical squib was fired without burning through the bridgewire. It was concluded that the squib was fired by discharge of static electricity accumulated on the unshielded wire connecting the right-hand ejection sequencers on the forward and aft seats. The unshielded wire was part of the test setup, rather than a test specimen component.
3. The arm restraint thruster cartridge in the aft seat on Test No. Q4 did not fire. Analysis revealed that a condition can exist (if one ejection sequencer fails) where there is insufficient power to fire the cartridge squib. Analysis and corrective action for this condition is discussed in Reference 20.
4. The catapult booster tube on the forward seat failed after approximately 15-inches of stroke, as a result of excessive pressure and heat. The failure resulted in a very low trajectory. As booster tube bending problems had occurred only on tests employing 95th percentile dummies, it was decided to modify booster tubes for all subsequent 95th percentile tests. Modification of rocket catapults for all remaining tests was not possible nor necessary, without jeopardizing test schedules. No further failures occurred, with rocket catapults incorporating modified booster tubes.
5. The vernier rocket sear puller was not retained after extraction of the sear. This condition was observed after seat ground impact, but there was no indication that STAPAC performance was affected.
6. The recovery parachute canopies on both seats sustained some burn damage in the skirt region as a result of mortar muzzle flash.

Test No. 5 (227 KEAS) — This test was conducted with a 5th percentile dummy (355-pound ejected mass). The recovery parachute inflated in 2.1 seconds after system initiation at the maximum trajectory height of 80 feet, Figure 114. The seat system demonstrated a satisfactory Mode-1 sequence and all subsystems functioned as intended. Rather severe burn damage was sustained by the parachute canopy, and a modification was made to the mortar and deployment bag prior to proceeding with test No. 6. The modification comprised installation of a bell-shaped extension to the end of the outer mortar tube (refer to Section X) and fabric pockets on the locking flap of the deployment bag to protect the exposed parachute suspension lines.

Test No. 6 (577 KEAS) — This test was conducted using a 5th percentile dummy (354-pound ejected mass). The seat attained a height of 39 feet and parachute inflation was observed at 3.0 seconds from system initiation, 1310 feet downrange from the point at which the rocket catapult was initiated, Figure 115. Seat stability was good with parachute inflation and dummy/seat separation accomplished prior to ground contact of the dummy. Except for minor structural damage to the recovery parachute, all subsystems per-

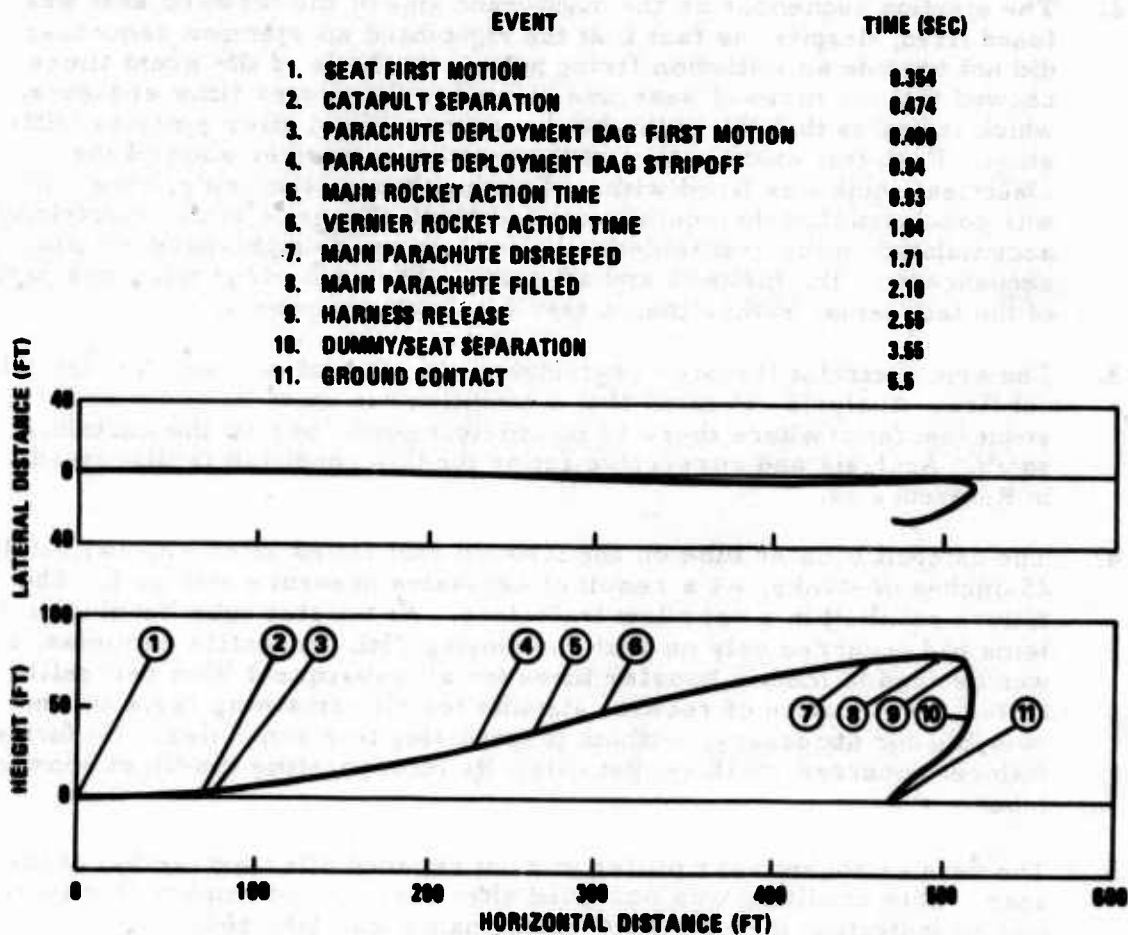


FIGURE 114. TRAJECTORY CURVE, ACES QUALIFICATION SLED TEST NO. 5 - 227 KEAS

formed as intended. The drogue began separating from the deployment sleeve slightly before line stretch, but deployment and inflation times were well within design values.

Test No. 7 (578 KEAS) - This test employed a 95th percentile dummy (424-pound ejected mass). The seat achieved a height of 52 feet, and parachute inflation occurred in 3.0 seconds from system initiation, 1390 feet downrange from the point at which the rocket catapult was initiated, Figure 116. All subsystems functioned properly with the following abnormalities observed:

1. The canopy experienced two small tears as a result of loading during recovery. One suspension line also suffered moderate burns from mortar muzzle flash and subsequently failed in tension during recovery.
2. A minor mechanical failure resulted in inadequate retention of the vernier rocket sear puller following actuation of the spin-up actuator. This condition had no effect on system performance.
3. The seat failed to separate from the dummy following initiation of the harness release actuator. Following first full inflation, the canopy did not fill completely again before ground contact.

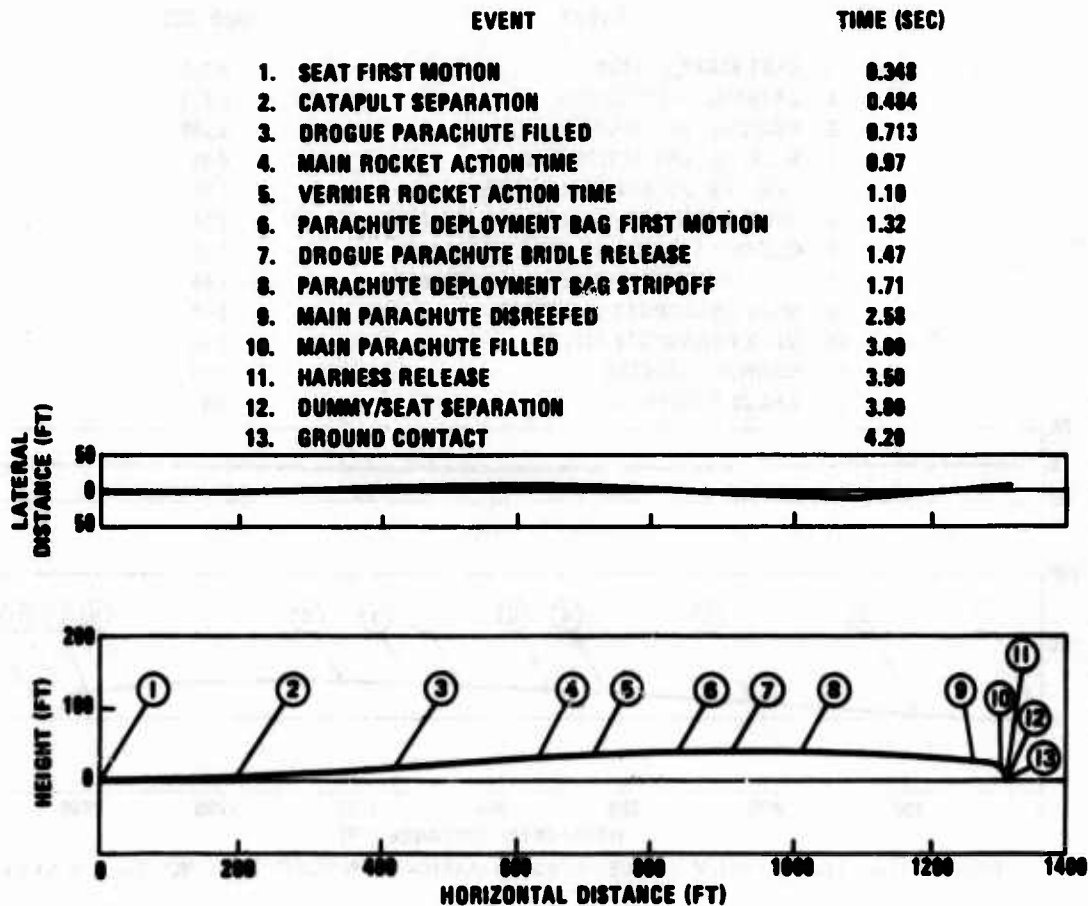


FIGURE 115. TRAJECTORY CURVE, ACES QUALIFICATION SLED TEST NO. 6 - 577 KEAS

Test No. 8 (437 KEAS, Fwd Seat; 438 KEAS, Aft Seat) - This was a dual ejection using a 5th percentile dummy in the forward cockpit and a 95th in the aft station. Ejected weights were 355 and 423 pounds, respectively. Both seats performed a Mode 2 ejection with successful recovery of the dummy and separation of the seat occurring in both cases, Figures 116 and 118. With the exception of the following items, all subsystems were observed to function as designed:

1. The right-hand ejection sequencer and arm restraint thruster on the forward seat did not function.
2. The recovery parachute used on the rear seat experienced some burn damage in the skirt area of the canopy and on the inside of the deployment bag. Evidence of small burns was noted on eight gores and two suspension lines. The damage did not adversely affect parachute performance.

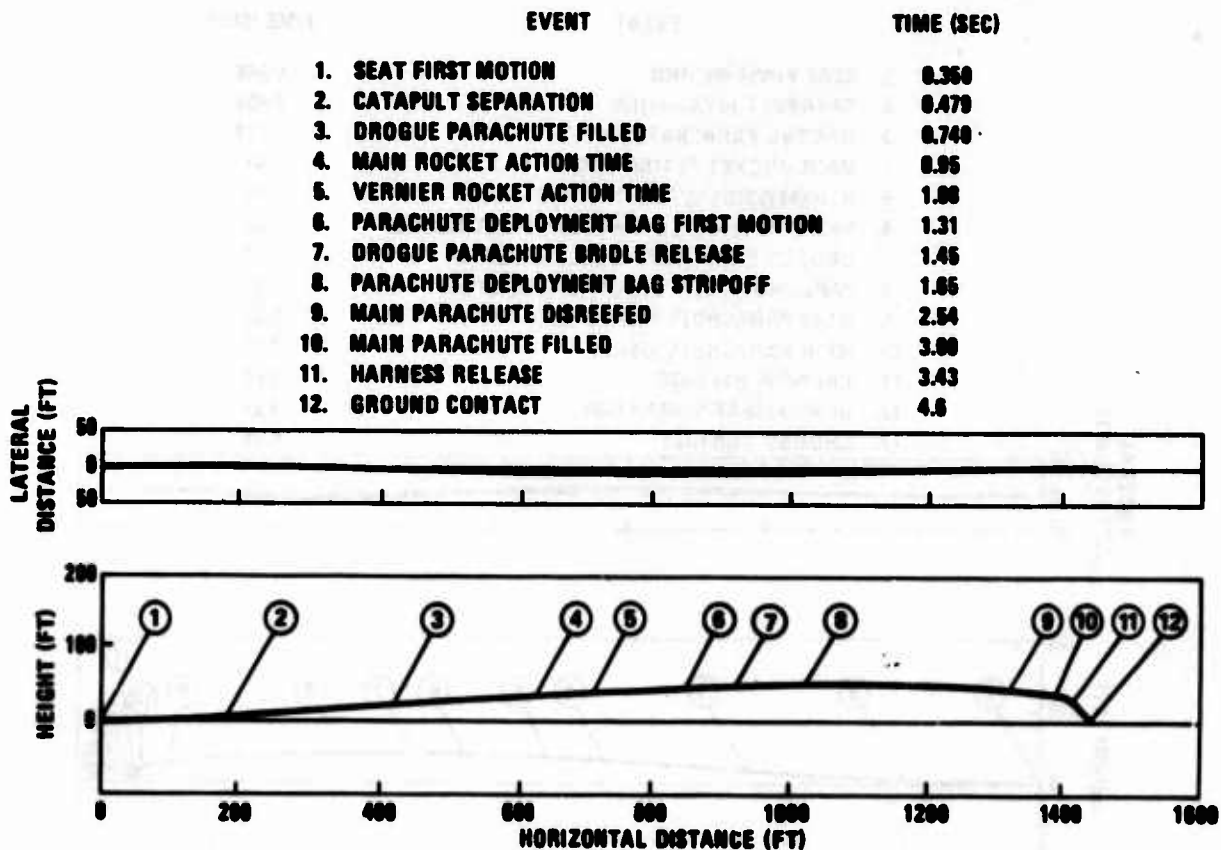


FIGURE 116. TRAJECTORY CURVE, ACES QUALIFICATION SLED TEST NO. 7 - 578 KEAS

- The contents of the survival kits on both dummies did not deploy, although the container flaps were released. Both kits utilized wooden blocks in the rucksack to simulate the GFE equipment items. The stiffness of the wooden blocks prevented the rucksack from falling freely from the survival kit container.

Qualification Inflight Ejection Tests

As part of the ACES qualification program, a series of six inflight ejection tests were made from the aft cockpit of an F-106 aircraft. Tests were conducted at El Centro, California during the period 16 through 30 September 1971, Reference 21. The purpose of these tests was to test the seat system under conditions that could not be simulated with the sled, i.e., high altitude and aircraft rate of descent conditions. One of the more important parameters evaluated was the rotation of the seat about the drogue axis in descent from 40,000 feet mean sea level (MSL) to approximately 15,000 feet. A summary of event data is presented in Table XXII and a synopsis of each test is given below. As in the track qualification tests, no attempt was made to ballast the seat system to achieve adverse cg/thrust line offsets. For tests with 5th percentile dummies, the system static cg ranged from 1.25 to 1.41 inches above the rocket thrust line, and from 0.90 to 1.02 inches for tests using 95th percentile dummies.

Test No. 1 (155 KEAS, 5219 feet MSL) - This test was conducted using a 5th percentile dummy (353-pound ejected mass).

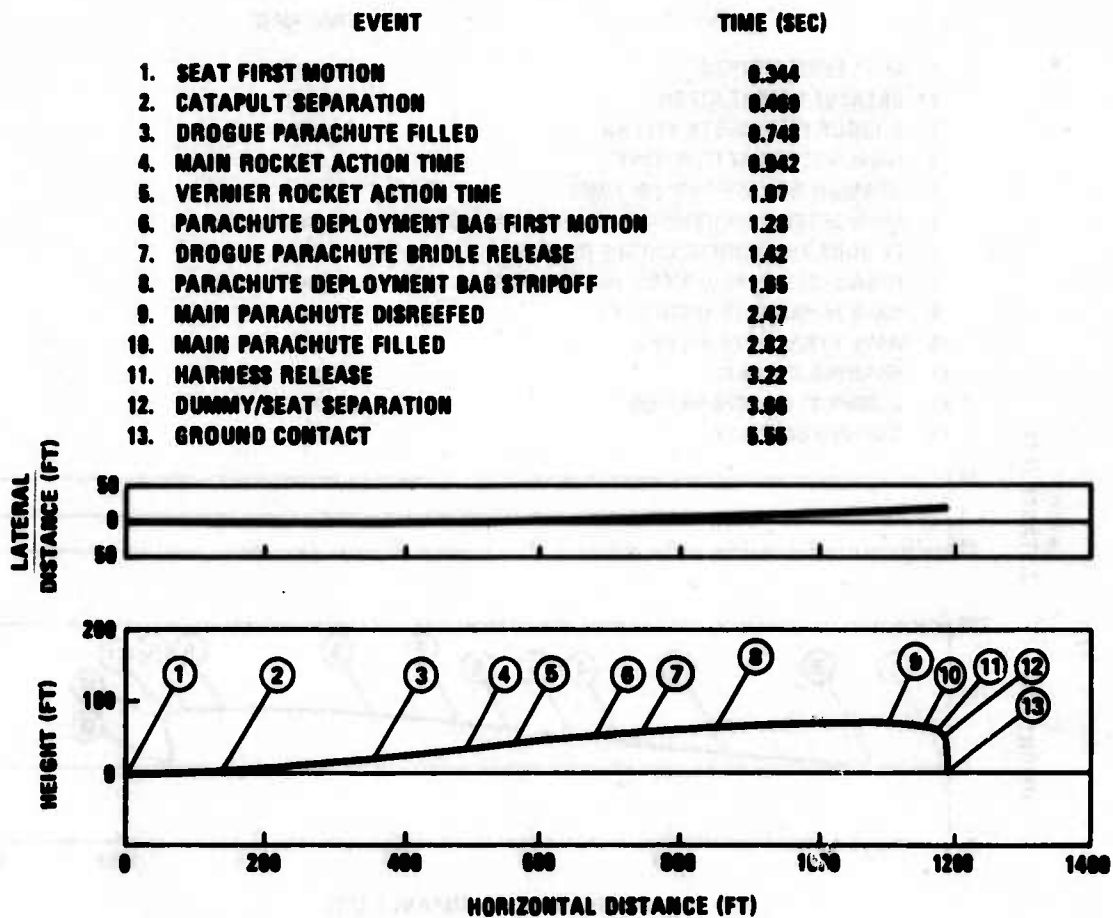


FIGURE 117. TRAJECTORY CURVE, ACES QUALIFICATION SLED TEST NO. 8 - 438 KEAS - AFT SEAT

As the ejection conditions were within the Mode 1 - Mode 2 crossover tolerance band, a shorting plug was attached to the recovery sequencer, in place of the environmental sensor cable assembly, to ensure operation in Mode 1.

The test was successful, with recovery parachute first-fill at 2.15 seconds after ejection initiation, followed by seat separation at 3.85 seconds, 38 feet above the ejection altitude, Figure 119.

System operation was normal throughout, except for four minor discrepancies:

1. The (redundant) left-hand ejection sequencer was not initiated because its triggering input cable assembly was connected incorrectly to the aircraft test firing circuit.
2. The arm restraint system thruster was not fired because of excessive current drain caused by shorting after firing of a parallel squib in the ejection sequencer, Reference 20.

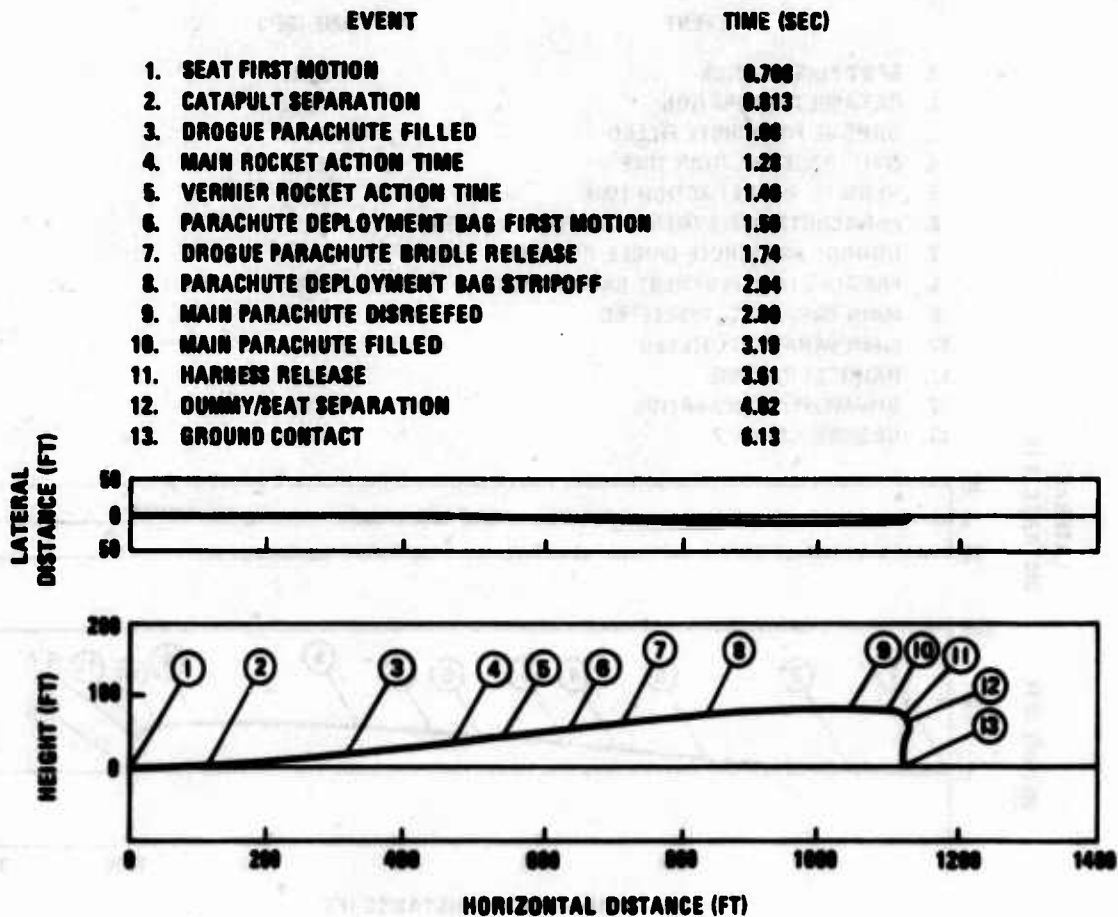


FIGURE 118. TRAJECTORY CURVE, ACES QUALIFICATION SLED TEST NO. 8 - 437 KEAS - FORWARD SEAT

3. A slight bend was evident in the catapult booster tube.
4. One of the two parachute reefing line cutters was not armed.

Test No. 2 (281 KEAS, 16,090 feet MS¹) - This test was conducted using a 5th percentile dummy (352-pound ejected mass).

The test was partially successful in that pre-ejection functions, ejection, stabilization, parachute deployment and reefed inflation, and dummy/seat separation were satisfactory. However, a failure of both reefing line cutters prevented disreefing and subsequent full inflation of the recovery parachute. The mode of failure was similar to the single failure experienced in test No. 1.

TABLE XXII

SUMMARY OF ACES INFLIGHT EJECTION
(FOR ABBREVIATIONS, SEE)

Event	Ref	AE1					AE2					AE3				
		T	ΔT	H	V(T)	V(E)	T	ΔT	H	V(T)	V(E)	T	ΔT	H	V(T)	V(E)
System Initiation	1	0.00 ^⑤	--	5,219	292	155	0.00		16,090	618	281	0.00 ^⑤		15,898	606	276
Seat First Motion	2	0.35 ^⑤	--	5,219	292	155	0.36		16,092	615	280	0.35		15,898	606	276
Catapult Separation	3	0.46	--	5,221	296	157	0.48		16,095	616	280	0.55		15,903	607	276
Main Rocket Ignition	3A	0.47	--	5,221	296	157	0.50		16,095	615	280	0.50		15,901	607	276
Drogue Gun Fires	4	②					0.52		16,096	614	279	--		--	--	--
Vernier Rocket Ignition	5	0.56	--	5,226	297	157	0.67		16,102	604	275	0.57		15,903	607	276
Extraction Chute Bag Stripoff	5A	②					0.75		16,107	592	269	0.62		15,905	607	276
Extraction Parachute Filled	6	②					0.79		16,110	585	266	0.68		15,908	604	274
Drogue Parachute Bag Stripoff	6A	②					0.81		16,112	581	265	0.79		15,915	595	271
Drogue Parachute Filled	7	②					0.89		16,118	568	258	0.95		15,924	575	261
Main Rocket Burnout	8	0.94	--	5,254	281	149	0.99		16,126	546	248	1.02		15,929	565	257
Vernier Rocket Burnout	10	1.10	--	5,226	260	138	1.13		16,136	513	233	1.14		15,936	542	246
Parachute Pack First Motion	11	0.55	--	5,225 (5,063)	④297	157	14.44	0.00	14,868 (14,312)	171	79.5	11.97	0.00	15,112 (14,653)	④170	78.2
Lower Drogue Bridle Severance	12	③					14.66	0.22	14,830	173	80.5	12.09	0.12	15,093	171	78.6
Upper Drogue Bridle Severance	13	②					14.76	0.32	14,814	173	80.5	12.20	0.23	15,075	171	78.8
Main Parachute Pilot Chute Filled	14	0.71	0.16	5,235	296	157	14.84	0.41	14,800	173	80.3	12.21	0.26	15,069	171	78.9
Main Parachute Bag Unlock	15	0.86	0.31	5,248	290	153	14.90	0.47	14,790	172	80.0	12.43	0.46	15,038	171	78.6
Main Parachute Bag Stripoff	16	0.98	0.43	5,257	276	146	15.02	0.59	14,770	169	78.6	12.48	0.50	15,031	170	78.4
Parachute Reefed Fill	17	1.12	0.67	5,273	236	126	15.51	1.08	14,692	154	71.6	12.71	0.74	14,993	166	76.5
Parachute Disreef	18	1.80	1.25	5,290	128	68.3	③					13.24	1.27	14,916	131	60.6
Parachute First-Fill	19	2.15	1.60	5,290	69.2	37.3	③					13.59	1.62	14,879	85.6	39.9
Harness Release	20	2.67	2.12	5,285	28.0	14.8	16.52	2.08	14,568	108	50.5	14.05	2.08	14,854	45.2	20.9
Dummy/Seat Separation	22	3.85	3.30	5,257	26.5	14.0	16.82	2.39	14,536	103	48.0	14.47	2.50	14,836	39.0	18.0
Parachute Final Fill	21	4.98	4.43	5,224	25.9	13.7	③					14.64	2.67	14,831	37.8	17.5
Impact	23	200.0	199	--	--	--	244.0	230.0	--	--	--	498.0	486.0	--	--	--

NOTES: ① indicated by these numbers on telemetry printout. ② not applicable, Mode 1. ③ reefing line cutter failure, no disreef. ④ pressure altitude (U.S. Std. Atmosphere)

ABBREVIATIONS: T = time, seconds ΔT = time after parachute first motion, seconds H = height, feet MSL V(T) = total velocity, true, feet/second. V(E) = Total Velocity, estimated, feet/second

TABLE XXII

INFLIGHT EJECTION TEST EVENT DATA
 (ABBREVIATIONS, SEE BELOW)

AE3			AE4					AE5					AE6				
H	V(T)	V(E)	T	ΔT	H	V(T)	V(E)	T	ΔT	H	V(T)	V(E)	T	ΔT	H	V(T)	V(E)
15,898	606	276	0.00		41,759	832	244	0.000		41,800	844	248	0.00		5,713	323	173
15,898	606	276	0.36		41,758	836	245	0.34		41,824	801	236	0.35		5,642	323	173
15,903	607	276	--		--	--	--	--		--	--	--	0.48		5,615	327	175
15,901	607	276	--		--	--	--	0.50		41,838	774	228	0.48		5,615	327	175
--	--	--	--		--	--	--	--		--	--	--	②				
15,903	607	276	--		--	--	--	0.50		--	--	--	0.58		5,596	326	175
15,905	607	276	--		--	--	--	--		--	--	--	②				
15,908	604	274	--		--	--	--	--		--	--	--	②				
15,915	595	271	--		--	--	--	--		--	--	--	②				
15,924	575	261	1.00		41,787	788	231	0.93		41,877	731	215	②				
15,929	565	257	--		--	--	--	1.05		41,888	722	212	0.83		5,552	316	170
15,936	542	246	--		--	--	--	1.16		41,898	702	206	0.98		5,526	302	162
15,112 (14,653)	④ 170	78.2	124.86	0.00	15,764 (15,129)	④ 176	80.0	123.81	0.00	17,277 (16,512)	④ 152	68.2	0.56	0.00	5,600 (5,382)	④ 327	175
15,093	171	78.6	124.96	0.09	15,746	173	79.0	123.85	0.04	17,270	151	67.6	②				
15,075	171	78.8	125.01	0.14	15,736	172	78.3	123.85	0.04	17,270	151	67.6	②				
15,060	171	78.9	124.92	0.06	15,752	174	79.3	124.06	0.25	17,235	144	64.5	0.70	0.14	5,573	324	174
15,038	171	78.6	125.28	0.42	15,683	164	75.0	124.33	0.52	17,197	132	59.6	0.85	0.28	5,549	315	169
15,031	170	78.4	125.43	0.56	15,655	160	73.2	124.47	0.66	17,178	125	56.9	0.94	0.37	5,534	308	165
14,993	166	76.5	125.63	0.77	15,620	153	70.1	124.68	0.87	17,149	116	52.7	1.20	0.64	5,493	273	147
14,916	131	60.6	126.06	1.20	15,556	134	62.0	125.14	1.33	17,097	95.9	43.4	1.83	1.27	5,422	161	87.2
14,879	85.6	39.9	126.40	1.54	15,503	119	54.6	125.47	1.66	17,075	81.7	37.8	2.20	1.63	5,397	78.2	43.1
14,854	45.2	20.9	126.84	1.98	15,460	99.0	46.3	125.92	2.11	17,046	62.5	28.5	2.69	2.13	5,379	35.3	19.0
14,836	39.0	18.0	127.22	2.36	15,429	81.1	38.3	126.17	2.36	17,037	54.4	24.8	3.03	2.46	5,368	34.4	18.5
14,831	37.8	17.5	127.88	3.02	15,397	56.9	26.8	126.92	3.11	17,021	33.9	15.5	3.65	3.09	5,349	29.5	15.9
--	--	--	671.00	546.00	--	--	--	766.00	6.42	--	--	--	195.00	195.00	--	--	--

pressure altitude (U. S. Std. Atmosphere) in parentheses. ④ System initiation apparently not indicated, times corrected from first motion.
 /second. V(E) = Total Velocity, KEAS

2

EVENT	TIME (SEC)
1. SYSTEM INITIATION	0.0*
2. SEAT FIRST MOTION	0.36
3. CATAPULT SEPARATION	0.46
4. PARACHUTE DEPLOYMENT BAG FIRST MOTION	0.96
5. MAIN ROCKET BURNOUT	0.94
6. PARACHUTE DEPLOYMENT BAG STRIPOFF	0.98
7. VERNIER ROCKET BURNOUT	1.10
8. MAIN PARACHUTE DISREEFED	1.80
9. MAIN PARACHUTE FILLED	2.16
10. HARNESS RELEASE	2.67
11. DUMMY/SEAT SEPARATION	3.06

*ESTIMATED

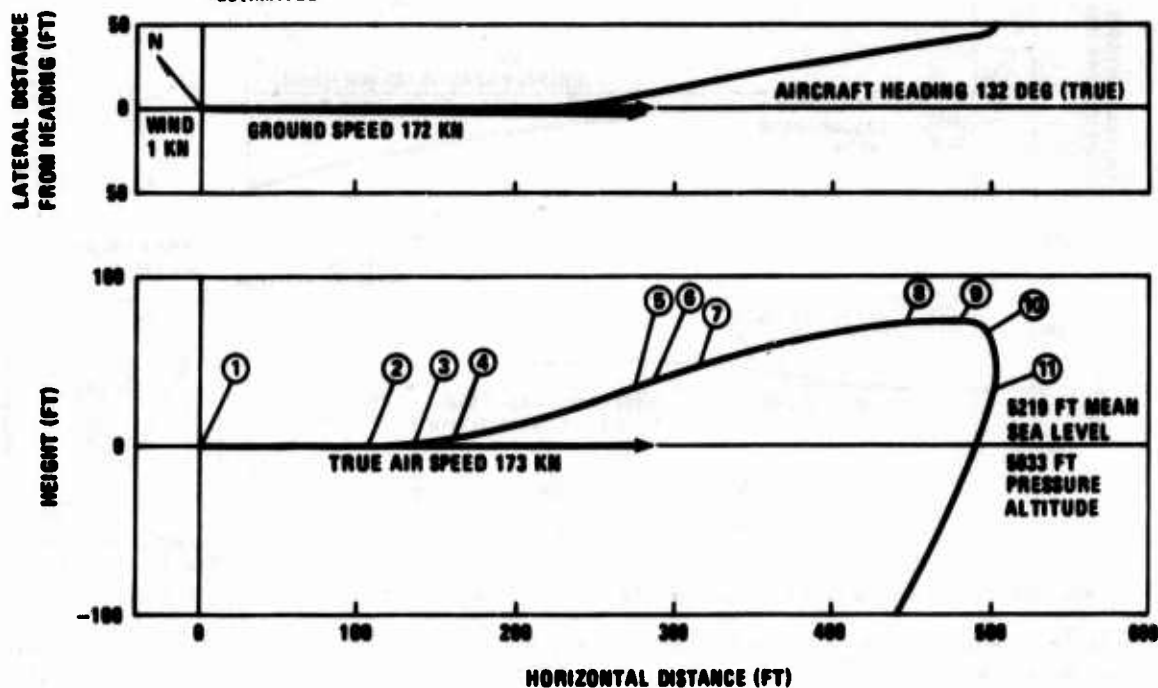


FIGURE 119. TRAJECTORY, ACES INFLIGHT EJECTION TEST NO. 1 (155 KEAS, 5219 FT MSL)

System operation was normal throughout, except for the reefing line cutter failure. This failure and the corrective action taken are described in ACES Failure Analysis Report No. 16, Reference 22.

Parachute mortar initiation occurred at 14,868 feet MSL (14,312 feet pressure altitude), 14.44 seconds after ejection initiation. Dummy/seat separation occurred at 14,536 feet MSL, 2.39 seconds after parachute mortar initiation, Figure 120.

Test No. 3 (276 KEAS, 15,898 feet MSL) - This test employed a 95th percentile dummy (424-pound ejected mass).

EVENT	TIME (SEC)
1. SYSTEM INITIATION	0.0
2. SEAT FIRST MOTION	0.36
3. CATAPULT SEPARATION	0.48
4. DROGUE INFLATION	0.80
5. MAIN ROCKET BURNOUT	0.80
6. VERNIER ROCKET BURNOUT	1.13
7. PARACHUTE DEPLOYMENT BAG FIRST MOTION	14.44
8. DROGUE BRIDLE RELEASE	14.76
9. PARACHUTE DEPLOYMENT BAG STRIPOFF	15.82
10. HARNESS RELEASE	16.82
11. DUMMY/SEAT SEPARATION	16.82

NOTE: PARACHUTE FAILED TO DISREEF

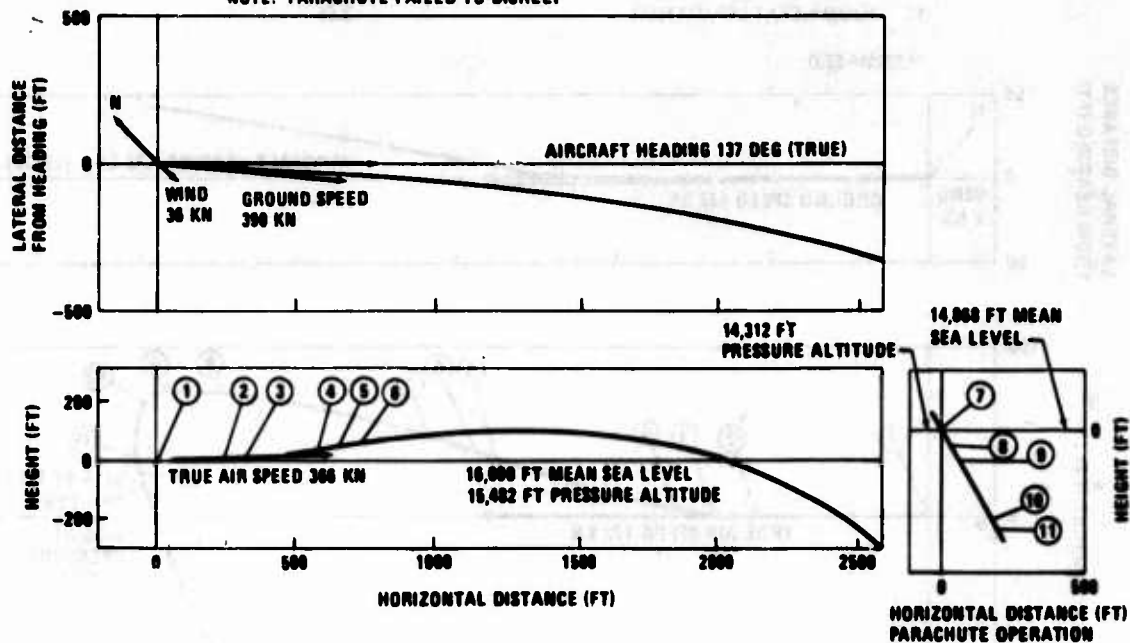


FIGURE 120. TRAJECTORY, ACES INFLIGHT EJECTION TEST NO. 2 (281 KEAS, 16,000 FT MSL)

The test was successful with recovery parachute first-fill at 14,879 feet MSL and dummy/seat separation at 14,836 MSL. System operation was normal throughout for a Mode 3 sequence.

Following ejection and stabilized descent by the drogue, parachute mortar initiation occurred 11.97 seconds after ejection, at 15,112 feet MSL (14,653 feet pressure altitude). Parachute first-fill occurred 1.62 seconds after mortar initiation, and dummy/seat separation at 2.50 seconds, Figure 121.

Test No. 4 (244 KEAS, 41,759 feet MSL) - This test was conducted using a 95th percentile dummy (421-pound ejected mass).

The test was successful, with stabilized descent, following ejection, to an altitude of 15,764 feet MSL where recovery was initiated. Parachute inflation occurred at 1.54 seconds after mortar initiation and dummy/seat separation at 2.36 seconds, Figure 122. System operation was normal except for two minor discrepancies:

1. A slight bend was evident in the catapult booster tube.

EVENT	TIME (SEC)
1. SYSTEM INITIATION	0.0*
2. SEAT FIRST MOTION	0.36
3. CATAPULT SEPARATION	0.55
4. DROGUE INFLATION	0.96
5. MAIN ROCKET BURNOUT	1.02
6. VERNIER ROCKET BURNOUT	1.14
7. PARACHUTE DEPLOYMENT BAG FIRST MOTION	11.97
8. DROGUE BRIDLE RELEASE	12.20
9. PARACHUTE DEPLOYMENT BAG STRIPOFF	12.48
10. MAIN PARACHUTE DISREEFED	13.34
11. MAIN PARACHUTE FILLED	13.50
12. HARNESS RELEASE	14.06
13. DUMMY/SEAT SEPARATION	14.47

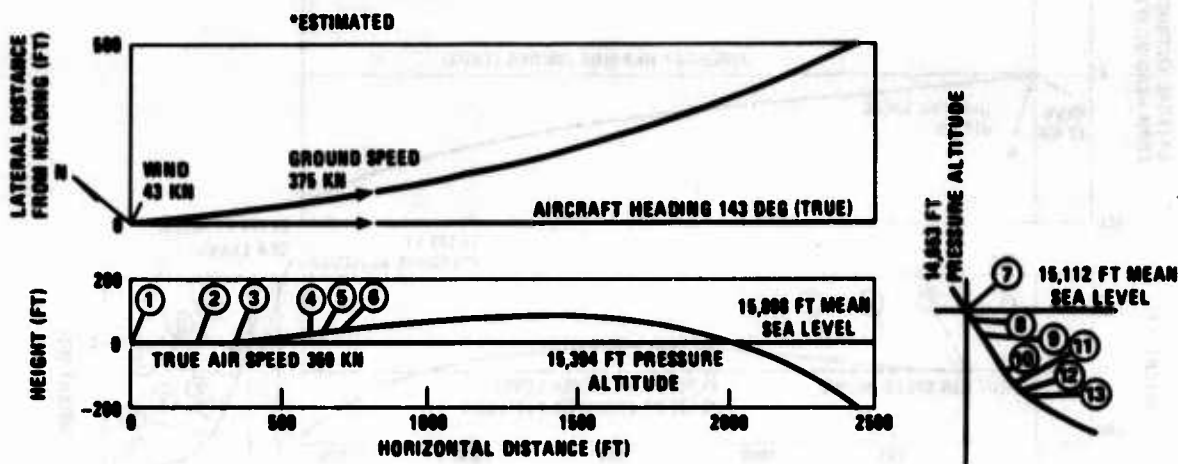


FIGURE 121. TRAJECTORY, ACES INFLIGHT EJECTION TEST NO. 3 (276 KEAS, 15,898 FT MSL)

- Both environmental sensor pitot tubes failed to erect because their release latches were not actuated. The malfunction was caused by a mislocation (on assembly in the test aircraft cockpit) of the pitot-release arms on a replacement torque tube which was installed for re-use of the extendable guide rails. As the seat was ejected in a Mode 3 environment, where the pitot-measured velocity is of no consequence, a normal Mode 3 recovery sequence occurred.

During the initial part of the ejection sequence the rate gyro record showed erroneous undamped oscillations. When the drogue became effective, an alternating rotation of the seat about the drogue axis was evident for periods of 20 to 25 seconds in each direction, with peak roll rates at about 200 degrees/second. Analysis of test films corroborated the rate gyro data.

Test No. 5 (248 KEAS, 41,800 feet MSL) - This test was conducted using a 5th percentile dummy (356-pound ejected mass).

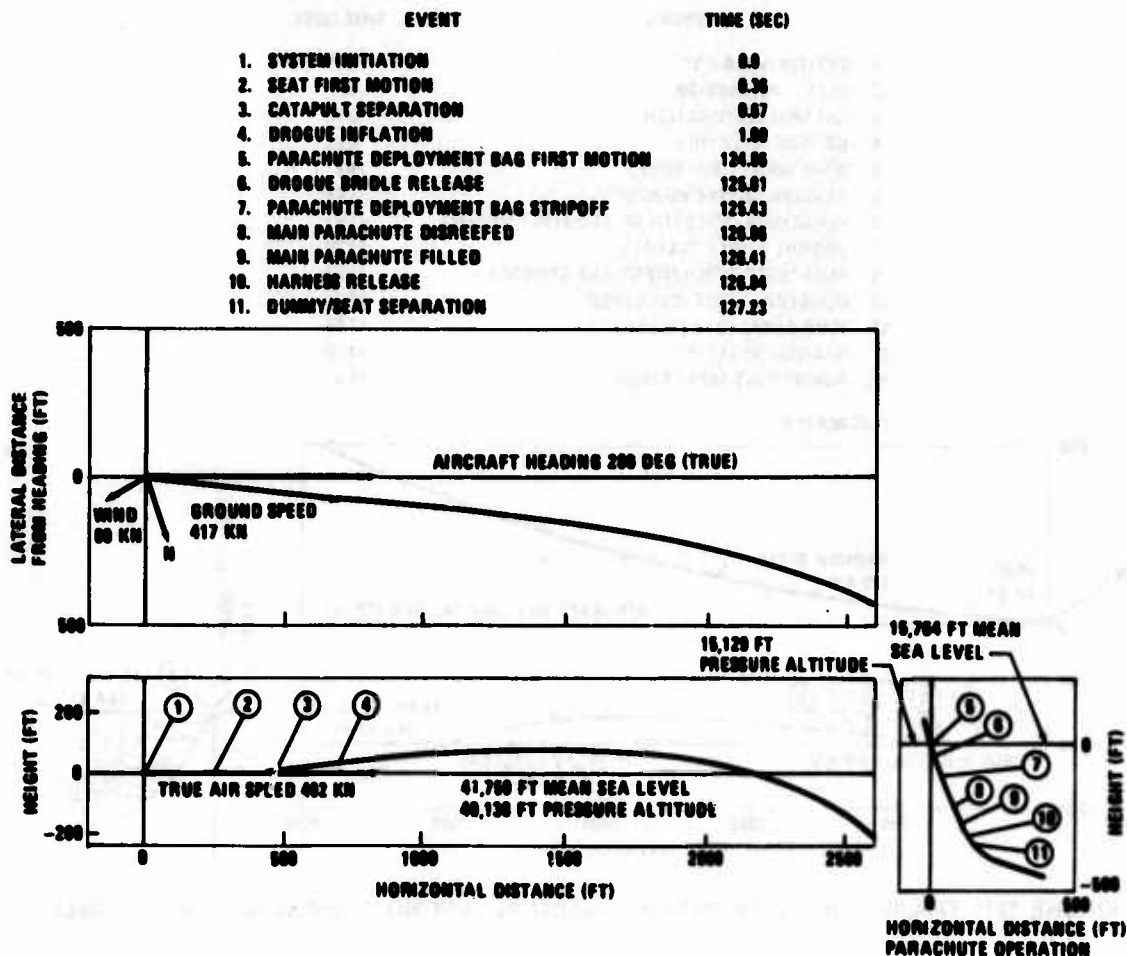


FIGURE 122. TRAJECTORY, ACES INFLIGHT EJECTION TEST NO. 4 (244 KEAS, 41,750 FT MSL)

The test was successful, with recovery initiation, following stabilized descent, at 17,277 feet MSL (pressure altitude 16,512 feet). System operation (sequencing and function) was normal throughout for a Mode 3 sequence. Following ejection, descent was stabilized by the drogue until parachute mortar initiation 123.81 seconds after ejection initiation. Parachute first-fill occurred 1.66 seconds after mortar initiation and dummy/seat separation at 2.36 seconds, Figure 123.

Test No. 6 (173 KEAS, 5,713 feet MSL) - This test was conducted using a 95th percentile dummy (421-pound ejected mass). The test airplane was in descending flight, at approximately 55 degrees nose-down attitude and flight-path angle, relative to the horizon, at the ejection point. The airplane rate of descent was 10,896 ft/min. when the test was initiated. As in test No. 1, a shorting plug was fitted to the recovery sequencer to ensure operation in Mode 1. The test was successful with recovery parachute inflation occurring 2.2 seconds after ejection initiation, followed by dummy/seat separation at 3.0 seconds, 345 feet below the ejection altitude, Figure 124. All subsystems functioned normally for a Mode 1 sequence.

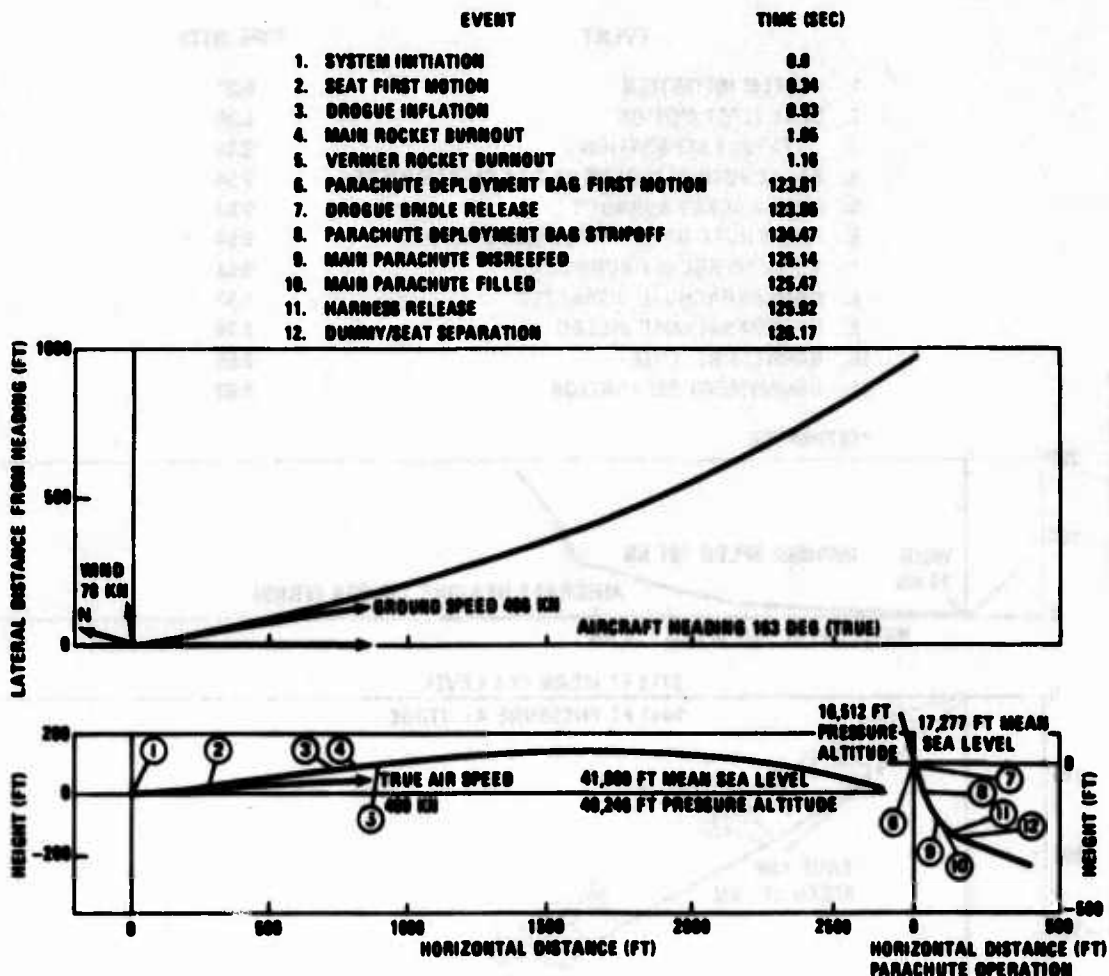


FIGURE 123. TRAJECTORY, ACES INFLIGHT EJECTION TEST NO. 5 (248 KEAS, 41,800 FT MSL)

DISCUSSION OF ACCELERATION DATA

All acceleration loads measured during the inflight tests were within the limits specified in MIL-S-9479A. Dynamic Response Index (DRI) values, calculated in accordance with the method described in MIL-S-9479A, resulted in acceptable values for the rocket catapult, stabilization and recovery phases of the ejection, Reference 21.

Accelerations measured on the seat system during the qualification track ejection tests exceeded, in some cases, the allowable values for the G_z axis (eyeballs down). In these cases, calculated DRI data were higher than that permitted by MIL-S-9479A for the catapult, stabilization and recovery phases of the ejection sequence, Reference 19.

Although the DRI values obtained on the rocket catapult compared reasonably well for all track ejection tests, the average DRI for the qualification tests was slightly lower than that obtained for the development ejection tests. This is explained by a change made in the catapult launch cartridge propellant following the development ejection tests. According to the Frankford Arsenal

EVENT	TIME (SEC)
1. SYSTEM INITIATION	0.0*
2. SEAT FIRST MOTION	0.35
3. CATAPULT SEPARATION	0.48
4. PARACHUTE DEPLOYMENT BAG FIRST MOTION	0.56
5. MAIN ROCKET BURNOUT	0.83
6. PARACHUTE DEPLOYMENT BAG STRIPOFF	0.94
7. VERNIER ROCKET BURNOUT	0.98
8. MAIN PARACHUTE DISREEFED	1.83
9. MAIN PARACHUTE FILLED	2.20
10. HARNESS RELEASE	2.80
11. DUMMY/SEAT SEPARATION	3.83

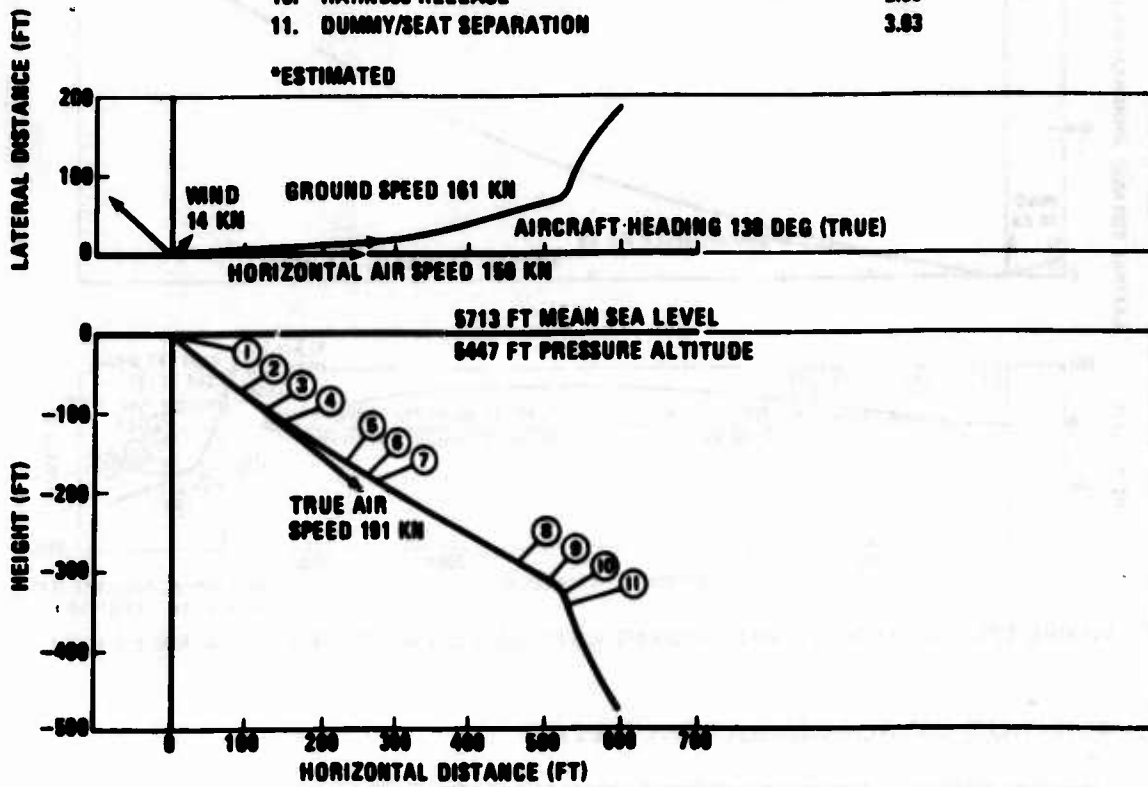


FIGURE 124. TRAJECTORY, ACES INFLIGHT EJECTION TEST NO. 6 (173 KEAS, 5713 FT MSL, AIRCRAFT RATE OF DESCENT 10,896 FT/MIN)

project engineer, the propellant alteration was intended to reduce DRI values but with no appreciable degradation of catapult end-velocity. A tabulation of DRI data resulting from the rocket catapult in the inflight, static and track ejection tests is presented below. In the qualification tests, the DRI limit of 18.0 was exceeded only in test No. Q8, aft seat.

Inflight Ejection Tests			Static and Track Ejection Tests					
			**Development (Static)			Qualification		
Test No.	Dummy % ile	DRI	Test No.	Dummy % ile	DRI	Test No.	Dummy % ile	DRI
AE-1	5th	NR*	4	5th	18.2	Q1	95th	17.8
AE-2	5th	NR	5	95th	15.2	Q2	5th	14.7
AE-3	95th	14.6	8	95th	18.4	Q3	95th	17.1
AE-4	95th	13.7	9	5th	18.2	Q4 (Aft)	5th	17.0
AE-5	5th	15.3				Q4 (Fwd)	95th	16.4
AE-6	95th	12.0				Q5	5th	16.1
						Q6	5th	15.2
						Q7	95th	17.6
						Q8 (Aft)	95th	18.8
						Q8 (Fwd)	5th	15.0

*NR - Not recorded (instrumentation malfunction)

**DRI data were not obtained for the track development tests (tests No. 10, 11, and 12), and DRI values have been omitted for test No. 7 and for tests No. 1, 2, 3, and 6 in which the Quantic rocket catapult was used.

The parachute loads, in some of the qualification ejection tests, exceeded the 17-g vertical acceleration limit (G_z) specified in MIL-S-9479A. This limit was exceeded during drogue parachute inflation in tests No. Q6, Q7, and Q8 and during main parachute reefed inflation in tests No. Q1 and Q5. The maximum vertical acceleration recorded during drogue parachute inflation was 20.0 g (test No. Q6) and, during main parachute reefed inflation, 19.7 g (test No. Q5). The G_x limit of 35 was not exceeded in any of the qualification ejection tests. Accelerations with respect to the G_z axis, measured during drogue and recovery parachute operation, are summarized for the track ejection qualification tests in Table XXIII. Total acceleration, G_t , the vector sum of the lateral, longitudinal and vertical acceleration values, is also listed for the recovery parachute, with G_x loads given for the drogue.

TABLE XXIII
DROGUE AND RECOVERY PARACHUTE ACCELERATION DATA
FOR TRACK EJECTION QUALIFICATION TESTS

Test No.	Ejected Weight (Lb)	Test Velocity (KEAS)	Drogue Acceleration (g)			Recovery Parachute Acceleration (g)					
			G _z	DRI	G _x	Reefed Inflation			Full Inflation		
						G _z	DRI	G _t	G _z	DRI	G _t
Q1	420	212	NA	NA	NA	18.6	21.8	19.1	12.5	13.1	15.2
Q2	355	Zero	NA	NA	NA	-1.0	NA	1.8	0.0	0.0	1.6
Q3	423	Zero	NA	NA	NA	NR	NR	NR	NR	NR	NR
Q4 (A)	355	151	NA	NA	NA	14.4	16.2	14.5	7.9	8.3	9.6
Q4 (F)	423	149	0.0	0.0	-4.4	5.3	5.5	5.5	9.1	9.5	10.5
Q5	355	227	NA	NA	NA	19.6	22.1	19.7	9.5	10.0	10.4
Q6	354	577	20.0	26.6	-24.3	8.7	8.9	13.8	8.6	9.5	11.2
Q7	424	578	18.2	21.9	-24.4	14.9	14.9	16.0	13.9	14.7	14.4
Q8 (A)	423	438	18.2	22.7	NR	13.5	14.7	NR	12.4	13.4	NR
Q8 (F)	355	437	16.2	21.1	NR	10.5	11.6	NR	9.7	9.9	NR

NA - Not Applicable
 NR - No Recording, Instrumentation Malfunction

Although the G_z drogue-induced accelerations exceeded the 17-g limit specified by MIL-S-9479A, the G_x loads were well below the specified 35-g limit. The problem of excessive G_z -axis acceleration could be solved by either reducing the drogue size, or by altering the drogue bridle geometry to trim the seat in a more upright attitude. The latter approach is more desirable because reducing the size of the drogue degrades system performance.

The recovery parachute G_z -axis acceleration loads can be attenuated by relocating the riser-to-seat attachment closer to the system cg or by revising the Mode 1 - Mode 2 crossover velocity downward. The former approach is somewhat complex while the latter results in degradation of system performance. Another alternative is to separate the crewman from the seat prior to the time any appreciable parachute loading is experienced. This approach allows the parachute-imposed accelerations to be distributed into the crewman's harness in the conventional manner.

EVENT TIMING

The timing for all the recovery sequencer-initiated events was within the specified tolerance during the inflight and track qualification ejection tests. To illustrate the accuracy and repeatability of the electronic timing, a comparison of design nominal and actual times for recovery sequencer-initiated events is shown below for the track tests.

MODE 1

EVENT	DESIGN	Q1	Q2	Q3	Q4(Aft)	Q5
STAPAC	0.46 ±5%	0.46	0.48	0.47	0.46	0.46
Parachute Mortar	0.50 ±3%	0.49	0.51	0.51	0.50	0.49
Lower Drogue Cutter	0.62 ±3%	0.61	0.63	0.62	0.62	0.61
Upper Drogue Cutter	0.65 ±3%	0.64	0.66	0.65	0.65	0.64
Harness Release	2.60 ±3%	2.54	2.69	2.60	2.66	2.55

MODE 2

EVENT	DESIGN	Q4(Fwd)	Q6	Q7	Q8(Aft)	Q8(Fwd)
STAPAC	0.46 ±5%	0.50	0.48	0.47	0.47	0.48
Drogue Gun	0.46 ±3%	0.53	0.47	0.46	0.46	0.48
Parachute Mortar (t)	1.30 ±3%	1.36	1.32	1.31	1.28	1.29
Lower Drogue Cutter	t+0.12 ±3%	0.12	0.12	0.11	0.11	0.12
Upper Drogue Cutter	t+0.15 ±3%	0.15	0.15	0.14	0.14	0.15
Harness Release	t+2.10 ±3%	2.13	2.18	2.12	2.06	2.02

Note: All times are in seconds.

Time zero is at system initiation.

The initiation time established for each event is based on an observed function following the ignition signal from the Recovery Sequencer; therefore, certain event times shown may be outside the required tolerance band.

SYSTEM IMPROVEMENTS

During the seat system development and qualification tests, various problems were encountered with the functional portions of the system. The specific problems and the corrective actions taken have been noted previously in this section.

Solutions provided for problems experienced in the overall research and development program were satisfactory, as evidenced in the final stages of the test program. However, the following improvements to the ACES-1 system would be beneficial in terms of performance and reliability:

1. The seat should be released earlier in the ejection sequence. This will provide more positive and rapid man-seat separation, as the parachute will be applying greater acceleration loading. In addition, an improvement in recovery performance will be achieved for all escape conditions.
2. The reefing line cutter should be modified to strengthen the sear pin. This would eliminate the necessity of special rigging of the arming lanyard and contribute to higher reliability.
3. The recovery parachute deployment bag should be modified to eliminate any mortar flash-burning of the canopy. This anomaly was only encountered in the track ejection tests, and the actual damage sustained by the canopy was not detrimental to its performance.
4. The survival kit should be altered to promote more rapid deployment of the kit contents.

SECTION XV SYSTEM PERFORMANCE

The performance of the ACES system has been analyzed for escape conditions other than those included in the test program. The analysis was performed using the McDonnell Douglas ESCAP-TRAC computer program (No. H5HA), which calculates escape system trajectories in three-degrees-of-freedom for all aircraft flight conditions in a vertical plane and, by approximation, for bank conditions. The program incorporates ICAO standard atmosphere data, aerodynamic coefficients for the ejection seat and occupant, Reference 23, and for the crewman and survival kit, Reference 24. A simulation of rocket catapult propulsion forces and the dynamics of the gyro-controlled vernier rocket also are contained in the program. Drogue and recovery parachute operation is simulated by a method incorporating the dynamics of parachute inflation and parachute mass effect following inflation (swing through).

The H5HA program is an outgrowth of several older Douglas computer programs including escape system trajectory (No. B9DA), STAPAC Vernier Rocket Dynamic Simulation (No. F2LA), Dynamic Response Index (No. L5WA) and Parachute Opening Dynamics (No. M7UA). The program is written in FORTRAN IV source language for the IBM 360/65 computer.

ACES performance predictions were computed originally on estimated and calculated input data, Reference 1. As the full-scale seat system test results became available, and were analyzed, the computer input parameters were progressively updated and adjusted to best simulate the performance observed. The original ACES performance predictions and the computed performance, based on seat ejection test results, are shown in Table XXIII. The difference in performance noted is attributable to the increased reefing time (1.0 to 1.3 seconds) and the fact that the computer program now better simulates the performance of the system. A factor that adversely affects performance of the present ACES is the 2.1-second delay between parachute mortar initiation and release of the seat. The parachute attains full inflation prior to seat release in nearly all cases, but unlike other contemporary seat systems, recovery is not accomplished until the seat is released. Reduction of the seat-release delay from 2.1 to 1.8 seconds would not only improve performance but would promote more rapid man/seat separation.

With reference to Table XXIV, it is evident that despite the difference in performance between the proposed and present ACES configurations, the MIL-S-9479A requirements are met or exceeded by the present ACES system.

Performance of ACES for various aircraft flight conditions is illustrated in Figures 125 through 129. All trajectories were computed with the H5HA program. The origin of all trajectories is the point at which the crewman pulls the firing control handle. In all cases except Figure 125, recovery is considered to occur at seat release, which follows full inflation of the recovery parachute. A 50th percentile seat occupant is assumed for all ejections, except in Figure 125, which shows seat trajectories with 5th and 95th percentile crewman for a 4-inch g excursion.

**TABLE XXIV
ACES SYSTEM PERFORMANCE**

Flight Conditions			Terrain Clearance Required at System Initiation (Ft) (1)			
Pitch (Deg)	Roll (Deg)	Airspeed (KEAS)	Rate of Descent (FPM)	MIL-S-9479A Requirement	ACES Performance (2)	
					Present	Predicted (Ref. 1)
0	60	120	0	0	0	0
0	180	150	0	200	187	200
0	0	150	10,000	300	133	103
-60 (3)	0	200	-	500	347	358
-60 (3)	60	200	-	550	463	446
-45 (3)	180	250	-	600	544	500

- NOTES:** (1) System initiation is 0.3-second prior to rocket catapult ignition
(2) Based on parachute inflation and man/seat release
(3) Dive conditions based on zero aircraft angle-of-attack

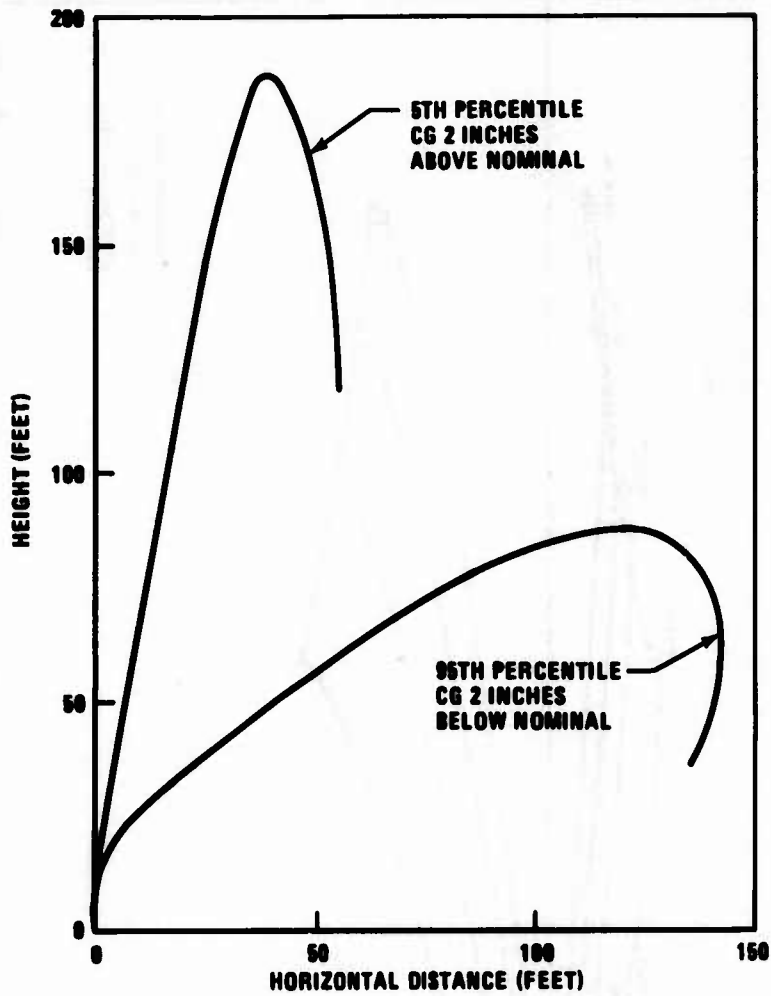


FIGURE 125. ACES ZERO/ZERO PERFORMANCE

A velocity decay profile for a 600-KEAS sea-level ejection is plotted in Figure 130. The significant events occurring during the ejection and recovery phases are noted on the velocity curve.

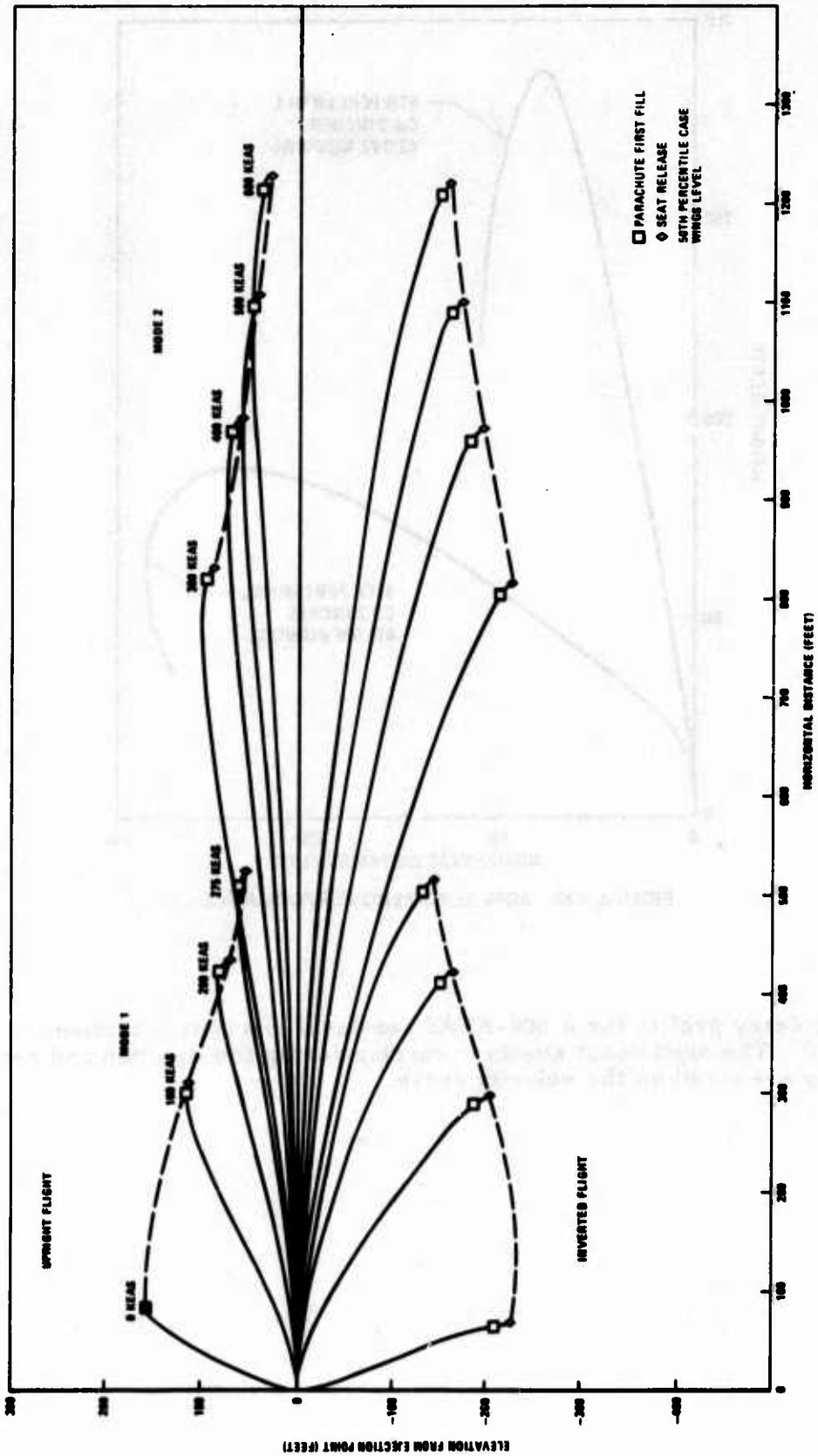


FIGURE 126. ACES PERFORMANCE FOR UPRIGHT AND INVERTED FLIGHT

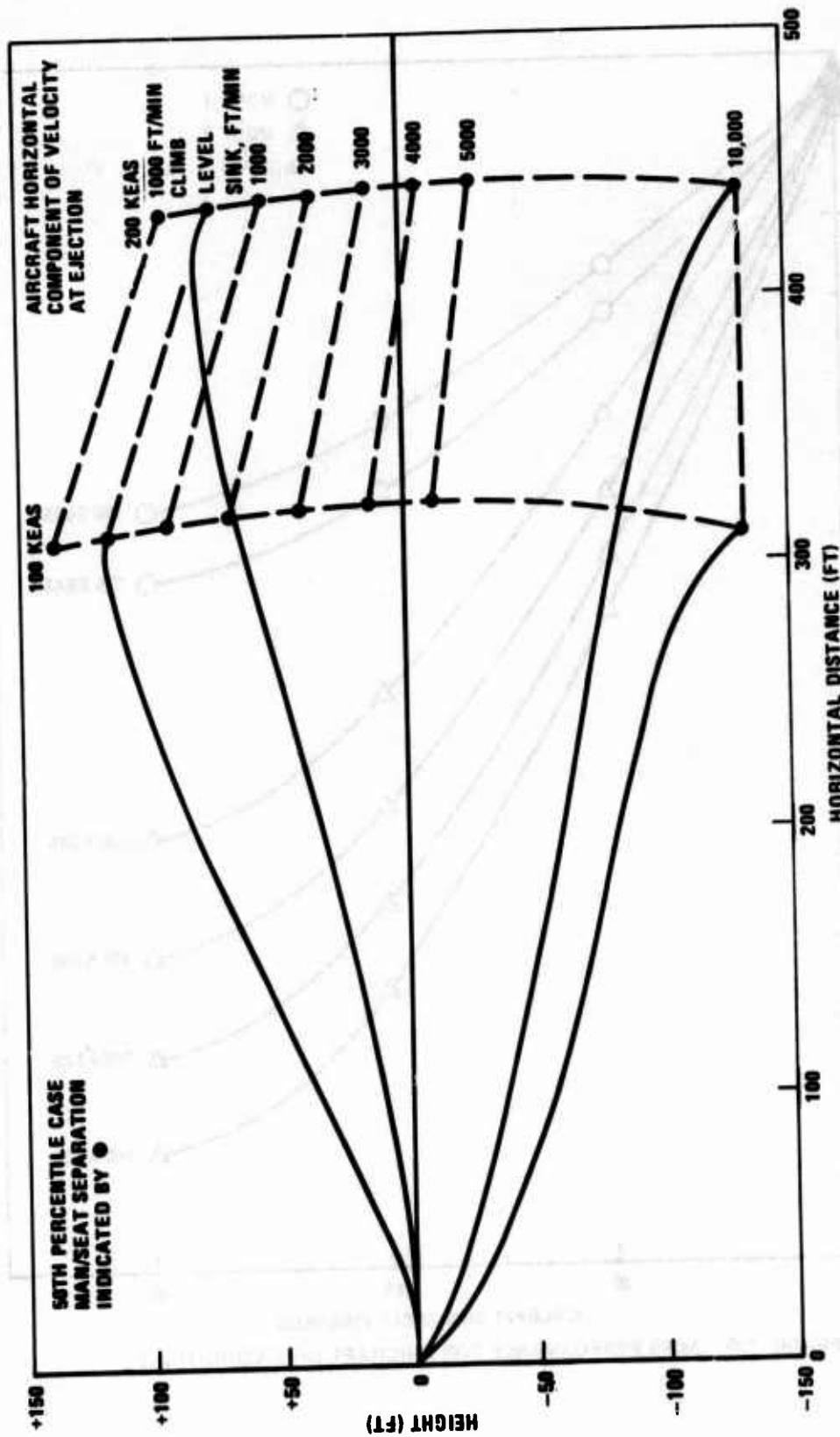


FIGURE 127. ACES SINK RATE PERFORMANCE

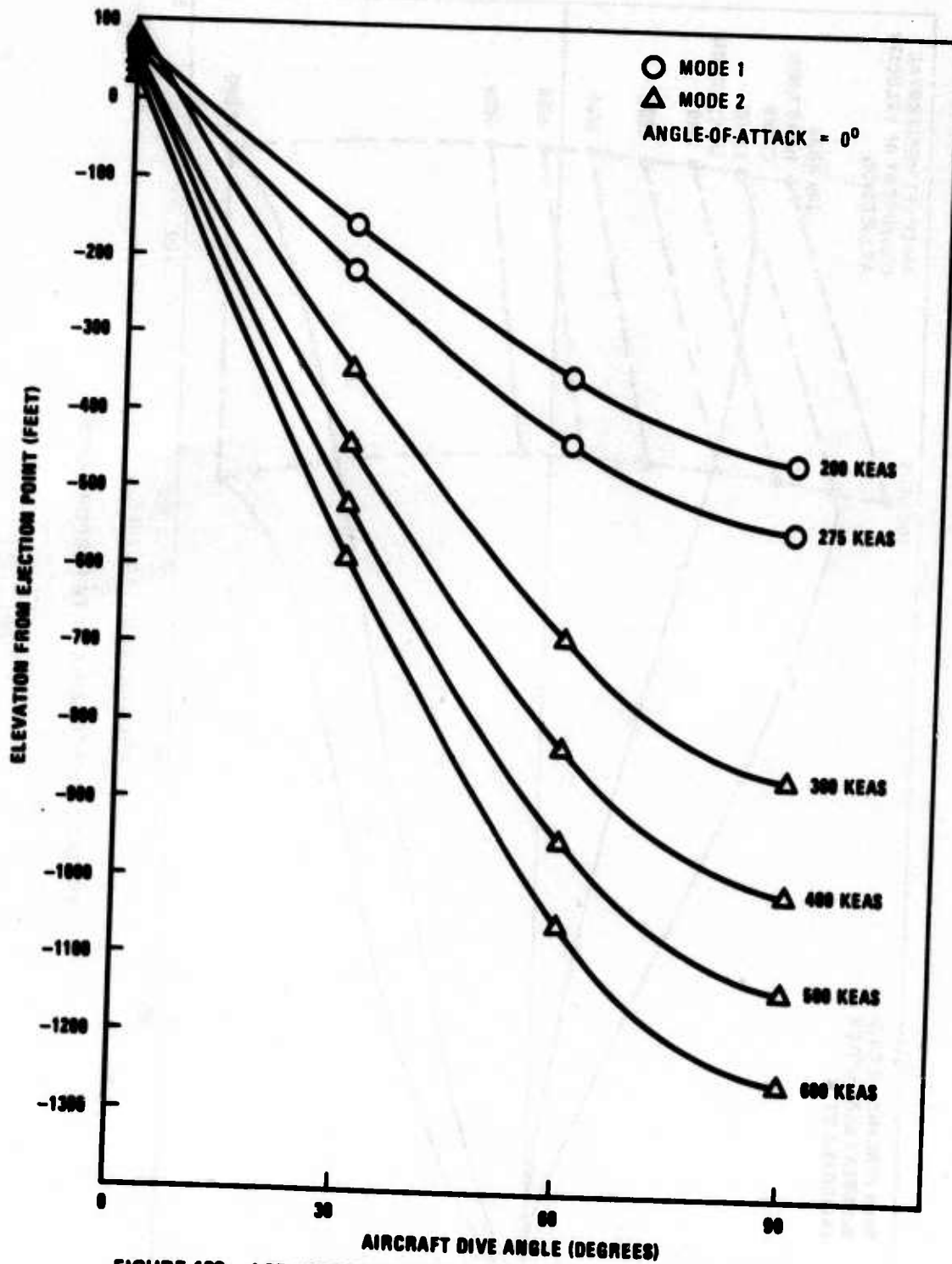


FIGURE 128. ACES PERFORMANCE FOR AIRCRAFT DIVE CONDITIONS

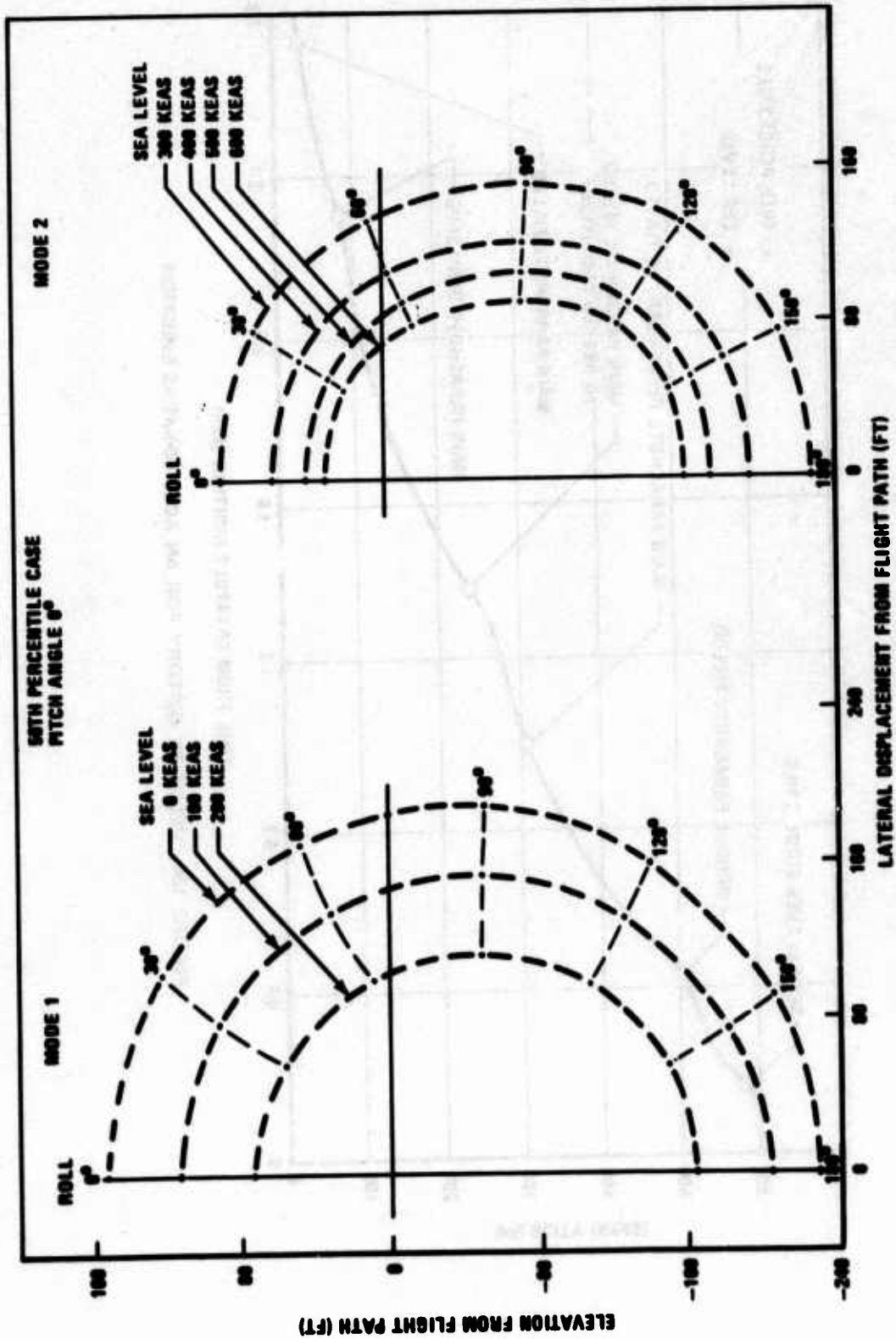


FIGURE 129. ACES PERFORMANCE FOR AIRCRAFT ROLL CONDITIONS

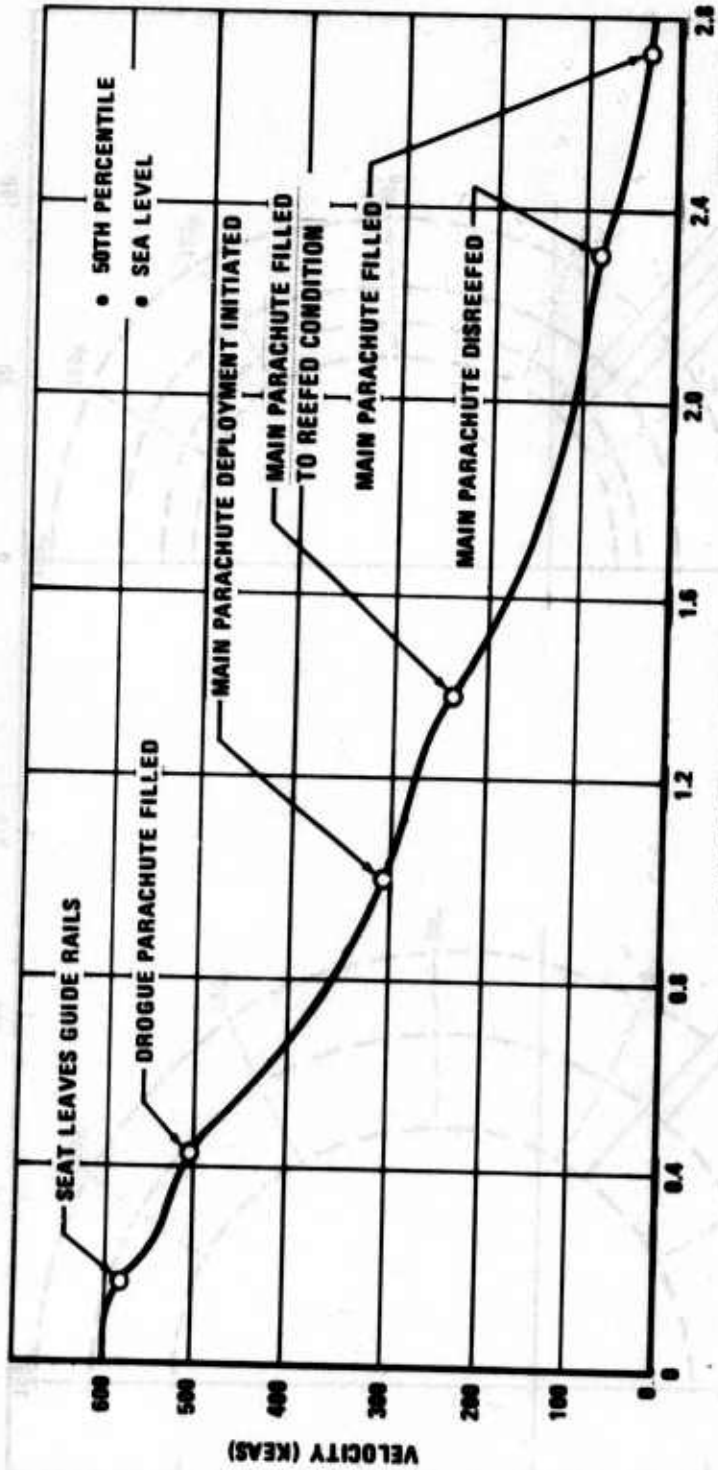


FIGURE 130. VELOCITY HISTORY FOR AN ACES 600-KEAS EJECTION

SECTION XVI

RELIABILITY AND MAINTAINABILITY

RELIABILITY

A reliability assessment of the ACES system was made in accordance with ground rules outlined in the Reliability Program Plan, Reference 25. The goal for probability of success for the seat system was established at 0.98 at the 90-percent lower confidence limit, as specified by MIL-S-9479A, which also requires a demonstrated system reliability of 0.90 at the 90-percent confidence level.

Because the ACES program did not include a series of tests specifically for reliability demonstration purposes, the final assessment was made using results of the qualification tests to establish the system-level reliability. For all subsystems and components, only qualification test results were used in the assessment. The results of the reliability analysis are summarized in Table XXV.

Assessment Criteria

To use results of a limited test program for reliability demonstration purposes, it is appropriate to employ a technique wherein certain failures are excluded from the chargeable failures. A chargeable failure is one in which the failure is random and the rationale for corrective design action cannot be established. A nonchargeable failure is one in which the mode of failure is identified and the validity of the corrective action demonstrated in subsequent tests. Design deficiencies are excluded from the analysis as chargeable failures, only if the following criteria are satisfied:

1. The system or component is redesigned to eliminate the failure mode.
2. The redesigned component is tested to verify that the failure mode has been eliminated.
3. The failure does not repeat in subsequent tests.

Successful Test - A successful test is a test that provides all the required data and demonstrates that all functional and sequencing requirements are accomplished. The test data must indicate that a crew member would have landed on the earth's surface without exceeding the human tolerance specified in the performance specification, Reference 26.

No Test - A no-test disposition is made for the following reasons:

1. Test apparatus malfunction such as unachieved vehicle velocity.
2. Human error such as misrigging
3. Insufficient data to justify a design revision in the case of a system anomaly in which malfunction of a specific component did not occur.

TABLE XXV
ACES RELIABILITY ASSESSMENT

System, Subsystem or Component	Report No.	Reliability Demonstrated at the 90% Confidence Level
Seat System	MDC-J5356 } MDC-J5327 }	0.85
Recovery Subsystem	MDC-J5219 } MDC-J5366 }	0.97
Parachute Mortar	Ogden F-70182	0.97
Gyro Spin-up Actuator	Ogden F-70181	0.97
Harness Release Thruster and Cartridge	Upco TR 1016	0.97
Mortar Cartridge (1)	Upco TR 1011A } Upco 1335 }	0.90
Arm Restraint Thruster and Cartridge	Upco TR 1023	0.97
Drogue Gun and Cartridge	Upco TR 1015 } and TR 1046 }	0.98
Seat Stabilization Rocket Motor	Talley 10700	0.96
Drogue Severance FLSC Assemblies	Teledyne H13194	0.96
Gas Generator and Initiator (for inertia reel)	Pacific Scientific } TR 718 }	0.93
Automatic Programmer	Dorsett ER-077	0.96
Reefing Line Cutter	Atlas ACDL 70-7	0.98
Environmental Sensors	HTL No. 300408	(2)

(1) Report No. TR 1011A covers qualification tests of cartridge P/N 1005-1. Report No. 1335 covers qualification tests of cartridge P/N 1005-2.

(2) Quantitative reliability data were not obtained on the environmental sensors, as the testing consisted only of dynamic and static pressure tests following exposure of the units to the prescribed environments.

When the above-described criteria are used to assess the results of the system qualification tests (Section XIV), 14 tests are counted as successful, with tests Number Q7 and AE-2 being designated as no tests. Fourteen successful tests provide a reliability of 0.85 at the 90-percent confidence level, Reference 27.

MAINTAINABILITY

The maintenance concept for the ACES system was developed by utilizing proven maintainability analysis procedures used on other Douglas ejection seat systems. The ACES maintenance analysis procedure considers direct-preventive and corrective maintenance at the organizational level.

Maintenance, inspection, and test procedures are established to the depth and at the interval necessary to assure and maintain the highest degree of operational safety and serviceability. This concept is based on the following:

1. Items such as rockets, cartridges, nylon components, initiators, and survival kits will be time-controlled on a scheduled preventive basis.
2. Items such as the power inertia reel and seat actuator assembly will be maintained on an unscheduled corrective basis.

The scheduled maintenance consists of preflight inspection, postflight inspection, replacement of time-compliance items, and phased inspection, which is based on aircraft maintenance interval requirements. During phased inspection, preventive maintenance is performed on the ejection seat and includes corrosion control, repairs to seat structure, and replacement or adjustment of any components not conforming to specifications or seat rigging requirements. All manual controls are actuated to ascertain compliance with pull-force specifications and to verify that linkages are intact and operating freely.

A maintainability program was conducted in accordance with the Maintainability Program Plan, Reference 27. This consisted of full maintenance engineering analysis with emphasis on the quantitative and qualitative maintainability parameters established within the design specification, MIL-S-9479A (USAF).

A value of 0.03538 maintenance man-hours per flight hour (MMH/FH) was achieved for all significant maintenance actions required to be performed at the Organizational Maintenance Level. This value is broken down as follows:

	<u>MMH/FH</u>
Preventive (Scheduled) Maintenance	0.03104
Time Compliance Items	0.00175
Corrective (Unscheduled) Maintenance	<u>0.00259</u>
TOTAL	0.03538

SECTION XVII

CONCLUSIONS

It is concluded that:

1. The Advanced Concept Ejection Seat meets the performance requirements of MIL-S-9479A, except for G_z -axis acceleration loads imposed on the occupant.
2. The use of an electronic programmer to sequence the initiation of pre-ejection and recovery events results in the precise control required for an advanced-performance emergency escape system. Logic and timing functions of the ACES automatic programmer satisfy all design criteria.
3. The concept of an erectable, on-board speed/altitude sensing system has been successfully demonstrated, and the performance of the system is considered compatible with the functional requirements of the ACES multi-mode system.
4. The stability of the ACES system is considered satisfactory throughout the ejection and recovery sequence for all speeds and altitudes tested.
5. The mortar-deployed recovery parachute, in combination with the variable effective reefing scheme, meets the escape system performance requirements.
6. The concept of releasing the seat following recovery of the man/seat combination eliminates the possibility of subsequent man/seat and/or seat/parachute interference.
7. Recovery of the crewman in the seat, and subsequent release of the seat, does not consistently result in positive separation of the seat. Actuation of the man/seat release system prior to recovery, when the parachute drag load is substantially higher, will improve the man/seat separation characteristics.
8. The ACES single-point release crew restraint system meets structural and performance criteria on the basis of evaluations made by Air Force flight personnel; however, additional development may be necessary to improve harness donning characteristics.
9. The ACES survival kit, in combination with the seat-mounted deployment selector meets the design requirements. A minor modification to the front corners of the outer container may promote more rapid deployment of the kit contents.

REFERENCES

1. Advanced Concept Ejection Seat for Model Ejection Seat Development Program, Report No. 3650T, Douglas Aircraft Company, 29 March 1969
2. U. S. Air Force Contract F33657-69-C-0223
3. H. R. Moy, Detailed Design Study, Advanced Concept Ejection Seat, Contract F33657-69-C-0223, Report DAC 67616A, Douglas Aircraft Company, February 1969
4. Rearward Vision Improvement, ECP-ACES-01
5. W. J. Chagaris, Drogue Parachute Study for Advanced Concept Ejection Seat (ACES), Report No. MDC J0028, Douglas Aircraft Company, 18 August 1969
6. Drogue Parachute Revision, ECP-ACES-04
7. Wilder, Deans and Kottler, Loads and Stress Analysis, ACES (Advanced Concept Escape System) Report No. DAC 67892
8. H. R. Moy, Advanced Stabilized Ejection Seat Development Program, Technical Report SEG-TR-67-51, January 1968
9. M. E. Wilfert, Recovery Subsystem Study for the Advanced Concept Ejection Seat (ACES), Report No. MDC J5030, January 19, 1971
10. H. R. Moy, R. McLaughlin, Advanced Concept Ejection Seat (ACES) Recovery Subsystem Qualification Drop Tests, Report No. MDC J5219, Revision A, January 6, 1972
11. A. R. Barker, Report No. DAC 67759, Test Plan Model 412A Advanced Concept Ejection Seat, Contract F33657-69-C-0223, February 17, 1969
12. R. W. Duer, Test Report of Leak Test at Room Temperature of One (1) McDonnell Douglas Corporation Part Number D114435-1, Sierra Engineering Report No. 266-936, Addendum I, March 5, 1971.
13. M. E. Wilfert and J. L. T. Williams, Report No. MDC J5259, Advanced Concept Ejection Seat (ACES) System Development Static and Dynamic Ejection Tests, Revision A, April 26, 1971.
14. Ogden Technology Laboratories, Inc. Report No. F-70182, Report of Environmental Test on ACES Parachute Mortar, October 1971.
15. Ogden Technology Laboratories, Inc. Report No. F-70181, Report on Environmental Tests on ACES Gyro Spin-up Actuator, September 1971.

16. D. L. Mundell, Report No. MDC J5366, Advanced Concept Ejection Seat (ACES) Recovery Subsystem Qualification Gravity-Launched Seat Tests, Revision A, March 3, 1972.
17. J. A. Buonauro, Report MDC J5146, Static Structural Tests - Advanced Concept Ejection Seat, Model 412A.
18. Ogden Technology Laboratories, Inc., Test Report No. F-70183, Report of Environmental Tests on ACES Escape System Assembly, September 1971.
19. A. R. Barker, Report No. MDC J5356-01, Advanced Concept Ejection Seat (ACES) System Qualification Static and Dynamic Ejection Tests, Revision B, October 31, 1972.
20. G. Mas, Advanced Concept Ejection Seat Failure Analysis Report No. 15, Revision A dated 24 September 1971.
21. J. L. T. Williams, Report No. MDC J5327, Advanced Concept Ejection Seat (ACES) System Qualification Inflight Ejection Tests, Revision A, March 13, 1972.
22. H. R. Moy, ACES System Failure Analysis Report No. 16, dated 20 October 1971.
23. D. E. Reichenau, Aerodynamic Characteristics of an Ejection Seat Escape System with Cold Flow Rocket Plume Simulation at Mach Numbers from 0.6 through 1.5, Report No. AEDC-TR-69-218, Arnold Engineering Development Center, Arnold Air Force Station, Tennessee, October 1969.
24. A. Rickards, and J. M. Collins; Full Scale Subsonic Wind Tunnel Tests on Fully Equipped 75 and 5 Percentile Dummies; Technical Report AFFDL-TR-67-44; Air Force Flight Dynamics Laboratory, Wright-Patterson Air Force Base, Dayton, Ohio; August 1957.
25. J. N. Dalrymple, Douglas Aircraft Company Report No. ER-247, Reliability Program Plan for Advanced Concept Ejection Seat, February 12, 1969.
26. MIL-STD-846 (USAF), 6 July 1967, Military Standard Escape System Testing: Ground, Track, and Flight Test.
27. J. N. Dalrymple, Report No. MDC-J1171, Advanced Concept Ejection Seat (ACES) Reliability Assessment and Analysis, Revision B, November 28, 1972.
28. R. L. Gaskey, Douglas Aircraft Division Report No. PS-MM01, Maintainability Program Plan for the Advanced Concept Ejection Seat, February 12, 1969.

UNCLASSIFIED

Security Classification

DOCUMENT CONTROL DATA - R & D		
<i>(Security classification of title, body of abstract and indexing annotation must be entered when the overall report is classified)</i>		
1. ORIGINATING ACTIVITY (Corporate author) Douglas Aircraft Co. McDonnell Douglas Corporation 3855 Lakewood Blvd., Long Beach, Ca. 90801		2a. REPORT SECURITY CLASSIFICATION UNCLASSIFIED
		2b. GROUP None
3. REPORT TITLE ADVANCED CONCEPT EJECTION SEAT (ACES) DEVELOPMENT AND QUALIFICATION		
4. DESCRIPTIVE NOTES (Type of report and inclusive dates) Final Report - September 1968 to April 1972		
5. AUTHOR(S) (First name, middle initial, last name) Hammond R. Moy		
6. REPORT DATE January 1973	7a. TOTAL NO. OF PAGES 196	7b. NO. OF REFS 27
8a. CONTRACT OR GRANT NO. F33657-69-C-0223	8a. ORIGINATOR'S REPORT NUMBER(S) None	
b. PROJECT NO. None		
c.	8b. OTHER REPORT NO(S) (Any other numbers that may be assigned this report)	
d.	ASD-TR-73-2	
10. DISTRIBUTION STATEMENT Distribution limited to U. S. Government agencies only; Test and Evaluation; 21 December 1972. Other requests for this document must be referred to ASD/SML, Wright-Patterson Air Force Base, Ohio 45433.		
11. SUPPLEMENTARY NOTES None	12. SPONSORING MILITARY ACTIVITY Life Support System Program Office Aeronautical Systems Division U. S. Air Force Systems Command	
13. ABSTRACT The development of the Advanced Concept Ejection Seat (ACES) was proposed by the Douglas Aircraft Company of the McDonnell Douglas Corporation as a solution to critical operational problems experienced with current U. S. Air Force escape systems and to provide a major improvement in escape capability, especially under low-level, adverse attitude situations where relatively high crew fatality rates have been encountered. A program encompassing design, as well as development and qualification testing, resulted in the successful demonstration of the ACES system at speeds up to 690 KEAS and at altitudes up to 41,000 feet (MSL). The major performance improvement was achieved by incorporation of a multi-mode recovery sequencing system, mortar-deployed recovery subsystem with variable effective reefing, and a gyro-controlled vernier rocket to pitch-stabilize the seat during the initial part of its trajectory. Onboard speed/altitude sensors and an automatic programmer, containing logic and electronic time delays, were used to establish the seat environment, select the recovery mode, and initiate ejection and recovery events. Performance requirements of MIL-S-9479A were satisfied, with the exception that accelerations (spinal axis), in some instances, exceeded specified limits. An improvement in ACES escape capability can be effected by releasing the seat from the crewman earlier, just as the recovery parachute initially inflates.		

14. KEY WORDS	LINK A		LINK B		LINK C	
	ROLE	WT	ROLE	WT	ROLE	WT
Ejection Seat						
Gyro-Controlled Pitch Stabilization						
Drogue Parachute						
Reefed Recovery Parachute						
Electronic Time-Delays						
Rocket Catapult						
Airspeed/Altitude Sensors						
Base Pressure Effects						
Electroexplosive Sequencing						
Survival Equipment						
Ejection Seat Testing						
Mortar-Deployed Parachute						